eman ta zabal zazu

Universidad del País Vasco

Euskal Herriko Unibertsitatea

DOCTORAL THESIS

Faculty of Medicine

Department of Neurosciences

Generation of new LGMDR1 models with CRISPR/Cas9 and studies to expand insight into the disease.

by

Martxel Pedro Dehesa Etxebeste, MSc

Memory to achieve a PhD in Molecular Biology and Biomedicine

by The University of the Basque Country

Under the direction of

Adolfo López de Munain, MD, PhD

Neia Naldaiz Gastesi, PhD

Donostia - San Sebastián, 2022

The work presented in this thesis was performed at Biodonostia Health Research Institute, Area of Neuroscience, under the supervision of Dr. Adolfo López de Munain and Dr. Neia Naldaiz Gastesi.

INDEX

INDEX

FIGURE AND TABLE INDEX

FIGURE INDEX

TABLE INDEX

ABBREVIATIONS AND ACRONYMS

ABBREVIATIONS AND ACRONYMS

A	AA	Amino acids
	AAV	Adeno-associated virus
	ADP	Adenosine diphosphate
	AFP	Alpha fetoprotein
	AKT	Protein kinase B
	ALDOA	Aldolase A
	AMPK	AMP-activated protein kinase
	ANKRD2	Ankyrin repeat domain-containing protein 2
	ATP	Adenosine triphosphate
B	BCAA	Branched chain amino acids
	BDNF	Brain derived neurotrophic factor
	BIP	Binding immunoglobulin protein
	BMD	Becker muscular dystrophy
	BP	Base pair
	BSA	Bovine serum albumin
C	CAMKII	Calcium/calmodulin-dependent protein kinase II
	CASQ	Calsequestrin
	C3KO	Calpain 3 knockout
	cAMP	Cyclic adenosine monophosphate
	CHOP	C/EBP homologous protein
	CK	Creatine kinase
	PCr	Phosphocreatine
	PCR	Polymerase chain reaction
	CNTF	Ciliary neurotrophic factor
	COC	Cumulus-oocyte complex
	CRISPR	Clustered regularly interspaced short palindromic repeats
	CSRP3	Cysteine and glycine-rich protein 3
	CTX	Cardiotoxin
	CTRL	Control
D	DM1	Myotonic dystrophy -1
	DM-2	Differentiation medium-2
	DMD	Duchenne muscular dystrophy
	DMEM	Dulbecco's modified eagle medium

	DMPK	Dystrophia myotonica protein kinase
	DMSO	Dimethyl sulfoxide
	DPBS	Dulbecco's phosphate buffered saline
	DSB	Double strand break
	DTT	1,4-Dithiothreitol
E	EB	Embryoid body
	ECM	Extracellular matrix
	ECMG	Extracellular matrix gel
	EDTA	Ethylenediaminetetraacetic acid
	EGF	Epidermal growth factor
	ERAD	Endoplasmic-reticulum-associated protein degradation
	ESC	Embryonic stem cell
F	FACS	Fluorescence-activated cell sorting
	FAP	Fibro/adipogenic progenitors
	FBS	Fetal bovine serum
	FGF-2	Fibroblast growth factor-2
	FSHD	Facioscapulohumeral muscular dystrophy
	FOXO1	Forkhead box O1
G	GFAP	Glial fibrillary acidic protein
	GFP	Green fluorescent protein
	GSK3β	Glycogen synthase kinase-3 beta
H	HBSS	Hank's Buffered Salt Solution
	HDR	Homology-directed repair
	HE	Haematoxylin and Eosin
	HGF	Hepatocyte growth factor
	HGF	Hepatocyte growth factor
	HR	Homologous recombination
	HSP	Heat shock protein
I	IBM	Inclusion body myositis
	IGF-1	Insulin-like growth factor 1
	IL	Interleukin
	INDEL	Insertion and/or deletion
	iPSC	Induced pluripotent stem cell
	IVF	*In vitro* fertilisation
	IVM	*In vitro* maturation
K	KBP	Kilo base pair
	KO	Knock-out

	KOSR	Knock-out serum replacement
L	LGMD	Limb girdle muscular dystrophy
	LGMD2A	Limb girdle muscular dystrophy type 2A, renamed LGMDR1
	LSGS	Low Serum Growth Supplement
M	MAPK	Mitogen-activated protein kinase
	MBP	Mega base pair
	MD	Muscular dystrophy
	MOI	Multiplicity of infection
	MRF	Myogenic regulatory factors
	MW	Molecular Weight
	MYHC	Myosin heavy chain
N	NADPH	Nicotinamide adenine dinucleotide phosphate
	NANOG	Homeobox protein
	NBCS	Newborn calf serum
	NEAA	Non-essential amino acids
	NF-***κ***B	Nuclear factor kappa B
	NGS	Next generation sequencing
	NHEJ	Non-homologous end-joining
	NMD	Nonsense mediated decay
	NMJ	Neuro-muscular junction
O	OCT	Optimal Cutting Temperature Compound
	OCT4	Octamer-binding transcription factor 4
P	PAGE	Polyacrylamide gel electrophoresis
	PAM	Protospacer adjacent motif
	PAX7	Paired Box 7
	PBS	Phosphate-buffered aline
	PCR	Polymerase chain reaction
	PCr	Phosphocreatine
	PMSF	Phenylmethanesulfonyl fluoride
	PI3K	Phosphoinositide 3-kinase
	PVA	Polyvinyl alcohol
R	RNP	Ribonucleoprotein
	ROCK	Rho-associated protein kinase
	ROS	Reactive oxygen species
	RT	Room temperature
	RYR	Ryanodine receptor
S	SCs	Satellite cells

	SCNT	Somatic cell nuclear transfer
	SD	Standard deviation
	SDS	Sodium dodecyl sulfate
	SEM	Standard error of the mean
	SERCA	Sarcoplasmic reticulum calcium ATPase
	SHH	Sonic Hedgehog Protein
	SNP	Single nucleotide polymorphism
	SOD	Superoxide dismutase
	SOX2	SRY-box 2
	SR	Sarcoplasmic reticulum
	SSEA3	Stage-specific embryonic antigen 3
	SSEA4	Stage-specific embryonic antigen 4
T	TA	Tibialis anterior
	TCA	The tricarboxylic acid
	TTN	Titin protein
	TALEN	Transcription activator like effector nucleases
	TBE	Tris/Boric Acid/EDTA
	TBS	Tris-buffered saline
	TBST	Tris-buffered saline tween
	TNF-α	Tumor necrosis factor-α
	TPC2	Two pore segment channel 2
	TRA-1-60	Tumor rejection antigens-1-60
	TRA-1-81	Tumor rejection antigens-1-81
	TUJ1	Neuron-specific class III beta-tubulin
U	UPR	Unfolded protein response
	UPS	Ubiquitin proteasome system
	UTR	Untranslated region
W	WT	Wild type
X	XBP1	X-Box binding protein 1
Z	ZFN	Zinc-finger nuclease
	α-SMA	α-smooth muscle actin
	%	Percent
	[ ]	Concentration
	ºC	Degree Celsius
	µg	Microgram

RESUMEN

RESUMEN

Las distrofias musculares constituyen un grupo de enfermedades genéticas que causan una degeneración progresiva del músculo esquelético. Entre estas enfermedades, las distrofias musculares de cinturas (LGMD, por sus siglas en inglés) forman un subgrupo de enfermedades que causan debilidad de los músculos proximales y los músculos de las cinturas pélvica y escapular. Según su patrón de herencia, las LGMD se clasifican en dos grupos: LGMD D para las autosómicas dominantes o LGMD R para las recesivas, seguidas de un número correspondiente al gen afectado.

Dentro de las LGMD recesivas, la LGMDR1 es la forma más común y está causada por mutaciones en el gen *CAPN3*. Este gen codifica la proteína calpaína 3, una proteasa no lisosomal que se expresa principalmente en el músculo esquelético. Desde que se descubrió la causa genética de la LGMDR1, se han descrito más de 500 mutaciones patogénicas en el gen *CAPN3*, que conllevan a resultados como la pérdida de la proteína, la pérdida de su actividad enzimática o cambios en su afinidad para unirse a otras proteínas en el músculo.

La enfermedad, que actualmente no tiene cura ni tratamiento disponible, se caracteriza clínicamente por una debilidad muscular progresiva que afecta tanto a las cinturas pélvica y escapular como a los músculos proximales de las extremidades. Los primeros síntomas suelen aparecer durante la segunda década de la vida, cuando los pacientes comienzan a tener dificultades para subir escaleras, correr, levantar peso o levantarse de una silla. A medida que aumenta la debilidad muscular, los pacientes comienzan a tener dificultades para caminar, lo que generalmente conduce a la pérdida de la deambulación en una o dos décadas después del inicio de los síntomas. A nivel histopatológico, las biopsias musculares de estos pacientes muestran características distróficas comunes como la variabilidad en el tamaño de las fibras, áreas necróticas con regiones regenerativas, miofibrillas desorganizadas y sustitución del tejido muscular por tejido adiposo y fibrótico, que aumentan con la progresión y severidad de la enfermedad. En las primeras etapas de la enfermedad se puede observar en estas biopsias inflamación e infiltraciones eosinofílicas, acompañadas de eosinofilia en sangre periférica, que va disminuyendo en las últimas etapas de la enfermedad. Los núcleos apoptóticos aumentan en el tejido y se

ha descrito que la cantidad de células satélite aumenta a medida que avanza la enfermedad.

Cabe destacar que existe una gran variabilidad fenotípica entre pacientes, incluso entre los afectados dentro de una misma familia. A pesar de que varios estudios han intentado correlacionar las diferentes mutaciones en el gen *CAPN3* y la gravedad del fenotipo, dicha correlación ha sido difícil de establecer, aunque en general los pacientes con dos mutaciones nulas (que dan como resultado la pérdida de la proteína) tienden a desarrollar un fenotipo más severo. La principal función de la calpaína 3 y el mecanismo mediante el cual su ausencia o pérdida de función conllevan a la distrofia aún se desconocen. Tampoco está clara la razón por la cual la deficiencia de calpaína 3 afecta más a unos músculos que a otros, y por qué la degeneración muscular no está presente en los recién nacidos y comienza a desarrollarse en la adolescencia o incluso en edades más avanzadas. Una de las principales funciones de la calpaína 3 parece estar relacionada con el ensamblaje y la remodelación del sarcómero, donde se sabe que interactúa y se une a la titina y proteoliza algunos de los componentes del sarcómero. Además, la calpaína 3 también participa en el mantenimiento de la homeostasis del calcio a través de su participación en la tríada y la interacción con varias proteínas que regulan los niveles de calcio como las proteínas RYR1 y SERCA. Además de estas funciones, diferentes estudios también han asociado la calpaína 3 con alteraciones en otras funciones y vías de señalización asociadas a la apoptosis, la adaptación muscular, la regulación mitocondrial y la regeneración muscular, entre otras.

Actualmente, el estudio de la fisiopatología de la LGMDR1 enfrenta varios desafíos. En primer lugar, al ser una enfermedad rara, el número de pacientes que aportan datos clínicos es reducido en comparación con otras enfermedades, y la disponibilidad de muestras musculares de los pacientes es muy limitada. Además, la calpaína 3 tiene una actividad autolítica que hace que la proteína sea altamente inestable, lo cual ha dificultado el estudio de los posibles roles e interacciones que realiza la calpaína 3, y muchas de las observaciones descritas en los modelos *in vitro* e *in vivo* aún no se han confirmado que ocurran en pacientes o no han sido reproducidos en otros modelos o estudios.

Otra de las limitaciones en el estudio de la LGMDR1 es la falta de modelos apropiados de la enfermedad. Con el fin de estudiar la enfermedad y desarrollar nuevos tratamientos,

se han generado diferentes modelos *in vitro* e *in vivo* para la LGMDR1. Los modelos *in vitro*, como los mioblastos primarios derivados de pacientes, además de ser escasos, solo pueden soportar un número limitado de pases en cultivo, y generalmente tienen una gran variabilidad entre pacientes. Alternativamente, el uso de mioblastos inmortalizados, si bien son útiles para estudiar ciertos aspectos, presentan otras limitaciones debido a sus modificaciones genéticas. Además de esto, dado que la LGMDR1 es una enfermedad degenerativa progresiva, los cultivos *in vitro* de corta duración y generalmente inmaduros no logran reproducir tales procesos degenerativos.

Por otro lado, los modelos *in vivo* desarrollados en ratones, como el ratón C3KO, desarrollan síntomas muy leves y no logran reproducir las características clínicas como una distrofia notable y la pérdida de la deambulación que ocurre en los pacientes. Esto sugiere que los modelos de ratón podrían tener mecanismos compensatorios para compensar la falta de calpaína 3. Este contexto pone de manifiesto la necesidad de nuevos modelos animales que reproduzcan las características de la enfermedad, lo que permitiría estudiar la enfermedad y probar la eficacia real de nuevas terapias, como las terapias génicas en desarrollo, antes de su transición a la clínica. En este sentido, la especie porcina se está convirtiendo en una alternativa interesante para modelar distrofias musculares como la LGMDR1. Siendo más similares a los humanos en tamaño, metabolismo y longevidad, los modelos genéticos que se han generado para enfermedades que afectan al músculo han mostrado un fenotipo más severo, similar al humano, postulando esta especie como una de las más adecuadas para futuros modelos *in vivo* de distrofias musculares.

Teniendo en cuenta la experiencia en nuestro grupo con algunos de los modelos mencionados, consideramos que, si bien estos pueden ser útiles para estudiar algunos efectos de la ausencia de calpaína 3 en el músculo, se requieren mejores modelos para avanzar en la comprensión de la enfermedad y en el desarrollo de nuevas terapias. Con esto en mente, este trabajo se ha centrado en contribuir a la investigación en la LGMDR1 en dos aspectos. Por un lado, nuestro objetivo era proporcionar nuevos modelos de LGMDR1, uno *in vitro* y otro *in vivo,* que esperábamos podrían mejorar algunas de las limitaciones encontradas en los modelos actuales, y por otro lado, realizamos estudios con el modelo de ratón C3KO existente y el modelo *in vitro* que desarrollamos, para evaluar aspectos clave de la enfermedad como la respuesta al daño, la miogénesis y el efecto del ejercicio en ausencia de calpaína 3, para obtener nuevas perspectivas de los mecanismos

de la enfermedad y las posibilidades para su tratamiento. Por ello, el trabajo de esta tesis se ha dividido en tres capítulos.

En el primer capítulo desarrollamos un modelo *in vitro* basado en líneas isogénicas de iPSCs KO para calpaína 3 generadas con CRISPR/Cas9. Hipotetizamos que el uso de líneas iPSCs isogénicas que solo difieren en la presencia o ausencia de calpaína 3 permitiría estudiar mejor el fenotipo *in vitro,* ya que se evitaría la variabilidad encontrada entre cultivos celulares derivados de diferentes individuos. Además, ofrecería una línea celular continua que podría expandirse indefinidamente. Para ello, diseñamos diferentes guías CRISPR/Cas9 para eliminar el codón de inicio del gen de la calpaína 3 en una línea control de iPSCs. Aislamos 4 clones KO de iPSCs que tenían deleciones bialélicas y seleccionando 2 de ellos para caracterizarlos por completo. Las líneas KO mantuvieron sus características de iPSCs después de la mutación bialélica y expresaron niveles apropiados de marcadores de pluripotencia mientras que no se detectaron mutaciones *off-target* de CRISPR/Cas9 y todas las líneas KO mostraron cariotipos normales. Para la obtención de células musculares a partir de estas iPSCs, se utilizó un protocolo miogénico que sobreexpresa *PAX7*, con el que se obtuvieron progenitores miogénicos PAX7-GFP+ proliferativos que diferenciaban a miotubos multinucleados, y en ellos se pudo confirmar la ausencia de proteína calpaína 3 en las líneas KO. A partir de este punto, optimizamos el protocolo probando diferentes medios de diferenciación terminal, suplementos y sustratos en el cultivo, y obtuvimos miotubos más maduros con mayores niveles de contracción al usar un sustrato a base de cultrex con ácido hialurónico y dos medios de diferenciación diferentes (S-Dex y DM-2).

En el segundo capítulo nos centramos en evaluar aspectos clave para el mantenimiento de la homeostasis en el músculo, donde la ausencia de calpaína 3 podría estar generando un impacto negativo, y para lo cual utilizamos nuestras líneas iPSCs isogénicas KO de calpaína 3, así como el modelo de ratón C3KO existente. Primero, realizamos un estudio proteómico para evaluar la respuesta al daño muscular agudo por inyección de CTX en el ratón C3KO. Observamos que la respuesta al daño era diferente en el C3KO, con muchas proteínas desreguladas en comparación con la respuesta al daño del WT, y también se observaron diferencias significativas entre los músculos TA y sóleo en su respuesta al daño, siendo este último un músculo más afectado. Además, observamos que las diferencias en los niveles de proteínas apuntaban a procesos mitocondriales, metabolismo de la glucosa, plegamiento de proteínas y miogénesis, e identificamos algunas proteínas

que podrían ser clave en estos procesos celulares como los reguladores miogénicos MYBBP1A, CSRP3 y ANKRD2 en el sóleo, así como varias chaperonas desreguladas en ambos músculos. A continuación, observamos que en ausencia de calpaína 3, la capacidad miogénica *in vitro* era menor, tanto en las líneas iPSCs humanas como en los cultivos de células satélite derivadas de ratones C3KO viejos.

Para evaluar si el ejercicio podía inducir un fenotipo más notable, realizamos varias pruebas de agotamiento en ratones C3KO viejos. Al medir su resistencia en estas pruebas, no observamos alteraciones motoras en los C3KO viejos, al contrario, observamos que los C3KO viejos tenían una mayor resistencia y cualitativamente a nivel histológico, tampoco mostraban signos claros de atrofia. Esto hizo evidentes las limitaciones de este modelo para realizar estudios funcionales y la necesidad de estudiar los mecanismos compensatorios de este modelo para evitar la atrofia. Tras las pruebas de agotamiento, observamos que a nivel molecular los C3KO viejos tenían diferencias significativas en niveles de proteínas mitocondriales, asociadas al metabolismo de la glucosa y en chaperonas citosólicas y asociadas al estrés de retículo/UPR. En este contexto, observamos que un tratamiento con 4-PBA, reducía significativamente los niveles elevados de dichas proteínas, pero sin afectar el rendimiento en las pruebas de agotamiento. Para evaluar si algunos de estos cambios y vías alteradas también estaban afectados en un contexto de miotubos humanos, inducimos contracciones *in vitro* en los miotubos obtenidos con nuestro modelo de iPSCs isogénico durante períodos prolongados, donde también probamos el tratamiento con 4-PBA. Se observó que las alteraciones en los niveles de proteínas TOM20, HSP70, GLUT4 y p-mTOR están presentes tanto en ratones C3KO después de las pruebas de agotamiento como en miotubos derivados de iPSCs humanos que carecen de calpaína 3. En cuanto al tratamiento con 4-PBA *in vitro,* este no mostró ningún resultado significativo en las condiciones probadas.

Finalmente, en el tercer capítulo, después de evidenciar que es necesario disponer de un mejor modelo de LGMDR1 *in vivo,* nos centramos en obtener un cerdo KO de calpaína 3. Para ello, utilizamos una estrategia de diseño de guías CRISPR/Cas9 similar a la utilizada en las células iPSCs, para eliminar el codón de inicio del gen de la calpaína 3 porcina, y guías adicionales, como estrategia alternativa, para generar una mutación en el exón 22. Las guías CRISPR/Cas9 se probaron y optimizaron en fibroblastos de cerdo y también en embriones de cerdo. A continuación, optimizamos el proceso para obtener embriones de cerdo con altas tasas de mutaciones bialélicas y viabilidad *in vitro* utilizando diferentes

combinaciones de guías y métodos para introducirlas en los ovocitos. Se realizaron varias transferencias de embriones a cerdas receptoras y se obtuvieron unas pocas gestaciones de las cuales la mayoría terminaron en abortos naturales. Solo obtuvimos 2 lechones que murieron al nacer y eran de genotipo WT, de modo que no logramos obtener un cerdo KO de calpaína 3. La razón por la que obtuvimos una tasa de éxito tan baja en la obtención de lechones vivos requerirá de más experimentos. No obstante, las herramientas y la optimización de los protocolos que se podrán ser útiles en los futuros intentos que se vayan a realizar para obtener el cerdo KO de calpaína 3, y que además allanarán el camino para obtener otros modelos de distrofias musculares.

SUMMARY

SUMMARY

Muscular dystrophies constitute a group of genetic diseases that cause a progressive degeneration of the skeletal muscle. Among these diseases, limb-girdle muscular dystrophies (LGMDs) form a subgroup of diseases that cause weakness of the proximal muscles and muscles of the pelvic and shoulder girdles. According to their inheritance pattern, LGMDs are classified into two groups: LGMD D for the autosomal dominants, or LGMD R for the recessive ones, followed by a number corresponding to the gene affected.

Within the recessive LGMDs, LGMDR1 is the most common form and is caused by mutations in the *CAPN3* gene. This gene encodes the calpain 3 protein, a non-lysosomal protease that is expressed mainly in skeletal muscle. Since the genetic cause of LGMDR1 was discovered, more than 500 pathogenic mutations have been reported in the *CAPN3* gene, which induce various protein outcomes, such as loss of the protein, the impairment of its enzymatic activity, or changes in its affinity to bind to other proteins in the muscle.

The disease, which currently has no cure or specific treatment available, is clinically characterized by a slow progressive muscular weakness that affects both pelvic and scapular girdles and proximal limb muscles. First symptoms usually appear during the second decade of life, where patients start to have difficulties climbing stairs, running, lifting weights, or getting up from a chair. As muscle weakness increases, patients start to have difficulties walking which generally leads to the loss of ambulation within one or two decades after onset. At the histopathological level, muscle biopsies from these patients display common dystrophic features such as fiber size variability, necrotic areas with regenerative regions, disorganized myofibrils and muscle tissue replacement by adipose and fibrotic tissue, which increases with disease progression and severity. In the early stages of the disease inflammation and eosinophilic infiltrations can be observed in these biopsies, accompanied by peripheral blood eosinophilia, which decreases in latter stages of the disease. Apoptotic nuclei are increased in the tissue and it has been reported that the amount of satellite cells continues to increase as the disease progresses.

Of note, there is great phenotypic variability existing among patients, even among those affected within the same family, and although several studies have tried to correlate the different mutations in the *CAPN3* gene and the severity of the phenotype, such correlation

has been hard to establish, although overall patients with two null mutations (resulting in the loss of protein) tend to develop a more severe phenotype. The main function of calpain 3 in the skeletal muscle and why its absence or loss of function results LGMDR1 is unknown. Also, the reason why calpain 3 deficiency affects some muscles more than others, and why muscle degeneration is not present in newborns and starts to develop in late childhood, adolescence, or even at later ages is not clear. Many functions have been attributed to calpain 3 in the muscle. One of the main functions seems to be related with sarcomere assembly and remodeling, where it is known to interact and bind to the titin spring protein, and proteolyzes some of the sarcomere components. Also, it seems that calpain 3 participates in the maintenance of calcium homeostasis through its participation in the triad and interaction with several calcium-handling proteins like RYR1 and SERCA proteins. Besides these functions, other functions and signaling pathways have been found altered in different studies, associated with apoptosis, muscle adaptation, mitochondria regulation and muscle regeneration among others. The multiple functions calpain 3 seems to have and the poor correlations that have been made between the mutations, pathogenic mechanisms and how this affects more to some muscles than others, highlights the need to further study this disease.

Currently, the study of LGMDR1 pathophysiology faces several challenges. First of all, being a rare disease, the number of patients providing clinical data is reduced compared to other diseases, and the availability of muscle samples from patients are very limited. Additionally, calpain 3 has an autolytic activity that makes the protein highly unstable, which has hindered the study of the potential roles and interactions that calpain 3 makes, and still many of the observations described in the *in vitro* and *in vivo* models have not been confirmed to occur in patients and have not been reproduced in other models or studies.

Another challenge when studying LGMDR1 is the lack of appropriate models of the disease. In order to study the disease and develop potential new treatments, different *in vitro* and *in vivo* models have been generated for LGMDR1. *In vitro* models such as the patient-derived primary myoblasts, besides being limited in availability and only being able to endure a limited number of passages in culture, they generally have a great inter-patient variability, which also occurs with patient-derived iPSC models. Alternatively, the use of immortalized myoblasts while being useful to study certain aspects, the modifications that these cells have makes them less relatable. On top of this, since

LGMDR1 is a slow progressive degenerative disease, short-lived and generally immature *in vitro* cultures fall short in reproducing such degenerative processes.

On the other hand, the *in vivo* models developed in mice such as the C3KO mouse, develop very mild symptoms, and fail to reproduce the clinical features such as the muscle wasting and loss of ambulation that occurs in LGMDR1 patients. This suggests that mouse models could have compensatory mechanisms that alleviate the muscle degeneration that the lack of calpain 3 causes in humans. This situation makes the development of new and potentially larger animal models that would reproduce the disease characteristics and progression highly desirable, which would allow to study the disease and to test the real efficacy of new therapies such as the gene therapies that are under development, before transitioning to the clinic. In this sense, the porcine species is becoming an interesting alternative to model muscular dystrophies such as LGMDR1, being more similar to humans in size, metabolic profile and longevity, so far, the genetic models that have been generated for muscular disorders in pigs have shown a more severe phenotype, similar to humans, postulating this species as suitable one for future *in vivo* models of muscular dystrophies.

Considering the mentioned issues and the existing experience in our group with some of the mentioned LGMDR1 models, we considered that while current models can still be used to study the effects of the absence of calpain 3 in the muscle, better models are required to advance in the understanding of the disease and the development of potential new therapies. With this in mind, the present study has focused on contributing to LGMDR1 research in two aspects. On the one hand, we aimed to provide new LGMDR1 models, one *in vitro* and one *in vivo,* which we expected could improve some of the limitations found in the current models. And on the other hand, we performed studies with the existing C3KO mouse model and the *in vitro* model that we developed, to evaluate key aspects of the disease such as the damage response, myogenesis and the effect of exercise in the absence of calpain 3 to obtain new insights of the disease mechanisms and treatment possibilities. Thus, the work in this thesis has been divided in three chapters.

In the first chapter, we developed an *in vitro* model based in isogenic calpain 3 KO iPSC lines generated with CRISPR/Cas9. We hypothesized that the use of isogenic iPSC lines that only differ in the presence or absence of calpain 3 would allow to better study the phenotype *in vitro,* and avoid the variability found between cell cultures derived from

different individuals. Additionally, it would offer a continuous cell line that could be expanded indefinitely. For this, we designed different CRISPR/Cas9 guides to target and eliminate the start codon of the calpain 3 gene in a control iPSC line. We isolated 4 iPSC KO clones that had biallelic deletions in the start codon of calpain 3, and selected 2 of them to be fully characterized. The KO lines maintained their iPSC characteristics after the biallelic mutation and expressed appropriated levels of pluripotency markers while no CRISPR/Cas9 off-target effects were detected and all KO lines showed normal karyotypes. To obtain muscle cells from these iPSCs, a *PAX7* overexpressing myogenic protocol was used, which resulted in proliferative PAX7-GFP+ myogenic progenitors that were capable to differentiate into multinucleated myotubes, and where the absence of calpain 3 protein in the KO lines could be confirmed. From this point, we optimized the terminal differentiation protocol by testing different terminal differentiation mediums, supplements and substrates in the culture, and obtained more mature myotubes with increased contraction levels by using a cultrex and hyaluronic acid-based substrate and two different differentiation mediums (S-Dex and DM-2).

In the second chapter, we focused on evaluating key processes important to maintain homeostasis in the muscle, where the absence of calpain 3 could be having an impact. For this, we used our isogenic calpain 3 KO iPSC lines as well as the existing C3KO mouse model. First, we performed a proteomic study to evaluate the acute damage response in the C3KO mouse after a CTX injection. Here, we observed that the damage response was different in the C3KO with many proteins dysregulated when compared to the WT damage response, but also, that there were significant differences between the TA and the soleus muscles in their response to damage, the latter being a more affected muscle. Also, we observed that the differences in protein levels pointed towards altered mitochondrial processes, glucose metabolism, protein folding and myogenesis in the C3KO muscles, and identified some proteins that could be key in these processes such as the myogenic regulators MYBBP1A, CSRP3 and ANKRD2 in the soleus, as well as several chaperones dysregulated in both muscles. Following this, we observed that in the absence of calpain 3, the myogenic capacity *in vitro* appears to be reduced, which we could observe both in the human isogenic iPSC lines as well as in the old C3KO mouse derived satellite cell cultures.

To evaluate if exercise could lead to a more notable phenotype, we performed several run to exhaustion tests in old C3KO mice. When measuring performance in these tests, we

did not observe any motor impairments in the old C3KO, on the contrary, the old C3KO mice showed increased endurance and there were no clear qualitative signs of atrophy at the histological level either. This made evident the limitations of this model to perform functional studies and the need to study the compensatory mechanisms of this model to avoid atrophy. At the molecular level, we did observe significant differences in proteins from mitochondria, glucose metabolism, and cytosolic as well as ER stress/UPR associated chaperones after run to exhaustion tests, and observed that a treatment with 4-PBA, which we tested on some of the old C3KO mice, significantly reduced some of the increased protein levels without affecting the performance in the run to exhaustion tests. To evaluate whether some of these observed changes and pathways would also be affected on the human myotubes obtained from our isogenic iPSC lines, we induced contractions of the myotubes *in vitro* for prolonged periods with EPS and also tested the 4-PBA treatment on them, and observed that alterations in TOM20, HSP70, GLUT4 and p-mTOR protein levels are present in both C3KO mice after the exhaustion tests and human iPSC derived myotubes lacking calpain 3 after EPS, while the 4-PBA treatment did not show any significant results in the *in vitro* studies.

Finally, in the third chapter, after evidencing that a better *in vivo* LGMDR1 model is needed, we focused on generating a new model by generating a calpain 3 KO pig with CRISPR/Cas9, which based on the severe phenotype pigs have shown in other muscular dystrophy models, we expected it would also develop a more severe atrophy and a clinical phenotype more similar to humans. For this, we used a similar guide design strategy to the one used in the iPSC cells, to eliminate the start codon on the porcine calpain 3 gene, and additional guides to alternatively target the exon 22 and cause a deleterious mutation. The CRISPR/Cas9 guides were tested in pig fibroblasts and also in pig embryos. Here, we optimized the process to obtain pig embryos with high mutation and viability rates *in vitro,* using different CRISPR/Cas9 guide combinations and delivery methods. However, after several embryo transfers to recipient pigs and obtaining few gestations, we could not achieve to obtain a calpain 3 KO pig, as most pregnancies resulted in natural abortions and only 2 piglets were born, which died at birth and were genotyped as WT. The reason why we obtained such a low success rate in obtaining live piglets requires further experiments, however, the tools and optimized protocols we obtained here will be helpful in future attempts that will be made to obtain the calpain 3 KO pig, and which also could be useful to develop porcine models for other muscular dystrophies.

INTRODUCTION

INTRODUCTION

Human muscular system

The muscular system is an organ system that permits movement of the body, blood circulation and maintains body posture. In vertebrates, muscles are classified in three types depending on the type of cells that make up the tissue and how their movement is controlled: skeletal, smooth and cardiac muscle. Skeletal muscle represents the majority of muscle tissue, it is controlled by voluntary movements and the muscles are attached to bones through tendons. Skeletal muscles are mostly comprised of striated and multinucleated cells called myotubes. Cardiac muscle is also comprised of striated cells, but these are called cardiomyocytes and in this case they are bound to each other through intercalated discs creating fiber-like structures. This muscle is only found in the heart, where it induces involuntary and continuous contractions. Smooth muscle is mostly found in internal organs, the digestive system and the circulatory system, and it is formed by non-striated slow-twitch smooth muscle cells controlled by involuntary movements.

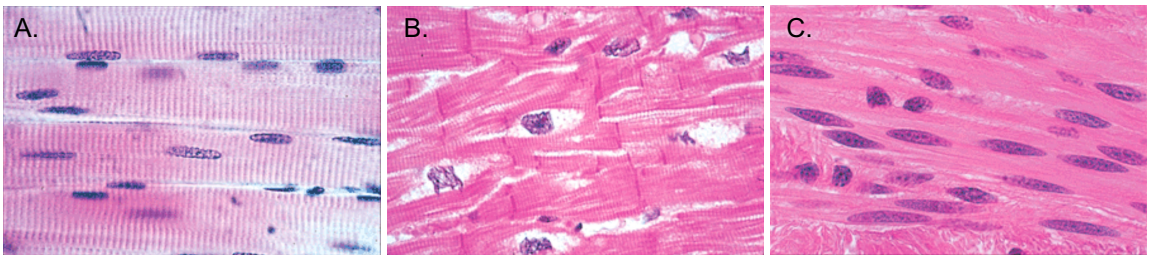

Figure 1. Representative histological images of the 3 muscle types. Hematoxylin and eosin staining of longitudinal sections of A) skeletal B) cardiac and C) smooth muscle. Source: The big picture: Medical Biochemistry (2012)

Skeletal muscle

Skeletal muscle is the most abundant type of muscle in the human body. The over 600 different muscles account for approximately 40% of the body weight, and besides the contractile and motor functions, it is a metabolically very active tissue, important for energy and amino acids storage and body temperature maintenance (Egan & Zierath, 2013; Frontera & Ochala, 2015). This type of muscle is also a very adaptive tissue, where resistance or strength trainings can cause hypertrophy and greatly increase their power, all while having a high regenerative capacity (Dumont, Bentzinger, et al., 2015).

Structure

Skeletal muscle is a highly structured tissue. The most abundant skeletal muscle cell, the myofiber or muscle fiber, is a long and thin multinucleated and post-mitotic cell that is formed by the fusion of mononuclear myoblasts. The nuclei in the myofibers are located on the outer perimeter of the cell below the cell membrane called sarcolemma. Right outside the sarcolemma, a layer of extracellular matrix (ECM) proteins such as laminins, collagens and glycoproteins form a coat for the myofiber called the basal lamina. Additionally, above the basal lamina there is a layer of connective tissue, the endomysium, which covers each myofiber. Groups of myofibers are bound together forming fiber fascicles by the conjunctive tissue of the endomysium. Each fascicle in turn, is covered by the conjunctive layer of the perimysium. This thin layer helps to provide an appropriate chemical environment for nutrient exchange, and also contains capillaries and nerves. Each muscle is made by sets of fascicles grouped, highly vascularized and innervated, and held together by the conjunctive tissue of the perimysium, where other cell types such as fibroblasts, pericytes and adipocytes are also present. The perimysium, is mostly made by collagen and the whole muscle is covered by an external cover called the epimysium, also made mostly by collagen (Figure 2). The conjunctive tissue that surrounds the muscle connects it to tendons and bones, transmitting the force generated by the contraction of the myofibers (Laurent, 2010; Susan Standring, 2021).

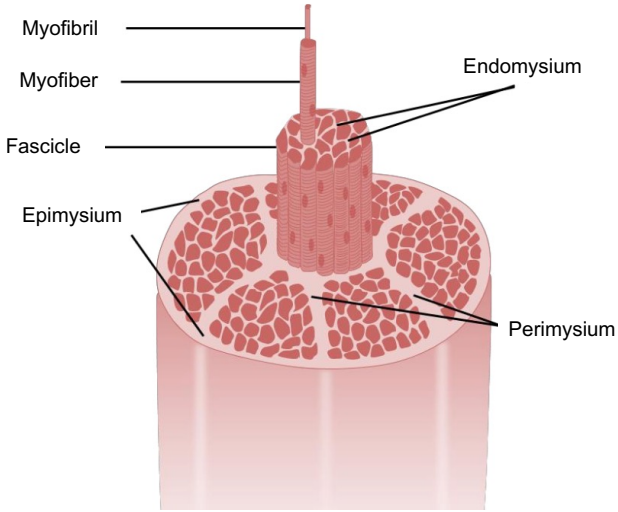

Figure 2. Structure of skeletal muscle. Myofibers surrounded by the endomysium form fascicles, and different fascicles that form the muscle are surrounded by the perimysium, and finally the whole muscle is covered by the epimysium. Source: Adapted from Mateos-Aierdi, 2017.

Within myofibers there are thousands of myofibrils, which are long rod like structures made of myofilaments (proteins) that when arranged together in a very orderly manner, form sarcomeres, the basic contractile unit of the skeletal muscle. The most abundant myofilaments are myosin (thick) and actin (thin) filaments, which slide along each other in contraction.

When sarcomeres are repeatedly aligned, these forms striations along the myofibers that can be observed in longitudinal sections of skeletal muscle tissue. Electron microscopy images of the sarcomere show light I bands and dark A bands. I bands only contain thin filaments and show a darker line known as the Z disk, where consecutive sarcomeres are joint together with α-ACTININ protein. Between I bands, A bands are the region where thin and thick filaments are in contact and the middle zone of the sarcomere, the H band, is where thin filaments are not present (Figure 3).

Other structurally important proteins are the dystrophin-glycoprotein complex, which bind the actin filaments to the extracellular laminin trough dystrophin (DMD); and the titin protein (TTN), a large elastic protein that stabilizes the thick filaments attaching them to the Z disk of the sarcomere. Other distinctive elements of the myofibers are the sarcoplasmic reticulum (SR), the transverse tubular system (T-tubule), and the mitochondrial network. Myofibrils are surrounded by the SR, which is a highly specialized smooth endoplasmic reticulum (ER) that plays a key role in contraction by controlling the release of calcium (Ca^{2+}), and the T-tubule system is an invagination of the cell membrane, the sarcolemma, towards the centre of the fiber that transmits the action potential from the nerves to the interior of the cells (Frontera & Ochala, 2015; Sweeney & Hammers, 2018).

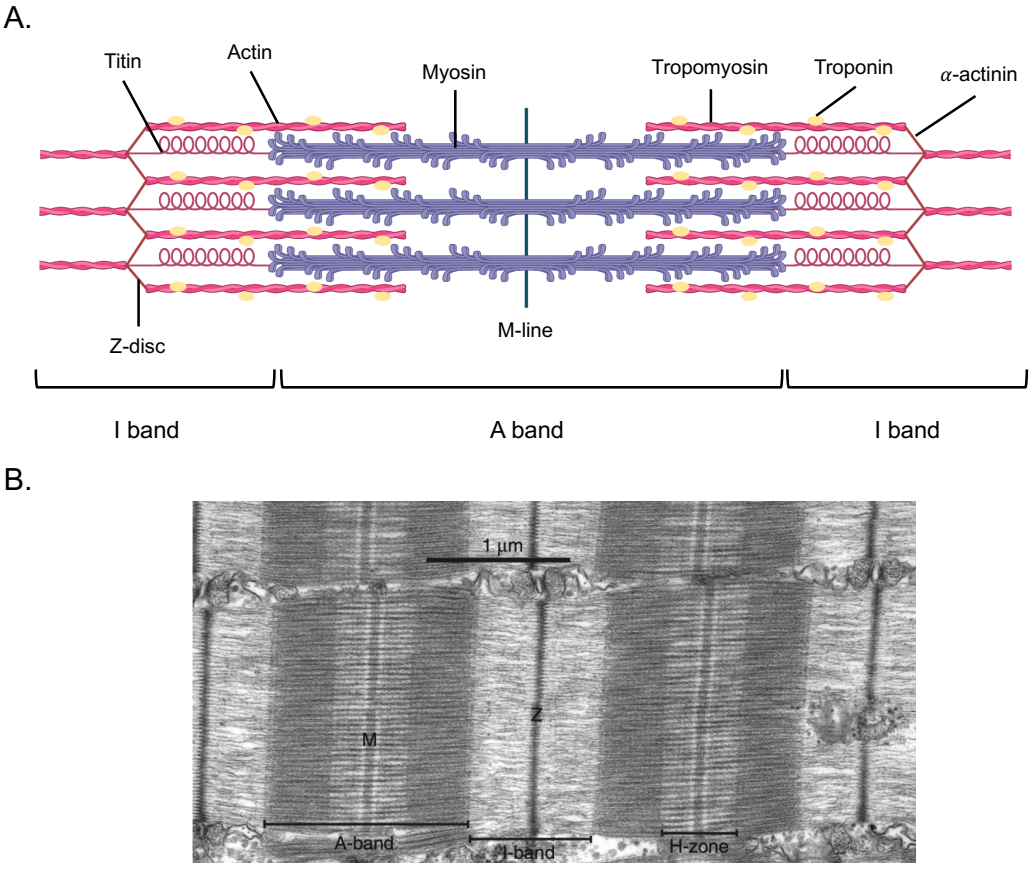

Figure 3. Structure of the sarcomeres. A) Simplified representation of the sarcomere, showing the main proteins that make up the different bands. B) Electron microscopy image of striated muscle sarcomere, with the different bands indicated. Source: Sweeney et al., 2018.

Fiber types

Fiber types are classified mainly depending on their metabolic activity, the speed of contraction and the type of myosin heavy chain isoforms they express. Each skeletal muscle can contain different proportions of fiber types (Westerblad et al., 2010):

- Type I: slow and oxidative fibers. These fibers appear reddish and contain large amounts of mitochondria with high levels of myoglobin and cytochrome complexes, and the main myosin heavy chain (MYHC) isoform is MYHCß (*MYH7* gene). The twitch of these fibers is slow with the lowest ATPase activity. They generate the lowest amount of force but are highly resistant to exhaustion. Muscles that contribute to body posture and perform slow and long-lasting contractions are enriched in this type of fiber.

- Type IIA: fast oxidative glycolytic fibers. These intermediate-sized fibers also contain a large number of mitochondria and high myoglobin content, but unlike type I fibers, they contain high amounts of glycogen and obtain energy also from anaerobic pathways. The main myosin isoform is MYHC-IIa (*MYH2* gene) and the contraction in these fibers is fast with intense peak strength and are also resistant to fatigue.

- Type IIX: fast glycolytic fibers. These fibers are large in size and appear lighter colored. They have fewer mitochondria and myoglobin and have a lower enzymatic rate of oxidation, but possess more anaerobic enzymatic activity and store high amounts of glycogen. The main myosin isoform is MYHC-IId/x (*MYH1* gene) and the twitch in these fibers is fast and produces the largest amounts of force, but they become exhausted rapidly due to the accumulation of lactic acid.

The fiber-type composition varies between people and muscles, and even within different parts of the muscle. Innervation, exercise, hormones and disuse can affect the fiber type composition of a muscle, and it has also been observed to be specifically altered in different muscular dystrophies (MDs). For instance, in sarcopenia and Duchenne muscular dystrophy (DMD), a fast to slow transition occurs in the proportion of fiber types found in the muscles, while in limb-girdle muscular dystrophy type R1 (LGMDR1), it has been reported that slow fibers are more affected (Kramerova et al., 2012; Nguyen-Tran et al., 2014; Ohlendieck, 2011).

Metabolism

Skeletal muscle also plays an important metabolic function in the body as a regulator of blood glucose levels and energy homeostasis, and is the largest glycogen storage of the body. The energy required to supply cellular demands, including muscle contractility, comes from the hydrolysis of ATP to ADP and Pi. A unique feature of skeletal muscle fibers is the fact that they can undergo a sudden increase in energy consumption when changing from rest to contraction. Most of the basal consumption of ATP in muscle fibers at rest comes from protein synthesis and maintenance of the sodium/potassium (Na^+/K^+) pump, an ATPase that maintains the resting membrane potential. This basal energy consumption is similar in the different types of muscle fibers (Rolfe & Brown, 1997). When the fiber contracts, myosin ATPase consumes 70% of the contractile energy, while ER

SERCA-mediated ion transport consumes around 30% (He et al., 2000). In order to supply these rapid energy changes, the muscle cell needs efficient ATP recovery mechanisms. The three most important mechanisms of ATP synthesis in muscle fibers are: creatine kinase activity, glycolysis and mitochondrial oxidative phosphorylation.

Phosphocreatine (PCr), a substrate for the enzyme creatine kinase (CK), is an available source of phosphoryl groups for rapid ATP synthesis through ADP phosphorylation. The speed of obtaining ATP for muscle contraction through the CK-adenylate kinase system is much higher than that of conventional catabolic pathways. In periods of relaxation, part of the ATP that comes from these routes is destined to the regeneration of PCr reserves. Both PCr content and CK activity are higher in type II glycolytic fast fibers (Karatzaferi et al., 2001). These fast fibers consume 30% of ATP and a large amount of PCr in only 10 seconds of maximum exercise, and an energy failure in them implies a considerable reduction in muscular power, leading to fatigue (Sargeant, 2007).

Glycolysis is the universal and central metabolic pathway of glucose metabolism. Throughout the consecutive reactions of this pathway, energy is released in the form of ATP and the reduction of NADH coenzyme, and two pyruvate molecules are obtained. Furthermore, glycolysis can be aerobic or anaerobic, depending on the fate of the pyruvate. If pyruvate is transformed into lactate through lactic fermentation, glycolysis is anaerobic since oxygen (O_2) does not participate as the last electron acceptor. On the other hand, if the fate of pyruvate is oxidation to carbon dioxide (CO_2) and water (H_2O) in the TCA cycle in the mitochondria, and the resulting reduced coenzymes are oxidized trough oxidative phosphorylation, it is considered aerobic glycolysis. Aerobic glycolysis is a slower but more efficient way of obtaining energy than anaerobic glycolysis. Accordingly, in fast anaerobic fibers the expression of glycolytic genes is higher than in slow fibers (Chemello et al., 2011; Plomgaard et al., 2006)

In muscle cells, glycolysis coexists with fatty acid oxidation as a source of energy. In certain physiological conditions such as fasting or an increased energy expenditure during sustained exercise, muscle cells are able to increase fatty acid oxidation in order to spare the utilization of plasma glucose during fasting, and to delay consumption of muscle glycogen during exercise. However, when cells are low in oxygen, they switch to lactic acid fermentation to regenerate the much needed NAD+ molecules that keep glycolysis active and producing ATP (Hargreaves & Spriet, 2020; Henriksson, 1995).

Contraction physiology

Excitation-contraction (EC) coupling is a coordinated process needed for force generation. Briefly, the action potential from the motor neuron arrives to the neuromuscular junction (NMJ) through its terminals, where it releases acetylcholine (Ach). Here, Ach receptors in the sarcolemma trigger depolarization of the sarcolemma, which triggers further depolarization of the membrane by activating voltage-sensitive sodium channels, allowing Na^+ entrance and propagating the depolarization. The depolarization then reaches the triads, which are structures where T-tubules are in close proximity with the membrane of the SR on both sides, and where voltage sensitive dihydropyridine receptor channels (DHPR) couple with the ryanodine receptors (RyR) located in the SR and induce a large Ca^{2+} release from the SR to the sarcoplasm (Figure 4) (Khonsary, 2017).

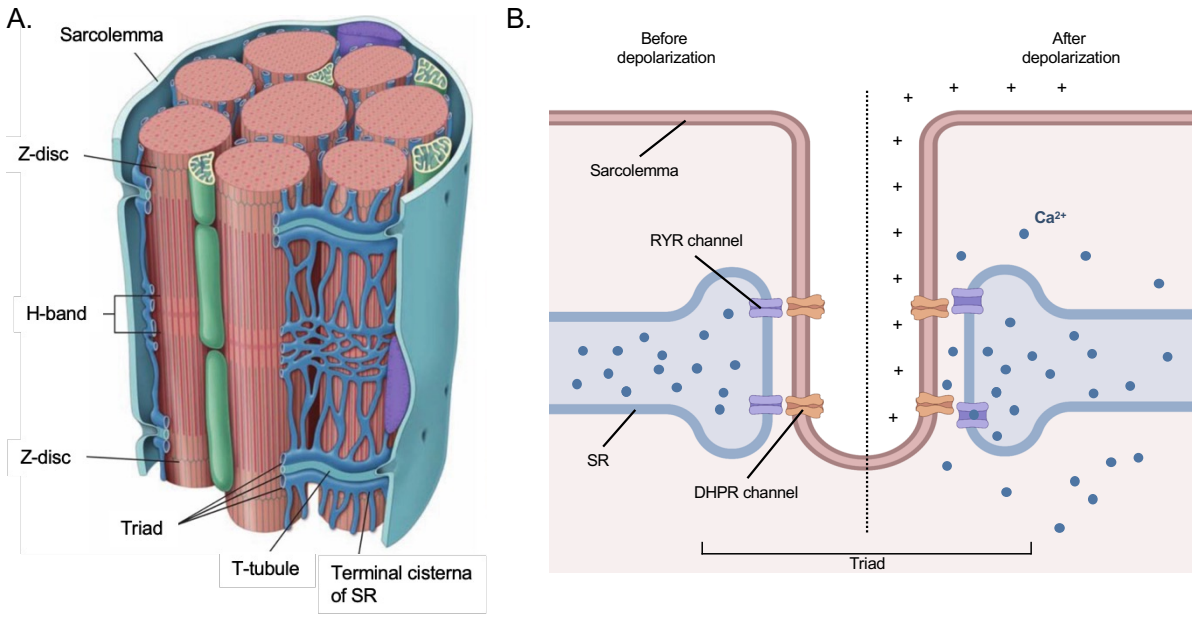

Figure 4. Structure of the sarcoplasmic reticulum and the triad. A) Structure of sarcolemma's T-tubules (in light blue) and SR (in blue), surrounding myofibrils. The figure shows the location of triads with regard to the sarcomeres. Source: adapted from Ross & Pawlina, 2016. B) Structure of the triad, representing calcium release from the SR following membrane depolarization.

The Ca^{2+} released into the sarcoplasm binds to troponin C on the actin thin filament, which changes its conformation producing tropomyosin movement and letting myosin bind to actin, forming a cross-bridge. Myosin uses energy released by ATP to change conformation and move along actin molecules forming new cross-bridges. When actin and myosin filaments are brought together and packed, the length of the I band and the entire

sarcomere shortens, which results in muscle contraction. This contraction is maintained until another ATP molecule binds to myosin, detaching it from actin back to the initial position, until another cross-bridge cycle occurs. Cross-bridge cycling is able to continue as long as there are sufficient amounts of Ca^{2+} and ATP. Ca^{2+} is actively pumped back into the sarcoplasmic reticulum by the ATP consuming SERCA pumps, reducing intracellular Ca^{2+} concentration, which moves tropomyosin back to the previous conformation blocking the actin binding sites and ending the muscle contraction (Stutzmann & Mattson, 2011; Sweeney & Hammers, 2018).

Muscle contractions require an intensive energy supply for myosin heads and SERCA pumps during the contraction process, which in some muscles can be constant, and therefore ATP producing mitochondria and glycogen molecules are distributed all around myofibrils. However, the type and frequency of contractions for different muscles can be very different and also their energy needs. Generally, high intensity fast and short contractions use anaerobic energy sources, whereas energy for prolonged low intensity contractions is obtained from aerobic pathways. Depending on these factors, there are different types of specialized muscle fibers, as described above (Sweeney & Hammers, 2018; Westerblad et al., 2010).

Myogenesis and regeneration

Skeletal muscle development also known as myogenesis, can be divided into embryonic and adult myogenesis (Tajbakhsh, 2009).

Embryonic myogenesis is a highly regulated process that develops from the paraxial mesoderm of the embryo, where the dermomyotome of the embryo contains multipotent progenitor cells that eventually give rise to skeletal muscle cells as well as muscle stem cells also known as satellite cells (SCs). At the molecular level, transcription factors paired box 3 and 7 (PAX3 and PAX7) are important regulators of myogenesis, acting upon myogenic regulatory factors (MRFs) that control the determination of muscle stem cells and the myogenic differentiation process. The better characterized MRFs are myogenic factor 5 (MYF5), myogenic factor 6 (MYF6 or MRF4), myoblast determination protein 1 (MYOD1) and myogenin (MYOG). PAX3 is expressed in the paraxial mesoderm and PAX7 is induced during the maturation of somites in the embryo. From this point, embryonic muscle development continues through different phases where cells expressing MRFs

migrate to form the myotome, the first muscle mass in the embryo and from where the rest of the muscles of the torso develop, and similarly others will start to migrate towards the limbs and form the muscles there. Some of these precursors will directly develop into muscle trough the expression of MRFs, while other cells will continue proliferating through the development to end up forming the reserve pool of myogenic precursors, the SCs. Overall, PAX3 plays a more relevant role in the development of trunk and limb muscles, while PAX7 is critical for post-natal muscle growth and the maintenance of SCs. MRFs are expressed at different points of the myogenic program (Figure 5), MYF5 and MYOD1 are critical factors for the determination of the myogenic linage of the multipotent cells, MYF5 plays a more critical role in the initial determination of the cell fate and its expression is necessary for SCs to proliferate, while MYOD1 directly induces the differentiation towards a muscle fiber cell. MYOGENIN is critical for the terminal differentiation of the proliferative myogenic precursors or myoblasts, and induces their fusion and differentiation, and MRF4 has a role in both the determination of the cells and in differentiation. (Buckingham et al., 2014; Relaix et al., 2006; Tajbakhsh et al., 1997).

Regarding cellular signaling pathways, the major players are WNT, NOTCH, sonic hedgehog (SHH) and bone morphogenetic protein (BMP) pathways, which all participate in myogenesis. In particular, WNT and SHH pathways are involved in early specification of muscle progenitors, essential for the maturation of cells in the dermomyotome into MYOD1 expressing cells. (Feng et al., 2006; Rudnicki et al., 1993; Tapscott, 2005; von Maltzahn et al., 2012; Zammit, 2017).

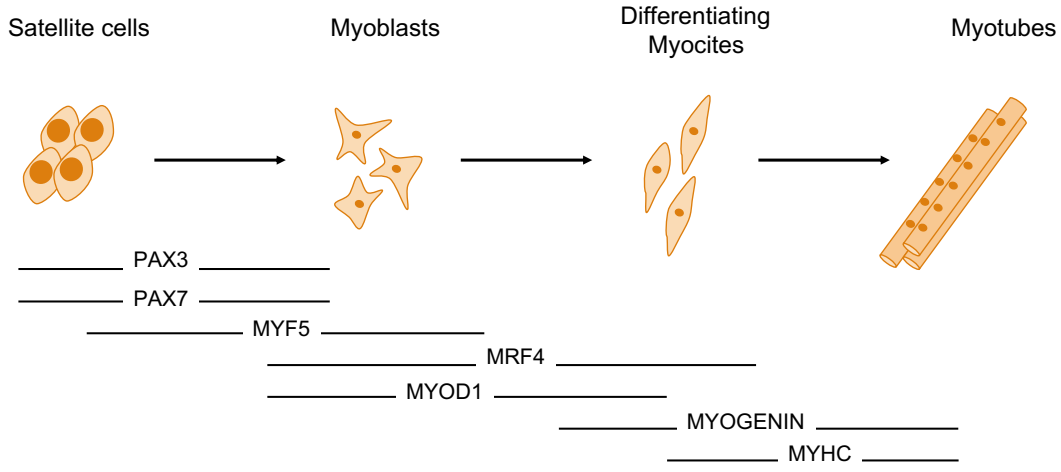

Figure 5. Myogenic program and MRFs that regulate myogenesis. The expression of different MRFs occur in a sequential but overlapping manner.

Adult myogenesis occurs whenever skeletal muscle regeneration is required, and to a large extent it relies upon the activation, proliferation, migration and differentiation of SCs. SCs are quiescent muscle stem cells that are located in a specific niche between the sarcolemma of muscle fibers and the basal lamina around it, hence their name; where they can be activated by different signals they receive from the muscle fiber, surrounding cells or bloodstream and adapt their response to the needs of the tissue in any specific moment (Mauro, 1961; Thomas et al., 2015).

SCs can be identified by the expression of several markers. PAX7 and to a lesser extent PAX3 are expressed in the nuclei, and cell surface markers such as α7/ß1-integrins, vascular cell adhesion molecule-1 (VCAM1), M-cadherin, or neural cell adhesion molecule-1 (NCAM1) among others are used to identify these cells (Fukada et al., 2007; Montarras et al., 2005). Genetical ablation of PAX7 has demonstrated the need of these cells in adult myogenesis, where their absence results in a failure to regenerate muscle tissue upon damage in adult mice (Sambasivan et al., 2011). However, SCs are also a heterogenic population that differ in the expression levels of PAX3, PAX7 and other genes, affecting their level of stemness, for instance, CD34 can differentiate sub-populations in mice SCs, some of them having a more genuine quiescent stem cell state while others are committed to myogenic differentiation (der Vartanian et al., 2019; García-Prat et al., 2020).

The repair of muscle tissue is a coordinated process that starts with a degenerative phase, where the necrosis and clearance of damaged muscle fibers occurs, followed by a regenerative phase that ends up with the formation of new fibers. The balance between these processes is critical to obtain a proper result since unbalances can result in the formation of scar tissue or fibro-adipose replacement of muscle tissue, as it occurs in several pathological processes (Baghdadi & Tajbakhsh, 2018; Tidball, 2011).

In the first degenerative phase myofibers lose the integrity of their sarcolemma, releasing cytosolic material to extracellular medium and producing an influx of extracellular Ca^{2+} which eventually leads to the degradation of cellular organelles, proteins and myofibrils (Alderton & Steinhardt, 2000). The released molecules act as chemotactic factors for immune cells, which have a critical role inducing inflammation and coordinating the regenerative process (W. Yang & Hu, 2018). Initially neutrophils and mast cells release pro-inflammatory cytokines, such as tumor necrosis factor-α (TNF-α), interleukin (IL)-1 and histamine, and together with complement system activation, recruit more immune

cells to the injury site (Dufaux et al., 1989; Frenette et al., 2000). Macrophages play a dual role at this stage, initially a population known as M1 helps clear up cellular debris and releases pro-inflammatory cytokines, while at a later stage a population known as M2 releases anti-inflammatory cytokines and activates SCs to initiate the regenerative phase (Chazaud et al., 2009; F. O. Martinez & Gordon, 2014; Sonnet et al., 2006).

In the regenerative phase, SCs are responsible for the formation of new muscle fibers. Activated by the dagame induced signaling in the tissue, they start to recapitulate the myogenic program similarly to how it occurs in the embryonic development. Once activated, PAX7 and MYF5 expressing SCs migrate to the damaged site and start proliferating. Most of these SCs will differentiate to myoblast cells while they start expressing MYOD1, and a small subset of SCs will renew their initial stem cell population in their niche. Based on these two options, SCs divisions can be either symmetric, dividing into two cells with the same fate; or asymmetric, where each cell takes a different path (le Grand et al., 2009). The proliferative stage is influenced by signaling pathways that promote cell cycle progression and repress differentiation. After proliferation, cells exit the cell cycle, decreasing PAX7 and MYF5 expression and start to differentiate. Myoblasts expressing MYOGENIN and MRF4 fuse to each other or to pre-existing myotubes, where they start to express proteins from the contractile and mature myotube structure (Buckingham & Rigby, 2014; le Grand & Rudnicki, 2007; Zammit, 2017). Besides SCs, other cell populations present in the muscles in the interstitial tissue such as mesoangioblasts and pericytes associated to blood vessels, fibro/adipogenic progenitors (FAPs), myoendothelial cells and fibroblasts participate and modulate the response to damage and the regenerative process in the muscle and have been shown to be necessary for an effective regeneration (Molina et al., 2021; Tedesco et al., 2017).

Finally, after a short period of denervation of the damaged muscle tissue, motor neurons can establish new contacts with the newly formed fibers in the proximity, which undergo a process of growth and maturation, first expressing embryonic or neonatal forms of MYHC and later expressing the slow and/or fast adult forms of this protein. The process culminates with the migration of the myonuclei towards the periphery (Sartore et al., 1982; Whalen et al., 1990). However, if denervation persists, the fibers loose the necessary trophic factors from the motor neurons and start to atrophy and degenerate (X. Yang et al., 2020).

Muscle homeostasis

The skeletal muscle is one of the most plastic tissues of the body where external stimuli such as exercise, variations in hormone levels, nutrients, and oxygen supply, as well as activity of motor neurons induces changes in its morpho-functional properties. Among different key signaling molecules, Ca^{2+} controls numerous cellular processes such as cell growth, proliferation, differentiation, and gene transcription in the skeletal muscle (Berridge et al., 2000; Scicchitano et al., 2018).

The morpho-functional properties of the muscle are modulated by the balance between net protein degradation and synthesis within each fiber, and by cell turnover and regeneration at the tissue level. When protein synthesis prevails, this leads to muscle growth and hypertrophy, whereas a reduction in protein synthesis and increase in protein degradation, results in muscle atrophy, and in pathological conditions can lead to muscle wasting (Kitajima & Suzuki, 2017). One of the key signaling pathways that regulates protein turnover is activated through insulin-like growth factor-1 (IGF-1) and an intracellular cascade of effectors including protein kinase B (AKT), that have the ability to modulate protein synthesis and degradation by activating the mammalian target of rapamycin (mTOR) kinase and repressing glycogen synthase kinase-3 beta (GSK3β) and forkhead box O1 (FOXO1) transcription factor (Figure 6) (Schiaffino et al., 2013; Schiaffino & Mammucari, 2011).

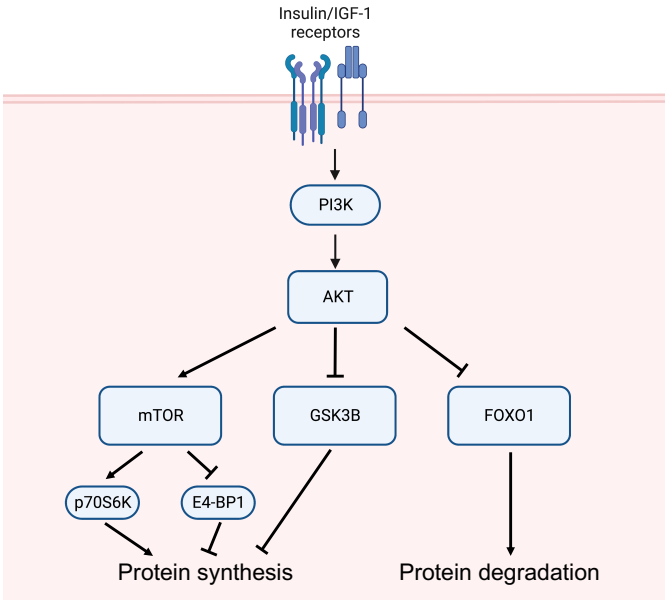

Figure 6. Schematic representation of the IGF-1/AKT pathway. IGF-1 increases the activity of AKT protein. This activation stimulates protein synthesis through mTOR and by inhibiting protein degradation by suppressing the activity of GSK3β and FOXO1.

Protein homeostasis in the muscle

Because of the dynamic nature of muscle, damage by wear and tear is inevitable as the tissue undergoes constant dynamic remodeling to remain healthy. Proteins can become misfolded for different reasons, from mechanical stress to changes in environmental conditions such as temperature, oxidative stress, pH, etc. Once they are misfolded, aggregation may occur through hydrophobic interactions, and to prevent this from happening, multiple systems are implicated in protein quality control in the muscle, including the chaperone system and the ubiquitin proteasome system (UPS) (Saibil, 2013; Smith et al., 2014).

Chaperones

Most proteins in the cell require assistance to achieve their tertiary structure, and to aid in this process, molecular chaperones bind to the hydrophobic amino acids (AA) of client proteins preventing aggregates and allowing the proteins to fold correctly, effectively helping to maintain protein homeostasis (proteostasis). In striated muscle, chaperones are necessary for both the assembly of the sarcomere and for the contractile function of its proteins (Carlisle et al., 2017; Saibil, 2013).

Many muscle diseases are associated with protein aggregation, such as inclusion body myopathy and protein aggregate myopathies, and also, mutations in several chaperones are associated with myopathies (e.g. LGMDD1 caused by mutations in *DNAJB6*, or distal atrophy caused by mutations in *DNAJB5*) that can lead to protein aggregates that overwhelm cellular processes and machinery and can lead to myo-apoptosis (Stein et al., 2014; Weihl et al., 2018).

Studies have shown that under stress or disease conditions, small chaperones such as HSP27 and alpha-crystallin B translocate to the sarcomeric Z-disc/I-band regions of skeletal myofibers (Paulsen et al., 2009). In fact, it has been observed that small chaperones binding to the titin spring can lead to an increase in passive tension of the myofiber, which has been observed in myofibers from patients with myofibrillar myopathy (MFM) and LGMDR1 (Unger et al., 2017), therefore although they might be preventing aggregation, they can also alter the sarcomeric function by increasing stiffness of the fiber.

Protein degradation

While protein synthesis is activated in the muscle, correct protein homeostasis also requires an efficient degradation of proteins. Among proteolytic systems, the ubiquitin-proteasome, calpain-, caspase-, and autophagy-mediated protein degradation are the main pathways active in the muscle, that in several pathologies can lead to myofiber degeneration, wasting and impaired regeneration (Vinciguerra et al., 2010).

The UPS involves an enzymatic cascade that starts with the targeting of substrate proteins with ubiquitin and terminates with the degradation of the targeted protein into small peptides and AA by the 26S proteasome complex. It has been shown that in several pathologic conditions that lead to muscle wasting or to muscle atrophy (e.g. glucocorticoid treatment, fasting, cancer or acidosis), an over-expression of the ubiquitin-proteasome pathway is a characteristic factor (Lecker et al., 2004; Mitch & Price, 2003; Scicchitano et al., 2018).

In the muscle, two of the critical elements of the UPS are the muscle E3 ubiquitin ligases, Muscle RING Finger 1 (MuRF-1) and atrogin-1 (MAFbx), which in some pathologic conditions are markedly up-regulated, and regulating these proteins are the key transcription factors of the FoxO family (Gomes et al., 2001; Mitch & Price, 2003). Within the muscle, it has been observed that atrogin-1 can target MYOD1 and the eukaryotic initiation factor of protein synthesis eIF-e (Lagirand-Cantaloube et al., 2008; Tintignac et al., 2005), whereas MuRF-1 targets myofibrillar proteins and can be transcriptionally activated by NF-κB in conditions favouring atrophy (Clarke et al., 2007; S. Cohen et al., 2009).

On the other hand, calpains consists of calcium-activated cysteine proteases that act based on the Ca^{2+} concentration. Two ubiquitous isoforms, calpain 1 (μ-calpain) and calpain 2 (m-calpain), are well characterized and referred as the conventional/ubiquitous calpains, while calpain 3 is mostly expressed in the muscle and maintains activity at physiological Ca^{2+} levels (Goll et al., 2003). In the muscle, calpains are generally localized at the Z disk in the sarcomere, where modulated by calcium levels and their endogenous inhibitor calpastatin, they can initiate cleavage of proteins that anchor in the sarcomere, which include titin, desmin, nebulin, filamin and others (Goll et al., 2008; Huang et al., 1998; Kumamoto et al., 1992), and participate in many cellular processes such as

cytoskeletal remodelling (Franco et al., 2005), myofibril maintenance (Goll et al., 2008), cell mobility, cell cycle progression and signal transduction (Evans et al., 2007; Jánossy et al., 2004). In fact, issues in calcium homeostasis can lead to sarcomeric alterations, mitochondrial swelling or disruption of the contractile tissue and muscle atrophy via calpain signalling and proteolysis (Artrong et al., 1991; Belcastro et al., 1998; Fareed et al., 2006; Nelson et al., 2012).

Autophagy, characterized by the autophagosome-lysosome system, is another essential mechanism by which besides other cellular components, protein turnover occurs. Basal levels of autophagy are essential to maintain homeostasis in all tissues, and in muscles, deregulation of autophagy genes have been identified as one of the major causes of several skeletal muscle disorders (Grumati et al., 2011; Xia et al., 2021). Its regulation is tightly controlled by various signalling pathways that control growth and metabolism, where signalling pathways such as the AMP-activated protein kinase (AMPK) pathway, that regulate ATP-producing catabolic pathways can activate it, and can be active in conditions such as starving while suppressing ATP-consuming biosynthetic processes, while other upstream nutrient and energy integrators such as mTOR can suppress it to promote hypertrophy (Sandri, 2010; Xia et al., 2021).

Finally, caspases represent another proteolytic system that is usually activated by extrinsic death stimuli, where specific ligands trigger a cascade that cleaves a broad spectrum of cellular targets and ultimately lead to cell death. However, it has been observed that activation of caspase -9, -3 and -2 are also necessary in myoblasts prior to fusion and differentiation and therefore their correct regulation is necessary for normal muscle differentiation (Fernando et al., 2002; H. Dehkordi et al., 2020).

ER stress and UPR in the muscle

The ER in the muscle (also known as the SR), besides being one of the main Ca^{2+} storages in the myotubes, has an essential function managing the synthesis, folding and structural maturation of cellular proteins, effectively helping to maintain proteostasis. To fulfil these functions, different enzymes and chaperons are needed in the ER, which requires high levels of ATP and Ca^{2+} to function properly (Michalak et al., 2002; I. C. Smith et al., 2013). In different physiological or pathological conditions where there might be stressors such as changes in Ca^{2+} concentration, inflammatory challenges or oxidative stress, unfolded proteins can accumulate in the ER, which activates the unfolded protein response (UPR). UPR involves the transcriptional induction of ER chaperones to improve the protein folding capacity and to avoid aggregation, attenuating the translation of proteins, and the removal of proteins through the degradation by the UPS (Afroze et al., 2019; Hetz et al., 2015). This response is mediated by the ER transmebrane sensors: inositol-requiring protein 1a (IRE1a), protein kinase R (PKR)-like endoplasmic reticulum kinase (PERK), and activating transcription factor 6 (ATF6) (Bohnert et al., 2018; Hetz, 2012).

One of the best-characterized ER chaperones, the 78-kDa glucose-regulated protein (GRP78), also referred as BIP, binds to those three proteins in basal conditions, blocking their activity and UPR signal transduction. However, upon ER stress, BIP binds to unfolded proteins, allowing those stress sensors to get activated (Figure 7). This results in the expression of CHOP, a transcriptional factor promoting apoptosis through down-regulation of pro-survival proteins, and on the other hand, splicing of a 26-base intron from X-Box Binding Protein (XBP1) is promoted, which allows it to translocate into the nucleus to induce the expression of ER-resident chaperones and ER-associated degradation (ERAD) components (Hetz, 2012; Yoshida et al., 2003), enabling misfolded proteins to be degraded by UPS or by the autophagy-lysosomal system (Deegan et al., 2013).

Of note, there is a vivid reciprocal interaction between ER-stress and oxidative stress, and both share key response mechanisms common to the integrated stress response (IRS), which optimizes the cellular response to stress depending on the nature and intensity of the stressors to restore cellular homeostasis (Mensch & Zierz, 2020; Pakos-Zebrucka et al., 2016). Similar to the IRS, UPR is necessary to promote cell survival; however, chronic unmitigated ER stress can lead to cell death (Afroze et al., 2019).

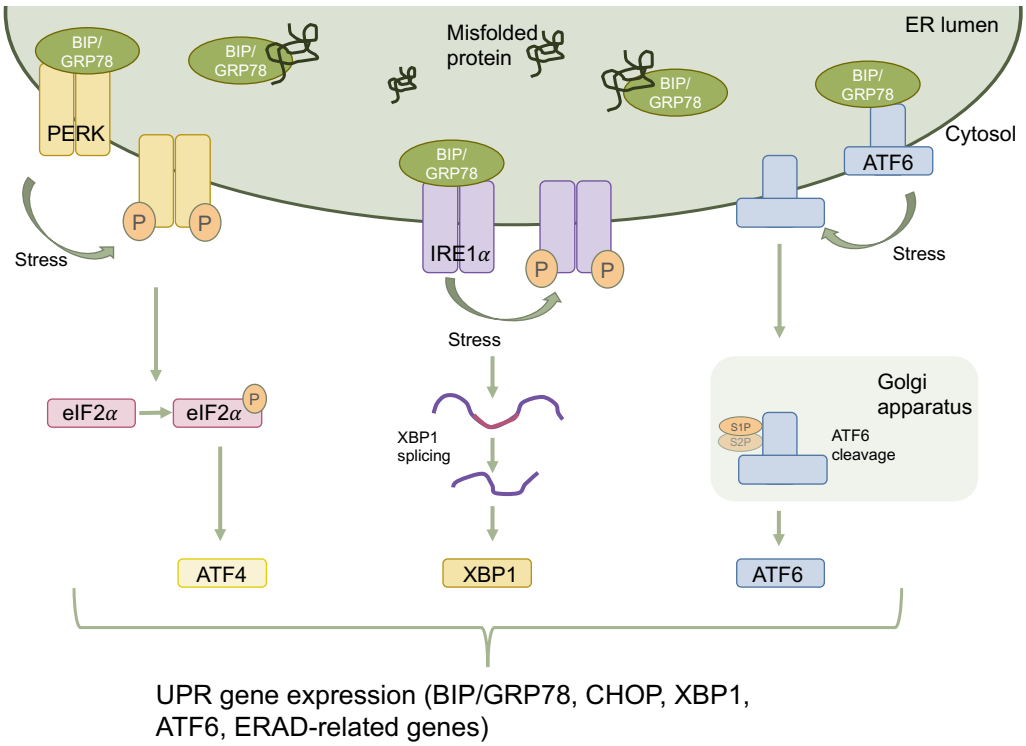

Figure 7. Schematic representation of UPR signaling pathways. When unfolded proteins accumulate in the ER lumen BIP/GRP78 dissociates from the three ER stress sensors IRE1α, ATF6 and PERK to bind the unfolded proteins. This activates the sensors that through different pathways, induce the expression of genes involved in protein folding, ER-associated degradation (ERAD), autophagy and amino acid metabolism. Source: adapted from Afroze et al., 2019.

Adaptation to exercise

Skeletal muscle has a remarkable capacity of functional adaptation and remodeling in response to contractile activity. Repeated bouts of muscle contraction associated with frequent exercise training, are potent inducers of physiological adaptation. These adaptations are reflected by changes in contractile proteins, metabolic regulation, mitochondrial function, transcriptional responses and intracellular signaling (Benziane et al., 2008; Coffey & Hawley, 2007; Egan & Zierath, 2013). Transient changes in gene transcription after exercise include myogenic regulators, genes of carbohydrate metabolism, mitochondrial metabolism and oxidative phosphorylation, lipid mobilization, transport and oxidation, and transcriptional regulators of gene expression and mitochondrial biogenesis (Louis et al., 2007; Mahoney et al., 2005).

In healthy conditions, these adaptations are intrinsic to the skeletal muscle, and collectively contribute toward maximizing substrate delivery, mitochondrial respiratory capacity, and contractile function. The adaptative effect is to promote optimal performance in a future exercise challenge, in order to have a robust defense of homeostasis in the face of a metabolic perturbation, and consequently, enhanced resistance to fatigue (Booth & Thomason, 1991; Egan & Zierath, 2013).

In fact, exercise represents a potential disruption to homeostasis by muscle activity that can be very different depending on the type of contraction (concentric, isometric, or eccentric) the modality of exercise (e.g., aerobic or resistance), the frequency, intensity, and its duration (Egan & Zierath, 2013). And all of these factors can impact the metabolic and molecular responses differently. Resistance exercise generally imposes a low-frequency, high-resistance demand on muscle contraction, whereas aerobic exercise generally imposes a high-frequency, low power output demand. Consequently, the metabolic and molecular responses to the different modalities are different. There are various muscle contraction signal transduction pathways implicated in the adaptive response, which include the changes in mechanical strain, calcium level oscillations, ATP turnover rate, reactive oxygen species (ROS) production, redox balance, and intracellular oxygen pressure (Chin, 2010; Maxwell et al., 1999; Powers et al., 2010).

An important signal transducer for metabolic adaptations during exercise is AMPK, which modulates cellular metabolism acutely through phosphorylation of metabolic enzymes and via transcriptional regulation (Jäer et al., 2007). AMPK activation is regulated allosterically by a cellular energy deficit, which is reflected by increases in the AMP/ATP and Cr/PCr ratios (Kahn et al., 2005). In skeletal muscle, glucose transport and lipid metabolism are promoted by the acute AMPK activation, which at the same time suppresses glycogen synthesis and protein synthesis (Bolster et al., 2002).

Other important mediators in muscle adaptation to exercise are the calmodulin-dependent protein kinases (CAMKs) and mitogen-activated protein kinases (MAPKs). Calcium oscillations during contraction, whose amplitude and duration are a function of the level of force output by the muscle, modulate the kinase activity of CAMKs, being CAMKII the dominant isoform in the skeletal muscle (Chin, 2010). CAMKs and calcium signaling influence glucose transport, lipid uptake and oxidation, and skeletal muscle plasticity and transition from fast to slow fiber types (Raney & Turcotte, 2008).

All forms of muscular contraction result in the application of force and increased tension. However, the adaptive muscle growth or hypertrophy consequent to high mechanical loads present during resistance exercise is largely determined by the activation of skeletal muscle protein synthesis consequent to the activation of mTOR, ribosomal protein S6K, and downstream targets (Bodine et al., 2001). On the other hand, molecular adaptation and regulation of the endurance phenotype associated with the aerobic exercise is characterized by an increase in mitochondrial biogenesis, and is defined by an increase in the number and volume of muscle mitochondria. After repeated exercise training, muscle mitochondrial density increases in all three fiber types, with the difference being somewhat greater in type IIa than in type I and type IIx fibers (Egan & Zierath, 2013). Specifically, these metabolic adaptations to endurance are reflected in the increased abundance of proteins involved in mitochondrial ATP production, mobilization, transport and oxidation of fatty acids, the TCA cycle, antioxidant capacity, glycolytic metabolism, glucose transport and glycogen synthesis, and oxygen delivery to and extraction from skeletal muscle (Bodine et al., 2001; Egan et al., 2011; Gavin et al., 2007).

Muscular dystrophies

MDs are a heterogeneous group of inherited disorders that mainly affect the skeletal and sometimes cardiac muscle, and are characterized by a progressive weakness and muscle tissue degeneration. Most of them are caused by mutations affecting myofiber proteins with either structural or enzymatic functions, that lead to the degeneration of the muscle tissue (Emery, 2002; Mercuri et al., 2019).

Classification

Classification of MDs can be done following different criteria since each type can show a specific pattern of predominantly affected muscles, progression rate, age of onset, and inheritance. Genetically, a given gene may be involved in several different clinical entities, and conversely a given clinical entity may be produced by defects in several possible genes. Nevertheless, the genetic origin of most MDs has already been elucidated. However, further investigation is still required to understand the pathogenic mechanism of many of these diseases, and new rare disease-causing mutations and associated genes are still being discovered relatively frequently (E. Cohen et al., 2021).

The main types of proteins involved in MDs are extracellular matrix and basement membrane proteins, nuclear membrane proteins, sarcomeric proteins, sarcolemma-associated proteins, enzymes, and endoplasmic reticulum proteins. Conditions with early onset that typically manifest before ambulation in children are frequently grouped under the congenital MDs, where mutations mostly affect to proteins located in the extracellular matrix or external membrane proteins (Mercuri et al., 2019; Zambon et al., 2021).

Myotonic dystrophy (DM) also known as Steinert's Disease, is the most common form of muscular dystrophy in adults. In its most frequent form (DM1), the disease is caused by a pathological (CTG) triplet expansion in the 3' untranslated region (UTR) of the dystrophia myotonica protein kinase (*DMPK*) gene. These patients suffer a progressive atrophy and myotonia, muscular weakness, and other clinical manifestations such as cardiomyopathy, insulin resistance, cataracts, and cognitive decline resembling an accelerated aging phenotype (Mateos-Aierdi et al., 2015)

Facioscapulohumeral muscular dystrophy (FSHD) is the second most common genetic myopathy, characterized by slowly progressing and highly heterogeneous muscle wasting with a typical onset in the late teens/early adulthood. Although the etiology of the disease for both FSHD type 1 and type 2 have been elucidated, attributed to gain-of-toxic function stemming from aberrant DUX4 expression, the exact pathogenic mechanisms involved in muscle wasting are also yet to be elucidated (Jagannathan et al., 2022).

Duchenne muscular dystrophy (DMD) and its milder form Becker muscular dystrophy (BMD) are the most common dystrophies affecting children. Caused by mutations in the dystrophin gene (*DMD)* located in the X chromosome, patients develop symptoms in the early childhood and the disease progresses rapidly, including cardiac abnormalities and respiratory difficulties that significantly shorten life expectancy (Carter et al., 2012; Duan et al., 2021).

Limb-girdle muscular dystrophies (LGMDs) are a group of MDs that despite being genetically heterogeneous, share common clinical features. Their inheritance pattern is autosomal, and can be dominant, recessive, or polygenic. They are relatively selective to skeletal muscle, with predominant proximal muscle involvement in the hip and shoulder girdles. LGMDs generally show elevated serum CK levels, and the degenerative muscle

changes can be seen in muscle histology and on medical imaging (Barton et al., 2020). Altogether, their prevalence is estimated at 1.6 per 100.000 persons in the world, being the fourth most frequent type of MDs (Mah et al., 2015). Their classification and nomenclature were recently updated, now being LGMD D for the autosomal dominants, or LGMD R for the recessive ones, followed by a number corresponding to the gene affected (e.g. LGMD D1: Dominant *DNAJB6*-related) (Straub et al., 2018).

LGMDR1

Limb-girdle muscular dystrophy recessive 1 (LGMDR1) or calpainopathy, previously known as LGMD2A, is caused by mutations in the calpain 3 gene (*CAPN3)* that encodes the non-lysosomal protease calpain 3 (CAPN3) (OMIM: 253600) (Richard et al., 1995).

The incidence of LGMDR1 represents almost 30% of all LGMD cases in the world (Straub et al., 2018; Zatz et al., 2003), and the prevalence is notably higher in specific regions with ancestral mutations such as in the Reunion island, with up to 48 cases per million (Fardeau et al., 1996) or in the Basque cluster in Spain, with up to 69 cases per million (Urtasun et al., 1998).

Genetics

Calpain 3, also known as p94, was first described in 1989, when Sorimachi and colleagues detected the expression of a skeletal muscle-specific transcript that showed high homology with the ubiquitously expressed calpain 1 and calpain 2 (Sorimachi et al., 1989), but its mutations were not associated with LGMDR1 until 1995 (Richard et al., 1995). The calpain 3 gene is located in chromosome 15 with a length of 52.8 Kbp (15q15.1-q21.1). Its 24 exons are variable in length, ranging from 12 to 309 nucleotides, and the main muscular isoform translates into an 821 AA long protein (Ono et al., 2016).

Since the genetic cause of LGMDR1 was discovered, more than 500 pathogenic mutations have been reported in the calpain 3 gene (*LOVD Database*, 2022). This includes point mutations that lead to premature stop codons, mutations that affect splice sites, mutations that alter the reading frame, or even bigger insertions and deletion. These mutations induce various protein outcomes, such as loss of the protein or the impairment of its enzymatic activity. Other mutations do not alter the enzymatic activity, but they

affect its affinity to bind to other proteins such as titin, which suggests that calpain 3 is a multifunctional protein. Interestingly, 20-30% of LGMDR1 patients present normal muscle calpain 3 levels in Western blot analysis (Fanin et al., 2003; Ono et al., 1998, 2016).

The condition is considered to have an autosomal recessive inheritance pattern, however recently, rare heterozygous mutations have been reported to cause autosomal dominant calpainopathy (LGMDD4), with later onset and a milder phenotype. However, whether these cases are truly dominant or depend on other unidentified variants is still a topic of debate (González-Mera et al., 2021; Sáenz & López de Munain, 2017; Vissing et al., 2016, 2020).

LGMDR1 phenotypes are variable among different patients regarding their severity, age of onset and progression rate. Several studies aimed to establish a relationship between the mutations observed in *CAPN3* gene and their disease outcomes. However, stablishing a correlation between the mutations found in different patients and their disease severity remains elusive (Chae et al., 2001; Fardeau, Eymard, et al., 1996; Sáenz et al., 2011; Urtasun et al., 1998). Of note, patient with two null mutations do appear to develop a more severe phenotype of the disease with an earlier onset, compared to patients that harbor at least one missense mutation (Fanin, et al., 2007; Sáenz et al., 2011, 2005)

Calpain 3

Calpain 3 belongs to a family of calcium-dependent non-lysosomal cysteine proteases known as calpains (Calcium-activated neutral proteinase 3, EC3.4.22.17) (Goll et al., 2003; Guroff, 1964). There are more than a dozen of calpains described, but calpain 1 and calpain 2 (m-calpain), being ubiquitously expressed, are the better studied ones (Sorimachi et al., 2011a, 2011b). Calpains participate in several cellular processes like cell motility, apoptosis, cell differentiation or cell cycle regulation, where their protease activity is regulated by intracellular Ca^{2+} levels and directed towards specific substrates by substrate recognition mechanisms (Croall & Ersfeld, 2007; Sorimachi et al., 2011b).

One of the most remarkable characteristics of calpain 3 is its high autodegradation rate, and the fact that it is able to regain proteolytic function after its autolytic dissociation. The native structure of calpain 3 has not been solved yet, nor the exact details of its

interactions with other proteins, but it is known to have more functions than the proteolytic ones (Ono et al., 2016).

Structure

Calpain 3 is considered a classical calpain, containing more than 50% homology with calpains 1 and 2 in the four main domains that characterize calpains (Campbell & Davies, 2012; Moldoveanu et al., 2002). These domains are:

I) The propeptide domain.
II) The catalytic domain (CysPc), which is divided into two subdomains: PC1 (or IIa) and PC2 (or IIb).
III) The calcium-binding and phospholipid-binding domain CBSW (Calpain-type Beta-Sandwich domain).
IV) The C-terminal calcium-binding domain, with five EF sequences (penta-EF, PEF).

Besides these domains, calpain 3 also has 3 unique domains:

NS) A 47 AA sequence in the N-terminal domain.
IS1) A 48 AA sequence in domain II.
IS2) A 77 AA sequence between domains III and IV, that contains a nuclear localization signal (NLS).

IS1 and IS2 sequences are calpain 3 specific, which suggests that these regions are performing calpain 3-specific roles and are believed to be responsible for the instability that the protein shows (Figure 8), in particular it has been shown that IS1 contains the autocatalytic activity of the protein (Kinbara et al., 1998; Ono et al., 2016; Sorimachi et al., 2011a).

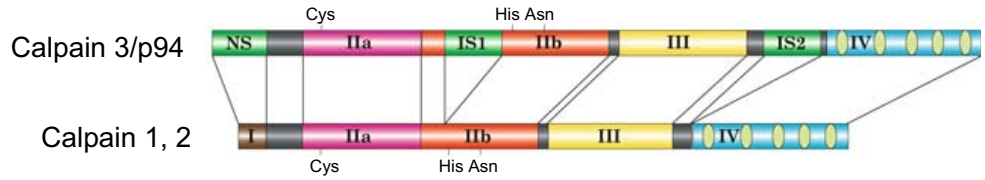

Figure 8. Schematic representation of the domains of calpain 3 and conventional calpains. Large subunits I, II+IIb, III, and IV represent the four calpain domains. NS, IS1, and IS2 are calpain 3 specific sequences. The active site of calpains is formed in the domain II by residues Cys, His, and Asn. Adapted from Ojima et al., 2005.

The first step of calpain activation is its intramolecular activation upon binding Ca^{2+} or Na^{+}. Initially, IS1 blocks the active site of calpain 3, preventing substrates to access the active site of calpain 3 until IS1 is autocatalyzed (Diaz et al., 2004). A second step of calpain activation occurs via extramolecular activation with Ca^{2+} or Na^{+}, which allows calpains to proteolyze different substrates without being dissociated in two fragments despite the nick in IS1. The subsequent proteolysis in IS2 inactivates CAPN3. In some cases, two CAPN3 fragments that have been cleaved only in IS1 dissociate, thereby inactivating CAPN3, and then can become active again by the CAPN3-specific mechanism called intermolecular complementation (iMOC), where two autolytic fragments of calpain 3 reconstitute the active core protease domain (Ono et al., 2014). On the other hand, IS2 enables the interaction between titin and calpain 3 in the sarcomere, which stabilizes calpain 3 preventing its autocatalysis and controlling its activity and its subcellular localization (Figure 9) (Lostal et al., 2019; Sorimachi et al., 1995).

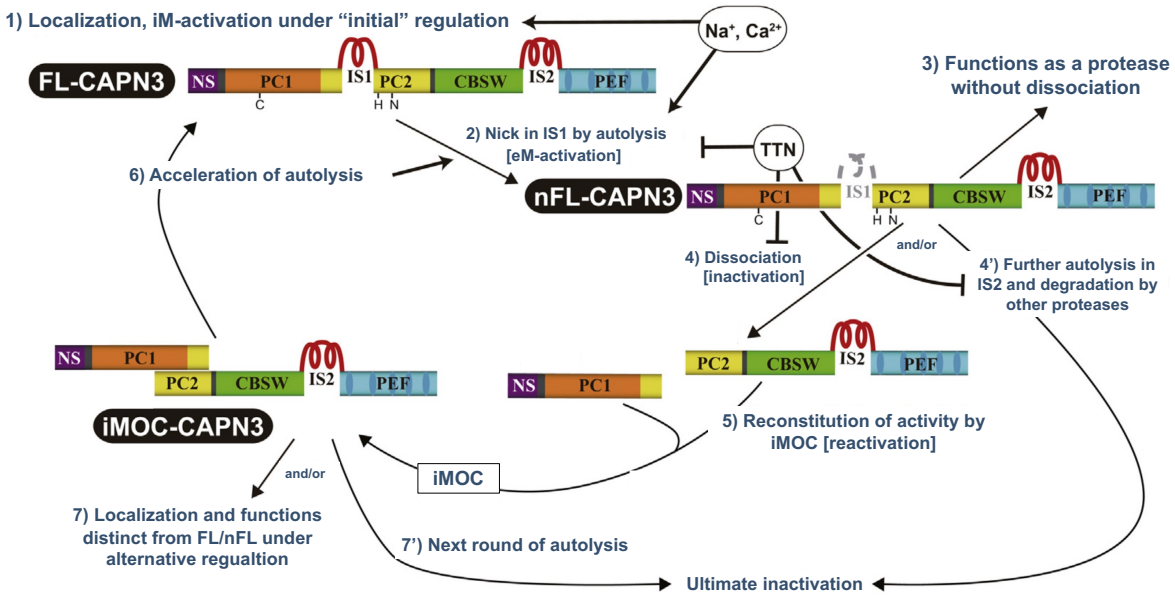

Figure 9. Schematic representation of the calpain 3 activity regulation. Translated full-length CAPN3 (FL-CAPN3) is iM-activated by physiological Na^{+} and Ca^{2+} (1), and autolyzes in IS1, producing nicked (but not dissociated) FL-CAPN3 (nFL-CAPN3) (2). Since nFL-CAPN3 is eM-activated and metastable, it functions as a protease (3). Then, nFL-CAPN3 is inactivated as its components dissociate from each other (4), and/or degradative reaction predominates through autolysis in IS2 and other sites with the aid of other proteases (4'). Dissociated fragments from IS1 can reconstitute the activity by iMOC (5), which accelerates autolysis of FL-CAPN3 (6). Reconstituted CAPN3 by iMOC (iMOC-CAPN3) localizes and functions distinctly from FL/nFL-CAPN3 under alternative regulation (7), and/or is ultimately inactivated by further autolysis (7'). Source: Modified from Ono et al., 2016.

At the quaternary structure level, it has recently been reported that instead of forming homodimers as previously thought (Partha et al., 2014; Ravulapalli et al., 2005), calpain 3 forms a homotrimer after being translated and remains as a homotrimer during and after autolysis (Hata et al., 2020).

Expression

The main isoform of calpain 3 (p94) has a skeletal muscle specific expression, however, there are several isoforms found in other tissues of the human body. The main isoform is much more abundant in the muscle, with over 10 times the levels of the ubiquitous calpains (Sorimachi et al., 1989). The other isoforms found in humans can be ubiquitous (isoforms Up84, Up49) or tissue specific (Tp36-Tp31 in testis and Mp18 in melanoma), but all of them lack at least one of the main calpain 3 isoform domains, and they use different promoters and initiation exons (Figure 10), in fact, the promoter and 5' sequences for these isoforms has been suggested to reside within another gene upstream *CAPN3,* the neutral α-glucosidase C gene (*GANC*), whose last 4 exons coincide with these isoforms and could be indicating a regulatory relationship between these two genes (Kawabata et al., 2003). In rodents, other isoforms have also been described however, most of these isoforms have been detected at the transcript level and there is little information about their function (Ono et al., 2016).

During embryonic muscle development, different splicing variants of calpain 3 are expressed, lacking either exon 6 coding for IS1 domain, or exons 15 and 16 which code for IS2 domain (Herasse et al., 1999). The full length calpain 3 appears relatively late compared to other muscle components, such as titin or sarcoglycans, and the same is true in mice (Fougerousse et al., 1998; Ojima et al., 2007). In adult mice the embryonic variants only appear in regenerating muscle, which suggests that IS1 and IS2 domains have specific roles in the matured muscle (Fougerousse et al., 1998; Herasse et al., 1999; Ojima et al., 2007). In humans the embryonic variants have been detected in fetal muscles at 10-12 weeks following specific patterns, which suggests different calpain 3 variants could play different roles in muscle development and in the mature tissue (Fougerousse et al., 1998; Kramerova et al., 2007).

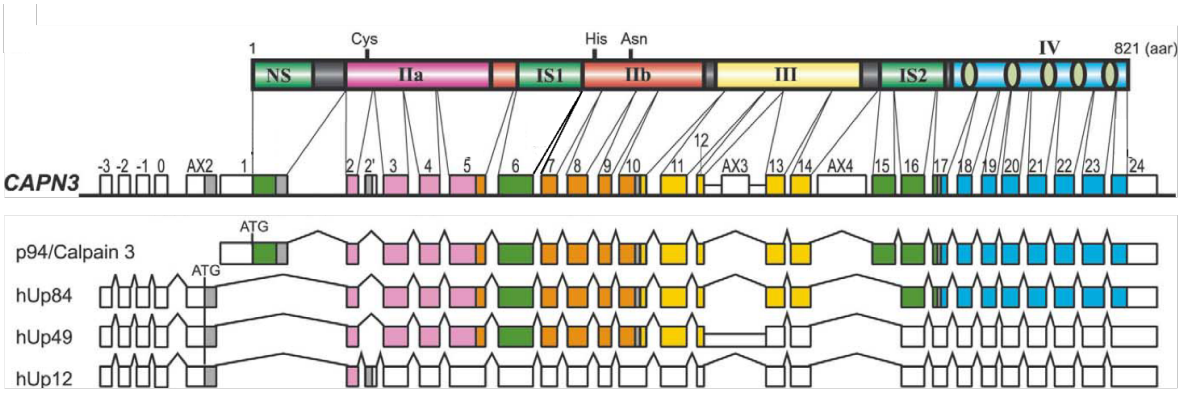

Figure 10. Calpain 3 exons and alternative isoforms. Domain structures are indicated by different colours and linked to the corresponding exons. White boxes indicated with "AX" are for alternative initiation exons, and boxes indicated with numbers -3 to 0 are the promoter region of the alternative isoforms that coincide with the last exons of the *GANC* gene. Source: Modified from (Kawabata et al., 2003).

Functions and role in the pathogenic mechanisms

Calpain 3 has both proteolytic and non-proteolytic functions. The proteolytic function of calpain 3 is activated with physiological intracellular concentrations of Ca^{2+} (100nM) and Na^{+} (15mM), both ions being complementary activators of its autolysis and therefore, its intracellular stabilization is dependent upon interactions with other proteins and in particular with titin (Lostal et al., 2019; Ono et al., 2006, 2010). Since calpain 3 potentially proteolyzes many different proteins *in vivo*, it could be regulating a wide range of functions such as apoptosis (Baghdiguian et al., 1999; Richard et al., 2000), myogenic differentiation and sarcomere remodeling (Kramerova et al., 2004; Yalvac et al., 2017), maintenance of calcium homeostasis (DiFranco et al., 2016; Toral-Ojeda et al., 2016), or the integrin signaling pathway (Jaka et al., 2017), which underlines its multifunctionality.

As mentioned before, calpain 3 has different domains each of which contributes to one or more specific role such as its autolytic or proteolytic activity, calcium sensitivity or dimerization ability. The fact that LGMDR1 patient mutations have been found across the entire gene (Ono et al., 2016), and that 32% of LGMDR1 patient-derived biopsies retain calpain 3 proteolytic activity (Milic et al., 2007) indicates that additional functions/interactions besides its proteolytic activity are essential to its function.

Sarcomere remodeling

Calpain 3 has been proposed to regulate muscle contraction and sarcomere stability by several studies (Kramerova et al., 2004, 2005; Ojima et al., 2007; Sorimachi et al., 1995), where it is believed to interact at the Z-line with different sarcomeric proteins such as α-actinin, tropomyosin, and most notably, with titin. Titin is a large scaffold protein essential in sarcomere assembly, responsible for the passive tension of the muscle that acts as a spring, unfolding under stretching force and refolding when tension is removed, and it integrates mechanosensory transduction pathways (Nishikawa, 2020). Interestingly, calpain 3 binds to titin at the Z-line region and in the N2A domain of titin, with different affinities depending on the stage of titin folding. This dynamism in its localization and affinity to titin affects its own proteolytic activity, being less active when it is bound to titin, which seems to be important for the release of MARP-2 protein from titin when transducing mechanosensory signals (Lostal et al., 2019; Ojima et al., 2007, 2010). In fact, titin can be found among other sarcomeric proteins as a substrate for the calpain 3 proteolytic activity, which may be regulating the turnover of these proteins, essential for the maintenance of the sarcomere structure (Isaacs et al., 1989; Zak et al., 1977). In this aspect, one of the calpain 3 KO mouse models (C3KO) showed abnormal A-bands at the sarcomere and apparently delayed myofibrillogenesis, as well as insoluble high molecular weight ubiquitin protein conjugates (Kramerova et al., 2004). Taken together, these studies indicate that a proper interaction between titin and calpain 3 is essential for sarcomere maintenance and remodeling (Beckmann & Spencer, 2008).

Besides strictly sarcomeric proteins, *in vitro* assays have shown that other structural cytoskeletal components can also be proteolyzed by calpain 3, such as filamin A, filamin C, talin, vinexin and erzin (Guyon et al., 2003; Ojima et al., 2007; Taveau et al., 2003), indicating calpain 3 mediated proteolysis might be necessary to modify the structure not only of the sarcomere but also of its surrounding cytoskeleton.

Calcium dysregulation

Calcium homeostasis is another key element that seems to be altered in LGMDR1 and also seems to be a common pathophysiological mechanism underlying other MDs (Lasa-Elgarresta et al., 2019; Vallejo-Illarramendi et al., 2014). Calpain 3 is known to interact with several calcium-handling proteins like the sarcoplasmic reticulum calcium release

channel ryanodine receptor 1 (RYR1), calsequestrin (CASQ), and the sarco/endoplasmic reticulum Ca^{2+}-ATPase (SERCA) proteins (Ojima et al., 2011), and knockout mice models have shown reduced levels of RYR1 expression as well as a reduction in calcium release from the sarcoplasmic reticulum (Dayanithi et al., 2009; Kramerova et al., 2008). The way it is believed that calpain 3 affects calcium release is through its participation in the triad as a structural stabilizer of RYR1 complexes, comprised of RYR1, Aldolase A (ALDOA) and CAMKII. In the absence of calpain 3, both RYR1 and CAMKII levels are decreased and ALDOA is mislocalized (DiFranco et al., 2016; Kramerova et al., 2012). This function again has to be taken into account partially, since some patients with specific mutations have not shown the reduced RYR1 levels, which could be preserved if the mutation does not affect this structural function of calpain 3 (El-Khoury et al., 2019).

SERCA protein, whose function is to transport calcium from the cytosol into the sarcoplasmic reticulum, has also been found decreased in calpain 3 knockout human myotubes, with a suggested increased ubiquitination leading to its degradation. Interestingly, this resulted in different outcomes in mouse myotubes and in human myotubes, where the human myotubes showed increased resting intracellular calcium levels, but mouse myotubes did not (Toral-Ojeda et al., 2016), which could be due to mouse myofibers having a higher calcium buffering capacity, with proteins such as parvalbumin, that are highly expressed in the mouse muscle (Ecob-Prince et al., 1989; Pertille et al., 2010).

Muscle adaptation

Related to the calcium dysregulation, calpain 3 also seems to affect muscle adaptation. Skeletal muscle is a very adaptable tissue that needs to respond to environmental and physiological challenges, and does so by altering its fiber type composition, size and metabolism. Absence of calpain 3 in the muscle has shown to affect CAMKII signalling pathway, which activates calcium-dependent transcriptional pathways to adapt to functional demand, that controls growth, myofiber type transition or mitochondrial biogenesis (Kramerova et al., 2012; Matsakas & Patel, 2009). In fact, in the C3KO mice, reduced CAMKII signalling after exercise results in a defective transition to slow type myofibers, which might explain why muscles enriched in these type of oxidative slow-twitch fibers like the diaphragm and soleus seem to be most affected in these models, and could be the reason why these type of fibers seem to be more affected also in patients

(Kramerova et al., 2004, 2012). As part of this transition to oxidative slow-twitch fibers, induction of genes involved in lipid metabolism and energy production are reduced in the C3KO mice (Kramerova et al., 2016), and this has also been found in some LGMDR1 cohorts (Siciliano et al., 2015).

Mitochondrial abnormalities

Alterations in mitochondria in the absence of calpain 3 have been observed in several studies and both LGMDR1 patients and C3KO mice present mitochondria with abnormal distribution, and in the case of the mice they seem to appear with swollen appearance and disrupted membranes, while human biopsies have shown several mitochondrial genes deregulated (N. Cohen et al., 2006; Kramerova et al., 2009; Sáenz et al., 2008). In this case too, some specific mutations have pointed towards mutation-specific patterns, in this case of mitochondrial dysfunction in LGMDR1 patients (N. Cohen et al., 2006; El-Khoury et al., 2019). Mitochondrial abnormalities could be tied to several pathological mechanisms in LGMDR1, since it can be induced by calcium dysregulation and produce energy deficits, oxidative stress, metabolic changes, and the release of pro-apoptotic factors into the cytosol. In the case of the C3KO mouse muscles, these showed increased oxidative stress and a reduced ATP production (Kramerova et al., 2009), and in patient muscles, cytochrome C mislocalization to the cytosol has been reported, which likely results in activation of caspases and apoptosis (Baghdiguian et al., 1999). Mitochondrial biogenesis also seems to be dysregulated in C3KO mice, as these were unable to increase mitochondrial DNA content during regeneration, as well as the peroxisome proliferator-activated receptor gamma coactivator 1-alpha (PGC1A) levels, a key regulator of mitochondrial biogenesis, which in turn can also be regulated by calcium trough the CAMKII signaling (Yalvac et al., 2017).

Oxidative stress

Oxidative stress has been associated to LGMDR1 and several other MDs as one of the causes of muscle wasting (Nilsson et al., 2014; Terrill et al., 2013). In LGMDR1 muscle biopsies, NAPDH oxidase has been proposed as one potential sources of the oxidative stress, where increased ROS has been detected, as well as increased lipid peroxidation and oxidized proteins (Nilsson et al., 2014; Rajakumar et al., 2013). In the muscles of the C3KO mouse model increased oxidative stress has also been detected where the defective

mitochondria could be a contributing factor since they are the source of most cellular free radicals. However, an increase in superoxide dismutase (SOD), a protective mechanism against ROS, was detected in C3KO mice while the patient muscles showed a reduction of SOD, which could be one of the factors contributing to the increased vulnerability of human LGMDR1 muscles compared to the mice models (Kramerova et al., 2009; Nilsson et al., 2014; Yalvac et al., 2017).

Impaired muscle regeneration

Impaired muscle regeneration is one of the main features of LGMDR1 muscles as once the muscle fibers start to degenerate, the formation of new fibers is unable to compensate the loss. The patients show fiber size variability with an increase in centrally nucleated regenerative fibers, and in correlation with age and disease duration, the dystrophic process spans from inflammation with necrosis and regeneration, to fibrosis and fatty infiltrations (Fanin et al., 2013; Rosales et al., 2013). Patient muscles have also been reported to have higher amounts of PAX7 positive SCs as disease progressed, correlating with a downregulation of micro RNAs miR-1, miR-133a, and miR-206 (Rosales et al., 2013). These micro RNAs regulate myogenesis by promoting differentiation (miR-1 and miR-206) and muscle proliferation (miR-133a), and inhibition of miR-206 and miR-1 is linked to an increase in proliferation of SCs (Chen et al., 2010; Liu et al., 2011). In addition to this, abnormal fusion has been observed *in vitro* in patient myotubes, presumably due to a lack of replacement of integrin ITGB1D, as a consequence of the overexpression of frizzled related protein (FRZB) and integrin beta 1 binding protein 2 or melusin (ITGB1BP2) and a reduced WNT signaling (Jaka et al., 2015, 2017).

In the C3KO mouse a similar pattern has been reported, with an impaired regeneration characterized by an increase of small lobulated fibers of the oxidative metabolic type (slow twitch), attenuated radial growth of muscle fibers and the same microRNAs dysregulated, accompanied by an increase in transforming growth factor beta (TGF-β) levels, which inhibits myogenic differentiation trough miR-206. However, this only occurred when these mice were subjected to damage by cardiotoxin (CTX) injections for multiple cycles of necrosis and regeneration (Winbanks et al., 2011; Yalvac et al., 2017). Underlying these differences, an increased AMPK phosphorylation, energy shortage and inhibition of AKT/mTORC1 has been suggested, as well as the abnormal sarcomere organization as a

potential contributor to the impaired regeneration (Kramerova et al., 2004; Yalvac et al., 2017).

Regarding to the ability of myoblasts to fuse during differentiation in the absence of calpain 3, some studies reported a higher capacity of these myoblasts to fuse, potentially due to an accumulation of the β-catenin M-cadherin complex at the membrane and a lack of ITGB1D replacement (Jaka et al., 2017; Kramerova et al., 2006), while others showed a decreased fusion (Yalvac et al., 2017). Finally, calpain 3 has been suggested to modulate MYOD1 by proteolyzing it in C2C12 murine cell cultures (Stuelsatz et al., 2010), and in myogenic progenitors and myotubes obtained from patient derived iPSCs, dystrophin transcripts were found to be decreased, which indicates calpain 3 could be a player in muscle differentiation from early myogenesis (Mateos-Aierdi et al., 2021).

Calpain 3 and NF-***κ***B-mediated apoptosis

Early studies in LGMDR1 associated an altered nuclear factor kappa B (NF-***κ***B) signaling with higher myonuclear apoptosis (Baghdiguian et al., 1999). In this study patients showed an accumulation of IkBα in the fibers, an NF-***κ***B inhibitor that retains NF-***κ***B in the cytoplasm and prevents it from inducing anti-inflammatory genes and cell survival genes in the nucleus, hence the increased apoptosis, which was found 100 times higher in patients compared to healthy controls and other MDs (Baghdiguian et al., 1999). Other study also showed that the mRNA and protein levels of the c-FLIP protein, an anti-apoptotic factor induced by NF-***κ***B signalling, were downregulated in LGMDR1 muscles (Benayoun et al., 2008). However, the total number of apoptotic nuclei in LGMDR1 was lower than 0.5% of all myonuclei, which generated doubts about the actual relevance of this fact as a causative element in the degeneration seen in LGMDR1 patients. In mouse models the presence of apoptotic myonuclei is more controversial as some studies reported elevated levels in the calpain 3 null -/- model (Richard et al., 2000), while similar studies in the C3KO model did not detect the apoptotic myonuclei (Kramerova et al., 2004).

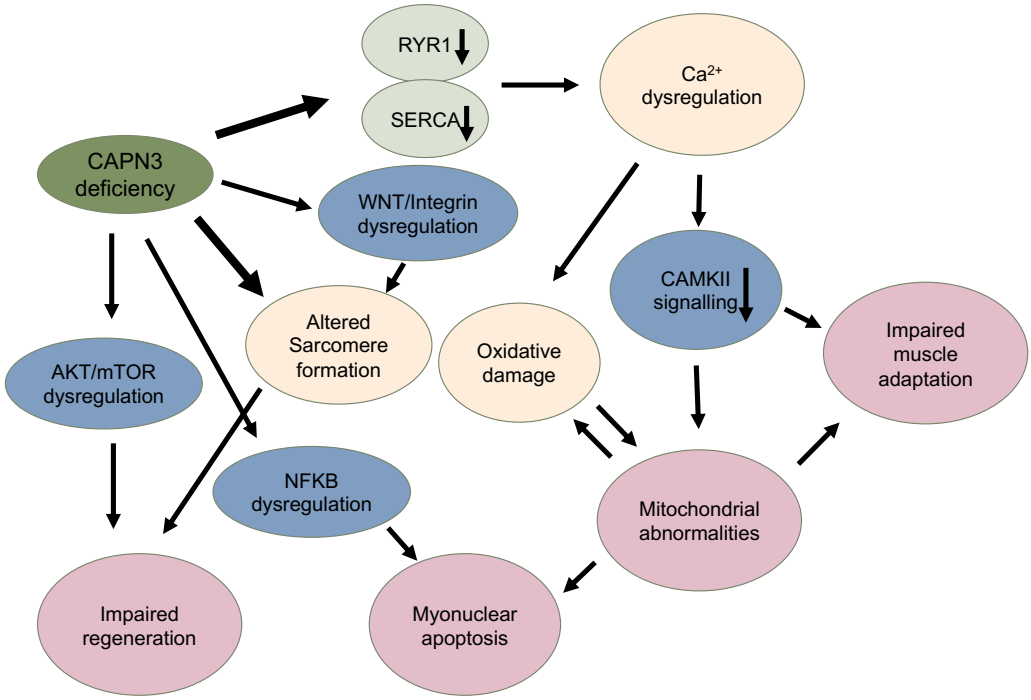

Figure 11. Schematic diagram of the suggested pathogenic mechanisms of calpain 3 deficiency.

Clinical and histopathological features

The disease is clinically characterized by a slow progressive muscular weakness that affects both pelvic and scapular girdles and proximal limb muscles. First symptoms usually appear during the second decade of life and generally lead to the loss of ambulation within one or two decades after onset in most patients, although delayed onset in the third or fourth decade has also been reported (Fardeau, Hillaire, et al., 1996; Richard et al., 2016). Muscle degeneration is progressive and patients may show difficulties to lift weight, climb stairs, get up from a chair or floor, running etc. and the difficulties keep increasing with disease progression. Posterior thigh muscles and trunk muscles suffer an accentuated atrophy, being the adductor magnus and semimembranous muscle some of the predominantly affected muscles together with soleus, vastus intermedius and biceps femoralis (Richard et al., 2016; Urtasun et al., 1998). Magnetic resonance imaging (MRI) has also shown that some distal muscles start to deteriorate in the early stages of the disease, although this becomes more evident in latter phases (Mercuri et al., 2005).

Considerable heterogeneity is found between patients in age of onset, disease progression, and histopathological features, even among affected members of the same family, making genotype-phenotype correlations hard to establish. However, some mutations such as the one found in the Basque cluster of patients in exon 22 (Arg788Serfs*14) tend to show a more severe phenotype, and in general patients carrying null alleles (i.e., predicting absence of calpain 3 protein) seem to show milder involvement (Barp et al., 2020; Sáenz et al., 2011). Contrary to other MDs, cardiac and facial muscles are not affected and patients do not show cognitive defects in LGMDR1. Some patients also experience mild respiratory insufficiency in advanced stages of the disease as a result of abdominal muscle weakness (Richard et al., 2016). Similar to other MDs, patients can show an increase of their serum CK levels 5 to 80 times over normal values in the early stages of the disease, which decreases to normal levels in wheelchair bound patients. Patients also show symptoms like contractures in the hips, knees, fingers or backbone area, and can develop shoulder bone protusions known as *scapula alata.* (Urtasun et al., 1998). Currently there are no effective treatments for LGMDR1 and only palliative care like physiotherapy can exert beneficial effects in the affected patients.

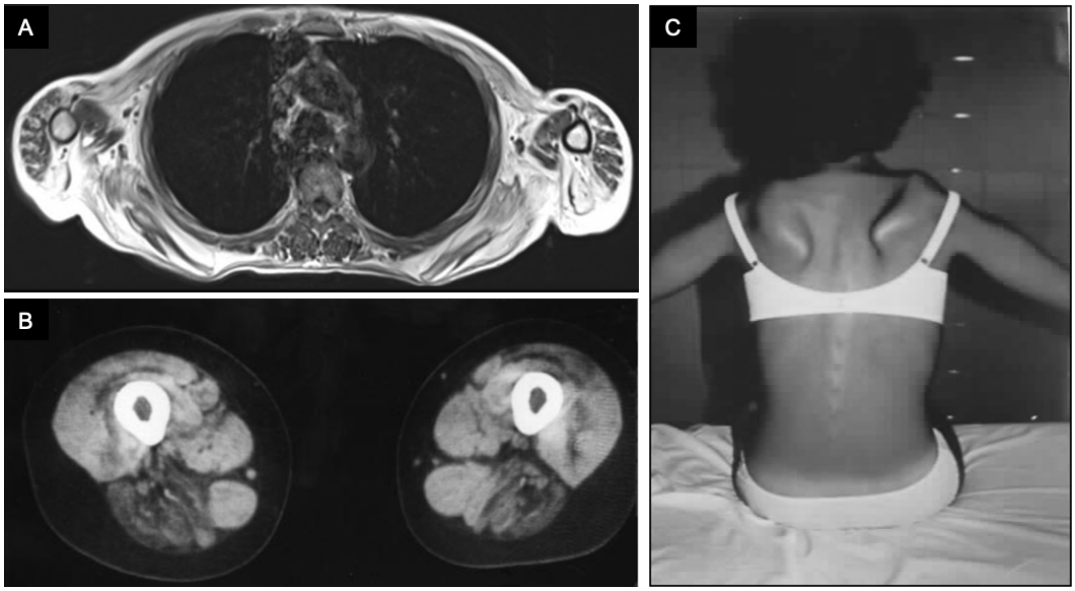

Figure 12. MRI images and *scapula alata* of LGMDR1 patients. MRI images of different patients. A) Scapular girdle B) thighs, and C) scapular winging *(scapula alata)* (From: Urtasun *et al.,* 1998 and Barp *et al., 2019*).

At the histopathological level, muscle biopsies of these patients display common dystrophic features such as fiber size variability, necrotic areas with regenerative regions, disorganized myofibrils and muscle tissue replacement by adipose and fibrotic tissue,

which increases with disease progression and severity (Chae et al., 2001; Fanin et al., 2003, 2013). In the early stages of the disease inflammation and eosinophilic infiltrations can be observed in these biopsies, accompanied by peripheral blood eosinophilia, which decreases in latter stages of the disease (Krahn et al., 2006, 2011). Apoptotic nuclei are increased in the tissue and it has been reported that the amount of SCs continues to increase as the disease progresses (Rosales et al., 2013).

Variability is also found between patients in the type of fibers affected, depending on the studied sample. For instance, some studies have reported an increased proportion and atrophy of type I fibers, while others reported a type II atrophy and loss, and type I fiber lobulation (Chae et al., 2001; Hermanová et al., 2006).

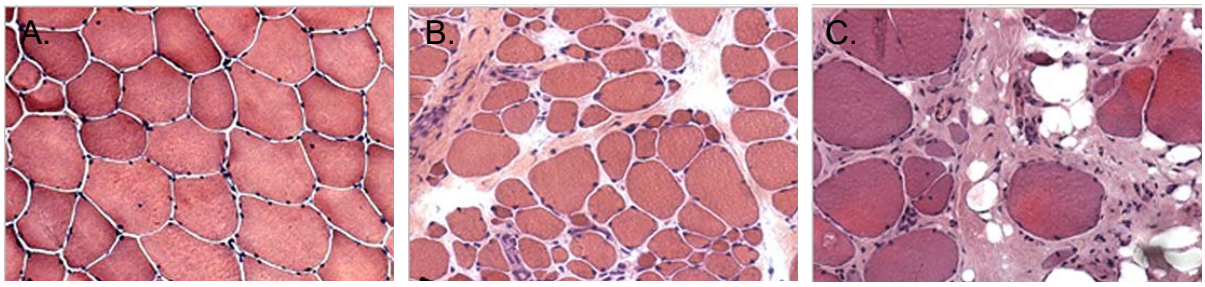

Figure 13. LGMDR1 patient muscle sections at different stages of the disease stained with hematoxylin-eosin. A) Early disease stage, only mild myopathic changes are present, such as fiber size variability, some atrophic fibers, and central nuclei. B) Advanced disease stages with muscle fibers of variable size surrounded by dense and diffuse connective tissue, that are finally replaced by adipose tissue C). Original magnification (200x) (From Fanin and Angelini, 2015).

LGMDR1 models

Besides all the information that patient's biological samples provide, different *in vitro* and *in vivo* models have been generated for LGMDR1.

In vitro models that have been used for LGMDR1 research include patient-derived primary myoblasts as well as patient-derived iPSCs that have been used to differentiate into myotubes and study different signalling pathways (Jaka et al., 2017; Mateos-Aierdi et al., 2021; Rico et al., 2021). Alternatively, the use of human and mouse immortalized myoblasts with calpain 3 silencing have also been used (Lasa-Elgarresta et al., 2022; Toral-Ojeda et al., 2016), as well as primary myoblast cultures from the different calpain 3 deficient mouse models (Jahnke et al., 2020; Kramerova et al., 2006; Yalvac et al., 2017).

A few mouse models of calpainopathy have been developed in order to investigate the role of calpain 3 in muscle biology and disease, as well as to develop therapeutic approaches. The first mouse model was developed by Richard and colleagues, where exons 2 and 3 of the mouse *Capn3* gene were replaced with a neomycin resistance cassette (Richard et al., 2000). The resulting mice (calpain 3 -/-) had no detectable calpain 3 protein in muscles, however, *in vitro* studies showed that during mRNA maturation the neomycin resistance cassette was eliminated and the resulting protein preserved the titin-binding ability, but did not preserve proteolytic nor autolytic ability. The knocked calpain 3 gene was preserved in the 129v mouse background and in mixed C57BL/6 - 129Svter background. At the histological level, these mice have mild dystrophic affliction, with some necrotic areas and some centrally nucleated regenerative fibers, as well as some immune cell infiltrations. Of note, this affection was muscle specific, being the psoas, deltoid and soleus the most affected, while the tibialis anterior (TA) and biceps showed milder affection and the rest of the analysed muscles were unaffected (Richard et al., 2000).

Another frequently used mouse model is the calpain 3 knockout (C3KO) mouse developed by Kramerova and colleagues (Kramerova et al., 2004). In this case, the knockout was generated with a genetrap construct that introduced a pre-mature translational stop signals after generation of fusions between the 5'- and 3'- end of the calpain 3 gene, and the resulting mice did not produce mRNA fragments or alternatively spliced products. These mice were smaller than the wild type (WT) counterparts and showed a reduced muscle mass, also developing a muscle-specific phenotype with some necrotic and regenerative areas in gastrocnemius, TA, soleus and diaphragm, and reduced fiber sizes. Here the soleus and the diaphragm were the most affected muscles and the authors mentioned a reduced maturity of the fibers (Kramerova et al., 2004).

Besides the knockout models of the disease, Tagawa and colleagues developed a transgenic mouse model which ubiquitously expressed a pathogenic variant of the calpain 3 gene, where a single amino acid substitution (C129S) results in a proteolytically inactive protein but maintains its structure protein binding abilities. Of note, these mice also expressed the endogenous WT calpain 3. The expression of the mutant calpain 3 increased with aging, while strength decreased progressively. However, there were no histological abnormalities detected in extensor digitorum longus (EDL) and soleus muscles, and only subtle dystrophic features were observed in 2 year-old mice (Tagawa et al., 2000). Later

on, a knock in mouse with the same mutation in calpain was developed, in this case replacing the endogenous WT calpain for the mutant one. This mouse developed some dystrophic features at the histological level, such as necrotic and regenerative areas, an increase in regenerative centrally nucleated fibers, and higher susceptibility to myofiber damage induced by exercise (Ojima et al., 2010).

All of these animal models of calpainopathy have provided valuable information to determine some of the roles of calpain 3 in the skeletal muscle, however, the phenotype that these models present is far from the degeneration observed in LGMDR1 patients. The dystrophic features of these mice are very mild, with essentially no fibrotic tissue nor fatty infiltrations in the skeletal muscle. They present slightly lower motor performance compared to the WT counterparts in some studies, but others report no differences (DiFranco et al., 2016; Kramerova et al., 2004; Sahenk et al., 2021), and motor function is not really compromised or lost at any point in their lifetime. At the same time, in order to study regenerative defects, muscles need to undergo extremely stressful conditions, such as repeated CTX injections or induction of atrophy by disuse (Kramerova et al., 2018; Yalvac et al., 2017). These differences are clear limitations of these models specially if they are intended to be used to test and develop potential therapies, and a better animal model with real loss of motor function and dystrophy would be of great help to develop new therapies.

Approaches to develop LGMDR1 therapies

Currently there are no effective therapies to treat LGMDR1, and similarly to the rest of LGMDs, treatments have been mostly symptomatic. However, new treatments both disease- and non-disease-specific are being investigated (Vissing, 2016). Most therapies in development can be divided into 3 categories: the ones focused on gene therapy, cell therapy approaches, and pharmacological approaches. Most research for LGMDR1 and also most LGMDs is focused on gene therapy approaches, either by introducing a correct copy of the mutated gene with the use of adeno-associated virus (AAV) or other vectoring technology, or trough approaches that target transcriptional modifications such as exon skipping (Straub & Bertoli, 2016). However, many of these approaches that showed promising results in mice have failed or delivered small improvements when transferred to humans, facing difficulties in delivering the treatment to the large amount of tissue that the skeletal muscle represents in the human body, and a great amount of effort is

being dedicated to the improvement of these vectors as well as the expression systems (Galli et al., 2018; Sarcar et al., 2019).

Early efforts in calpain 3 gene therapy were made in the calpain -/- mouse model with AAV9 (Bartoli et al., 2006). The treatment induced expression of an active calpain 3 in the sarcomere, but with modest clinical improvement. Importantly, an increase in the dose led to cardiac toxicity, rising concerns about calpain 3 toxicity in cardiac muscle. Later on, this issue was avoided by improving the expression vector and restricting the expression to skeletal muscle with a miRNA-regulated cassette that downregulated transgene expression in cardiac tissue (Roudaut et al., 2013). In any case, it was recently discovered that the cardiac toxicity in mice was due to the splicing differences that reduced ability of mice titin to buffer calpain 3 activity, since when the therapy was tested in non-huma primates (NHP), no cardiac toxicity was observed even when the transgene was being expressed in the heart (Lostal et al., 2019). More recent studies with a different AAV serotype (AAVrh74) and in the C3KO mouse model, showed motor and histological improvements and no cardiac toxicity was reported (Sahenk et al., 2021). Despite the efforts, these approaches are still in pre-clinical stages and no clinical trials in humans have started to date (ClinicalTrials.Gov), with only one company currently developing a AAVrh74 based gene therapy, also in preclinical stages (Sarepta therapeutics in collaboration with Nationwide Children's Hospital).

Cell therapy approaches have also been proposed to treat MDs in general. Being able to harness the outstanding regenerative capacity of SCs has been a goal for some time, however, the technical difficulties in their culture and maintenance of stemness in culture and after the engraftment in autologous therapies has hindered the advancement of therapies with SCs (Chang & Rudnicki, 2014; Judson & Rossi, 2020). Many current hopes rely on the use of iPSCs, which have shown to be able to differentiate into myogenic progenitor cells, and to engraft and differentiate into muscle fibers *in vivo* in mice, which in conjunction with gene therapy applied *ex vivo* in those cells, opens the possibilities to perform cell and gene therapies for MDs (Darabi et al., 2012; Incitti et al., 2019; Maffioletti et al., 2018a). One of the advantages of this approach is that when using iPSC derived myogenic progenitors, these have shown the potential to not only differentiate into muscle *in vivo*, but also to seed the SCs niche and respond to multiple injuries, contributing to long-term regeneration and thus, opening the possibility to repopulate the SCs free of the pathogenic mutations (Chan et al., 2018; R. He et al., 2020; Xie et al., 2021). In the case

of LGMDR1, both patient-derived iPSCs and CRISPR/Cas9 based gene editing methods to correct mutations have been developed and the derived muscle progenitors have been engrafted into C3KO-NSG mice as an early proof of concept (Mateos-Aierdi et al., 2021; Selvaraj, Dhoke, et al., 2019). Despite the promising results of these approaches, they are still far from the clinical context as both iPSCs and CRISPR/Cas9 are relatively new technologies and safety, efficacy and scalability of such autologous therapies will need to improve before they reach clinical trials.

Finally, pharmacological approaches have also been proposed to treat LGMDR1. Promoting muscle growth and inhibiting atrophy trough WNT pathway activation and/or GSK3β inhibition have been the focus of recent studies showing promising results in the C3KO mice and patient cells respectively (J. Liu et al., 2020; Rico et al., 2021), while other approaches such as myostatin inhibitors resulted less effective (Kramerova et al., 2020). Other groups have suggested targeting the ubiquitin-proteasome system aiming to avoid the reduction in SERCA proteins and reduce the increased ubiquitination (Lasa-Elgarresta et al., 2022).

Research models for human muscle disorders

Traditionally, skeletal muscle and its biology has been studied using muscle biopsies from either healthy or diseased individuals, cell culture experiments or animal models. Despite using human subjects and tissues is ideal, tissue availability is generally limited and in the case of diseased muscle, many of the muscle biopsies that were performed previously with diagnostic purposes can now be replaced with molecular or genetic diagnostic methods to avoid the invasive procedure (Aartsma-Rus et al., 2016; Joyce et al., 2012).

In vitro models

Patient-derived myoblasts, as well as healthy donor-derived myoblasts, have been broadly used to study the physiopathology of MDs as well as to test the efficacy of molecules with possible therapeutic potential (Bou Saada et al., 2016; Delaporte et al., 1990; Volonte et al., 2003). Obtaining primary myogenic progenitors is performed either by enzymatic digestion or cell outgrowth from muscle biopsies where specific populations of interest such as myoblasts or SCs can be further purified (Motohashi et al., 2014; Yoshioka et al., 2020). In any case, myoblasts and SCs cultured *in vitro* have a limited amount of passages

they can withstand before they stop dividing or start to differentiate, and in the case of SCs they generally lose their stem cell identity, quiescence and self-renewal capacity once they are cultured *in vitro* (Gilbert et al., 2010; Sacco et al., 2008).

Thus, in order to maximize this material, several authors have chosen to immortalize myoblasts, despite the fact that this process can slightly alter their properties (Mamchaoui et al., 2011; Yoon et al., 2013). Alternatively, researchers have been investigating for other easy-access cell types with myogenic potential to establish patient-specific cellular models. In this regard, skin-derived fibroblast transdifferentiation into myotubes through exogenous MYOD1 expression has been very useful to establish myogenic *in vitro* models of a wide range of MDs (J. Choi et al., 1990; Cooper et al., 2007). Cell culture studies that use animal primary cells or immortalized cell lines such as the mouse C2C12 or rat L6 myoblasts, have also been extensively used to study muscle biology *in vitro* (Khodabukus et al., 2018).

To differentiate these cells into multinucleated myotubes, traditional 2D cultures usually involve the expansion and culture of the precursors in a high-serum media until near-confluence and then inducing differentiation into myotubes by decreasing serum content (Khodabukus, 2021). Due to the rapid rate of fusion (3-5 days) and ease of this setup, this 2D model is the most frequently used system to evaluate a pathological condition and the impact of different small molecules, growth factors or genetic manipulations by measuring the levels of differentiation and fusion achieved (Zschüntzsch et al., 2022).

Culturing satellite cells

In order to study SCs biology, single myofibers can be dissected and isolated from the muscle, and cultured for several days (Renzini et al., 2018). This model has become the gold-standard to study SCs activation *in vitro*, since SCs stay retained within their niche and this allows to study SC dynamics with multiple modalities, which have been used to help decipher the molecular mechanisms and transcription factors regulating SC activation (Beauchamp et al., 2000; Kuang et al., 2007), polarity (Dumont et al., 2015), and symmetric divisions (Wang et al., 2019).

However, these methods generally don't allow the expansion of SCs in quantities as to generate engineered muscle models or potential cell therapies. Therefore, alternative

methods have also been developed aimed at culturing SCs while maintaining their characteristics. Aiming to maintain a similar environment to the SC niche, 3D myospheres can be generated with SCs (Sarig et al., 2006; Westerman et al., 2010), following the examples of neurosphere cultures that were previously developed (Reynolds et al., 1992). With these methods SCs purified from dissociated muscle are cultured in suspension where they form the myospheres and are able to proliferate both in number and size and maintain their myogenic capacity *in vitro* and *in vivo* for prolonged culture periods (Naldaiz-Gastesi et al., 2019; Westerman et al., 2010). Also, this type of myospheres can incorporate additional cell types such as non-myogenic precursors similar to FAPs and mesenchymal precursors, besides the cells expressing SC markers PAX7 and α7-integrin (Naldaiz-Gastesi et al., 2019; Wei et al., 2011; Westerman, 2015).

Methods to improve differentiation, function, and maturation

Complete adult muscle development and maintenance requires functional innervation and electrochemical stimuli from motor neurons. *In vitro,* electrical stimulation can be applied to muscle cultures as a surrogate for neuronal activity, where an optimized protocol can minimize electrochemical damage and can allow continued stimulation over multiple weeks (Huang et al., 2006; Khodabukus et al., 2012). In 2D cultures it has been shown that depending on the stimulation patterns, these can increase specific isoforms from sarcomeric and calcium-handling proteins and induce muscle hypertrophy. For instance, when keeping a constant stimulation frequency work:rest ratio, with contraction lengths greater than 6 seconds (s), these induced a fast-to-slow MYHC shifts and maturation (Khodabukus et al., 2015). However, 3D engineered muscles seem to support tissue contraction for longer periods better and up to 2 weeks, and similarly to how it occurs in native muscle, the resulting hypertrophy is associated with an increased mTORC1 activity (Donnelly et al., 2010; Maleiner et al., 2018; Wehrle et al., 1994).

Complementary to electrochemical stimulation, mechanical load can also be used *in vitro* using deformable substrates to induce recurring levels of stretch to the culture to emulate both muscle length increase that occurs during development and muscle strain that occurs during exercise and locomotion (Pavesi et al., 2015; Rangarajan et al., 2014), which can induce hypertrophy of *in vitro* cultures, but also atrophy when reducing the mechanical load or shortening the tissue length (Lee et al., 2013). However, these systems are

generally custom made and there are few studies replicating the results that different research groups have obtained.

A plethora of small molecules and growth factors have been studied and are routinely used to improve differentiation, maturation, and function (Syverud et al., 2016). Generally, these compounds aim to induce the pathways that are involved naturally in the myogenic process and compensate the shortcomings of the *in vitro* environment, for which media supplementation with these compounds/factors has to be adequate to each phase and markedly different in the proliferative and differentiation phases. Both in embryonic and post-natal myogenesis, NOTCH signalling and WNT proteins are essential regulators of myogenic precursors, and although more associated with hypertrophy and homeostasis, mTOR also can regulate SCs activity and myogenesis by upregulating MRFs (Bentzinger et al., 2012; P. Zhang et al., 2015). Hypertrophy and regeneration are primarily regulated by a signalling pathway initiated by insulin-like growth factor 1 (IGF-1) that activates AKT and indirectly mTOR, while simultaneously inhibiting GSK3β. At the same time, AKT prevents protein degradation and muscle atrophy by blocking the FoxO family of transcriptions factors (Sandri, 2008). Hence, it is common to supplement media supplied during the initial proliferation phase with HGF and FGF, which promote activation and proliferation of myogenic progenitor cells and delay terminal differentiation, prior to switching to a media supplemented with IGF-1 or insulin for the induction of differentiation, as well as small compounds that modulate the mentioned pathways such as GSK3β inhibitors (Lee et al., 2013).

Other compounds on the other hand can be used to emulate signaling provided by other supporting cells, such as motor neurons, where the use of synapto-genic molecules such as agrin have been shown to increase contractile force of the culture (Bian et al., 2012).

Finally, co-culturing muscle cells with other cells of the muscle tissue such as fibroblasts but mostly motor neurons, has shown to prompt the formation of advanced structures such as NMJs and increase contractility and maturation of engineered muscles (Bakooshli et al., 2019; Khodabukus, 2021).

Biomaterials

Traditional 2D cell cultures over plastic surfaces with muscle cells results in developmentally immature myotubes with reduced physiological relevance (Engler et al., 2006; Khodabukus et al., 2018). This functional immaturity is partially the result of using hard surfaces like glass or plastic for cell growth and differentiation. It was demonstrated that cells are very sensitive to their physical environment and that culturing myotubes on soft substrates with a stiffness similar to the muscle (12-18kPa) can improve myotube structure, gene expression and also reducing the detachment of contractile myotubes which can shorten the culture duration (Engler et al., 2004, 2006). In this aspect, using muscle ECM proteins to enhance cell adhesion improves the quality of the 2D cultures. However, despite 2D cultures can be practical to make comparative studies, they still don't reproduce the complex 3D environment of native muscle (Engler et al., 2006). To overcome the limitations of the 2D muscle culture, several 3D culture models have also been developed mostly using either hydrogels from specific proteins or from decellularized tissue, as well as self-organized materials, with the aim being to create a biomimetic muscle microenvironment to provide cells with an appropriate ECM with biological and mechanical signals to induce muscle development, maturation and function (Wang et al., 2019; Zschüntzsch et al., 2022).

Collagen I is the most abundant protein in the muscle ECM and it has been shown that myoblasts can proliferate and differentiate within collagen hydrogels and provide growth stimulus (Shansky et al., 1997). However, myofibers in a healthy muscle mostly interact directly with proteins form the basal lamina and some studies indicated that high collagen content has adverse effects on functional maturation of the muscle, which is consistent with findings that in cases of fibrosis where collagen levels are elevated, are associated with poor regeneration and function of the muscle. In addition to this, collagen I is not easily remodelled and it has been suggested it may not provide optimal stiffness for differentiation (Hinds et al., 2011; Stearns-Reider et al., 2017).

This promoted the use of hydrogels supplemented with basal lamina extracts such as Matrigel (basal lamina extracts isolated from mouse Engelbreth-Holm-Swarm tumors) to improve tissue formation, which have been extensively used and have shown to improve tissue structure (Grefte et al., 2012).

Another widely used substrate for tissue engineering skeletal muscle is fibrin. Unlike collagen, fibrin has the ability to be extensively remodelled, degraded and replaced by endogenously derived ECM, as it naturally occurs in the wound healing process where fibrin plays an important role. Moreover, fibrin fibrils have a stiffness similar to native muscle and also has been shown to promote angiogenesis and neurite extension, which are required for the formation of a fully functional muscle *in vivo* (Grassl et al., 2002; Ross et al., 2003; Thorrez et al., 2018).

iPSC-derived muscle cultures

Induced pluripotent stem cells (iPSCs) marked a crucial milestone in the field of tissue engineering and biomedical sciences in general. Generated for the first time in 2006, these cells are generated by re-programming cell identity to an undifferentiated state and exhibit both transcriptional and epigenetic signatures similar to those of embryonic stem cells, making theoretically possible to create tissues or organs with patient-derived cells (Takahashi et al., 2006). Consequently, iPSCs have also been extensively studied to engineer muscle *in vitro* and *in vivo.*

In order to differentiate iPSCs from their pluripotent state into myogenic cells, two main approaches have been described: 1) Transgenic approaches by overexpressing myogenic transcription factors (e.g., PAX3/7, MYOD1) and 2) direct differentiation by induction with small molecules and growth factors. Both approaches focus on differentiating iPSCs into myogenic progenitors *in vitro*, which can be subsequently differentiated into myotubes (Iberite et al., 2022). When aiming to develop protocols for potential cell therapies, their myogenic potential can be evaluated *in vivo* in immunosuppressed mice to quantify the progenitor's ability to generate new myofibers and most importantly, to repopulate the stem cell niche, as this would be key to ensure long-term viability of the therapy, being able to respond future tissue regeneration requirements (Xie et al., 2021). In contrast when the differentiation protocols are aimed at generating *in vitro* platforms to study disease with patient-derived iPSCs or to create drug screening platforms, 2D or 3D culture protocols can be used in a similar way to the myoblast cultures mentioned above (Iberite et al., 2022; Khodabukus, 2021).

Several successful transgenic differentiation approaches have been reported based on the transient or stable expression of MRFs MYOD1 and PAX3/7 (Darabi et al., 2012; Tanaka

et al., 2013; Tedesco et al., 2012). These methods generally have an initial differentiation phase towards a mesodermal phenotype guided by specific mediums and small molecules, as well as the formation of embryoid bodies (EBs) in some cases, and then involve the use of an inducible system to control the expression of the transgene by the addition of an antibiotic in the culture medium to differentiate the cells towards myogenic progenitors. A reporter system for the transgene such as GFP or mCherry can also be used to enrich the transgene expressing cell population by fluorescence-activated cell sorting (FACS) (Darabi et al., 2012; Tanaka et al., 2013).

The use of MYOD1 for the myogenic induction generally results in a stronger differentiation towards myoblast-like progenitors, and it is possible to directly induce MYOD1 overexpression from the beginning of the differentiation process bypassing early embryonic differentiation (Abujarour et al., 2014; Shoji et al., 2015; Uchimura et al., 2017). However, MYOD1-reprogrammed progenitors cannot replenish the muscle stem cell niche, since they do not express PAX3 or PAX7, and therefore do not show the regenerative potential of adult stem cells (Sato et al., 2019).

From the viewpoint of a therapeutic potential, the induction of PAX3/7 in iPSCs can be more interesting since these progenitors can repopulate the muscle stem cell niche when implanted *in vivo* and repair injured muscles (Xie et al., 2021). In fact, a study showed that starting from PAX7-induced myogenic progenitors and enriching for ICAM1+ /integrin α9β1+ /SDC2+, the triple-positive cells replenished the SCs pool and generated new fibers 10 months post-transplantation (Magli et al., 2017).

Despite the success of long-term studies on mouse models, the use of overexpressed genes may limit the translation of this technology to the clinic since most of them use integrative vectors and transient vectors possess the risk of random integration and lead to a less efficient differentiation (Warren et al., 2010).

Therefore, alternative non-transgenic approaches have also been developed. This type of directed differentiation of iPSCs consists of using just defined culture conditions in a spatiotemporal controlled manner, where sequential addition of different morphogens, growth, and differentiation factors responsible for cell proliferation, migration, and differentiation *in vivo* are added, many of which modulate the mentioned NOTCH and WNT pathways among others (Awaya et al., 2012; Iberite et al., 2022; Maffioletti et al.,

2018a; Tanoury et al., 2020). These non-transgenic protocols, however, usually lead to a more heterogeneous cell populations where in some cases cell populations can be enriched by FACS for myogenic progenitor markers in order to enrich the desired population and remove non-myogenic cells. However, these are also longer differentiation protocols that can take up to 10 weeks before mature myotubes are observed (Hosoyama et al., 2014).

One application in which using iPSCs is advantageous is in the generation of iPSC derived, complex, multilineage 3D muscle organoids that contain key isogenic cellular constituents of skeletal muscle, such as vascular endothelial cells, pericytes, or motor neurons, all developed from the same iPSC line. These models, despite being technically complex to develop, offer the opportunity to generate and study patient-specific multicellular muscle cultures (Ajalik et al., 2022; Maffioletti et al., 2018; Shin et al., 2022).

However, one of the limitations that iPSCs have is their increased variability over other *in vitro* models, which mostly comes from the inter-donor variability, but which also can come from the inter-clonal variability in the iPSC generation process, as well as in the overall longer myogenic differentiation protocols, which altogether can decrease the statistical power of the system (Beekhuis-Hoekstra et al., 2021; Mirauta et al., 2020; Volpato & Webber, 2020).

Animal models

The most common species used in experiments for muscular dystrophy research are mice, dogs, pigs, fruit flies (*Drosophila melanogaster*), and zebrafish (*Danio rerio*). Although other animals such as rats, hamsters and cows have also been used to study the different pathogenetic mechanisms of muscular disorders, they have been less frequently used (Gaina & Popa, 2021). Some MDs can occur naturally in some of these species whereas in others they must be genetically induced. In both cases, these animals are used to identify the properties of the disease-causing gene, to understand the cellular and molecular mechanisms underlying genetic disease, and to identify its potential treatments (Egorova et al., 2021; van Putten et al., 2020).

In order for an animal model to resemble the human muscular dystrophy, it should resemble human muscle structure, develop the key clinical aspects of the disease, and have similar gene expression patterns. Often all of these aspects are not found in a single

animal model, and different animal models can be used, each model having its advantages and limitations.

Non-mammalian models

Non-mammalian models to study muscle disorders have mostly been generated in *Caenorhabditis elegans, Drosophila melanogaster* and in *Danio rerio*. These type of animal models have some advantages over mammalian models such as their small size, high reproduction rate, fast growth and development, and a large number of offspring. Also, the lower cost of maintenance associated with these models as well as the laxer ethical and regulatory requirements to work with these animals makes them very useful for activities such as drug screenings (Ellwood et al., 2021; M. Li et al., 2017; Plantié et al., 2015).

Compared to the *Drosophila* and zebrafish models, *C. elegans* has more restricted applications, owing to a lack of muscle cell fusion, restricted gene conservation and a short lifespan, and although some models for diseases such as FSHD, DMD or LGMDR2 among others have been generated (Ellwood et al., 2021; Krajacic et al., 2009; Q. Liu et al., 2010), models in *Drosophila* and zebrafish seem to be more useful for screening applications and to make preliminary studies in general (Plantié et al., 2015). Besides a higher degree of genetic similarity, *Drosophila* and zebrafish muscles share more structural, histological and functional similarities with human muscle (Baylies et al., 1998; McKeown et al., 2009; Taylor, 2013). These models are also easily amenable to genetic manipulation and therefore a growing body of new models for muscular diseases are being created. Some of the most relevant models in these animals have been developed for DMD (Kucherenko et al., 2008; Waugh et al., 2014), DM1 (de Haro et al., 2006; Todd et al., 2014), and FSHD (Jones et al., 2016; Pakula et al., 2019).

However, despite the practicality of these models for some type of studies such as drug screenings and early phases of drug development, many of the gene orthologs responsible for some diseases are still quite different to the human proteins and being phylogenetically and physiologically far from humans, limits their use for more advanced studies where other aspects such as disease natural history and the overall physiology of the model needs to be closer to humans (Plantié et al., 2015).

Mammalian models

Rodents

The mouse remains the most widely and extensively used animal model for the study of MDs, and has played a key role in the understanding of the molecular mechanisms underlying the pathogenesis of many of these diseases. Owing to the advancements in gene editing technologies such as CRISPR/Cas9 and the relative ease of generating genetically modified mice, a variety of mouse models have been developed for the majority of MDs (Gaina et al., 2021; van Putten et al., 2020).

Mice have some advantages for preclinical studies given their small body size, short gestation and life span and the abundance of experimental reagents available for this species. Also, being one of the most studied animal models, the amount of studies and the knowledge about its physiology and genetics is greater than in other mammalian models. However, many MD mouse models are limited in their presentation of the human disease characteristics (Sztretye et al., 2020). These limitations also add to the fact that the effects of a drug observed in mice may not necessarily predict the outcome in the clinical setting. To better confront these limitations, the research community has highlighted the need for detailed natural life-history data from both the patients as well as the mouse models of the most commonly used MD models (Kornegay et al., 2014; Mercuri & Muntoni, 2013; Nagaraju & Willmann, 2009).

An example of the limited phenotype that these models present besides the already mentioned LGMDR1 calpain 3 KO models, are the DMD models. There are several DMD mouse models available, some of them being from naturally occurring dystrophic mouse strains, while most of them have been genetically engineered (Egorova et al., 2021). All dystrophin-deficient mice have dystrophic symptoms, however the severity of them does not often correlate with the disease severity in DMD patients. For example, the lifespan of the commonly used mdx mouse model is about 80% of normal while the lifetime of a human with DMD is generally not more than one third of a healthy individual (Broomfield et al., 2021; van Putten et al., 2019).

Besides mouse models, other rodents such as rats and hamsters have been also used for modelling MDs (Larcher et al., 2014; Nigro et al., 1997). For instance, a considerable

number of animal models for sarcoglycanopathies have been developed, but the hamster was the first animal model used and is the most well described for this diseases (Blain & Straub, 2011).

Pigs

Larger animals such as pigs and dogs develop a more similar phenotype to humans when modelling MDs, probably due to their closer genetic, physiologic and anatomic similarities (Lunney, 2007; Selsby et al., 2015; Wernersson et al., 2005). Pigs in particular are also more similar to humans in size, metabolic profile and longevity, which makes them an attractive animal model to study highly prevalent genetic MDs (Gutierrez et al., 2015; Klymiuk et al., 2016). In fact, there seems to be a relationship between the size of the animal model and the biomechanical characteristics of the fibers, which could be key to develop the clinical symptoms in the animal models (Cone et al., 2017; Klymiuk et al., 2013).

Until recently, most pig models were used to model metabolic diseases such as diabetes or cardiovascular diseases, however, technical improvements in *in vitro* reproductive technologies in this species, somatic cell nuclear transfer (SCNT) protocols, as well as the introduction of gene editing technologies like CRISPR/Cas9 have made obtaining genetic models for MDs more accessible (Crociara et al., 2019; Selsby et al., 2015; Tanihara et al., 2021).

The first muscular dystrophy model in pigs was developed for DMD, which was developed by homologous recombination and SCNT of cells where the exon 52 of the dystrophin gene had been deleted (Klymiuk et al., 2013). These animals displayed key elements of DMD such as the lack of dystrophin, a decrease in the dystrophin glycoprotein complex, hyperCKemia in blood and a progressive fibrosis of skeletal muscle that resulted in a very severe form of DMD. A natural model of Becker's disease, a milder form of DMD, has also been described in pigs where a mutation in dystrophin can cause death as a porcine stress syndrome, and these models have also been suggested to be used in the study of preclinical therapies for DMD (Hollinger et al., 2014). Recently, and developed with the same homologous recombination and SCNT methods, a commercially available model of DMD in a minipig breed has also become available (Echigoya et al., 2021). These minipigs, unlike the mouse model of DMD, manifested early disease onset with severe bodywide

skeletal muscle degeneration accompanied by poor growth. With this model, different exon skipping strategies to treat DMD were evaluated *in vitro* in primary muscle cells from this model.

In pigs, a few models have already been developed with CRISPR/Cas9 (Tanihara et al., 2021). However, the higher requirements in terms of logistics for the animal housing facilities, the longer gestation periods and less developed and optimized procedures of *in vitro* fertilization as well as a lower success rate in the gestations after the embryo transfers results in a much higher cost when developing new pig models (Chen et al., 2022). On the other hand, the demand for such models for research is increasing and an improvement of these processes is very much in demand (H. Yang & Wu, 2018).

Despite the challenges, these strategies are currently being used to develop many genetic models in pigs, such as another DMD pig model that was developed with CRISPR/Cas9 microinjection in the zygote (Yu et al., 2016). This model was obtained by a knockout of exon 27 of the dystrophin gene, which resulted in a severe form of the disease that led to the death of the piglets within weeks. On top of this, the born piglets were mosaics, harbouring different mutations throughout the body, which emphasizes the need to optimize the processes to develop new pig models.

Besides DMD models, pigs have also been used to develop genetic models of amyotrophic lateral sclerosis (ALS), a neuromuscular disorder that also severely affects the muscle, and where pigs showed a more severe affection than their mouse counterparts (Crociara et al., 2019; G. Wang et al., 2015).

The fact that there are already therapeutic strategies for MDs that were proven successful in mice, but failed in the translation to humans, shows that there is still a gap between the mice models and humans that needs to be filled with better models to test the efficacy and safety of the new treatments at the preclinical stage. In this aspect pigs possess the requirements to become better models than mice to tests therapies in MDs, however in order to achieve this, it is essential to improve the process of generating new pig models to make them available in a cost and time efficient manner.

Other large animal models

Other large animals have also been used to model muscular dystrophy, in particular for DMD models. Canine and feline models have been identified in natural populations for DMD, whereas monkey models have been developed with CRISPR/Cas9 (Y. Chen et al., 2015; McGreevy et al., 2015).

About 20 different dog breeds have been identified with dystrophyn deficiency, and in particular the Golden retriever and Beagle breeds have become fundamental tools for the evaluation of the different therapeutic strategies under development for DMD (Wells, 2018).

However, in terms of the generation of new models for MDs, dogs are being avoided in favor of other large animal species such as pigs due to the high cost and mostly due to the increased ethical concerns implicated when using dogs, and the same can be said about the possibilities of using primates to generate new models, which carry even higher costs and ethical concerns (Goñi-Balentziaga et al., 2022; Kang et al., 2019; Prescott, 2020).

CRISPR/Cas9 gene editing

Most recent animal and cellular genetic models are being developed thanks to the precise genetic modifications obtained with sequence specific nucleases, in particular with CRISPR/Cas9 (Jinek et al., 2012). The high efficiency of the CRISPR/Cas9 system, in addition to its simplicity and ease of design has made it a common tool for the generation of genetic modifications *in vitro* and is now routinely used to generate new genetic mice models (Singh et al., 2015).

Since it was discovered that DNA double strand breaks (DSBs) allows generating loss of function alleles and increases the efficiency for homologous recombination (HR) (Choulika et al., 1995), many targeted endonucleases have been developed. Initially, tools for genome editing relied on programable nucleases that use their AA sequence to target a specific DNA sequence, such as meganucleases, zinc-finger nuclease proteins (ZFN), and transcription activator like effector nucleases (TALEN) (Silva et al., 2011). CRISPR/Cas genome editing uses a single bacterial endonuclease (Cas) protein that contains nuclease and RNA/DNA binding domains. To guide the endonuclease activity, it requires a small

single stranded RNA molecule to target the DNA sequence through sequence complementary. This allows to decouple the target specificity from the protein structure allowing the same endonuclease to be used with different guide RNAs. The resulting system has a major advantage as it can be rapidly reprogrammed to target different DNA sequences by redesigning the RNA guide (Cong et al., 2013; Jinek et al., 2012).

The RNA-guided CRISPR endonucleases were derived from a prokaryotic adaptive immune system against nucleic acid sequences from bacteriophages and have been optimized for their use in mammalian cells, where the Cas9 endonuclease from *S. pyogenes* (SpCas9) has become the standard CRISPR/Cas endonuclease used for genetic engineering in mammals (Mali et al., 2013; Mojica & Montoliu, 2016). The guide RNAs are formed by two RNA molecules: crRNA and tracrRNA. crRNAs are complementary to the target DNA sequence on one end and hybridize with the tracrRNA molecule in the other and the resulting RNA duplex is then assembled with Cas proteins into a ribonucleoprotein complex (RNP). Then this RNP complex starts searching for a nucleic acid sequence complementary to the target sequence of the crRNA, however, target binding of the RNP also requires a specific motif called the protospacer adjacent motif (PAM) right next to the crRNA complementary sequence in the target DNA strand for the Cas protein stay bound. Once the Cas effector has bound to the PAM motif, the target sequence is unwound and hybridizes to the crRNA, allowing Cas nuclease activity to activate and cut the DNA strand (Anders et al., 2014). For practical applications the tracrRNA and crRNA have been engineered into a single-guide RNA (sgRNA) reducing the overall size of the tracrRNA by fusing the two RNAs together using a small loop (Figure 14) (Jinek et al., 2012). The targeting sequence of the crRNA for SpCas9 is typically 20 nucleotides long, although it is possible to shorten this sequence to 17-18 bases without losing much activity (Fu et al., 2014; Jinek et al., 2012).

Once the DSB occurs in the target DNA, this is repaired by the organism using its own DNA repair mechanisms, which can be used for genome editing to introduce a genetic modification of interest (Jasin & Haber, 2016). The two main DNA repair pathways are the non-homologous end-joining (NHEJ), which occurs most of the times and is active in nearly all cell types, and the homology-directed repair (HDR), which relies on copying the genetic information from a homologous template to the site of the DSB. Briefly, NHEJ rejoins the ends of the DNA fragments that were cut by the break, however, this process is inaccurate and error prone, and often results in the introduction of insertion or deletion

mutations (indels) in the site. If this occurs within a protein coding gene, these often result in frameshift mutations that end up in a premature stop codon, generating a loss of function either by truncating the protein or eliminating its expression via nonsense-mediated mRNA decay, although it can also cause mRNA dysregulation and splicing modifications (Tuladhar et al., 2019). On the other hand, HDR relies on copying the genetic information from a homologous template, which naturally would occur by copying the sequence from the other allele of the same gene via homologous recombination, however, if an exogenous template is provided, this can participate in the homologous recombination and introduce its sequence into the repaired DNA, which is how precise sequence modifications or insertions can be introduced (Figure 14). This process tends to be much less efficient and is generally only active during mitosis (Chapman et al., 2012; Jasin & Haber, 2016; J. P. Zhang et al., 2017).

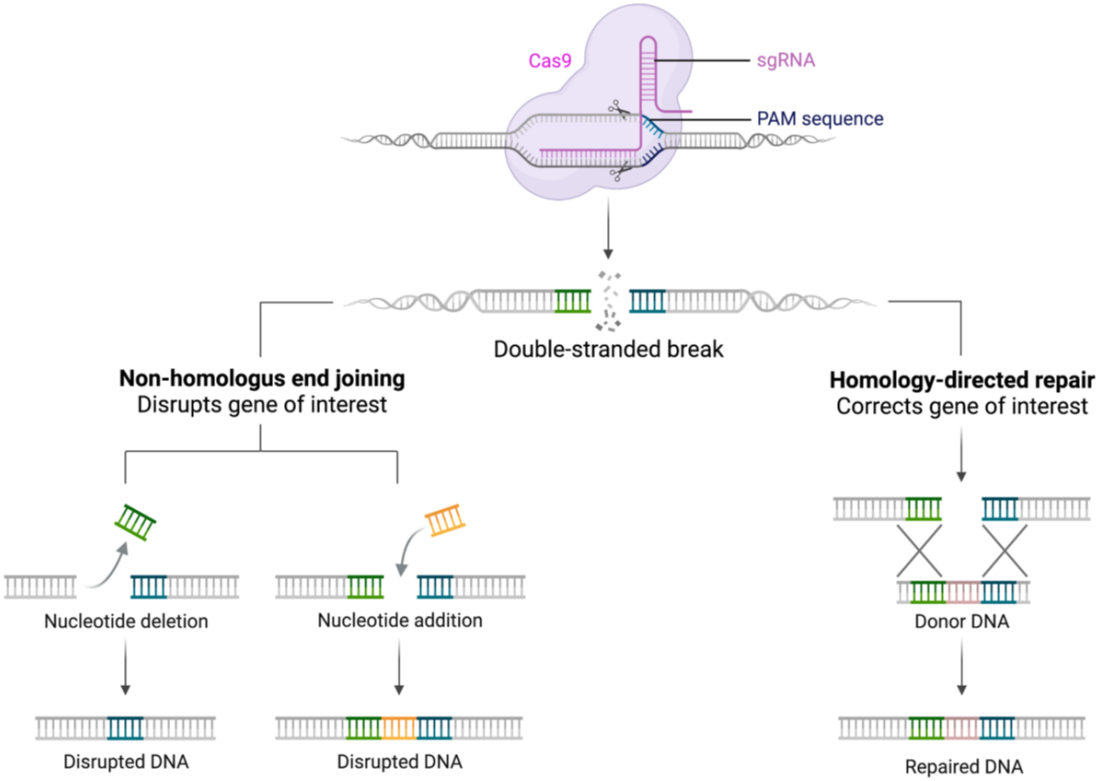

Figure 14. CRISPR/Cas9 and DSB repair mechanisms. Cas9 endonuclease with a sgRNA molecule targets a specific DNA sequence and generates a DSB. DSBs are repaired either by the NHEJ repair mechanism, which generate indel mutations, or by the HDR mechanism using a donor DNA template with homology arms. Source: Biorender.

One of the potential issues of this technology is that DNA cleavage by CRISPR/Cas endonucleases does not require complete complementarity between the guide RNA and DNA target sequence which can lead to off-target DNA cleavage, and although less

frequently, it can also induce larger deletions and chromosomal re-arrangements (Kosicki et al., 2018; X. H. Zhang et al., 2015).

Since the development of the CRISPR/Cas system, new applications and modifications have been developed mostly by either using Cas proteins from other species which can have different PAM sequences, affinities and efficiencies; or engineering these Cas proteins to perform new functions. For example, Cas9 nickase mutants have been developed which are only able to introduce a cut in one of the DNA strands, which still allow for the induction of homology-directed repair but reduce the occurrence of NHEJ and can be used to increase the specificity of the system (Ran et al., 2013). Also, catalytically dead SpCas9 (dCas9) have been developed with no nuclease activity, that still bind sgRNAs and find target DNA sequences, effectively turning dCas9 into a highly specific DNA-binding platform which allows to recruit functional elements to target sites and can be used to regulate transcription, introduce epigenetic modifications, chemically modify single bases and many other applications for genome engineering (Adli, 2018; Gaudelli et al., 2017; G. Liu et al., 2022).

HYPOTHESIS AND AIMS

HYPOTHESIS AND AIMS

Currently there are several caveats and pitfalls in human muscular disorder research, as well as unmet medical needs that require better tools for the research of disease pathophysiology and the development of new treatments.

In the case of LGMDR1, the study of its pathophysiology faces several challenges due to the multiple features of the disease. In the first place, being a rare condition, the number of patients providing clinical data is reduced compared to other diseases. In addition to this, currently genetic diagnosis can be performed from blood samples (Blázquez et al., 2008) without the need of a muscle biopsy, therefore reducing the availability of the much-appreciated muscle samples from patients that were used both to study the sample itself or to stablish patient-derived muscle primary cell cultures.

An additional difficulty when studying LGMDR1 and the role of calpain 3 lies in the autolytic activity of calpain 3, which makes the protein highly unstable and with a very short half-life (Fanin, et al., 2007). This has prevented the determination of its three-dimensional structure, and the fact that most commercially available antibodies against calpain 3 have specificity issues, has hindered the study of the different potential roles of calpain 3. Generally, there is not a clear genotype-phenotype correlation in patients (Sáenz et al., 2005), and despite the proposed roles of calpain 3 discussed in the introduction, none of these functions appears to precisely explain how mutations in the calpain 3 gene lead to the muscle degeneration observed in LGMDR1 patients. Moreover, many of the observations described in the *in vitro* and *in vivo* models have not been confirmed to occur in patients and have not been reproduced in other models or studies.

From the different *in vitro* models that have been used for LGMDR1 research, patient-derived primary myoblasts as well as patient-derived iPSCs have been used to differentiate them into myotubes and make comparative studies, however, variability between individuals both within controls and patients is a recurring problem that added to the intrinsic variability of the long protocols for myogenic differentiation, poses inconveniences when using these models (Jaka et al., 2017; Mateos-Aierdi et al., 2021; Rico et al., 2021). Alternatively, the use of immortalized myoblasts with calpain 3 silencing while being useful to study certain aspects (Lasa-Elgarresta et al., 2022), the

modifications included in those lines to avoid senescence and the potential incomplete silencing of the gene make these models potentially less accurate.

On the other hand, the *in vivo* models developed in mice (Kramerova et al., 2004; Ojima et al., 2010; Richard et al., 2000), despite providing valuable information about the role of calpain 3 in the skeletal muscle, fail to reproduce the clinical features and muscle wasting that occurs in LGMDR1 patients. Which suggests that mouse models could have compensatory mechanisms that alleviate the muscle degeneration that the lack of calpain 3 causes in humans.

Taking everything into account and the existing experience in the group with various of the mentioned models, we considered that while it is worth to use the available models to try to elucidate the implications of the absence of calpain 3 in the muscle, better models are required to progress in the understanding of the disease and the development of new therapies.

With this in mind, the work in this thesis has been focused in 3 main objectives, that have been developed in 3 chapters, 1) for the development of an *in vitro* model based in isogenic calpain 3 KO iPSC lines, 2) to evaluate the implications of the absence of calpain 3 in some of the described processes as well as exploring new mechanisms that could be affected using the developed *in vitro* model as well as the existing C3KO mice model, and 3) to develop a new *in vivo* model based in the porcine species that we expect could overcome the limitations found in the current mouse models.

OBJECTIVES:

1. The generation of isogenic calpain 3 KO iPSC lines with CRISPR/Cas9 for the development of an *in vitro* model.

    1.1. To obtain isogenic calpain 3 KO iPSC lines with CRISPR/Cas9 from a control iPSC line.
    1.2. To characterize the generated isogenic lines for pluripotency maintenance and CRISPR/Cas9 off-targets.
    1.3. To establish an optimized myogenic differentiation protocol from iPSCs to myotubes.

2. To study damage response, myogenesis and protein homeostasis in calpain 3 KO models of LGMDR1.

    2.1. To study the early response to acute muscle damage in the C3KO mouse model.
    2.2. To evaluate the myogenic capacity *in vitro* of mouse SCs and human isogenic iPSCs derived myogenic progenitors in the absence of calpain 3.
    2.3. To evaluate C3KO running performance in functional studies and pathways associated with protein homeostasis.
    2.4. To evaluate the response to electrostimulation of human isogenic iPSCs derived myotubes in the absence of calpain 3.
    2.5. To evaluate the use of 4-PBA to improve proteostasis in the C3KO mice and human isogenic iPSCs derived myotubes in the absence of calpain 3.

3. The generation of a LGMDR1 pig model with CRISPR/Cas9

    3.1. To design and test CRISPR/Cas9 guides to generate calpain 3 KOs in pig fibroblasts.
    3.2. To test and optimize the obtention of calpain 3 KO embryos in pigs and transfer the embryos to recipient sows to obtain a calpain 3 KO pig.
    3.3. To characterize the obtained calpain 3 KO pig model.

MATERIALS AND METHODS

MATERIALS AND METHODS

iPSC culture

All iPSCs used had been previously generated by reprogramming human skin fibroblasts and maintained pluripotency markers expression and iPSC morphology (Mateos-Aierdi et al., 2021). Unless stated otherwise, iPSCs were cultured on cell culture dishes coated with Matrigel (1:50) in mTeSR1 medium supplemented with 100 U/ml penicillin and 100 μg/ml streptomycin (1% pen-strep). Cell medium was replaced daily. Cells grew forming colonies and these were passaged before colonies reached confluence with accutase or ReLeSR reagent depending on the purpose, neutralized with the same medium and centrifuged for 5 minutes at 300g. Following passaging and in order to improve cell survival, cells were seeded in culture medium supplemented with 5 μM Y-27632 rock inhibitor for 24 hours when passaged with ReLeSR and supplemented with 10% CloneR for 24 hours when passaged with accutase. For freezing the cells, FBS with 10% DMSO was used.

iPSC calpain 3 KO generation with CRISPR/Cas9

Guide design

CRISPR/Cas9 RNA guides were designed using the Breaking-Cas CNB software(Oliveros et al., 2016) and the calpain 3 exon 1 sequence from the NCBI Reference Sequence: NG_008660.1. From the available target sites for Cas9 in exon 1 of calpain 3, 4 guides were selected either directly targeting the start codon of the protein or within 100 bp of the start codon and taking into consideration the overall score given by the software (Table 1).

#	Sequence
Guide 1	5′-ATAAGATACAGCTACCTTCA-3′
Guide 2	5′-GACCGTCATTAGCGCATCTG-3′
Guide 3	5′-ATGACGGTCGGCATGGCAAG-3′
Guide 4	5′-CAGCCTCAGTGGCCTTGCTC-3′

Table 1. CRISPR/Cas9 guide sequences to target exon 1 of human calpain 3.

CRISPR/Cas9 transfection and clonal selection

iPCSs were detached from the culture dishes by incubating them with accutase until colonies were completely disaggregated. The cells were then neutralized with culture media, centrifuged for 5 min at 300g and seeded in 24-well (1.9 cm^2/well) cell culture dishes coated with Matrigel (1:50) in mTeSR1 Medium supplemented with 10% CloneR at a density of 50,000 cell/well for 24 hours.

To prepare the CRISPR/Cas9 RNA guides, two-part crRNA:tracrRNA oligo duplexes were used. Equimolar quantities of each oligo were mixed and diluted in Annealing buffer to a final concentration of 80 μM, and incubated at 95°C for 5 minutes followed by 60°C for 1 minute to anneal the oligos. In order to form a ribonucleoprotein complex (RNP) with Cas9 nuclease, 8μL of each duplex-guide were incubated with 3.2 μL of Cas9 nuclease (4μg/μl) in 13.8 μL DMEM-F12 medium for 10 minutes at RT. Both RNA guides and Cas9 purchased from Stemcell Technologies. The RNP-complex was then diluted 1:2 in DMEM-F12 and TransIT-X2 transfection reagent was added to a final concentration of 2% and incubated for 20 minutes at RT. Finally, 50μL of this solution was added per well of iPSC with freshly replaced media. In the cases where 2 guides were used simultaneously, 25μL of each preparation were added.

48 hours after the transfection the cells from each well were detached with accutase, and half of the cells were diluted and seeded in 24-well cell culture dishes. The other half of the cells were used to analyze whether the expected mutations were detectable in the cell pool. If the mutation was detectable, the 24-well dish was analysed in order to select the well that was most enriched in mutations and this was subcloned at a density of 0.7 cells/well into a 96-well cell culture dishes in order to isolate clonal populations and genotype them.

CRISPR/Cas9 mutation detection and analysis in iPSCs

DNA was extracted from cell pellets with the Purelink Genomic DNA kit following manufacturer's instructions. The calpain 3 start codon region of 316bp was amplified by PCR (Table 2) and analysed in a 2% agarose gel electrophoresis in TBE buffer.

Calpain 3 start codon region PCR	
hEx1_Fwd	5'-GGACATAACCTGTACGACCTTC-3'
hEx1_Rev	5'-GGCTGATGATGGCTGAATAGA-3'
PCR Program	95ºC – 5 min 35 cycles (95ºC – 30 sec, 52ºC – 30 sec, 72ºC – 30 sec) 72ºC – 5 min

Table 2. PCR primers and program for human calpain 3 start codon region.

In the cases were the iPSCs were transfected with two RNA guides simultaneously, the resulting deletions were directly observed in the agarose gel. In the cases where the RNA guide was directly targeting the start codon and to evaluate if the mutation had taken place, the PCR product was digested with Hin1II restriction enzyme. For this the PCR product was purified with QUIAquick PCR purification kit following manufacturer's instructions and 400µg of the purified product was digested over-night at 37ºC with 10U of Hin1II and 1x Buffer G. The digestion products were analysed in a 2% agarose gel electrophoresis in TBE buffer. In order to sequence different fragments from a PCR, these were separated in a 2% agarose gel electrophoresis, cut out and purified with GeneJET Gel Extraction Kit following manufacturer's instructions, diluted 1:100 in water and sequenced.

iPSC Characterization

Off-target analysis

Potential off-target sites for each CRISPR/Cas9 RNA guide were calculated using Cosmid software (Cradick et al., 2014), allowing up to 3 mismatches in case of no indels and up to 2 mismatches in case of 1 base indels. For each guide, the top 5 potential off-targets were selected based on the score given by the software. These regions were amplified by PCR (Table 3) and sequenced by Sanger sequencing at the Genomics Platform of the Biodonostia HRI. The obtained sequencing chromatograms of the KO clones were aligned with the control with Snapgene software to determine if an off-target mutation had occurred.

Off-target	Forward primer	Reverse Primer	Tm(ºC)
Guide 1 off-1	5′-GGGTCCTTAGCACTGTTTT-GTCAC-3′	5′-CAAAGAAGCAGGATCTGAA-ATCTCACAGC-3′	57
Guide 1 off-2	5′-TCCAGGCATGAGCCACTGCA-3′	5′-CCCCCTTGTTATCTCACTGGTC-3′	56
Guide 1 off-3	5′-GCCTCTTCTCATGTTCATT-CTCAAAGGTTTTC-3′	5′-GTAAGGAGGCAATTTTTCT-GGTTATTTTGCTGTC-3′	61
Guide 1 off-4	5′-GGATTTGTTTGTTTGTTTT-TGAACAGGGTCTGG-3′	5′-CTCTACCTACCCTGTTTGA-AAAGTTCATCAC-3′	60
Guide 1 off-5	5′-GCTCTTTCATCATTTAAG-GTATCAGGCATTTTATGCA-3′	5′-CATATGAGTCTCTGTAA-ACACATAGACCACTG-3′	61
Guide 2 off-1	5′-CACAAACAACCGGTTGCT-GGTTGC-3′	5′-GCAATTGGGTTGACTTTG-GATTTAGAGAGG-3′	59
Guide 2 off-2	5′-TTGCCATCGGAACTCTTCCACC-3′	5′-CAGAGTGGAGGGCAGACAGA-3′	56
Guide 2 off-3	5′-GAGCAGGATAGGAGTGAGCC-3′	5′-TGAGTCACTCTGCTGGGTGC-3′	56
Guide 3 off-1	5′-CTGTTTCCACAGGCTT-TTCAGGAG-3′	5′-CCAAGAAGCCAATTTTCT-CTGCCC-3′	57
Guide 3 off-2	5′-AGAGGAGCTCAAAACA-CTGAGCTG-3′	5′-TTCTGCCTCTCCCTACCCAC-3′	56
Guide 3 off-3	5′-GTGTCAGAGGACAGCA-TCAAACAG-3′	5′-CACAACCTCCCTCAGTTC-CATAG-3′	57
Guide 3 off-4	5′-TTAACATATGTTTCGCA-ATTTACACTGCAGATCTGCT-3′	5′-GTAGGCCATATGTAAATGATC-TTTCATGCATTAACAC-3′	51
Guide 3 off-5	5′-GACAGTGTCCCTGGAGGTAC-3′	5′-ACTTCAGCCTGGGCCAGGAAGA-3′	58

Table 3. PCR primers for the CRISPR/Cas9 off-target sites analysed for each RNA guide. Melting temperature (Tm) indicates the temperature utilized in the annealing step for each PCR.

In vitro differentiation into primordial germ layers

Differentiation of iPSCs into cell types derived from each of the three primordial germ layers of the embryo was performed culturing the cells in specific culture medias. First, the iPSCs were culture in suspension in mTeSR1 medium supplemented with 5 μM Y-27632 rock inhibitor without Matrigel and on Nuclon Sphera Dishes, until cell aggregates known as embryoid bodies (EBs) were visible after 2-5 days. Endodermal differentiation was induced by culturing EBs in KO-DMEM medium supplemented with 10% FBS, 2mM GlutaMAX, 1x NEAA, 50 μM 2-mercaptoethanol and 1% pen-strep for 3-4 weeks. For Mesoderm differentiation, EBs were cultured in 0.1% gelatin-coated plates with KO-DMEM medium supplemented with 10% FBS, 2 mM GlutaMAX, 1x NEAA, 50 μM 2-mercaptoethanol, 100 μM ascorbic acid and 1% pen-strep for 3-4 weeks. Ectodermal differentiation was induced culturing the EBs 10 more days in suspension in N2B27 medium, which consisted of a 1:1 mix of DMEM/F12 medium and Neurobasal medium, with 2 mM GlutaMAX, 0.5x B-27 supplement, 0.5x N-2 supplement, 10 ng/ml FGF2 and 1% pen-strep followed by 3-4 weeks of culture in matrigel-coated plates in N2B27 medium without FGF2. In all cases the media was replaced every 2-3 days.

Karyotype analysis

Karyotype analysis was performed on proliferating iPSC control and selected calpain 3 KO clones. Cells were incubated for 45 minutes in mTeSR1 medium with 20 ng/ml colcemid, washed twice in PBS, detached using 0.25% trypsin-EDTA to ensure maximal cell separation, neutralized, centrifuged and washed with PBS again. The cell pellet was resuspended in 10 ml of warmed hypotonic solution (0.075 M KCl) that was added to the cells dropwise, while the cells were being vortexed. Cells were incubated at 37°C for 10 minutes and 1 ml of chilled Carnoy's fixative solution was added to the cells drop wise (methanol:acetic acid, 3:1), also while vortexing. Finally, cells were centrifuged and resuspended in 10 ml of cold Carnoy's fixative solution, and stored at -20°C until karyotype analysis was performed at the Donostia University Hospital by a cytogeneticist with the G-banding method. For each KO clone 20 metaphase karyotypes were analysed.

iPSC Myogenic differentiation and medium optimization

Infection of iPSCs with doxycycline-inducible PAX7 system

The doxycycline-inducible PAX7 system with GFP reporter comprised of the rtTA-FUGW and hPAX7-pSAM2 vectors (kindly provided by Dr. Perlingeiro, University of Minnesota)(Darabi & Perlingeiro, 2016) were packaged in VSV-G 2nd generation Lentivirus by the Viral Vectors Unit (CNIC, Madrid). iPSCs were detached with accutase to ensure cell disaggregation prior to infection and $6 \cdot 10^5$ cells per well were seeded in matrigel-coated 6-well plates in mTeSR1 medium supplemented with 1% pen-strep and 10% CloneR for 24 hours. The following day, cells at 40-50% confluence were infected using hPAX7-pSAM2 and rtTA-FUGW lentivirus at MOI 5.0 with 4 µg/ml polybrene in the freshly added medium. The medium was not changed for the next 48 hours to allow infection to happen. When the infected cells reached 70-80% confluence they were expanded and infection efficiency was determined by incubating cells with 1 µg/ml doxycycline for 24 hours and estimating the percentage of GFP-positive cells by flow cytometry in a Guava EasyCyte 8HT Flow Cytometer. If infection rates were over 20% it was considered sufficient and the expanded infected cells were frozen to generate stocks of infected iPSCs.

Differentiation of iPSCs into PAX7-GFP+ myogenic progenitor cells

iPSCs with the *rtTA-hPAX7* system were detached using accutase and plated in 60mm Nuclon Sphera dishes without any coating, at a density of $1 \cdot 10^6$ cells in 5 ml mTeSR1 medium with 10 µM ROCK inhibitor. After 2 days, homogeneous EBs formed in the plates. Culture medium was switched to myogenic EB medium (IMDM medium supplemented with 15% FBS, 10% horse serum, 2 mM GlutaMAX, 50 µg/ml ascorbic acid, 1% chick embryo extract, 4.5 mM monothioglycerol and 1% pen-strep) supplemented with 10 µM GSK3β - inhibitor (CHIR 990217) and 5 µM ROCK inhibitor. After 2 days, the medium was switched to EB medium supplemented with 200 nM BMP pathway inhibitor (LDN-193189). 10 µM of Activin/BMP/TGF-B pathway inhibitor (SB-431542) and 5 µM ROCK inhibitor for 24 hours. At this point, the medium of the plates was supplemented with 1 µg/ml doxycycline to induce *PAX7* expression for 24 hours and then the medium of the plates was the replaced with EB medium supplemented with 1 µg/ml doxycycline for 48 hours. At day 8 of the induction protocol, EBs were transferred to 0.1% gelatin-coated T75

flasks in EB medium supplemented with 1 µg/ml doxycycline and 5 ng/ml FGF_2. Flasks were incubated for 72 hours avoiding movement to maximize EB attachment to the surface. After that, medium was renewed and 24 hours later the cells were FACS sorted for GFP to purify the PAX7 positive (PAX7-GFP+) myogenic progenitors. For FACS sorting, the cells were detached using 0.25% trypsin and taken to the cell sorting facility in ice chilled sorting buffer (DPBS with 0.5% BSA, 25 mM HEPES and 5 mM EDTA, pH 7.2). The cells were sorted at the Cytometry platform at CIMA research center. Sorted PAX7-GFP+ myogenic progenitors were plated in 0.1% gelatin-coated EB medium with 1 µg/ml doxycycline and 5 ng/ml FGF_2. These progenitors were expanded every 3 days for up to 4-5 passages and frozen stocks were generated for future experiments.

Terminal differentiation of PAX7-GFP+ myogenic progenitors into myotubes

iPSC-derived myogenic progenitors were plated at a density of 37.000 cell/cm^2 on 6-well or 24-well plates and on 2- or 4-well chamber slides for immunofluorescence detection. The cells were cultured in EB medium with 1 µg/ml doxycycline and 5 ng/ml FGF_2 to allow them to proliferate until 80-100% confluence was reached. At this point cells were washed with DPBS and differentiation medium was added. The differentiation medium was not changed for the first 72 hours, and after that it was renewed every 48 hours.

Different differentiation mediums and variations were tested. Medium A consisted of high glucose DMEM supplemented with 15% KOSR, 2 ng/ml IGF1, 10 ng/ml HGF and 1% pen-strep (Chal et al., 2016). Medium S consisted of KnockOut DMEM supplemented with 20% KOSR, 1% NEAA, 1% GlutaMAX and 1% pen-strep and was supplemented with small molecules SB-431542, DAPT, froskolin and dexamethasone at 10 µM each (Selvaraj, Dhoke, et al., 2019). Variations of this medium tested included removing dexamethasone after day 3 of differentiation, supplementing it with 2 ng/ml IGF1, or adding a FOXO1 inhibitor (AS1842856) at 33 nM. Differentiation medium-2 (DM-2) was only added after day 8 of culture and consisted of Neurobasal A medium with B27 supplement, 1x GlutaMAX, 20ng/mL of BDNF, 50ng/mL SHH, 10ng/mL IGF-1, 5ng/mL CNTF, 20ng/mL NT-3, 4µg/mL laminin, 100ng/mL agrin and 50µg/mL gentamicin (Toral-Ojeda et al., 2018).

Different coating and overlay combinations were also tested. Coating consisting of 0.1% gelatin with 2.4 µg/mL laminin was prepared in water and incubated on the wells for 20

minutes. Cultrex-HA coating consisting of cultrex at 2.77 mg protein/mL and hyaluronic acid (HA) at 2.5 mg/ml was prepared in PBS pH 7.4 and incubated on the wells for at least 48 hours at 37ºC (García-Parra et al., 2012). Overlays consisted of applying different extracellular matrix preparations on top of confluent progenitor cells at the start of the differentiation protocol. ECMG was diluted 1:3 in differentiation medium and added to the cells in enough volume to cover them, incubated 30 minutes at 37ºC and removed replacing the solution for the differentiation medium. Matrigel was added in 1:100 dilution on differentiation medium and left there until media was changed. The cultrex with hyaluronic acid overlay (cultrex-HA) consisted in the same solution used for the coating diluted 1:4 in differentiation medium, incubated 30 minutes at 37ºC on top of the cells and removed replacing the solution for the differentiation medium. All coating and overlay preparations were made in ice to avoid their premature polymerization until they were added to the cell wells.

Electrical pulse stimulation (EPS) of myotubes

At day 6 of differentiation, myotubes plated in 6-well plates were incubated with electrodes from C-Pace EP (Ion Optix). EPS stimulation parameters were 6 ms, 4 V and 0.2 Hz for 48 hours. At day 8 of differentiation, the parameters were changed to 6 ms, 15 V, 0.1 Hz for 4 more days.

To calculate pulsating myotube ratios, 9 areas per well were recorded for 2 minutes and the number of myotubes that were visibly contracting during the recording was divided by the total amount of myotubes in the field.

Gene expression analysis

RNA was extracted from cells with Qiazol and the miRNeasy Mini Kit and 1.25 µg of RNA was retrotranscribed using the High-Capacity cDNA Reverse Transcription Kit, following manufacturer's instructions.

Gene expression analysis of pluripotency markers

Expression of endogenous *SOX2, OCT4, KLF4, cMYC, CRIPTO, NANOG*, and *REX1*, and transgenic *OCT4*, *SOX2*, *KLF4* and *cMYC* pluripotency genes were determined through qPCR, using specific primers for each of the genes (Aasen et al., 2008) (Table 4) and KiCqStart SYBR Green qPCR ReadyMix, in a Bio-Rad CFX384 Touch machine.

Target	Forward primer	Reverse primer
Trans-*OCT4*	5′-TGGACTACAAGGACGACGATGA-3′	5′-CAGGTGTCCCGCCATGA-3′
Trans-*SOX2*	5′-GCTCGAGGTTAACGAATTCATGT-3′	5′-GCCCGGCGGCTTCA-3′
Trans-*KLF4*	5′-TGGACTACAAGGACGACGATGA-3′	5′-CGTCGCTGACAGCCATGA-3′
Trans-*cMYC*	5′-TGGACTACAAGGACGACGATGA-3′	5′-GTTCCTGTTGGTGAAGCTAACGT-3′
Endo-*OCT4*	5′-GGGTTTTTGGGATTAAGTTCTTCA-3′	5′-GCCCCCACCCTTTGTGTT-3′
Endo-*SOX2*	5′-CAAAAATGGCCATGCAGGTT-3′	5′-AGTTGGGATCGAACAAAAGCTATT-3′
Endo-*KLF4*	5′-AGCCTAAATGATGGTGCTTGGT-3′	5′-TTGAAAACTTTGGCTTCCTTGTT-3′
Endo-*cMYC*	5′-CGGGCGGGCACTTTG-3′	5′-GGAGAGTCGCGTCCTTGCT-3′
NANOG	5′-ACAACTGGCCGAAGAATAGCA-3′	5′-GGTTCCCAGTCGGGTTCAC-3′
CRIPTO	5′-CGGAACTGTGAGCACGATGT-3′	5′-GGGCAGCCAGGTGTCATG-3′
REX1	5′-CCTGCAGGCGGAAATAGAAC-3′	5′-GCACACATAGCCATCACATAAGG-3′
GAPDH	5′-GCACCGTCAAGGCTGAGAAC-3′	5′-AGGGATCTCGCTCCTGGAA-3′

Table 4. qPCR primers for the expression analysis of pluripotency genes. To distinguish transgenic and endogenous expression of reprogramming genes, gene names are indicated with endo- (endogenous) and trans- (transgenic) prefixes.

Gene expression analysis of differentiated myotubes

Gene expression levels were determined through qPCR, using commercially available TaqMan probes and TaqMan Gene Expression Master Mix, in a Bio-Rad CFX384 Touch machine (Table 5).

Target	Reference	Brand
DMD	Hs00758098_m1	Thermo Fisher
GAPDH	Hs99999905_m1	Thermo Fisher
MYH2	Hs00430042_m1	Thermo Fisher
MYH3	Hs01074230_m1	Thermo Fisher
MYOD1	Hs00159528_m1	Thermo Fisher
MYOGENIN	Hs01072232_m1	Thermo Fisher
PAX7	Hs00242962_m1	Thermo Fisher
TBP	Hs00427620_m1	Thermo Fisher
CAPN3	Hs00544982_m1	Thermo Fisher
FBXO32	Hs01041408_m1	Thermo Fisher
HSF1	Hs00232134_m1	Thermo Fisher
HSP70 (HSPA1A)	Hs00359163_s1	Thermo Fisher
HSP90 (HSP90AA1)	Hs00743767_sH	Thermo Fisher
DNAJA4	Hs00388055_m1	Thermo Fisher
MELUSIN (ITGB1BP2)	Hs00900209_g1	Thermo Fisher
HSP60 (HSPD1)	Hs01941522_u1	Thermo Fisher
CRYAB	Hs00157107_m1	Thermo Fisher
HSP27 (HSPB1)	Hs00356629_g1	Thermo Fisher
CHIP (STUB1)	Hs00195300_m1	Thermo Fisher
Spliced *XBP1*	Hs00231936_m1	Thermo Fisher
Unspliced *XBP1*	Hs03929085_g1	Thermo Fisher
GRP94 (HSP90B1)	Hs00427665_g1	Thermo Fisher
BIP (HSPA5)	Hs99999174_m1	Thermo Fisher
GRP75 (HSPA9)	Hs00269818_m1	Thermo Fisher
MYH7	Hs01110632_m1	Thermo Fisher
PPARD	Hs04187066_g1	Thermo Fisher
GLUT4 (SLC2A4)	Hs00168966_m1	Thermo Fisher

Table 5. TaqMan probes used to analyse gene expression. Names in parentheses are gene name aliases.

Protein extraction

Protein from mouse muscles was extracted by placing 10-20 mg of frozen muscle in 1:20 weight to volume ratio with Nicholson protein extraction buffer (Anderson & Davison, 1999) and mechanically disrupting the sample. Nicholson protein extraction buffer consists of 1.25 M tris hydrochloride pH 6.8, 5% 2-mercaptoethanol, 4M urea, 4% Sodium dodecyl sulfate (SDS), 1% Glycerol, 0.001% Bromophenol blue, 50 mM ß-glycerophosphate, 5 mM Sodium pyrophosphate and 1 tablet of Complete Protease Inhibitor Cocktail. To disrupt the sample a 2.4 µm stainless steel bead (Omni-Inc) was placed with the sample and buffer and shaken at 6 m/s for 45 sec in a Bead Ruptor 12 (Omni-Inc). The samples were chilled on ice for 20 sec and the process was repeated 4 to 6 times until the muscle was completely dissolved. At this point the samples were centrifuged for 5 minutes at 524 g and supernatants containing the protein were stored at -80ºC.

To extract protein from cultured myoblasts, protein extraction buffer consisting of 20 mM Tris HCl pH 8, 1 mM DTT, 0.1 mM EDTA, 28 µM E-64, 20 µg/ml soybean trypsin inhibitor and 2 mM PMSF, 5% 2-mercaptoethanol and 1x loading buffer was used. Culture plates were washed twice with DPBS, put on ice and protein extraction buffer was directly added to each well (10µl/cm^2). Cells were harvested using cell scrapers and the sample was directly stored at -80ºC.

To quantify protein concentration, samples were diluted 1:50 in water and Bio-Rad protein-assay reagents were used following manufacturer's instructions. Absorbance at 595 nm was measured in a microplate reader in technical triplicates for each sample.

Western blot analysis

For Western blot analysis, the same amount of protein from each sample (8-20 µg) was diluted in the extraction buffer and 1x loading buffer and heated at 95°C for 5 minutes to denature the proteins. The samples were loaded into Min-PROTEAN TGX 4-20% gradient SDS-PAGE precast gels with the Precision Plus Kaleidoscope Protein ladder as protein size marker. Gels were run at 100V in a Tris-glycine buffer (25mM Tris, 200mM glycine, 0.15% SDS). Proteins were transferred to nitrocellulose membranes using the Mini Trans-Blot Electrophoretic Transfer system for 1 hour at 400 mA. Membranes were stained with

Ponceau S solution to ensure proteins were transferred and the membrane was cut at specific heights guided by the protein ladder if multiple proteins were going to be analysed in the same membrane at different heights for different molecular weights (MW). Membranes were blocked with 5% skimmed milk in TBST (0.05 M Tris, 0.2 M NaCl, 1% triton X-100, pH8) in agitation for 1 hour at RT. Membranes were rinsed and incubated overnight with the primary antibodies diluted in 5% BSA in TBST (Table 6) in a shaker at 4ºC. The next day, membranes were washed three times in TBST and incubated in secondary antibody diluted in 5% skimmed milk in TBST for 1 hour at RT. Secondary antibodies were always HRP conjugated against the host species of the primary antibody (P0448, P0447, P0449, Dako). Finally, membranes were washed two times in TBST and once in TBS and proteins were detected by chemilluminescence using the SignalFire ECL reagent as substrate, or Immobilon ECL Ultra if stronger signal was required. Chemiluminescence signals were acquired with an iBright apparatus (Thermo scientific) and quantified using Image Studio Lite 4.0 software.

Target	**Host species**	**Dilution**	**Reference**	**Brand**
α-ACTININ	Mouse	1:1000	A7811	Sigma
β-CATENIN	Mouse	1:1000	sc-7963	Santa Cruz
A-CRYSTALIN B	Mouse	1:1000	sc-137129	Santa Cruz
AKT	Rabbit	1:1000	9272	Cell Signalling
BIP	Rabbit	1:1000	ab21685	Abcam
CALNEXIN	Rabbit	1:250	2433	Cell signalling
CALPAIN 3	Mouse	1:250	MONX10794	Sanbio
CAMKIIB	Mouse	1:1000	13-9800	Thermo Fisher
CHIP/STUB1	Mouse	1:1000	sc-133083	Santa Cruz
CHOP	Mouse	1:1000	2895	Cell Signalling
CI-NDUF	Mouse	1:1000	ab110411	Abcam
CII-SDHB	Mouse	1:1000	ab110411	Abcam
CIII-UQCRC2	Mouse	1:1000	ab110411	Abcam
CSRP3	Rabbit	1:250	NBP2-92797	Novus Biologicals
CV-ATP5A	Mouse	1:1000	ab110411	Abcam
DMD	Mouse	1:300	MANDYS1(3B7)	DSHB
GAPDH	Rabbit	1:5000	2118	Cell Signalling
GLUT4	Mouse	1:300	2213	Cell Signalling
GRP94	Rabbit	1:1000	2104	Cell Signalling
GSK3-β	Rabbit	1:1000	9323	Cell Signalling
HSP27	Mouse	1:1000	sc-13132	Santa Cruz
HSP70	Mouse	1:1000	sc-32239	Santa Cruz
ITGB1D	Mouse	1:500	MA5-17103	Thermo Fisher
LC3	Rabbit	1:1000	4108	Cell Signalling
mTOR	Rabbit	1:1000	2983	Cell Signalling

MYBBP1A	Rabbit	1:1000	NBP2-13630	Novus Biologicals
MYH3	Mouse	1:300	F1.652	DSHB
MYHC	Mouse	1:1000	MF20	DSHB
MYOD1	Rabbit	1:500	138125	Cell Signalling
MYOGENIN	Mouse	1:500	F5D	DSHB
NF-κB-1	Rabbit	1:1000	8242	Cell Signalling
p-AKT	Rabbit	1:500	4060	Cell Signalling
p-AMPK	Rabbit	1:500	2531	Cell Signalling
p-CAMKII	Mouse	1:500	PA537833	Thermo Fisher
p-GSK3-β (S9)	Rabbit	1:500	9323	Cell Signalling
p-mTOR (S2448)	Rabbit	1:1000	2971	Cell Signalling
p-P53	Mouse	1:500	9286	Cell Signalling
p-S6	Rabbit	1:1000	2211	Cell Signalling
P53	Mouse	1:1000	sc-126	Cell Signalling
PGC1-α	Rabbit	1:500	NBP1-04676	Novus Biologicals
RYR	Mouse	1:500	MA3-925	Thermo Fisher
SERCA2	Rabbit	1:500	9580	Cell Signalling
TOM20	Mouse	1:250	sc-17764	Santa Cruz
UBIQUITIN	Mouse	1:2500	GTX630148	Genetex

Table 6. Table of antibody references used for Western blot analysis. Secondary antibody dilution was always 1:5000.

Immunofluorescence analysis

Immunofluorescence detection of pluripotency and lineage-specific markers

Cells were fixed in 4% paraformaldehyde for 10 minutes and stored at 4°C in tris-buffered saline (TBS). For immunofluorescence detection, cells were washed three times in 0.1% triton-X100 in TBS for 5 minutes, and blocked in 0.5% triton-X100 and 6% donkey serum in TBS for 2 hours at RT. Samples were incubated with the primary antibodies, diluted in 0.1% triton-X100 and 6% donkey serum, for 48 hours at 4°C. Next, samples were washed three times with 0.1% triton-X100 in TBS for 5 minutes, blocked for 1 hour in 0.1% triton-X100 and 6% donkey serum, and incubated with the secondary antibodies diluted in 0.5% triton-X100 and 6% donkey serum, for two hours at RT and protected from light (Table 7). Finally, samples were washed 3 times, incubated 5 minutes in 10 µg/mL Hoechst, washed twice in TBS and mounted in Fluoro-Gel.

A panel of pluripotency markers were assessed in the control and selected calpain 3 KO clones, comprising the nuclear transcription factors SOX2, OCT4 and NANOG, the glycolipid antigens SSEA3 and SSEA4, and keratin sulfate antigens TRA-1-60 and TRA-

1-81. Immunofluorescence detection was performed on the iPSC lines cultured in top of 4-well chamber slides coated with Matrigel (1:50).

Primary Antibody		Secondary Antibody	
Target	**Dilution**	**Antibody**	**Dilution**
OCT4	1:60	Donkey-anti-MouseIGG-555	1:200
SSEA3	1:3	Goat-anti-RatIgM-488	1:200
SOX2	1:100	Donkey-anti-GoatIgG-488	1:200
SSEA4	1:3	Donkey-anti-MouseIgG-647	1:200
TRA-1-60	1:200	Donkey-anti-MouseIgM-Cy3	1:200
NANOG	1:50	Donkey-anti-GoatIgG-488	1:200
TRA-1-81	1:200	Donkey-anti-MouseIgM-Cy3	1:200

Table 7. Primary and secondary antibodies for the detection of pluripotency markers by immunofluorescence.

The same protocol was used to analyze the differentiation to different lineages with lineage-specific markers (Table 8).

Primary Antibody		Secondary Antibody	
Target	**Dilution**	**Antibody**	**Dilution**
AFP	1:400	Donkey-anti-RabbitIgG-488	1:200
SMA	1:400	Donkey-anti- MouseIgG-488	1:200
TUJ1	1:500	Donkey-anti- MouseIgG-555	1:200
GFAP	1:1000	Donkey-anti-RabbitIgG-488	1:200

Table 8. Antibodies for the detection of lineage-specific markers.

Immunofluorescence analysis of differentiated myotubes

Cells were fixed in 4% paraformaldehyde for 10 minutes, washed and stored at 4°C in DPBS. Cells were blocked in DPBS with 5% donkey serum (DS) + 0.3% triton-X100 for 1 hour at RT. Then samples were incubated with the primary antibodies, diluted in DPBS with 0.3% triton-X100 for 24 hours at 4°C. Next, samples were washed 2 times in DPBS and incubated with the secondary antibodies diluted in DPBS with 0.3% triton-X100 for 1 hour at RT and protected from light. Finally, samples were washed 2 times, incubated 5 minutes in 10 µg/mL Hoechst, washed twice in DPBS and mounted in Fluoro-Gel.

Primary Antibody		Secondary Antibody	
Target	**Dilution**	**Antibody**	**Dilution**
MYHC	1:100	Donkey-anti-MouseIgG-488	1:200
MYOG	1:50	Donkey-anti-MouseIgG-555	1:200
PAX7	1:50	Donkey-anti-MouseIgG-488	1:200
α-ACTININ	1:100	Donkey-anti-MouseIgG-488	1:200

Table 9. Antibodies used in immunofluorescence analysis of differentiated myotubes. Differentiation index was defined as the number of nuclei in myotubes expressing MYHC divided by the total number of nuclei in a field, and fusion index as the number of nuclei in myosin heavy chain expressing myotubes with 2 or more nuclei, divided by the total number of nuclei in a field.

Mouse procedures

Calpain 3 KO mouse (C3KO) mouse was generated in a C57BL/6 background and kindly provided by Kramerova and colleagues (Kramerova et al., 2004) Experiments were conducted in accordance with protocols approved by the Institutional Animal Care Ethical Board Committee of Biodonostia HRI (CEEA 17_015, OH17-27 PRO-AE-SS-104) and the Regional Government of Gipuzkoa, in accordance with the Spanish Royal Decree (53/2013), the European Directive 2010/63/EU and the guidelines established by the National Council on Animal Care.

Genotyping C3KO mouse

A small piece of ear tissue was obtained with an ear punch and mixed with lysis solution (NaOH 25 mM, EDTA 0.2 mM, pH 12) at 95ºC in agitation for 30 minutes. Right after, the solution was cooled in ice and neutralized with neutralization buffer (Tris-HCl 40 mM, pH 5). 0.5 µL of each sample were used in 24.5 µL of standard PCR master mix containing 3 primers for genotyping (Kramerova et al., 2004).

Primer	Sequence	Tm	Size(bp)
C3up	5′–GAAAGGGACAGGAGAAATGGAG –3′	60ºC	576 (WT) 324 (C3KO)
C3down	5′– CCTGAAACTTCAAGCCTCTGTTC–3′		
LTR2	5′– AAATGGCGTTACTTAAGCTAGCTTGC–3′		

Table 10. Primers for C3KO mouse genotyping. Melting temperature (Tm) indicates the temperature utilized in the annealing step for the PCR, and Size the length of the amplified fragment.

Cardiotoxin injection

TA and soleus muscles from four WT and four C3KO mice were injured with a cardiotoxin (CTX) injection. To do so, mice were anesthetized by inhaled isoflurane, administered at 5% concentration for induction and at 3% for maintenance during surgery. TA and soleus muscles from the right leg were injected with 20 µl and 10 µl respectively of cardiotoxin from Naja mossambica at 100 µM using a beveled 26G needle. The left legs of each mouse were used as undamaged controls. Mice were housed for 3 days and then sacrificed.

Mouse sacrifice and muscle extraction

To extract the muscles, mice were sacrificed by inhalation of 5% isoflurane followed by inhalation of CO_2. Muscles for protein analysis were extracted and frozen within an eppendorf tube in liquid N_2. Muscles for histological analysis were embedded in OCT (Optimal Cutting Temperature Compound) and frozen in liquid nitrogen-cooled isopentane. All muscles were stored at -80°C until sectioning or further processing.

4-PBA Treatment

Sodium phenylbutyrate (4-PBA) was dissolved at a concentration of 200 mg/dl in drinking water and mice were treated ad-libitum for 5 weeks, starting the treatment a week earlier than the exhaustion and voluntary running tests.

Exhaustion tests

Exhaustion tests were performed in mice running on a treadmill (Columbus Instruments). Before starting the tests, all mice were accustomed to the treadmill with a 20 minutes run at 16 cm/min for 3 days in a row. Based on a previously described protocol (Kramerova et al., 2016), mice ran at 8 cm/s for the first 5 minutes, at 16 cm/s for 10 minutes, at 20 cm/s for 20 minutes and at 23 cm/s for 30 minutes. At this point speed was increased +3 cm/s every 5 minutes until the mice were unable to continue. Mice were considered exhausted when they were not able to continue running on the treadmill for 1min, and when within that time it received 3 or more electrical shocks for staying in the static plate. All mice groups were subjected to 3 exhaustion tests every week in alternating days for 4 weeks, while during the weekends voluntary running was measured.

Voluntary running

Mice were placed individually into a cage with a running wheel that records distance, time and maximum speed (Med Associates Inc.). To get them used to running in the wheel, they were placed with the wheel for 2 days before starting the measurements. Voluntary exercise data was collected over the weekend for 48 hours by Wheel Manager Software (Med Associates Inc.).

Proteomics analysis

The proteomics study was performed at CIC Biogune's proteomics platform. Label Free nLC MS/MS of the soleus and TA muscles was performed in the WT and C3KO mouse in control (basal) muscles or CTX damaged muscles 3 days post damage, with 4 samples of each condition.

For the digestion, an equal volume of 7M urea, 2M thiourea, 4% CHAPS was added to the samples, and these were further incubated for 30 min at RT under agitation. Samples were digested following the filter-aided FASP protocol (Wiśniewski et al., 2009). Trypsin was added to a trypsin:protein ratio of 1:10, and the mixture was incubated overnight at 37ºC, dried out in a RVC2 25 speedvac concentrator (Christ), and resuspended in 0.1% FA. LC was performed using an NanoAcquity nano-HPLC (Waters), equipped with a Waters BEH C18 nano-column (200mm x 75 um ID, 1.8um). A chromatographic ramp of 120 min (5 to 60% ACN) was used with a flow rate of 300 nl/min. 0.5 ug of each sample were loaded for each run.

A Synapt G2Si ESI Q-Mobility-TOF spectrometer (Waters) equipped with an ion mobility chamber (T-Wave-IMS) for high definition data acquisition analyses. All analyses were performed in positive mode ESI. Data were post-acquisition lock mass corrected using the doubly charged monoisotopic ion of [Glu1]-Fibrinopeptide B. Accurate mass LC-MS data were collected in HDDA mode that enhances signal intensities using the ion mobility separation step. Progenesis LC-MS (version 2.0.5556.29015, Nonlinear Dynamics) was used for the label-free differential protein expression analysis. One of the runs was used as the reference to which the precursor masses in all other samples were aligned to. Only features comprising charges of 2+ and 3+ were selected. The raw abundances of each

feature were automatically normalized and logarithmized against the reference run. Samples were grouped in accordance to the comparison being performed. A peak list containing the information of all the features was generated and exported to the Mascot search engine (Matrix Science Ltd.). Database searching was performed using MASCOT 2.2.07 (Matrixscience, London, UK) against a UNIPROT - Swissprot database Release 2016_03 (550,740 entries) filled only with entries corresponding to Mus musculus (without isoforms). For protein identification the following parameters were adopted: carbamidomethylation of cysteines (C) as fixed modification and oxidation of methionines (M) as variable modifications, 15 ppm of peptide mass tolerance, 0.2 Da fragment mass tolerance and up to 3 missed cleavage points, Peptide charges of +2 and +3. The list of identified peptides was imported back to Progenesis LC-MS and protein quantitation was performed based on the three most intense non-conflicting peptides (peptides occurring in only one protein), except for proteins with only two non-conflicting peptides. The significance of expression changes was tested at protein level, and proteins identified with at least two peptides and an ANOVA p-value ≤ 0.05 and a ratio>1.5 in either direction were selected for further analyses.

Functional analysis of protein lists was determined by gene ontology (GO) enrichment of biological processes, molecular pathways and functions, using the DAVID Bioinformatic Resources Enrichment analysis tool (Sherman et al., 2022).

Histological analysis

Muscles embedded in OCT and frozen in liquid nitrogen-cooled isopentane were sectioned in cross-sections of 8 µm in a CM1950 Leica cryostat. For hematoxylin and eosin (HE) staining, slices were immersed into hematoxylin solution for 1min, and the excess was removed with washing water and then introduced into eosin 3 times. From this point on, the samples were cleaned and dehydrated by passing them through repeated solutions of 96º alcohol (x2), 100º alcohol (x2) and xylol (x2), immersing them 4 times in each bucket of solution. Finally, sections were mounted with a thin layer of Shandon Consul mounting medium and a coverslip. Images were taken at a Nikon 80i microscope.

Mouse satellite cells separation and culture

Satellite cell separation

SCs from diaphragms of mice were isolated using magnetic beads (MACS Separator, LS and MS columns, (Miltenyi Biotec) with the Satellite Cell Isolation Kit and the Anti-Integrin α-7 MicroBeads. Diaphragms were collected in HBSS with 2% pen-strep in ice and dissociated in a sterile petri dish using a scalpel and tweezers. After this the muscle was digested in 8 ml of collagenase IA (previously filtered) at 2,100 U/ml in HBSS, shaking at 180 rpm and at 37ºC for 60-90 minutes until it was well digested. Collagenase was inactivated with 15 mL of distilled water and the solution was filtered with a 40 µm cell strainer, centrifuged for 5 minutes at 524 g. Supernatant was removed and the pellet was incubated 2 minutes with 3 mL/sample of red blood cell lysis buffer, then inactivated with 10 mL of MACs buffer and centrifuged for 10 minutes at 524 g. Following this step the cell pellet was processed as described per manufacturer's instructions in the "Saltallite Cell Isolation Kit". The resulting cell population was centrifuged for 10 minutes at 300 g and processed with the Anti-Integrin α-7 MicroBeads kit to further purify α-7 integrin positive SCs population.

Sphere formation

α-7 integrin positive population from mouse diaphragms were plated on untreated p12 cell culture dishes (3.5 cm^2) in suspension at a density of 50,000 cell/well to allow the cells attach to each other and form spheres. The medium consisted of Neurobasal medium with 2% B-27, 1% of L-Glutamine 200mM and 1% pen-strep and each well was supplemented with 40 ng/ml rrEGF, 80 ng/ml rrFGF2 and 2% 1X LSGS. The first 3 days the medium was changed daily to clean the culture of cell debris, by centrifuging the cells 5 minutes at 524 g and resuspending them in fresh medium. After the 3rd day media was changed every 2 days. The number of spheres formed in each well were counted at day 7 and day 14 of culture. The size of the spheres was measured on optical images taken from the culture with D90 digital camera (Nikon) attached to Eclipse TS100 optical microscope (Nikon) and with ImageJ software to measure the diameter of each sphere.

Myogenic differentiation of spheres

Spheres obtained from SC culture in suspension were disaggregated by incubating spheres from each p12 well in 1mL of trypsin-EDTA 0.25% solution for 5 minutes at 37ºC. Once a suspension of single cells was obtained, trypsin was neutralized with 5mL of PBS and removed by centrifugation for 5 minutes at 524 g. The cell pellet was resuspended in 1 mL of differentiation medium consisting of Neurobasal medium with 10% FBS, 2% B-27, 1% of L-Glutamine 200mM, and 1% pen-strep. The cells were counted and plated in 4-well cell culture plates (1.9 cm^2) at a density of 80,000 cells/well. As coating for the plates, cultrex-HA coating was used, consisting of cultrex at 2.77 mg protein/mL and HA at 2.5 mg/ml, prepared in PBS pH 7.4 and incubated on the wells at 37ºC for at least 48 hours prior to plating the cells. The medium on the cells was left unchanged for the first 2 days of differentiation and then half of the medium was renewed every 2 days until the end of the culture, generally about 7 days later.

Calpain 3 KO pig generation with CRISPR/Cas9

Pig fibroblast culture

Primary pig fibroblasts were obtained from the skin of a male pig from a local farm and the skin biopsy was transported in RPMI 1640 medium with 1% pen-strep. 1 mm^2 skin bits were attached on T25 cell culture flasks for 3h at 37ºC vertically before being slowly submerged in medium consisting of DMEM, 13% NBCS, 1x Glutamax and 1% pen-strep. The explants were cultured without changing the medium for 3 weeks to allow fibroblasts to outgrow from the explants. At this point the cells were detached with 0.25% trypsin and expanded in MPF medium consisting of DMEM, 10% FBS and 1% pen-strep. Stocks were generated freezing $0.5 \cdot 10^6$ cells/cryotube in FBS with 10% DMSO.

Guide design

CRISPR/Cas9 RNA guides for the porcine calpain 3 gene were designed using the Breaking-Cas CNB software (Table 11). To design the guides Reference Sequence NC_010443.5 was used and the target regions were sequenced by sanger sequencing the fibroblasts and the pig colonies that were going to be used to generate the model. From the available target sites for Cas9 in exon 1 of calpain 3, 7 guides were selected to be used

in pairs flanking the start codon of the protein. 2 guides for exon 22 were designed targeting codon ARG788.

#	Sequence	Target
Guide 1	5′-GTCGGCATGACAGGCAAATT-3′	Exon 1
Guide 2	5′-CAGGCAAATTTGGAAGGGAA-3′	Exon 1
Guide 3	5′-ACAAGATACGGCTACCTTTA-3′	Exon 1
Guide 4	5′-ATAGACGCGCTAATGACAGT-3′	Exon 1
Guide 5	5′-TTAGCGCGTCTATGGCCCCA-3′	Exon 1
Guide 6	5′-GTCCCCAGGACCGATGCCCC-3′	Exon 1
Guide 7	5′-ATGGCTGAGTATTTACCACC-3′	Exon 1
Guide 22.1	5′-TCTATGACATCATCACCATG-3′	Exon 22
Guide 22.2	5′-TATCTGCTGCTTCGTCAGGC-3′	Exon 22

Table 11. CRISPR/Cas9 guide sequences to target exon 1 and exon 22 of porcine calpain 3.

CRISPR/Cas9 nucleofection in pig fibroblasts

CRISPR/Cas9 RNA guides were used either as two-part crRNA:tracrRNA oligo duplexes or as single-guide RNA oligos (sgRNA) both from IDT DNA. To form the RNP complex, 1.2μL of 100μM sgRNA or crRNA:tracrRNA guides were mixed with 2.1μL PBS and 1.7μL of Cas9 nuclease at 61μM and incubated at RT for 10-20 minutes. Pig fibroblasts grown in MPF medium were detached with 0.25% trypsin, neutralized with MPF medium, counted and centrifuged 5 min at 524 g. $0.5 \cdot 10^6$ cells were resuspended in P3 Primary Cell Nucleofector Solution where 5μL of the prepared RNP was added and the cells were electroporated twice with the DS-150 program in a 4D-Nucleofector system (Lonza). Following electroporation, fibroblasts were plated in T25 flasks with MPF medium for at least 48 hours before being analysed.

CRISPR/Cas9 mutation detection and analysis in pig fibroblasts

DNA was extracted from cell pellets with the Purelink Genomic DNA kit following manufacturer's instructions. For the detection of deletions or mutations in the target site, the regions were amplified by PCR (Table 12) and analysed in a 2% agarose gel electrophoresis, where deletions could be observed and guide combination efficiencies

were quantified by relative quantification of band density with Fiji software. PCR products were also Sanger sequenced and analysed with ICE CRISPR Analysis Tool (Conant et al., 2022) to determine the most frequent mutations being generated.

Primer	Sequence	Tm	Size(bp)
sEx1_Fwd_1	5′-GTTTTAAGACGGACGCAAGC-3′	57ºC	307
sEx1_Rev_1	5′-TTACCACCTGGGTTTCCAAC-3′		
sEx1_Fwd_2	5′-TTGGTTTTCCTGGCTCAAGC-3′	61ºC	842
sEx1_Rev_2	5′-CCTGAGTTCCAATTAATGCAAGGT-3′		
sEx22_Fwd	5′- AGGCTTCCACCTCAACAACC-3′	61ºC	202
sEx22_Rev	5′- AGGTGATCAGGCAGAGATGC -3′		

Table 12. PCR primers for porcine calpain 3. "sEx1" primers are for the start codon region in exon 1 and "sEx22" for the codon ARG788 region in exon 22. Melting temperature (Tm) indicates the temperature utilized in the annealing step for each PCR, and Size the length of the amplified fragment.

CRISPR/Cas9 guide testing in pig blastocysts

Pig procedures

All the procedures related with pig embryo obtention, *in vitro* fertilization (IVF) or embryo transfer to recipient sows was performed at the Physiology Dept. of the University of Murcia, (Murcia, Spain), in collaboration with the Physiology of Reproduction group. The study was developed according to the Spanish Policy for Animal Protection (RD 53/2013) and this project was approved by the Ethics Committee at the University of Murcia and Murcia Regional Government for the use of Genetically Modified Organisms (Reference A/ES/16/79).

In vitro maturation (IVM) of pig oocytes

Ovaries were obtained from Landrace and Large White crossbred sows from a slaughterhouse, transported in saline solution at 38ºC and washed in 0.04% cetrimide solution and saline solution at 38ºC. Cumulus-oocyte complex (COCs) were collected from follicles 3-6 mm in diameter, washed in DPBS with 1mg/ml polyvinyl alcohol (PVA) and in maturation medium NCSU37 (Petters & Wells, 1993). COCs were cultured for maturation in NCSU37 medium supplemented with dibutyryl cAMP, eCG and hCG for

22h at 38,5°C and 5% CO_2 and for 22 more hours in NCSU37 without the supplementation.

CRISPR/Cas9 microinjection and electroporation in pig oocytes

After IVM, matured oocytes were decumulated with a micropipette after incubating with hyaluronidase at 0.5% for 5 minutes and washed with 1mg/ml PVA in DPBS. For electroporation 50-100 oocytes were put in a drop with CRISPR/Cas9 RNP with 25ng/µl of each guide in a 1:2 or 1:1 Cas9:sgRNA molar ratio, and electroporated using 2,4 or 6 pulses, and 30V 1ms pulse with 100ms pulse intervals (Qin et al., 2015), in a ECM 830 Electroporation System (BTX, Harvard Apparatus, USA). In the case of introducing CRISPR/Cas9 by microinjection, oocytes were put in pairs in 6 µl PBS drops covered in mineral oil and then microinjected with an Eppendorf CellTram microinjector system (Navarro-Serna, Hachem, et al., 2021). CRISPR/Cas9 RNP were prepared as described above for testing in fibroblasts, and diluted to the desired concentration in PBS.

In vitro fertilization (IVF) of pig oocytes

In vitro matured oocytes were washed and placed in TALP medium with 0.3% BSA, 1 mM sodium pyruvate, and 50 µg/mL gentamycin (IVF-TALP) (Rath et al., 1999). 0.25mL frozen boar spermatozoa was thawed and selected by swim-up procedure (Navarro-Serna, Hachem, et al., 2021) diluting the semen in 2ml NaturARTsPIG sperm swim-up media at 38ºC and adding 1mL sperm swim-up media over the thawed-diluted sperm in a conical tube, incubated for 20 minutes at 38ºC at 45º angle and aspirating the sperm at the top. Concentration was adjusted to 10.000 spermatozoa/mL diluted in IVF-TALP and 250µL were added to 50-55 oocytes in 0.5mL total volume. Gametes were cocultured at 38.5ºC 5% CO2, and 7% O2 for 20-22 hours. Putative zygotes were cultured 24 hours in NCSU23a medium, cleavage was evaluated and 2-4 cell embryos were either transferred or cultured for an additional 156 hours in NCSU23b (Canovas et al., 2017). On day 6.5, blastocysts were collected.

CRISPR/Cas9 mutation detection and analysis in pig blastocysts

Blastocysts were denuded with 0.5% pronase and washed in nuclease free water. DNA extraction and PCR were performed with Phire Animal Tissue Direct PCR Kit following manufacturer's instructions. For the PCR, 1 µL of sample were used in 12.5 µL PCR reaction mix using 0.5 µM of primers (Table 12). With this PCR kit, annealing temperatures were modified, being 64.9ºC for exon 1 primers and 64.4ºC for exon 22. To detect the exon 1 mutations, PCR products were run in electrophoresis in 1.5% agarose gels and deletions were directly observed. To detect mutations in exon 22, fluorescent PCR-capillary gel electrophoresis was performed (Ramlee et al., 2015). PCR was carried out using fluorescently labeled forward primers (6-FAM). PCR products were diluted 1:100 in TE buffer and subsequently 1 µL in 11.5 µL Hi-DiTM formamide with 0.1 µL GeneScanTM 500 LIZ Size Standard. The mix was incubated 3 mins at 95°C, chilled in ice and analysed by capillary gel electrophoresis on a 3500 Genetic Analyzer (Applied Biosystems). Gene Mapper software was used to analyze the results.

Pig embryo transfers

In vitro produced embryos were transferred to females using cycling multiparous sows after weaning and synchronized gilts. Gilts were synchronized as previously described (Coy et al., 1993), by 1250 IU eCG equine chorionic gonadotropin followed by 750 IU hCG 56 h later. Embryo transfers were performed 44–46h after hCG injection. Multiparous sows showing heat symptoms at an interval of 2 days before and after the timing of IVF were selected for embryo transfers. For embryos in day 2 (D2) with 2-4 cells were transferred surgically into the oviduct to the uterotubal junction or to the oviduct. Alternatively, day 6 (D6) blastocysts were transferred non surgically to the uterus. All the embryo transfer procedures were carried out by University of Murcia veterinarians from the Physiology of Reproduction group.

Statistical analysis

Unless otherwise stated, results are expressed as mean ± standard deviation (SD) when working with data from individual animals, or standard error of the mean (SEM) when working with biological replicates of a cell line or culture condition. Outlier data was removed if detected, and distribution data was analysed by Saphiro wilk's test. If sample number was too small, it was considered normal distribution and Student's t-test was used in comparisons of two groups and one-way analysis of variance (ANOVA) when comparing 3 groups or more and Tukey's multiple comparison test was used. When multiple measures were taken from mice exhaustion experiments, one-way ANOVA for repeated measures (Mixed Model) was employed, applying Geisser-Greenhouse correction. For pig embryo statistics the variables in all experiments were tested for their normality by a Shapiro-Wilk test and data that was not normally distributed was analysed by a Kruskal-Wallis test. When data had significant differences ($p<0.05$), values were compared by a Conover-Inman test for pairwise comparisons. Data with normal distribution was analysed by one-way ANOVA. When data showed significant differences ($p<0.05$), values were compared by a pairwise multiple comparison post hoc test (Tukey). The level of significance was set at $p<0.05$ (*), $p<0.01$ (**) and $p<0.001$ (***). GraphPad Prism version 8.2.1 was used to perform statistical analysis.

Materials reference list

Product	Reference	Brand
Agarose	AG-0120	Ecogen
Agrin	550-AG-100	R&D Systems
Amersham™ Protran™ Nitrocellulose Membrane 0,2 µm	10600001	Cytiva
Annealing buffer	76020	Stemcell Technologies
Anti-Integrin α-7 MicroBeads	130-104-261	Miltenyi Biotec
B-27™ supplement	17504044	Gibco
BDNF	450-02	Peprotech
Bio-Rad protein-assay	5000002	Bio-rad
Biotaq DNA Polymerase (PCR kit)	BIO-21060	Bioline
Buffer G	BG5	Thermo Fisher
Cas9 nuclease ArciTect™	76002	Stemcell Technologies
Cas9 Nuclease V3 Alt-R®	1081058	Integrated DNA Technologies
Cetrimide	M7635	Sigma-Aldrich
Chamber slides 2-wells	177429	Thermo Fisher Scientific
Chamber slides 4-wells	177437	Thermo Fisher Scientific
Chick embryo extract	MD-004D-UK	Life Science Group
CHIR 990217	72054	Stemcell Technologies
CloneR™	05888	Stemcell Technologies
CNTF	557-NT	R&D Systems
Collagenase IA	C-2674	Sigma-Aldrich
Complete protease inhibitor cocktail	11836170001	Roche
crRNA Alt-R®	Custom generated	Integrated DNA Technologies
crRNA ArciTect™	76010	Stemcell Technologies
Cultrex Basement Membrane Extract	3432-005-01	R&D Systems
DAPT	72082	Stemcell Technologies
Dexamethasone	D4902	Merck
Dibutyryl cAMP	D0627	Sigma-Aldrich
DMEM	10569010	Gibco
DMEM high glucose	11965-092	Gibco
DMEM-F12	31331-028	Gibco
Donkey-anti-GoatIgG-488	A11055	Thermo Fisher Scientific
Donkey-anti-MouseIgG-555	A31570	Thermo Fisher Scientific
Donkey-anti-MouseIgG-647	A-31571	Thermo Fisher Scientific

Donkey-anti-MouseIgM-Cy3	715-165-140	Jackson ImmunoResearch
E-64	E3132	Sigma-Aldrich
eCG	2828 ESP	Provesa
ECMG Extracellular Matrix Gel	E6909	Sigma-Aldrich
Fetal Bovine Serum (FBS)	10270-106	Gibco
Fetal Bovine Serum (FBS)	10270-106	Gibco
FGF2	100-18B	Peprotech
Fluoro-Gel	17985-10	Electron Microscopy Sciences
Forskolin	72114	Stemcell Technologies
FOXO1 inhibitor	S8222	Shelleck
GeneScan™ 500 LIZ Size Standard	4322682	Thermo Fisher Scientific
Gentamicin	15750-037	R&D Systems
GlutaMAX™	35050061	Gibco
Goat-anti-NANOG	AF1997	R&D Systems
Goat-anti-RatIgM-488	A21212	Thermo Fisher Scientific
HBSS	14175053	Gibco
hCG	CG10	Sigma-Aldrich
HGF	GF116	Merck-Millipore
Hi-Di™ formamide	4311320	Thermo Fisher Scientific
High-Capacity cDNA Reverse Transcription Kit	4368814	Thermo Fisher Scientific
Hin1II	ER1831	Thermo Fisher
Hoechst	B2883	Sigma-Aldrich
Horse serum	26050-088	Gibco
Hyaluronic acid	GLR001	R&D Systems
IGF-1	4326-RG	R&D Systems
IMDM	12440053	Gibco
Immobilon ECL Ultra HRP substrate	WBULS0100	Merck
Isoflurane (Forane)	SPPL030	Abbott
KiCqStart® SYBR® Green qPCR ReadyMix	KCQS00	Sigma-Aldrich
KO-DMEM	10829018	Gibco
KOSR	10828028	Gibco
Laminin	23017015	Thermo Fisher Scientific
LDN-193189	72147	Stemcell Technologies
LS Columns	130-042-401	Miltenyi Biotec
LSGS	S00310	Gibco

Min-PROTEAN® TGX™ 4-20 Precast Protein Gels	4561096	Bio-rad
miRNeasy Mini Kit	217004	Qiagen
Monothioglycerol	M6145	Sigma-Aldrich
Mouse-anti-α-ACTININ	A7811	Sigma-Aldrich
Mouse-anti-MYHC	AB_2147781	DSHB
Mouse-anti-MYOGENIN	F5D	DSHB
Mouse-anti-OCT4	Sc-5279	Santa Cruz
Mouse-anti-Pax7	AB_528428	DSHB
Mouse-anti-SSEA4	MC-813-70	DSHB
Mouse-anti-TRA-1-60	MAB4360	Chemicon
Mouse-anti-TRA-1-81	MAB4381	Chemicon
mTeSR1™ Medium	85850	Stemcell Technologies
N-2 supplement	17502001	Gibco
NaturARTsPIG sperm swim-up media	NaturARTs-SUM	EmbryoCloud
NBCS	16010159	Gibco
NEAA	11140050	Gibco
Neurobasal A medium	10888022	Gibco
NT-3	450-03	Peprotech
Nuclon™ Sphera™ dishes	174932	Thermo Fisher Scientific
OCT	N/A	Sakura
P3 Primary Cell 4D-Nucleofector X Kit L	V4XP-3012	Lonza
Penicillin-streptomycin	15140-122	Gibco
Phire Animal Tissue Direct PCR Kit	F140WH	Thermo Fisher Scientific
PMSF	78830	Sigma-Aldrich
Polybrene	TR-1003-G	Merck
Polyvinyl alcohol	P8136	Sigma-Aldrich
Ponceau S solution	P7170	Sigma-Aldrich
Precision Plus™ Kaleidoscope™ Protein ladder	1610375	Bio-rad
Pronase	P8811	Sigma-Aldrich
PureLink™ Genomic DNA Mini Kit	K182001	Thermo Fisher
Qiazol™	79306	Qiagen
QUIAquick™ PCR purification kit	28106	Qiagen
Rat-anti-SSEA3	MC-631	DSHB

Red blood cell lysis buffer	130-094-183	Miltenyi Biotec
ReLeSR™	05872	Stemcell Technologies
ROCK inhibitor Y-27632	72304	Stemcell Technologies
RPMI 1640	11875093	Gibco
rrEGF	3214-EG	R&D Systems
rrFGF2	3339-FB	R&D Systems
Saltallite Cell Isolation Kit	130-104-268	Miltenyi Biotec
SB-431542	72234	Stemcell Technologies
sgRNA	Custom generated	Integrated DNA Technologies
Shandon Consul mounting	9990441	Thermo Fisher Scientific
SHH	1845-SH-025	R&D Systems
SignalFire™ ECL Plus Reagent	12630S	Cell Signaling
Sodium phenylbutyrate (4-PBA)	4-PBA	Scandinavian Formulas
SOX2	GT15098	Immune Systems
Soybean trypsin inhibitor	T6522	Sigma-Aldrich
StemPro™ Accutase™	A1110501	Thermo Fisher Scientific
TaqMan™ Gene Expression Master Mix	4369514	Thermo Fisher Scientific
TBE 10x (Tris / Boric Acid / EDTA) Buffer	1610733	Bio-Rad
TracrRNA Alt-R®	1072533	Integrated DNA Technologies
TracrRNA ArciTect™	76017	Stemcell Technologies
TransIT-X2®	Mir 6004	Mirus Bio
Trypsin-EDTA 0.25%	25200056	Gibco
ß-Mercaptoetanol	M3148	Sigma-Aldrich

Table 13. Product references.

CHAPTER 1

CHAPTER 1: GENERATION OF ISOGENIC CALPAIN 3 KO iPSC LINES WITH CRISPR/CAS9

Hypothesis and objectives

Current cellular models available to study LGMDR1 pathophysiology present several limitations. In the case of patient-derived cells, variability between cell cultures derived from individuals both within controls and patients is a problem that added to the scarcity of muscle biopsies available for research, and the finite nature of patient derived primary cultures, limits researcher's ability to study the disease *in vitro*.

We hypothesize that the use of isogenic iPSC lines that only differ in the presence or absence of calpain 3 will allow to better study the phenotype *in vitro* and avoid the variability found between cell cultures derived from different individuals.

Therefore, to develop this model, the following specific objectives were set:

1. To obtain isogenic calpain 3 KO iPSC lines with CRISPR/Cas9 from a control iPSC line.
2. To characterize the generated isogenic lines for pluripotency maintenance and CRISPR/Cas9 off-targets.
3. To establish an optimized myogenic differentiation protocol from iPSCs to myotubes.

Results

Obtention of calpain 3 KO iPSC clones from an isogenic control with CRISPR/Cas9

In order to obtain isogenic calpain 3 KO iPSC lines, a control iPSC line previously developed in our group by reprogramming skin fibroblasts with the 4 Yamanaka factors (Mateos-Aierdi et al., 2021) was used. Considering LGMDR1 is a recessive disease, it is necessary to disrupt the expression of calpain 3 from both alleles of the gene. The CRISPR/Cas9 RNA guides were designed to target the start codon of the protein in exon 1, which also corresponds to the calpain 3 specific domain "NS". Two strategies were devised to generate the mutations: 1) The single-guide strategy consisted of using a single-guide that directly targeted the start codon using the closest available PAM sequence which would generate a double strand DNA break 3 bp upstream of the start codon, which likely would result in a mutation in the start codon caused by the NHEJ mechanism of the cell. 2) The dual-guide strategy consisted of using two guides simultaneously that flanked the start codon and which generate a deletion of the sequence between the two guides. 4 guide sequences were designed: guide #3 for the single-guide strategy, and two pairs, guide #1 with guide #2 and guide #3 with guide #4, for the dual-guide strategy (Figure 15).

CRISPR/Cas9 ribonucleoprotein (RNP) with the different guide strategies were transfected into iPSCs and single cell clones were isolated and expanded (Figure 16A). With the single-guide strategy, a total of 101 clones were analysed. 49 clones (48.5%) were WT clones for the expected mutation with no modification detected, 51 clones (50.5%) were heterozygous for the mutation, with only one allele mutated, and 1 biallelic KO clone (<1%) was obtained. With the dual-guide strategies, higher efficiencies were observed.

A.

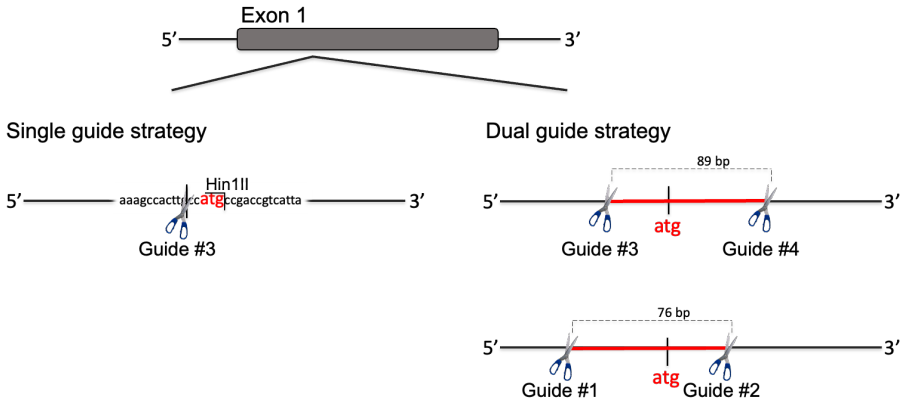

B.

#	Strand	Sequence	Ontarget	Score
1	-	ATAAGATACAGCTACCTTCAAGG	1	78.3
2	+	GACCGTCATTAGCGCATCTGTGG	1	94.2
3	-	ATGACGGTCGGCATGGCAAGTGG	1	87.9
4	-	CAGCCTCAGTGGCCTTGCTCTGG	1	62.5

Figure 15. CRISPR/Cas9 guide design strategy for calpain 3 KO generation in iPSC. A) Squematic representation of the exon 1 in calpain 3 gene and CRISPR/Cas9 cut sites in single-guide strategy, including Hin1II restriction enzyme recognition site, and dual-guide strategies. B) Designed guide sequences. PAM sequences are highlighted in orange, ontarget stands for the amount of genes found containging a matching sequence, and the score given by the guide design software.

With guide pairs #3 and #4, 2 biallelic KO clones were obtained (3.8%) out of 52 clones. In these cases one allele had a deletion corresponding to the action of both guides, while the other only had a mutation in the start codon generated by guide #3. With guides #1 and #2, 5 biallelic KO clones were obtained (23%) out of 22, which present biallelic deletions corresponding to the action of both guides in both alleles. From all the KO clones obtained, 4 were selected to continue with the characterization and the mutations were confirmed by sequencing. KO-1 was selected from the single-guide strategy, KO-2 and KO-3 (generated with guides #3 and #4) and KO-4 (generated with guides #1 and #2) from the dual-guide strategy (Figure 16B).

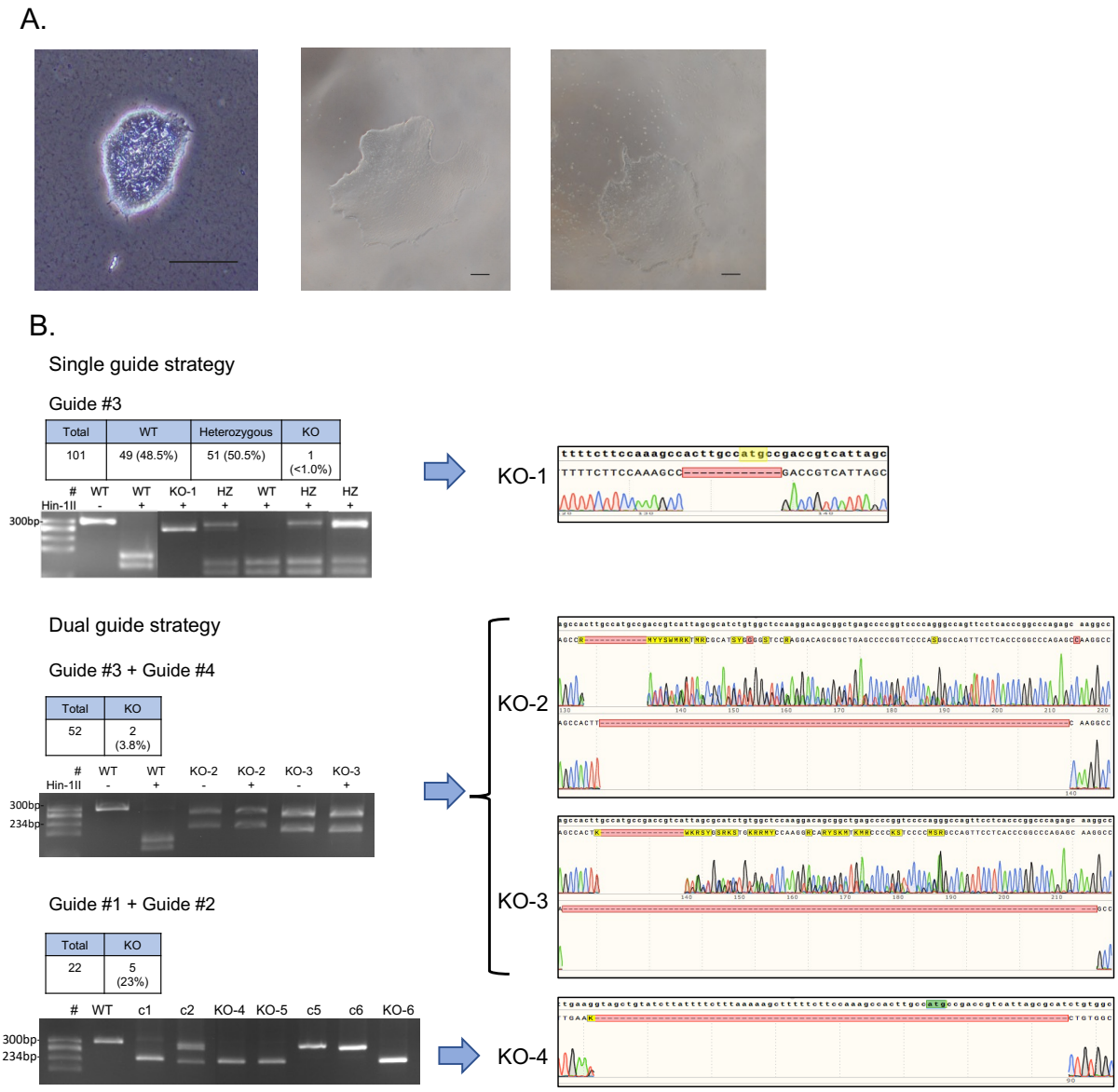

Figure 16. Genotyping and selection of calpain 3 KO iPSC clones. A) Representative brightfield images of iPSC colonies obtained by clonal isolation. Scale: 100 µm. B) Summary of isolated clones and their genotype with each CRISPR/Cas9 guide strategy and combinations. Tables indicate the efficiency obtained generating biallelic KO clones with each strategy. DNA electrophoresis gels show genotyping of clones by resisting digestion with Hin1II (clones obtained with guide #3), by resisting digestion in one allele and having a larger observable deletion in the other allele (clones obtained with guides #3 and #4) and by having a larger observable deletion in both alleles (clones obtained with guides #1 and #2). On the right side, 4 selected KO clones and their sequencing chromatograms indicating with a red line the deleted sequence in each case.

Characterization of calpain 3 KO iPSC clones

Detection of pluripotency markers

Calpain 3 KO clone cultures were similar to the control line cultures being highly proliferative and displayed no evident morphologic differences. The morphology resembled that of embryonic stem cells (i.e., homogeneous surface of the colonies with smooth and well-defined edges) (Figure 16A), and were able to stay stable without spontaneous differentiations occurring over several passages. In order to confirm that the generated KO lines maintained pluripotency after the gene edit, pluripotency assessments were performed based on stablished indicators (Martí et al., 2013). Gene expression analysis was performed to evaluate the levels of a set of pluripotency genes (Figure 17), here, the expression levels of these genes in the KO lines was considered sufficient taking the control line as a reference, as this was an already stablished and characterized iPSC line. *KLF4* and *cMYC* levels were particularly low for both control and KO lines.

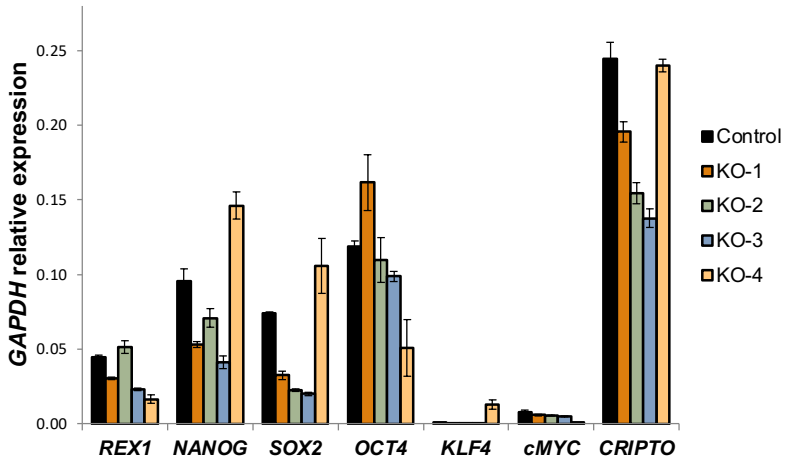

Figure 17. Expression of pluripotency genes in KO clones quantified by qPCR. Expression levels represented relative to *GAPDH* expression. Data expressed as mean of 2 biological replicates ±range.

At the protein level, pluripotency markers were evaluated by immunofluorescence. In all the KO clones nuclear proteins OCT4, SOX2 and NANOG were detectable, and cell surface markers SSEA3, TRA-1-60 and TRA-1-81 were also present (Figure 18).

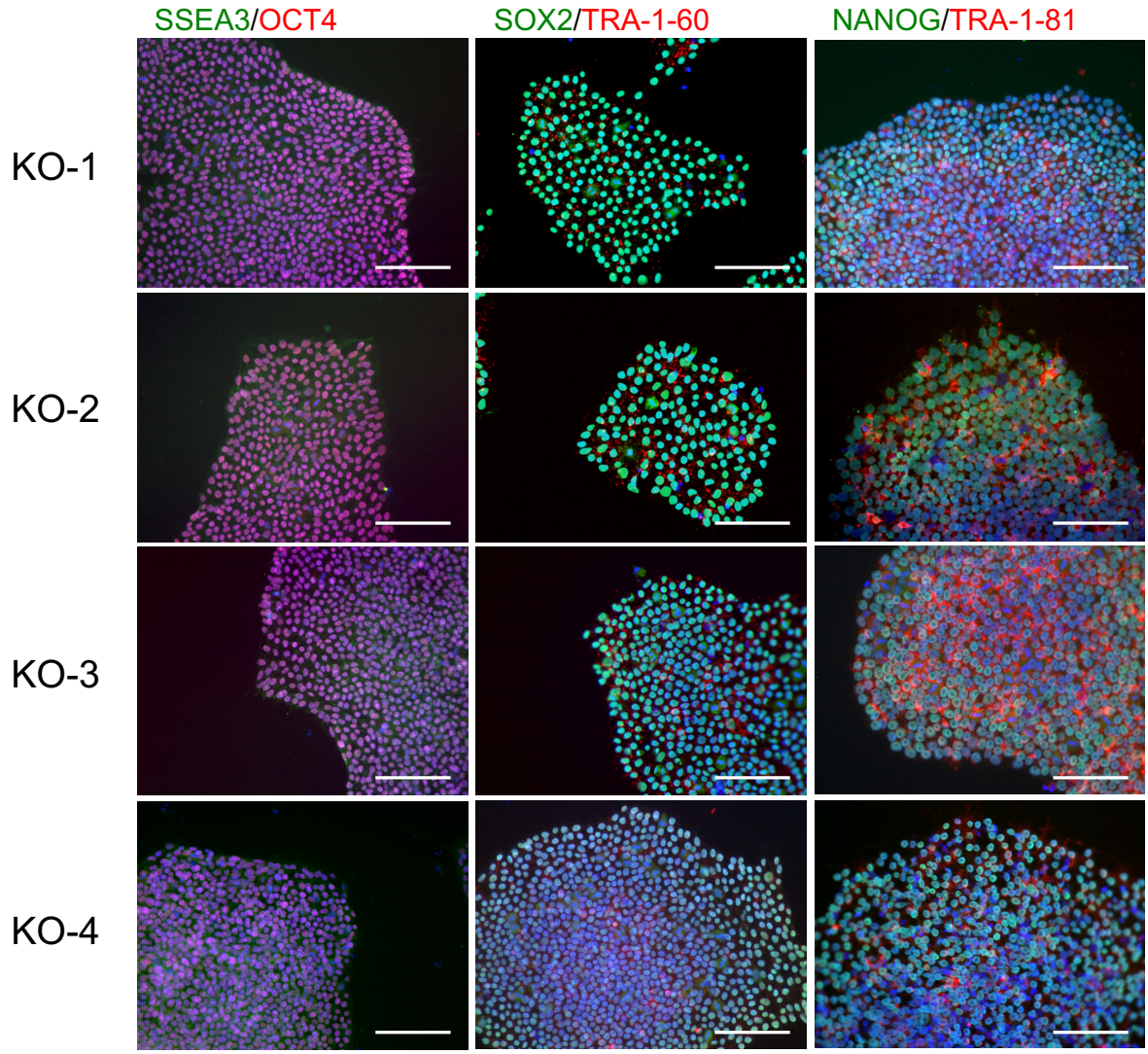

Figure 18. Immunofluorescence analysis of KO clones for the detection of pluripotency markers. Images from column 1 show the expression of SSEA3 (green) and OCT4 (red), column 2 of SOX2 (green) and TRA-1-60 (red), and column 3 of NANOG (green) and TRA-1-81 (red). Nuclei were counterstained with Hoechst (blue). Scale bars: 100 µm.

Karyotype stability

Gene editing together with clonal expansion and extensive culture can facilitate the emergence of chromosomal abnormalities. To ensure these were not present in the KO lines, karyotype analysis through G-banding was performed in each of the lines (Figure 19). None of the KO clones had detectable chromosomal abnormalities and all were considered unaffected.

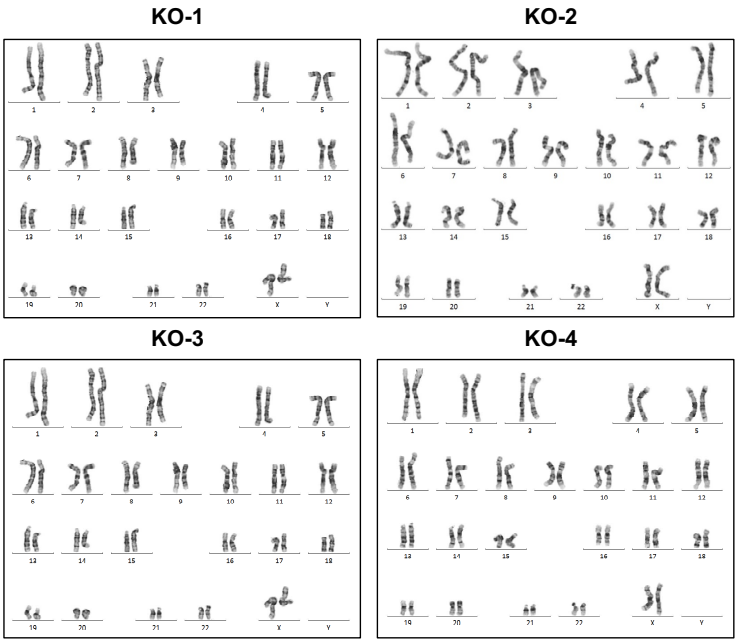

Figure 19. Representative karyotype images for each of the isolated calpain 3 KO iPSC clones.

In vitro differentiation potential

At this point, even though all KO clones had shown appropriate markers of pluripotency and iPSC features, KO-1 and KO-4 clon lines were selected to continue with the characterization and further experiments as two KO lines were considered enough. In particular KO-1 and KO-4 were selected because each represented one of the CRISPR/Cas9 guide strategies and both had their respective mutations in homozygosis with the same deletion in both alleles, contrary to what KO-2 and KO-3 had. Also, KO-2 and KO-3 were generated with a pair of guides that had a lower score, therefore higher chances of having unwanted off-target effects.

Once the expression of pluripotency markers was proven, the next test was performed to demonstrate that these lines had the potential to differentiate into cell types from the primordial germ layers of an embryo. The KO lines were cultured in specific conditions to induce their differentiation and immunofluorescence detection of lineage-specific markers were used to identify their successful differentiation. For the differentiation towards endoderm germ layer, expression of α-fetoprotein (AFP), considered as the fetal form of serum albumin, was detected in the samples. For the mesoderm differentiation, α-smooth muscle actin (α-SMA) was detected, and for ectodermal differentiation, expression of the

neuron- specific class III beta-tubulin (TUJ1) and glial fibrillary acidic protein (GFAP) were detected (Figure 20). Both KO lines expressed all the analysed proteins and were considered to possess the potential to differentiate into cell types derived from the three primordial cell layers, providing evidence of their pluripotency maintenance.

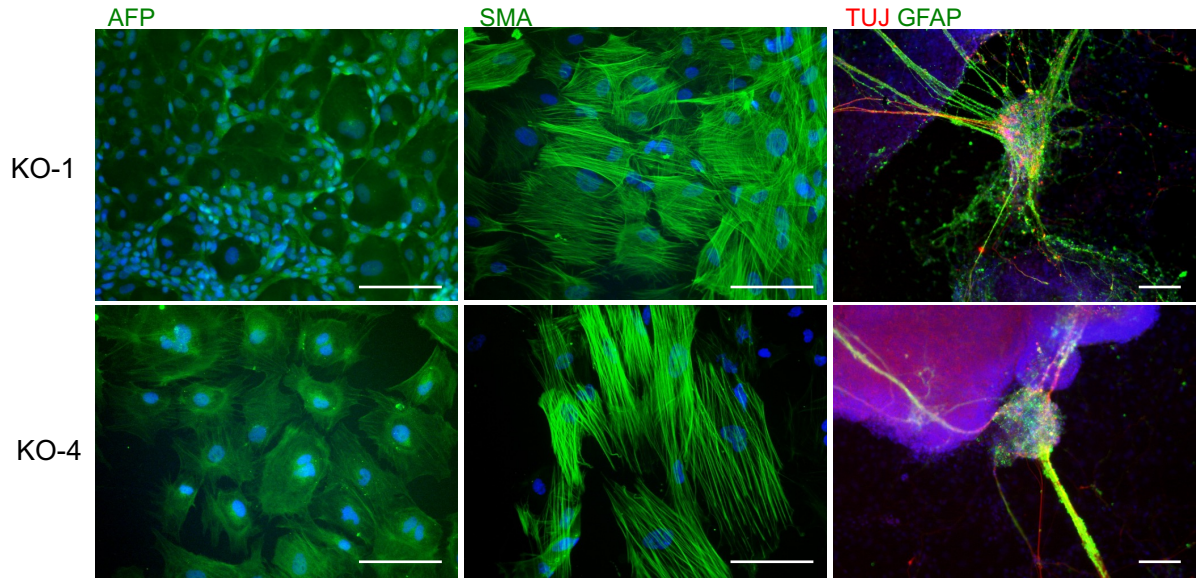

Figure 20. Immunofluorescence detection of lineage-specific markers. Images in column 1 show the detection the endoderm marker AFP (green), in column 2 the expression of α-SMA (green) used as mesoderm marker and in column 3 TUJ1 (red) and GFAP (green) used as ectoderm markers. Nuclei were counterstained with Hoechst (blue). Scale bars: 100 µm.

CRISPR/Cas9 off-target analysis

Finally, CRISPR/Cas9 off-target analysis was performed to evaluate whether any unwanted off-target mutations had occurred elsewhere in the genome as a consequence of the Cas9 unspecific activity. For each guide used to generate clones KO-1 and KO-4, the most probable off-target sites were analysed based on the guide sequence similarity to other loci using Cosmid software (Cradick et al., 2014). In the case where more than 5 potential off-target sites were found, with search parameters allowing up to 3 mismatches and no indels or up to 2 mismatches and 1 base indels, only the 5 most probable loci were analysed. None of the potential off-target sites evaluated by PCR amplification of the region and sequencing had mutations and all the sequences perfectly aligned to that of the control line, indicating no off-target events occurred in the evaluated sites (Figure 21).

KO-1: Guide #3 off-target analysis

Name	Result	Mismatch	Chr Position	Alignment with KO-1
G #3 off 1	AGGAGGTCAGCATGGCAAGAGG -- hit ATGAGGTCGGCATGGCAAGNGG -- query	2	Chr18:8712100-8712121	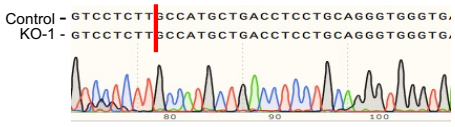
G #3 off 2	AGACGGTGGGCCTGGCAAGTGG -- hit AGACGGTCGGCATGGCAAGNGG -- query	2	Chr2:239683321-239683342	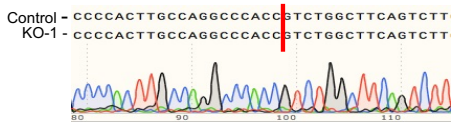
G #3 off 3	ATGACGGCTGCTTGGCAAGGGG -- hit ATGACGGCGGCATGGCAAGNGG -- query	2	Chr10:6702409-6702430	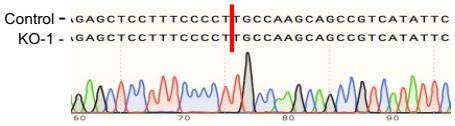
G #3 off 4	ATGAGGTTGGCATGGTAAGGGG -- hit ATGAGGTCGGCATGGCAAGNGG -- query	2	Chr10:85198349-85198370	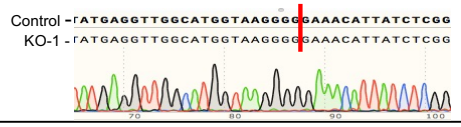

KO-4: Guide #1 and #2 off-target analysis

Name	Result	Mismatch	Chr Position	Alignment with KO-4
G #1 off 1	ATAAAGCACAGCTACCTTCAAG G -- hit ATAAGATACAGCTACCTTCANGG -- query	3	Chr2:54931898-54931920	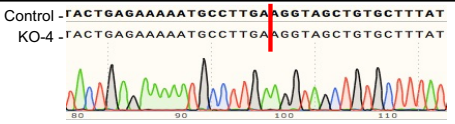
G #1 off 2	ATAGGTGCAGCTACCTTCAGGG -- hit ATAGATACAGCTACCTTCANGG -- query	2	Chr9:23379735-23379756	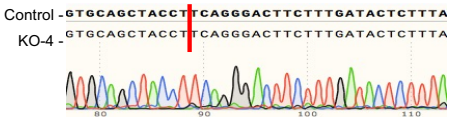
G #1 off 3	AAAAATAAAGCTACCTTCAGGG -- hit AAAGATACAGCTACCTTCANGG -- query	2	Chr4:77680719-77680740	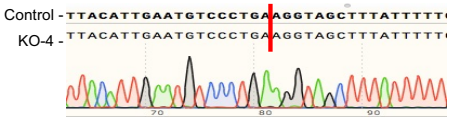
G #1 off 4	AAAGAAACATCTACCTTCATGG -- hit AAAGATACAGCTACCTTCANGG -- query	2	ChrX:41343815-41343836	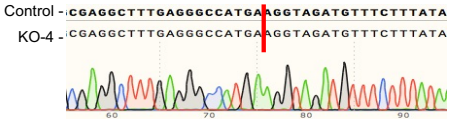
G #1 off 5	ATGAGATTCACTACCTTCATGG -- hit ATAAGATACACTACCTTCANGG -- query	2	Chr3:6282511-6282532	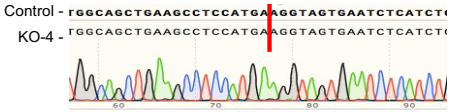
G #2 off 1	GACCCTCATTAGCCCATCTGGG G -- hit GACCGTCATTAGCGCATCTGNG G -- query	2	Chr13:96867999-96868021	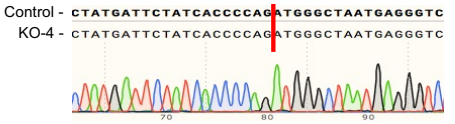
G #2 off 2	GACCTCACTAGTGCATCTGAGG -- hit GACCTCATTAGCGCATCTGNGG -- query	2	Chr4:7618253-7618274	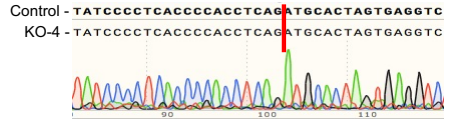
G #2 off 3	GACCGTCACAGTGCATCTGGGG -- hit GACCGTCATAGCGCATCTGNGG -- query	2	Chr22:30448347-30448368	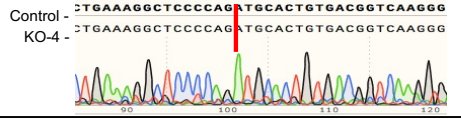

Figure 21. CRISPR/Cas9 off-target analysis in calpain 3 KO iPSC clones. Most probable off-target sites for each guide (G #) used to generate clone KO-1 and KO-4. "Name" indicates each off-target. "Result" shows the query (guide) sequence and the hit sequence found in the genome. "Mismatch" indicates the number of mismatches between query and hit. "Chr Position" indicates the position in the chromosome where the potential off-target is located, "Alignment with KO" shows KO sequencing result at the off-target site aligned with the control sequence, where the vertical red line indicates the precise point where the off-target mutation would be expected.

Myogenic differentiation of calpain 3 KO iPSC clones

For the myogenic differentiation of the iPSC lines, a *PAX7* conditional expression system was used (Darabi & Perlingeiro, 2016). Here the iPSC lines were infected with a doxycycline inducible *PAX7-GFP* expression system, and a myogenic induction protocol was performed through the formation of EBs and specific culture conditions. In order to obtain proliferative PAX7-GFP+ myogenic progenitors, cells were sorted with FACS and GPF+ cells were separated and amplified to be used for myogenic terminal differentiations into myotubes. During the process, no qualitative differences were observed between the control and calpain 3 KO lines (Figure 22A-C).

At this point, myogenic progenitors could be differentiated into myotubes by culturing them into high confluence and switching the medium to terminal differentiation medium. Around the 4th day of culture elongated myocytes started to fuse and form myotubes, which were generally cultured until the 8th day of culture with terminal differentiation medium to allow the myotubes to fully form and mature. Both control line and KO lines were able to differentiate into myotubes and myosin heavy chain (MYHC) and sarcomeric α-actinin (α-ACTININ) could be detected by immunofluorescence in the three lines (Figure 22D). Calpain 3 protein expression, which is expressed mostly in latter stages of the myogenic process, could also be detected in protein extracts from the myotubes of the control line, but not in the KO lines, thus confirming the effective knockout of the KO-1 and KO-4 isogenic clone lines at protein level (Figure 22E).

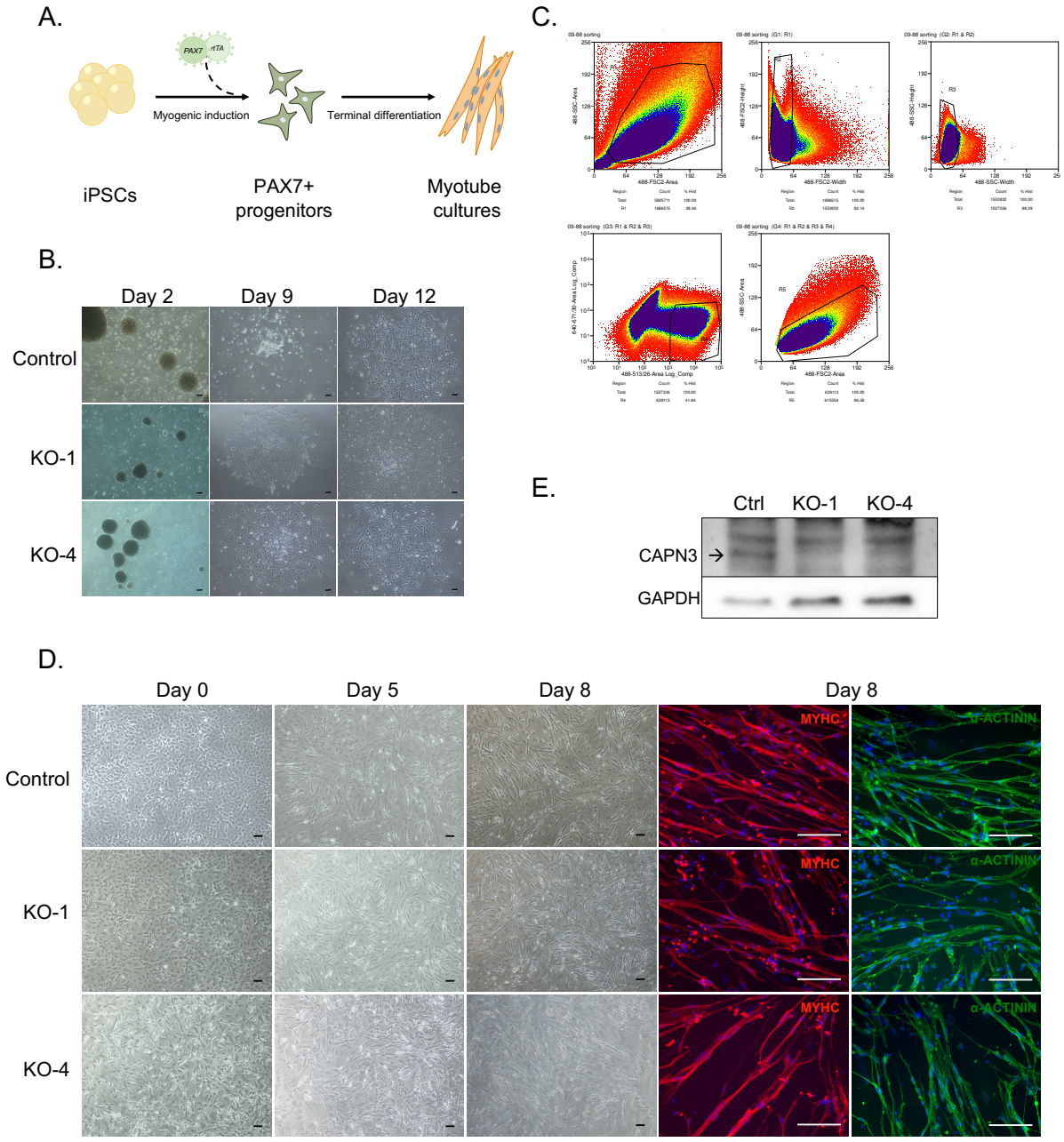

Figure 22. Myogenic differentiation of calpain 3 KO iPSC clones. A) Schematic representation of the myogenic protocol. B) Brightfield images of the myogenic induction process showing day 2 embryoid bodies, and day 9 and day 12 myogenic progenitors previous to FACS sorting. C) Representative plots of FACS sorting of the PAX7-GFP+ fraction of the myogenic progenitors. D) Terminal differentiation of the PAX7-GFP+ myogenic progenitors into myotubes. Brightfield images of the differentiation shown in days 0, 5 and 8, and immunofluorescence detection of MYHC in red and α-ACTININ in green in the myotubes at day 8 of differentiation. Nuclei were counterstained with Hoechst (blue). Scale bars: 100 µm. E) Calpain 3 Western blot of differentiated myotubes from control and KO iPSC lines, with GAPDH as loading control.

Optimization of the terminal differentiation protocol

Aiming to optimize the terminal differentiation protocol to obtain better differentiations with more mature and pulsating myotubes, different culture mediums, supplements and substrates were tested with the control line. First, qualitative comparison of two terminal differentiation mediums was performed with two mediums previously described and used in this group, medium A and medium S. Overall, medium S obtained a higher density of myotubes distributed evenly across the culture plate and with apparently thicker bodies (Figure 23A).

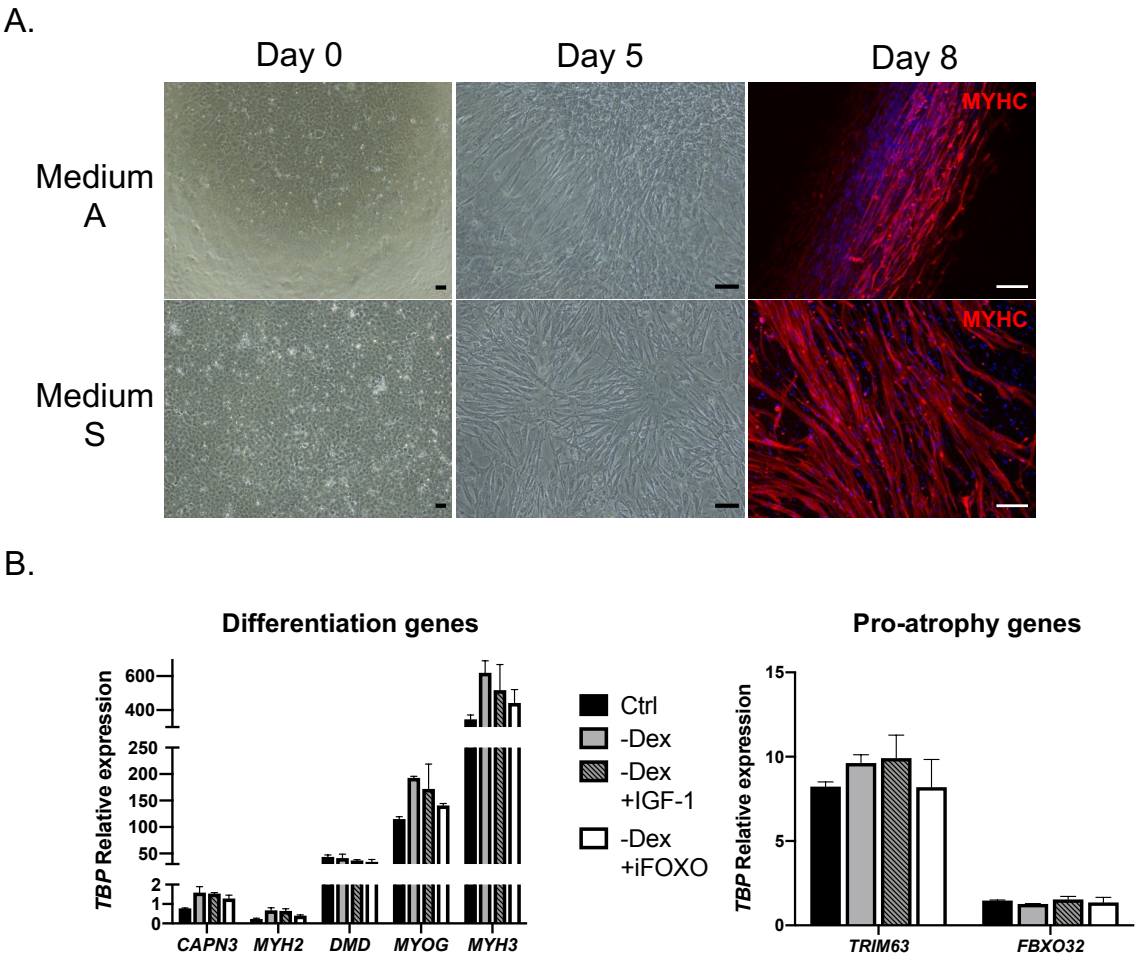

Figure 23. Differentiation medium optimization. A) Qualitative comparison of terminal differentiation mediums A and S in the control line. Brightfield images show myogenic progenitors at confluence at day 0 and differentiating at day 5. Immunofluorescence detection of MYHC in red in the myotubes at day 8 of differentiation. Nuclei were counterstained with Hoechst (blue). Scale bars: 100 µm. B) Variations of the medium S and the effects in the expression levels of myotube differentiation genes and pro-atrophy genes analysed by qPCR. "Ctrl" stands for the standard medium S, "-Dex" for medium S without dexamethasone applied to the culture after day 3 of differentiation, "+IGF-1" with IGF added, and "+ iFOXO1" with a FOXO1 inhibitor added. Legend and colors are same for both graphs. Data expressed as mean of 2 biological replicates and error bars for standard error of the mean (SEM).

Variations of the medium S composition were also tested to evaluate if these changes could improve indicators of myogenic differentiation, which were evaluated at the gene expression level. Among these changes were withdrawing dexamethasone from the S medium, a glucocorticoid that has been described to improve myogenic differentiation in the initial phases but detrimental in latter stages (Han et al., 2017); and together with dexamethasone withdrawal supplementing the medium with IGF-1, a major regulator of skeletal muscle growth (Schiaffino & Mammucari, 2011) and the use of a FOXO1 inhibitor, which acts as a repressor of myogenesis (M. Xu et al., 2017). There were no statistically significant differences detected in the expression of myogenic differentiation indicators nor in the expression of pro-atrophic genes, however medium S without dexamethasone had a tendency to show slightly higher levels of myogenic differentiation indicators, and therefore this modification was chosen for future differentiations with medium S (Figure 23B).

Aiming to obtain more mature and functional myotubes, the use of an additional differentiation medium (DM-2) over prolonged culture times of up to 14 days was tested. DM-2 contained additional supplements like neurotrophic factors and agrin, which can help in the maturation of the excitation-contraction coupling mechanism (Bandi et al., 2008). When switching to DM-2 after day 8 day of differentiation compared to staying with the S medium, a tendency could be observed where more myotubes were pulsating and also more myotubes per area could be detected (Figure 24A). At the gene expression level, the adult form of myosin heavy chain (*MYH2)* and dystrophin (*DMD*) also showed a tendency for higher expression with DM-2, while the embryonic myosin (*MYH3*) seemed to decrease and the other genes analysed seemed unaltered (Figure 24B).

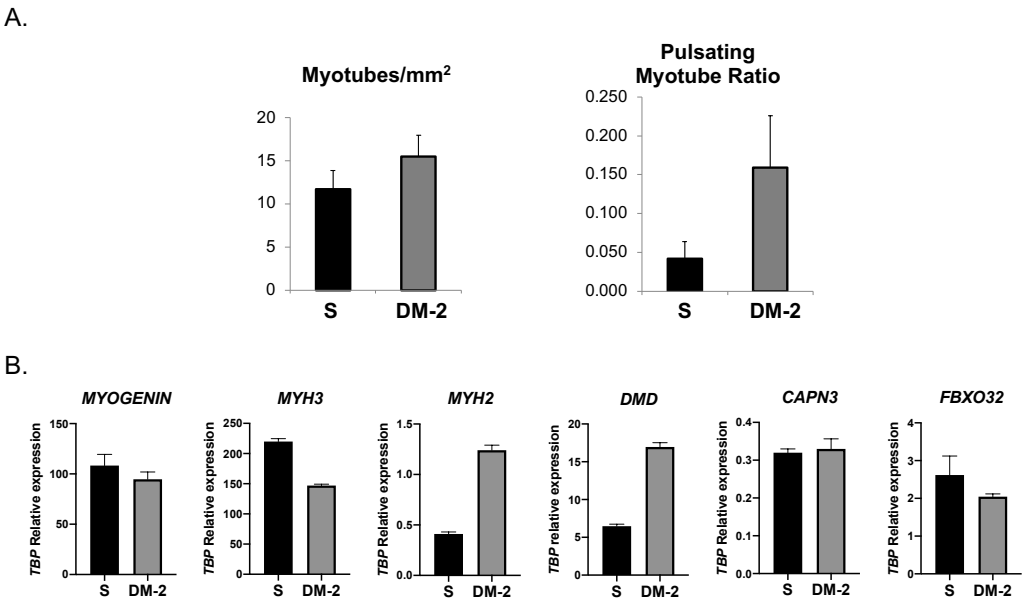

Figure 24. Maturation medium optimization. Comparison of medium S and medium DM-2 in myotubes from day 8 to day 14 of differentiatinon A) Quantitative comparison of the number of myotubes found per mm2 at day 14, and the ratio of pulsating myotubes detected with each medium. B) Gene expression levels of myotubes at day 14 of differentiation analysed by qPCR. Data expressed as mean ± standard error of the mean (SEM) of 2 biological replicates.

Finally, different substrates were tested as cell culture dish coatings and cell overlays for the differentiation of the myogenic progenitors. The use of 0.1% gelatin with laminin (G+L) as dish coating without overlay or with different commercially available extracellular matrix protein preparations (ECM, Matrigel) were tested, and also the use of one such preparation (cultrex) with low molecular weight HA as a coating or coating and overlay (cultrex-HA). Visual inspection of the differentiations showed overall longer and better aligned myotubes in cultures where cultrex-HA was used (Figure 25A). In the case of myotube density in the culture, the use of cultrex-HA without overlay seemed to result in higher densities, and also appeared to increase the pulsating myotube ratio when compared to the other substrates (Figure 25B).

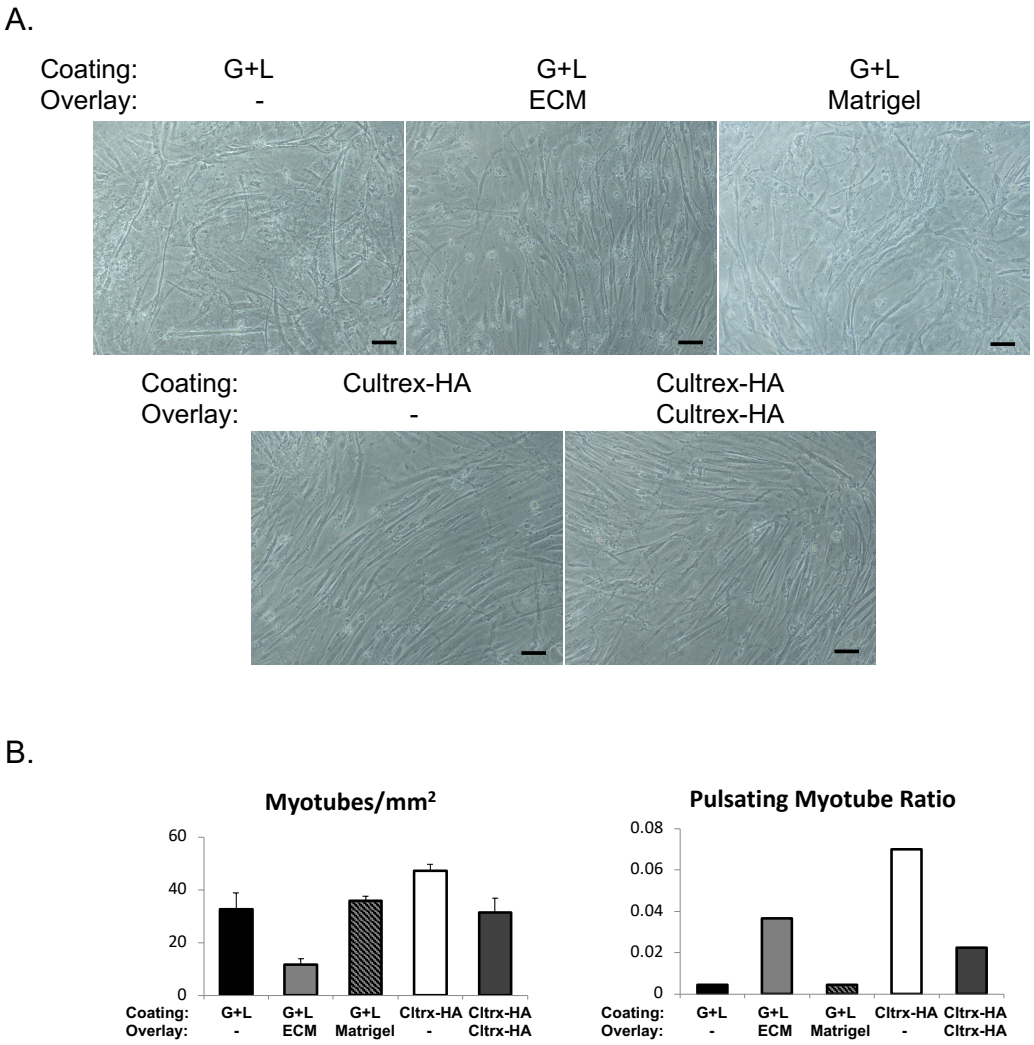

Figure 25. Differentiation substrate optimization. Comparison of different plate coatings and cell overlay combinations for myotube differentiatinon. "G+L" stands for gelatin and laminin, "ECM" stands for extracellular matrix proteins, "Cultrex-HA" stands for cultrex with hyaluronic acid and "-" stands for when no overlay was used. A) Representative images of myotubes differentiated in each coating and overlay combination tested. Scale bars: 100 µm B) Quantitative comparison of the number of myotubes found per mm^2 and the ratio of pulsating myotubes detected. Data for myotubes/mm^2 expressed as mean ± SEM of 2 biological replicates and one replicate for the pulsating myotube ratio.

Gene expression analysis also seemed to indicate that the use of cultrex-HA with or without overlay resulted in higher levels of embryonic and adult forms of myosin heavy chain, *MYOGENIN* and *DMD*, while the differences on the pro-atrophic *FBXO32* seemed more subtle but also appeared slightly higher on average (Figure 26).

Overall, the use of cultrex-HA seemed to provide a better substrate for the differentiation of the myogenic progenitors compared to the other substrates tested, particularly at the morphological level, the induction of pulsations, and the expression of genes associated

with myotubes. The use of an overlay in the cultrex-HA coating did not seem to exert any additional benefit over simply using the cultrex-HA coating, therefore a cultrex-HA coating was selected as optimal substrate for future differentiations.

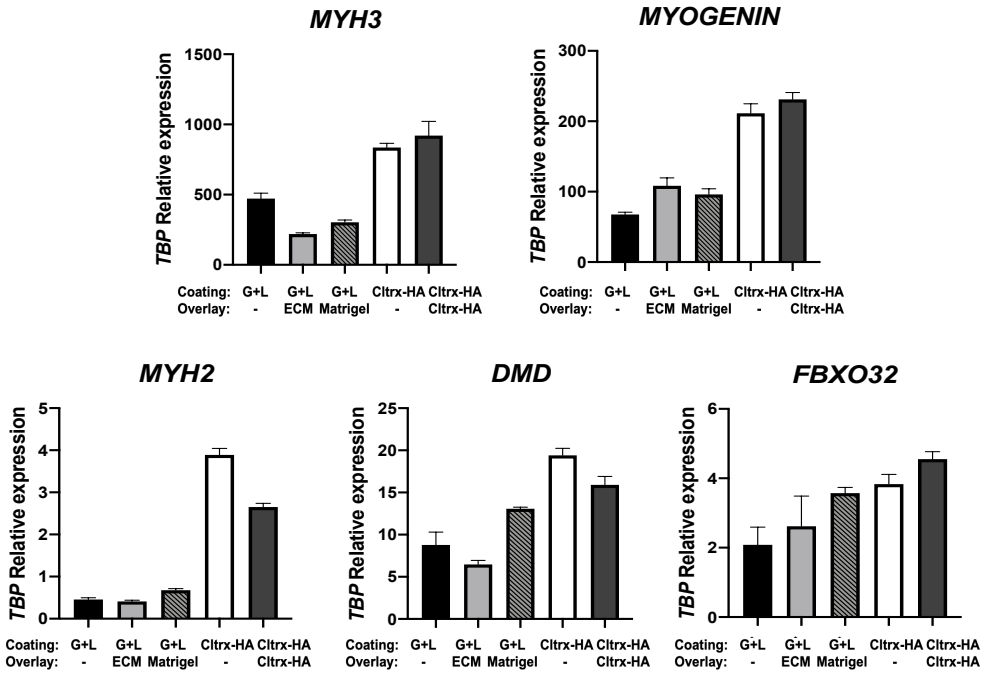

Figure 26. Gene expression analysis with different differentiation substrates. Gene expression levels of myotubes differentiated with different plate coatings and cell overlay combinations analysed by qPCR. Data expressed as mean ± SEM of 2 biological replicates.

After the different experiments performed in the optimization of the terminal differentiation protocol, this was defined with the use of cultrex-HA as substrate for the cells, the use of differentiation medium S and removal of dexamethasone from the medium from day 3 to day 8 of the differentiation, followed by a switch to DM-2 from day 8 to day 14. The resulting protocol differentiated myogenic progenitors into myotube cultures that were densely packed, showing spontaneous contractions and with improved expression of myotube maturation genes. Immunofluorescence images of these myotubes also showed thick multinucleated myotubes with visible striations indicative of maturation and sarcomeric structure formation (Figure 27).

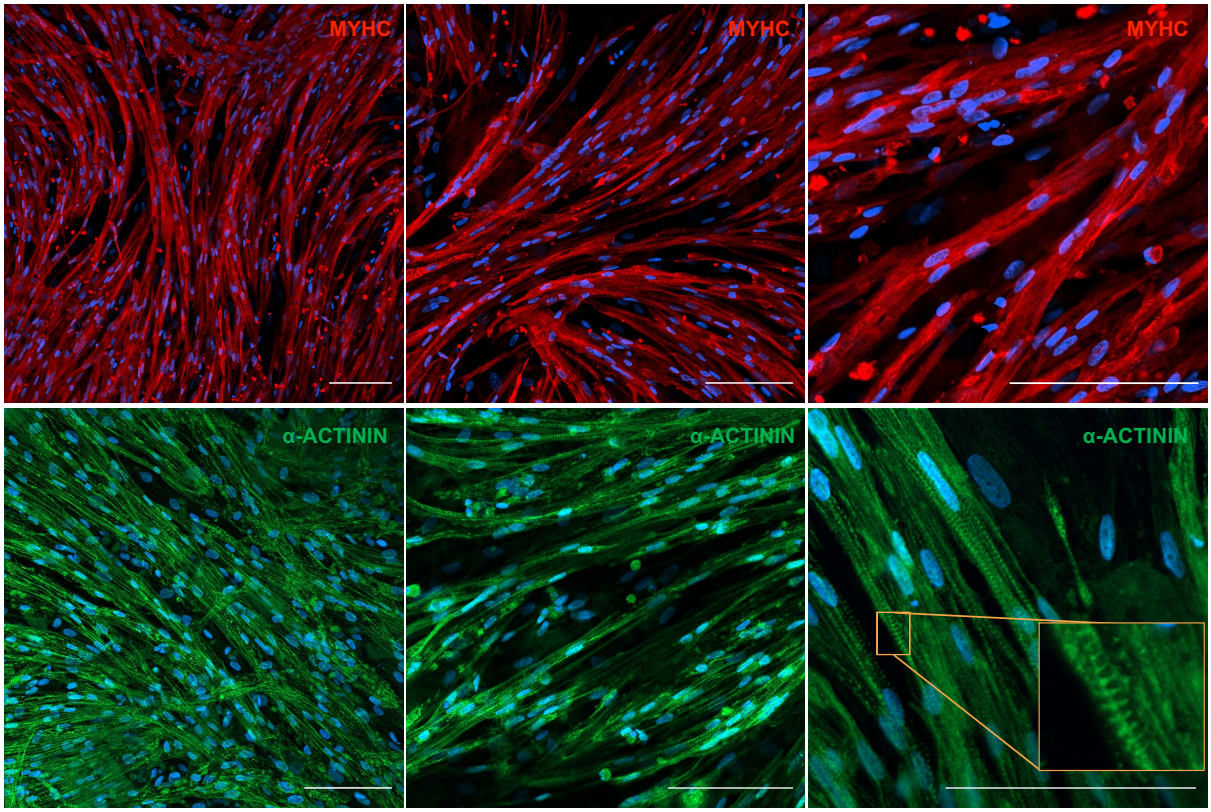

Figure 27. Immunofluorescence images of myotubes obtained with the optimized protocol. MYHC in red and α-ACTININ in green in the myotubes at day 14 of differentiation. Bottom right image shows myotube striations in an amplified region highlighted in the orange box. Nuclei were counterstained with Hoechst (blue). Scale bars: 100 µm.

Discussion

LGMDR1 research over the last years has lacked appropriate *in vitro* and *in vivo* models that could clearly represent the pathological features observed in patients.

The *in vitro* models have shown different type of limitations, on the one hand there are issues with the source of the cells, as patient-derived biopsies are scarce and the amount of myoblasts that can be obtained from the explants and culture passages that these cells can withstand are limited. Also, the patient-derived cells often present variability that can be due to the different pathogenic mutations they might be carrying, but also can be derived from the differences in age, sex or disease progression, making it difficult to draw conclusions (I. Y. Choi et al., 2016; Volpato & Webber, 2020). Alternatively, immortalized myoblasts have also been used to overcome some of these issues of patient variability and cell culture senescence, although in the case of human LGMDR1, only calpain 3 gene silencing approaches have been used instead of CRISPR/Cas9 gene editing in the immortalized cells (Lasa-Elgarresta et al., 2019; Toral-Ojeda et al., 2016). More importantly, immortalized myoblasts do not allow to study earlier satellite cell or pre-myoblast progenitor stages, and evaluate whether satellite cells could be also affected, while the iPSC derived PAX7-GFP+ myogenic progenitors have shown to be able to repopulate the satellite cell niche *in vivo* and regenerate muscle from there (Darabi et al., 2012). Here we have developed a model based on iPSCs using a control line and isogenic CRISPR/Cas9 generated calpain 3 KO lines, with the goal of having a highly proliferative cellular model that is able to differentiate into myotubes from PAX7-GFP+ myogenic progenitors, that can potentially avoid the issues of previous cellular models mentioned above and also offers the possibility to study the stem cell like stage and more flexibility for *in-vitro* muscle engineering since having iPSCs as the starting point offers more potential options than immortalized myoblasts to generate different cell types.

Obtention of isogenic calpain 3 KO iPSC clones and their characterization

To obtain the isogenic calpain 3 KO iPSC lines, we took an iPSC control line previously developed in our group that had been properly characterized (Mateos-Aierdi et al., 2021) and transfected it with CRISPR/Cas9 ribonucleoprotein and guides targeting the start codon of the gene.

Using a single-guide strategy to generate a DSB in the DNA and generate a mutation via NHEJ is the original and most frequent approach with CRISPR to inactivate a gene (Jinek et al., 2012), however, it is known that the use of two simultaneous sgRNAs at a relatively close distance from each other also induces DNA repair by NHEJ and generates a loss of the sequence between both guides (López-Manzaneda et al., 2020; Zheng et al., 2014). In our case, the dual strategy with both guide combinations also showed slightly higher efficiencies obtaining biallelic KOs. Besides the improved efficiency, using a dual-guide strategy has also a technical advantage on the genotyping of the isolated clones, since the deletion can be identified by a simple gel electrophoresis of the PCR product of the target region, whereas in the case of using a single-guide, the indel generated is usually too small to be detected this way and an additional process such as a digestion with a restriction enzyme or sequencing is required to detect if the mutation has occurred, which becomes time consuming when genotyping large amounts of clones.

Regarding the use of the start codon as a target to generate a KO, it has been described that in order to induce nonsense-mediated mRNA decay (NMD) it is more efficient to target exons further away from the start codon (J. H. Lee et al., 2020), however, in this case exon 1 of calpain 3 is one key exon of the p94 muscle specific isoform, and there were no other alternative in-frame start codons in exon 1, therefore this approach was selected and the lack of calpain 3 protein was confirmed once these lines were differentiated into myotubes. Also, despite some LGMDR1 patients carry mutations that allow them to express mutated calpain 3, lack of calpain 3 in muscle biopsies whether from mRNA NMD or from autocatalytic degradation, is a common feature of LGMDR1 biopsies (Fanin & Angelini, 2015). One of the issues we detected with our RNA guides was with guide #4 in KO clones KO-2 and KO-3. The target sequence for guide #4 in our control iPSC line had a silent mutation in heterozygosis in that locus and therefore this guide was not working in one allele. The result could be observed when sequencing these clones, where one allele had the deletion of the entire sequence between both guides, while the other had only a smaller deletion caused by the action of guide #3. Nonetheless, both alleles had the start codon eliminated.

After selecting the 4 KO clones, these were characterized for their maintenance of iPSC characteristics, karyotype stability and off-targets. These type of characterization tests, particularly the ones concerning pluripotency are a standard that new iPSCs lines are generally required to pass for their deposition in cell banks such as at the Spanish

National Bank of Cell Lines (Banco Nacional de Líneas Celulares, Instituto de Salud Carlos III), and are widely used trough the literature (Martí et al., 2013; Raya et al., 2009). At the gene expression level, except for KLF4 and cMYC which had very low levels of expression also in the control line, the rest were detectable in all the lines. Despite there seemed to be some differences between the lines, these were not considered of importance since expression level of these genes can fluctuate while in culture and can be different at the clonal level. This fact as well as the variable gene expression rates were similar to those reported in the literature, however, it might be one of the sources of variability between clones that can be found with iPSCs (Mason et al., 2014; Sánchez-Danés et al., 2012; Volpato & Webber, 2020). Pluripotency maintenance of the KO lines was also confirmed by the detection of pluripotency markers by immunofluorescence, and in the case of KO-1 and KO-4, which were the KO-clones finally selected to continue with experiments, their ability to differentiate into cell types from different lineages also is indicative of pluripotency.

Prolonged *in vitro* culture of iPSCs as well as DNA modifications generated by CRISPR/Cas9 can cause chromosomal abnormalities, and to circumvent this karyotype analyses are recommended (Assou et al., 2020; Cullot et al., 2019). None of the four KO lines analysed showed large chromosomal aberrations, however, it is worth mentioning that the G-banding method used in this study, despite being the most commonly used method for this type of characterizations, has its limitations since it does not have a high enough resolution to detect small deletions, inversions or other alterations that might be occurring under the 5Mbp range, for which other methods such as a SNP array would be required (Weisheit et al., 2021).

When off-target analysis was performed by sequencing in the KO lines to evaluate if CRISPR/Cas9 had generated unintended mutations in other loci, no off-target mutations were detected in the predicted sites with higher risk. This analysis was only focusing on the most probable but yet few sites where potential off-target mutations could occur, and while a more exhaustive analysis could have been done, the issue of off-target mutations and their relevance and real frequency has been controversial in the literature. It is known that some mutations in the guide-target sequence are tolerated, and that the nucleotides closer to the CRISPR recognition PAM site are less tolerant (Hsu et al., 2013). In fact, initial studies from different labs using high-throughput sequencing of cell cultures found many more off-targets than expected (Kim et al., 2015; Tsai et al., 2014),

however, most of the off-targets were based on sequence similarity and many of the guides that were used were very unspecific with a lot of potential off-target sites. Nowadays guide design software allows to pick guides with far less off-target potential and initial concerns about off-targets became more manageable with a good guide design (Sheridan, 2018). Also, other key aspects for the off-target cleavage frequency are Cas9 concentration and its exposure time, where the use of CRISPR/Cas9 as a RNP reduces exposure time over Cas9 overexpression from a plasmid (Vakulskas & Behlke, 2019). In fact, some studies were unable to find off-targets in genetically modified mice generated with brief CRISPR/Cas9 exposure, which has led some authors to dismiss the off-targets found through high-throughput assays as entirely irrelevant in practice (Iyer et al., 2015). In our case, in order to avoid potential off-targets RNP transfection was used with carefully selected guides, and as no off-targets were identified in the predicted sites of higher probability, high throughput whole-genome sequencing approaches to detect other potential off-targets were not considered a necessary nor a sensitive option.

Myogenic differentiation and optimization of the differentiation protocol

An efficient and reproducible differentiation of iPSCs into specific cell types is essential to generate *in vitro* models as well as for future therapeutic applications. Despite a great variety of differentiation protocols have been reported, *in vitro* myogenic differentiation of iPSCs remains being a challenge, generally showing low efficiencies and reproducibility (Iberite et al., 2022; Mirauta et al., 2020). For this reason and in order to optimize the differentiation rate of the cultures, most efficient and fast protocols generally include transient expression of transgenes and/or FACS-mediated selection of cells with myogenic potential (Kodaka et al., 2017).

Considering the different approaches described to date, we decided to use a protocol using transgene expression for the myogenic induction of our isogenic lines, due to the higher efficiency and shortened duration of these protocols. In particular, we decided to use transient *PAX7* overexpression, with an adapted protocol of the one originally developed by Darhabi and colleagues and later optimized by Selvaraj and colleagues (Darabi et al., 2012; Selvaraj, Dhoke, et al., 2019), which uses a myogenic induction phase to obtain a pool of PAX7-GFP+ myogenic progenitor cells, in order to be able to study the role of calpain 3 in earlier "stem cell like" cells, as well as later myogenic differentiation stages. Using other approach such as *MYOD1* overexpression was discarded due to the potential

interaction of calpain 3 with MYOD1 (Stuelsatz et al., 2010). Also, the PAX7-GFP+ myogenic progenitors possess a transcriptomic profile more similar to fetal myoblasts and are able to seed the SCs niche *in vivo*, therefore this method could be a more appropriate approach in order to study myogenesis from earlier phases (Incitti et al., 2019; Magli et al., 2017).

Throughout the myogenic induction protocol, cell morphology was comparable between the various lines, and both infection efficiencies and the amount of PAX7-GFP+ myogenic progenitors obtained for these lines every time the myogenic induction was performed was similar at the qualitative level. Also, all the lines were able to terminally differentiate into multinucleated myotubes and express the myogenic markers MYHC and α-ACTININ, and despite calpain 3 expression is generally low in *in vitro* cultures and the available antibodies do not offer a strong specific signal, we were able to detect it in the control line and not in the KO lines, which confirmed at the protein level that we had efficiently obtained isogenic calpain 3 KO lines from the control line.

When testing the protocols of myogenic differentiation, we aimed to obtain a robust and reproducible method to differentiate the isogenic lines, that would be able to obtain myotubes with a minimum level of maturation with elements such as striations, indicative of sarcomere formation, or the ability to generate contractions. Initially, we did run some experiments to optimize and tests some variations in the myogenic induction phase of the protocol, considering that an improved mesoderm induction at the early stages of the myogenic induction protocol could positively act on the myogenic capacity of the muscle progenitor cells. However, this protocol had previously been optimized (Selvaraj et al., 2019) and already included small molecules such as BMP and TGF-B pathway inhibitors, or CHIR990217, one of the most selective GSK3β inhibitors described to date, that has been shown to activate the canonical WNT signaling pathway and lead to an enhanced myogenic differentiation, and has been included in many myogenic differentiation protocols for iPSCs and human ESC (van der Velden et al., 2007; C. Xu et al., 2013). For this reason and the fact that we were already obtaining enough amounts of PAX7-GFP+ myogenic progenitors, we decided to focus on optimizing terminal differentiation phase, where the obtained myotubes were still considered to be a little thin and irregularly shaped.

The results obtained when directly comparing medium A and medium S, clearly showed at the qualitative level, the improved myotube formation with medium S. Medium A is a more traditional medium for terminal myogenic differentiation, which are characterized by a low serum or serum replacement preparations and the use of some growth factors, in this case IGF-1 and HGF, and had been previously used by our group and others (Chal et al., 2015; Mateos-Aierdi et al., 2021). On the other hand, medium S besides having serum replacement media and AA supplementation, it contains SB-431542, DAPT, forskolin and dexamethasone. These molecules have been proven to improve myogenesis by inhibiting TGF-B pathway (SB-431542), inhibiting NOTCH pathway (DAPT), increasing AMP by activation of adenylyl cyclase (forskolin), and promoting kinesin-1 motor activity (dexamethasone) (Lin et al., 2021; Watt et al., 2010; C. Xu et al., 2013; H. Zhang et al., 2021). This suggests that these type of PAX7-GFP+ myogenic progenitors still need some additional aid to differentiate properly into myotubes compared to primary myoblasts, which in previous experiences in our group and the literature achieved proper differentiation with simpler mediums (Jaka et al., 2017; Lasa-Elgarresta et al., 2022). However, this would also be expected as these cells would be in an earlier progenitor state and PAX7 is not a MRF that induces differentiation, but a regulator and marker of SCs (Zammit et al., 2006).

We did some tests to try to optimize the terminal differentiation by further optimizing medium S and testing a second differentiation medium, the DM-2. Based on a study that indicated that the use of dexamethasone can promote myogenesis in early phases but can induce atrophy *in vitro* when applied at the myotube state (Han et al., 2017) we tested its withdrawal from the medium after day 3 of differentiation, as well as supplementing the medium with IGF-1, a major regulator of skeletal muscle growth (Schiaffino & Mammucari, 2011) and the use of a FOXO1 inhibitor, which acts as a promoter of myogenesis (M. Xu et al., 2017). From the tested combinations, removing dexamethasone showed a tendency for higher levels of expression of differentiation genes, and adding IGF-1 or the FOXO1 inhibitor did not seem to exert additional benefits. This lack of benefit from adding IGF-1 or the FOXO1 inhibitor could mean that the insulin that the medium S has in its serum replacement components, could be already activating the IGF-1 pathway, which in turn also inhibits FOXO1, and therefore there would be no additional benefit from further activating/inhibiting these pathways. On the other hand, when extending the culture time to 14 days, the use of DM-2 did seem to improve culture by increasing myotube density, expression of genes indicative of myotube maturation, and

particularly the pulsating myotube ratio in the culture. This tendency was in line with our expectation that the addition of this medium with components such as agrin, BDNF or laminin would improve maturation and contraction capability of the culture as other studies have shown (Halievski et al., 2020; Toral-Ojeda et al., 2018; B. G. X. Zhang et al., 2016).

Similarly, when testing the different materials as substrates for the differentiations, the use of cultrex with HA showed a qualitatively better morphology and a tendency towards more densely packed cultures, increased contractibility and higher expression of differentiation genes, although adding an overlay of this material to the cells did not seem to improve the results. Unlike extracellular matrix preparations such as cultrex that are widely used as a substrate for *in vitro* muscle culture, HA is less frequently used and mentioned in the bibliography as a substrate for muscle cell culture (Dienes et al., 2021; Khodabukus, 2021). In part this is because some initial studies showed it can inhibit myogenesis *in vitro* (Calve et al., 2010), however other studies have shown that its synthesis is required for differentiation and it can also improve regeneration *in vivo* (Dienes et al., 2021; Hunt et al., 2013) where the molecular weight of the HA could be important and have different effects depending on this factor (Stern, 2003). In our experience, the best results were obtained with the cultrex-HA substrate, a material that was initially developed for neural differentiation (García-Parra et al., 2012, 2013) but that had also worked well for SCs differentiation in our group (García-Parra et al., 2014; Naldaiz-Gastesi et al., 2019).

It is worth mentioning that most mediums and substrates we tested were based on previous studies or publications, and that using the same components, many more combinations could have been tested. However, each differentiation takes at least 3 weeks if starting already from the PAX7-GFP+ progenitors, therefore time constrains are an issue when trying many variables and experiments. In order to further optimize this type of protocols, it would be ideal to access some level of automation in the analysis process, similar to the ones used in screening platforms that can measure myoblast differentiation levels among other parameters (Sun et al., 2020; Young et al., 2018), which would allow to test more components. Also, it should be noted that some of our experiments were guided by qualitative assessment of the culture morphology which are hard to represent and despite the results were consistent, the experiments lacked statistical power to show statistical significance, therefore it would be appropriate to increase the replicates which

we believe would make the results show statistical significance. Finally, despite we decided to use PAX7 transgene expression for the reasons discussed above, it is likely that in terms of differentiation efficiency and maturation, the use of MYOD1 overexpression could have been more efficient, as it is a direct inducer of myogenesis. Also, in order to further improve culture maturation, a 3D culture could probably reach a higher level of complexity as some studies have shown (Maffioletti et al., 2018; Urciuolo et al., 2020), however protocols for developing such 3D cultures are considerably more time consuming, which depending on the target application, might not be the most appropriate.

Overall, we achieved an improved method to differentiate iPSC derived PAX7-GFP+ myogenic progenitors into myotubes with an increased expression of differentiation markers and contraction capacity, that show that not only mediums and substrates are important but also timing of their addition throughout the differentiation process.

CHAPTER 2

CHAPTER 2: DAMAGE RESPONSE, MYOGENESIS AND PROTEIN HOMEOSTASIS IN CALPAIN 3 KO MODELS OF LGMDR1.

Hypothesis and objectives

Lack of calpain 3 in LGMDR1 muscle tissue leads to atrophy, muscle loss and degeneration in humans. However, whether this deficiency arises from a defective SCs, reduced myogenic capacity, a failure to adapt and maintain muscle cell homeostasis, a defective signalling or a combination of more than one of these functions is not clear. To study these aspects of the disease the following objectives were set:

1- To study the early response to acute muscle damage in the C3KO mouse model.
2- To evaluate the myogenic capacity *in vitro* of mouse SCs and human isogenic iPSCs derived myogenic progenitors in the absence of calpain 3.
3- To evaluate C3KO running performance in functional studies and pathways associated with protein homeostasis.
4- To evaluate the response to electrostimulation of human isogenic iPSCs derived myotubes in the absence of calpain 3.
5- To evaluate the use of 4-PBA to improve proteostasis in the C3KO mice and human isogenic iPSCs derived myotubes in the absence of calpain 3.

Results

Proteomic analysis of damage response in the C3KO mouse

In order to study potential differences in how muscles that lack calpain 3 respond to acute damage and how this differential response could result in a failure to regenerate or lead to a dystrophic process, a proteomic damage response analysis was performed in the C3KO and WT mice. To exert the damage, CTX injections were performed in the soleus and TA muscles of the right hindlegs of C3KO and WT mice. 3 days after the injections, mice were sacrificed and the damaged muscles as well as the control undamaged muscles from the left hindlegs were extracted for proteomic analysis (Figure 28).

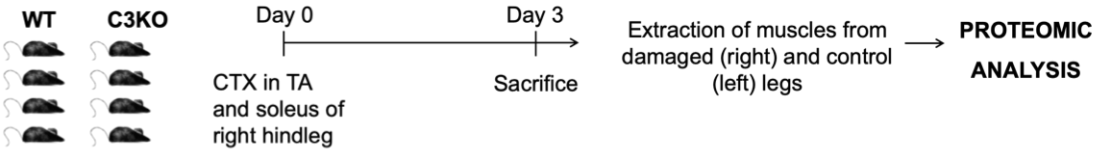

Figure 28. Schematic outline of the experiment for the proteomic analysis of damage response in the C3KO mouse.

The first thing that was evaluated were the differences that could be found between the two genotypes in the muscles at basal state, without considering the damaged muscles, in order to understand the basal differences between the WT and C3KO mice. For this, proteins with a differential ratio greater than 1.5 (up or down) that were statistically significant were analysed.

In the soleus muscle, 30 proteins were found differentially expressed. Some of the most downregulated proteins in the C3KO mice corresponded to mitochondrial proteins like isovaleryl-CoA dehydrogenase and the mitochondrial import receptor subunit TOM70, while among the most upregulated ones were flavin reductase (NADPH), 10 KDa heat shock protein and myogenic regulatory cysteine and glycine-rich protein 3 (CSRP3) (Figure 29A). When performing functional enrichment analysis of these proteins, terms associated with mitochondrial processes were significantly upregulated (Figure 29B).

In the case of the TA muscle, 57 proteins were found differentially expressed. Among the most downregulated ones, isovaleryl-CoA dehydrogenase, spliceosome RNA helicase Ddx39b, the mitochondrial 2,4-dienoyl-CoA reductase or the ubiquitin-40S ribosomal protein S27a were found, while the most upregulated proteins were actin associated Myristoylated alanine-rich C-kinase, DNA replication licensing factor MCM7 and flavin reductase (NADPH) (Figure 29C). Functional enrichment analysis of these proteins indicated processes like protein folding, protein processing in the ER, glucose metabolisms and RNA splicing were altered (Figure 29D). In line with previous studies, the affection appeared different for each muscle, with the soleus having a high number of proteins associated with mitochondrial functions (Kramerova et al., 2004, 2009).

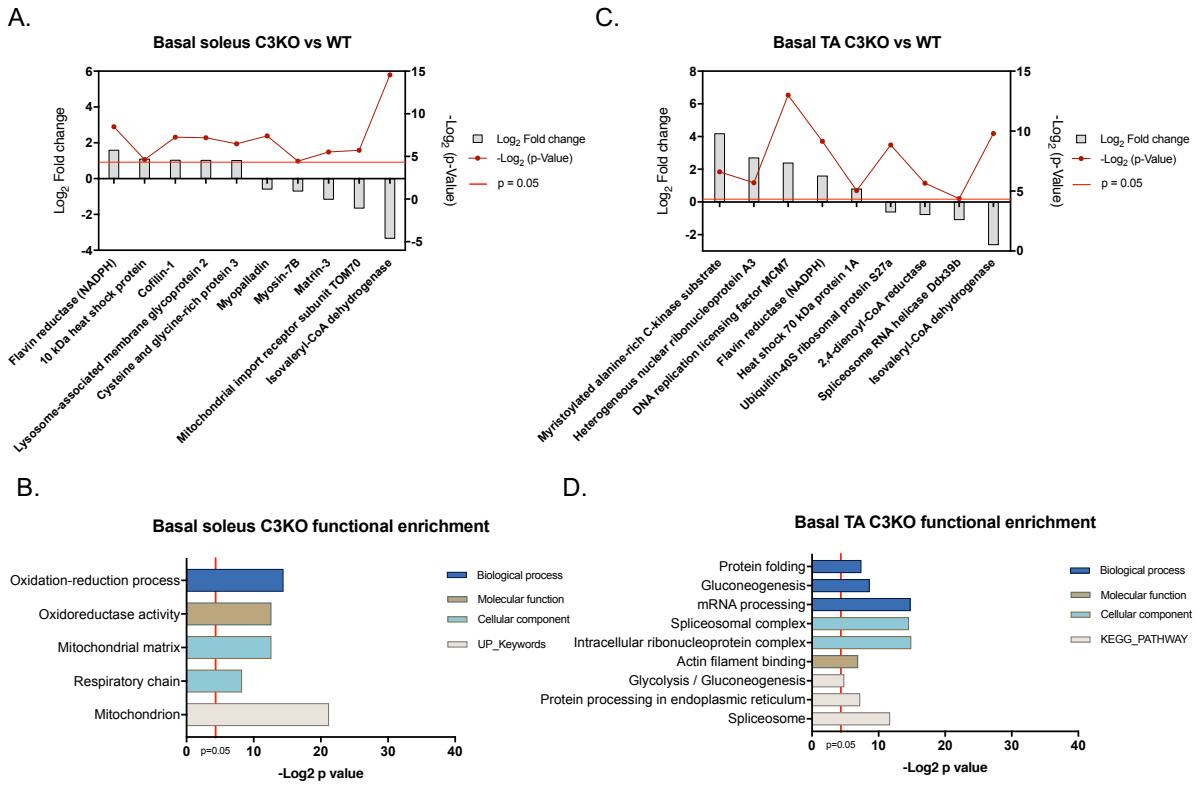

Figure 29. Basal differences between control legs of the WT and C3KO mice in soleus and TA muscles. A) Some of the most differentially expressed proteins in the soleus of the C3KO mice in basal (control) state compared to WT. B) Functional enrichment analysis of the 30 differentially expressed proteins in the C3KO soleus. C) Some of the most differentially expressed proteins in the TA of the C3KO mice in basal (control) state compared to WT. D) Functional enrichment analysis of the 57 differentially expressed proteins in the C3KO TA. Gene ontology (GO: DAVID Bioinformatics Resources) terms (Biological process, Molecular function and Cellular component) and upregulated keywords or KEGG pathways associated to these proteins.

For comparing damage response differences in the soleus, damage response (i.e. protein level differences between the damaged muscle compared to the undamaged control muscle) of the WT were compared against those of the C3KO. WT mice had 61 proteins in its damage response that were not present in the C3KO damage response (24 upregulated and 37 downregulated), while the C3KO had 171 proteins that were not present in the WT damage response (110 upregulated and 61 downregulated) (Figure 30A). Among the proteins specific for WT damage response, proteins like isovaleryl-CoA dehydrogenase, sarcomeric myopalladin, heat shock protein beta-6 and sodium/potassium-transporting ATPase subunit alpha-2 were downregulated, while actin-related protein 2/3 complex subunit 1B, TAR DNA-binding protein 43 or prolyl 4-hydroxylase subunit alpha-1 were upregulated (Figure 30B). To perform functional enrichment analysis, the entire WT damage response was analysed. The functions that were enriched in WT but not in C3KO included processes like response to calcium ion, regulation of mitochondrial membrane potential and ER-Golgi vesicle-mediated transport. M band and cytoskeleton proteins, propanoate metabolism and protein processing in the ER pathways were also specific functions that only appeared enriched in the WT response to damage (Figure 30C).

On the other hand, the C3KO damage response besides lacking the changes in proteins and enriched functions mentioned for the WT, had a larger set of proteins in its damage response. Among these, the myogenic regulatory protein cysteine and glycine-rich protein 3 (CSRP3), together with ankyrin repeat domain-containing protein 2 (ANKRD2), also a muscle differentiation regulatory protein and stress sensor, were the most downregulated proteins in the C3KO damage response. In addition to these, chaperones, dystrophin and troponin T were among the most downregulated proteins. In the upregulated side, proteins like ras-related protein rab-11A, high mobility group protein B1 or Tropomyosin alpha-4 chain were among the most upregulated, as well as the myogenic repressor myb-binding protein 1A (MYBBP1A) (Figure 30D). The functions that were enriched in C3KO but not in WT included processes like translation, regulation of muscle contraction, pyruvate metabolism and protein catabolic processes (Figure 30E).

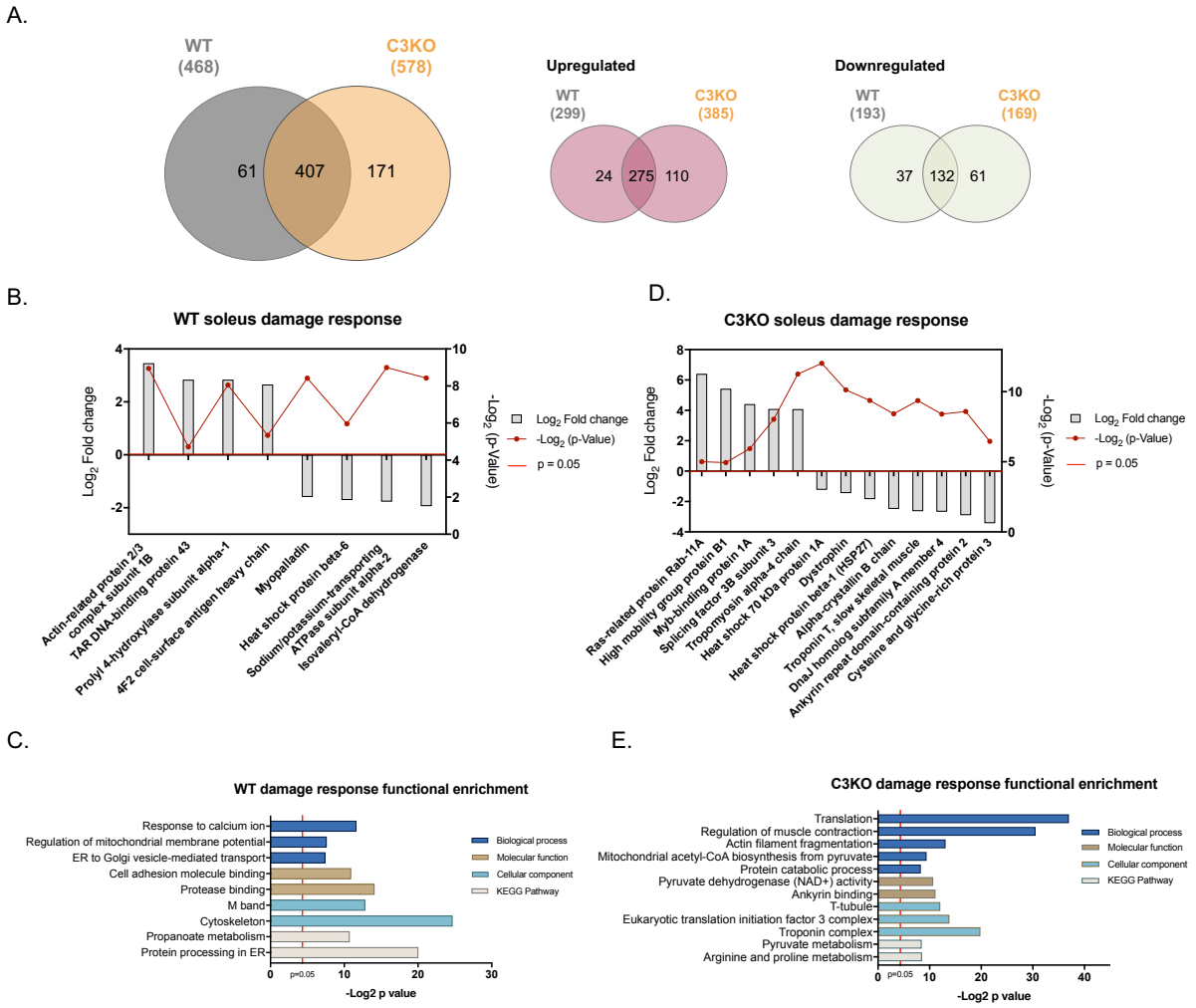

Figure 30. Damage response differences in the soleus muscle of the C3KO mouse. Venn diagrams showing the number of common and differentially expressed proteins identified in damage response of the WT and C3KO mice and the total proteins identified in each group. Diagrams in red just with the upregulated proteins of each group and diagrams in green only with the downregulated ones. B) Fold change and p-value of some of the most differentially expressed proteins in the soleus damage response of the WT mice. C) WT specific terms obtained from the functional enrichment analysis of the 468 proteins in the WT damage response. D) Fold change and p-value of some of the most differentially expressed proteins in the soleus damage response of the C3KO mice. E) C3KO specific terms obtained from the functional enrichment analysis of the 578 proteins in the C3KO damage response. Gene ontology (GO: DAVID Bioinformatics Resources) terms (Biological process, Molecular function and Cellular component) and upregulated keywords or KEGG pathways associated to these proteins.

In the case of the TA, the same damage response comparisons between the WT and the C3KO resulted in fewer differences. WT damage response had 32 proteins differently regulated compared to the C3KO, all of which were upregulated, and in the case of the C3KO response there were 96 proteins specific to its damage response (53 upregulated and 43 downregulated) (Figure 31A). The most upregulated proteins in the WT response were galectin-3, exportin-1 and transmembrane glycoprotein NMB among others; and the functional enrichment analysis pointed towards RNA splicing, intracellular protein

transport processes, and extracellular matrix components as the main WT specific responses (Figure 31B-C). For the C3KO TA damage response, immune response related proteins Ig gamma-1 chain C region, membrane-bound form, and neutrophil cytosol factor 1 proteins were among the most upregulated ones together with Rho-related GTP-binding protein RhoG, Actin-related protein 2/3 complex subunit 1B, Coronin-1B, and chaperones heat shock protein beta-1 (HSP27) and DnaJ homolog subfamily A member 1. The most downregulated proteins included calcium handling parvalbumin alpha, myosin-4, creatine kinase, and fast skeletal muscle troponin T (Figure 31D). The functional enrichment analysis of the C3KO TA damage response differed in the enriched presence of pyruvate metabolism, glycolysis/gluconeogenesis, and amino acid biosynthesis pathways; processes of muscle contraction regulation, actin binding, unfolded protein binding, and the cellular components of the troponin complex, mitochondrial matrix, and cell-cell adherens junctions (Figure 31E).

It was observed that soleus and TA damage responses were differed in WT and C3KO mice, and the damage response also changed from muscle to muscle within the same genotype. To compare how the C3KO is differentially affected in each muscle, both muscles were compared. In basal state, from the differentially expressed proteins in the C3KO, only 2 proteins coincided in the TA and the soleus, which were isovaleryl-CoA dehydrogenase and flavin reductase (NADPH) (Figure 32A). When comparing the damage response differences in genotype and muscles, the C3KO soleus had 153 proteins specific to its damage response, while the C3KO TA only had 13 unique proteins in its response. In the case of the WT specific damage response for both muscles, 1 protein appeared upregulated in both muscles after damage only in WT, precisely this was flavin reductase (NADPH), the one protein already upregulated in the basal state in C3KO that did not increase after damage. In the case of the C3KO specific damage response, in common between both muscles and not present in either muscle WT damage response were 14 proteins (Figure 32B). Specific analysis of these 14 proteins revealed proteins inter alpha-trypsin inhibitor, heavy chain 4, Arginase-1, chloride intracellular channel protein 4 or matrin-3 as the most upregulated proteins in this set and the most downregulated were hydroxyacyl-coenzyme A dehydrogenase, tripartite motif-containing protein 72 and triosephosphate isomerase. Heat shock protein beta-1 (HSP27) responded differently, being up in TA and down in soleus (Figure 32C).

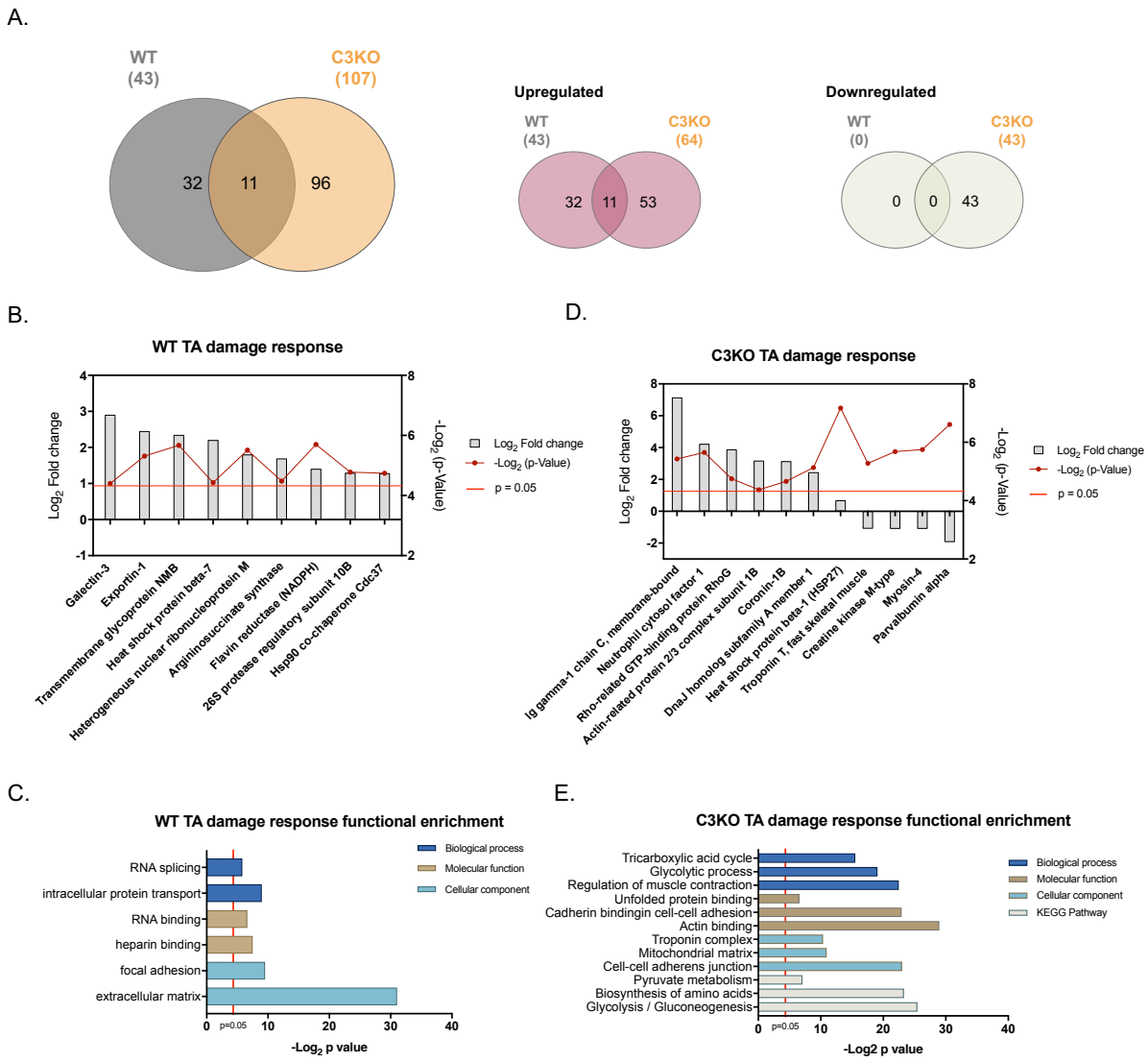

Figure 31. Damage response differences in the TA muscle of the C3KO mouse. A) Venn diagrams showing the number of common and differentially expressed proteins identified in damage response of the WT and C3KO mice and the total proteins identified in each group. Diagrams in red just with the upregulated proteins of each group and diagrams in green only with the downregulated ones. B) Fold change and p-value of some of the most differentially expressed proteins in the TA damage response of the WT mice. C) WT specific terms obtained from the functional enrichment analysis of the 43 proteins in the WT damage response. D) Fold change and p-value of some of the most differentially expressed proteins in the TA damage response of the C3KO mice. E) C3KO specific terms obtained from the functional enrichment analysis of the 107 proteins in the C3KO damage response. Gene ontology (GO: DAVID Bioinformatics Resources) terms (Biological process, Molecular function and Cellular component) and upregulated keywords or KEGG pathways associated to these proteins.

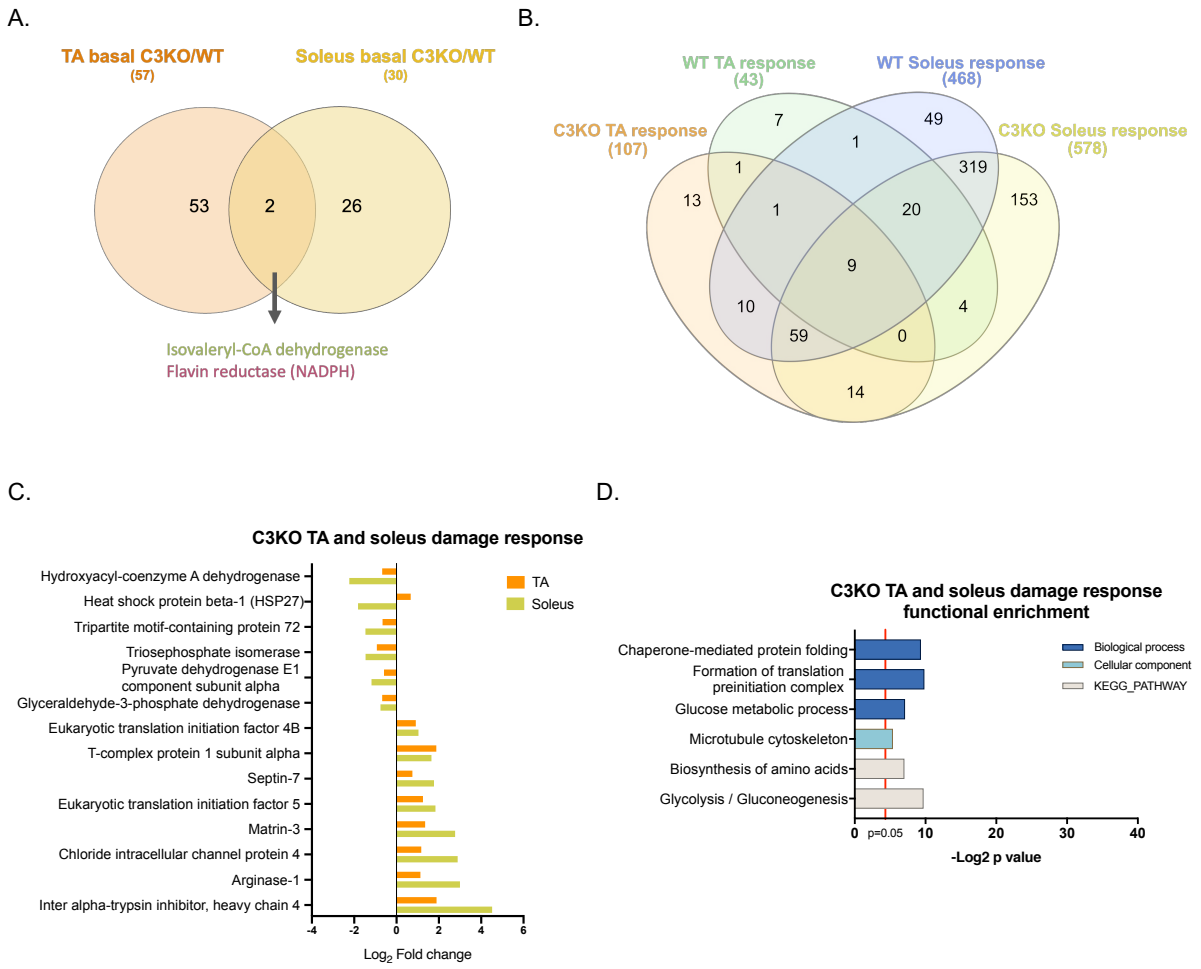

Figure 32. Comparison of the differentially expressed proteins between TA and soleus of the C3KO mouse and the WT in basal state and in damage response. A) Venn diagram showing the number of common and differential proteins identified in the TA and soleus comparisons between the WT and C3KO mice in basal state, the total amount of proteins identified in each group. B) Venn diagram showing the number of common and differential proteins identified in the damage response of the TA and soleus in WT and C3KO mice and the total amount of proteins identified in each group C) Fold change of the 14 proteins identified in common between the soleus and TA damage response in the C3KO mouse that were not detected in the WT damage response of either muscle. D) Functional enrichment analysis of the 14 proteins identified in (C). Gene ontology (GO: DAVID Bioinformatics Resources) terms (Biological process and cellular component) and KEGG pathways associated to these proteins.

Functional enrichment analysis of the 14 C3KO specific damage response proteins pointed towards processes of chaperone-mediated protein folding, formation of the translation preinitiation complex, and glucose and amino acid metabolism, as well as microtubule cytoskeleton as the functional context for these proteins (Figure 32D).

To summarize, proteomic data indicated that already in the basal state, the C3KO has a different affection in soleus muscle compared to TA, with only 2 proteins in common dysregulated in the C3KO muscles. The differences between the muscles are also notable in the damage response, where overall soleus shows more dysregulated proteins. The C3KO specific damage response had many dysregulated proteins, many of them being muscle specific. In the case of the soleus, myogenesis regulators appeared among the most dysregulated proteins, which were not present in the C3KO TA damage response. However, 14 proteins were found to be specific to the C3KO damage response in both muscles, which associated with processes such as the chaperone-mediated protein folding, protein translation, and glucose and amino acid metabolism.

Myogenic evaluation of C3KO mouse satellite cells

Considering the failure to regenerate muscle that occurs in LGMDR1 patients, previous reports indicating altered myoblast fusion in C3KO mice (Kramerova et al., 2006; Yalvac et al., 2017), as well as our proteomic damage response study where various proteins related to myogenesis were dysregulated in the C3KO, we decided to evaluate the state of C3KO SCs *in vitro*. To evaluate the proliferative and myogenic capacity of C3KO SCs and how ageing could be affecting these aspects in the C3KO mouse, SCs from young (3 month) and old (18 months) diaphragms were studied. SCs were isolated using magnetic beads to purify them based on SCs specific markers and these were cultured in suspension to allow them to form spheres which were counted, measured and then plated to differentiate into myotubes. At 7 days of culture, there were no statistical differences in the number of spheres between the young WT and C3KO, however the old C3KO had significantly fewer spheres than the old WT and young C3KO. At 14 days, old C3KO also had significantly fewer sphere than the old WT and young C3KO, while no statistically significant differences were found on the sphere sizes (Figure 33).

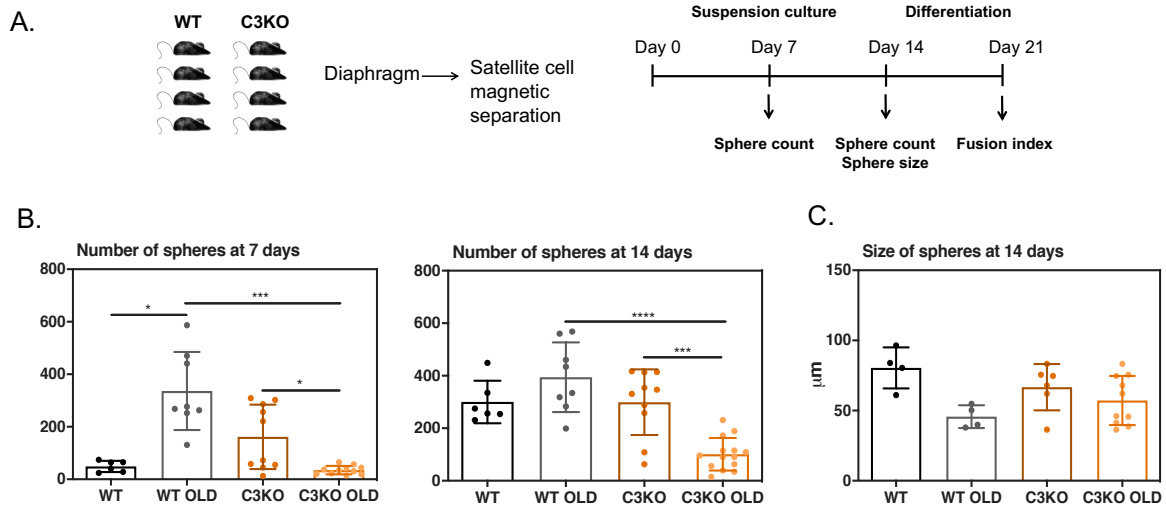

Figure 33. Sphere formation assay with young and old C3KO mouse satellite cells. A) Workflow of the sphere formation assay. B) Quantification of spheres at 7 days and 14 days of suspension culture. C) Quantification of sphere size at 14 days of culture. Data expressed as mean ± SD. One-way Anova is used to calculate p-value *p<0.05, ***p<0.001, ****p<0.0001.

When set to differentiate into myotubes, spheres from the old C3KO formed smaller and shorter myotubes, and the differentiation index was significantly lower than the myotubes obtained from the old WT spheres, however this difference was not noticeable in the myotubes from the young C3KO spheres (Figure 34).

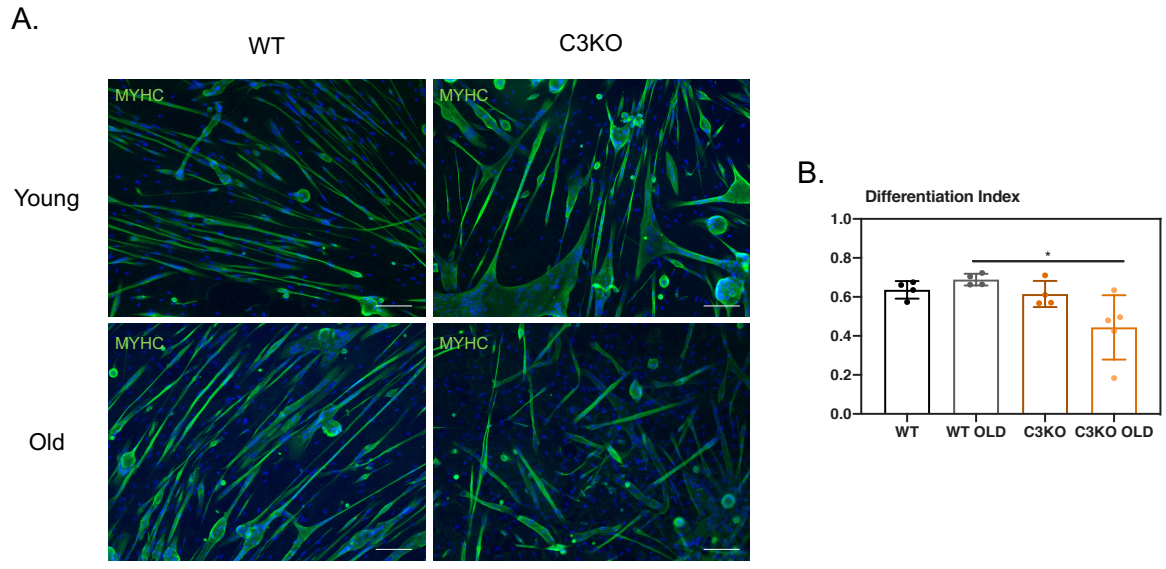

Figure 34. Sphere differentiation from young and old C3KO mouse satellite cells. A) Representative images of immunofluorescence detection of MYHC at day 7 of sphere differentiation. Nuclei were counterstained with Hoechst (blue). Scale bars: 100 µm. B) Quantification of the differentiation index. Data expressed as mean ± SD. One-way Anova was used to calculate p-value. *p<0.05.

Overall, SCs from the C3KO mice had a reduced capacity to form spheres and differentiate only in old age, while the young C3KO did not show statistically significant differences compared to the WT. Thus, it seemed that aging in the absence of calpain3 affects the stemness and myogenic capacity of the SCs.

Myogenic evaluation of human isogenic iPSCs derived myotubes

In order to evaluate whether the observed reduction of myogenic capacity in the C3KO mouse SCs would also occur in human cells, myogenesis was evaluated in human isogenic iPSC-derived PAX7-GFP+ myogenic progenitors. Two isogenic groups were used, "group 1" consisted of the control line and the two calpain 3 KO lines developed in the first chapter of this thesis (KO-1 and KO-4), and "group 2" consisted of a patient-derived line and two isogenic lines that had the mutation in calpain 3 corrected, which were developed in a previous collaborative work with the group of Dr. Perlingeiro (Selvaraj et al., 2019).

Here, the results obtained with the isogenic group 1 are presented first. When performing terminal differentiation of the isogenic group 1 into myotubes, the control line and both KO lines were able to differentiate, formed myotubes and showed differentiation markers MYOGENIN, MYHC and α-ACTININ in immunofluorescence analysis, as well as a few PAX7 positive nuclei. However, the differentiation index measured was slightly lower in the KO-1 line and significantly lower in the KO-4 line. The fusion index was also significantly lower in the KO-4 line and when measuring the MYHC area per nuclei, the ratio was significantly lower in both KO lines (Figure 35).

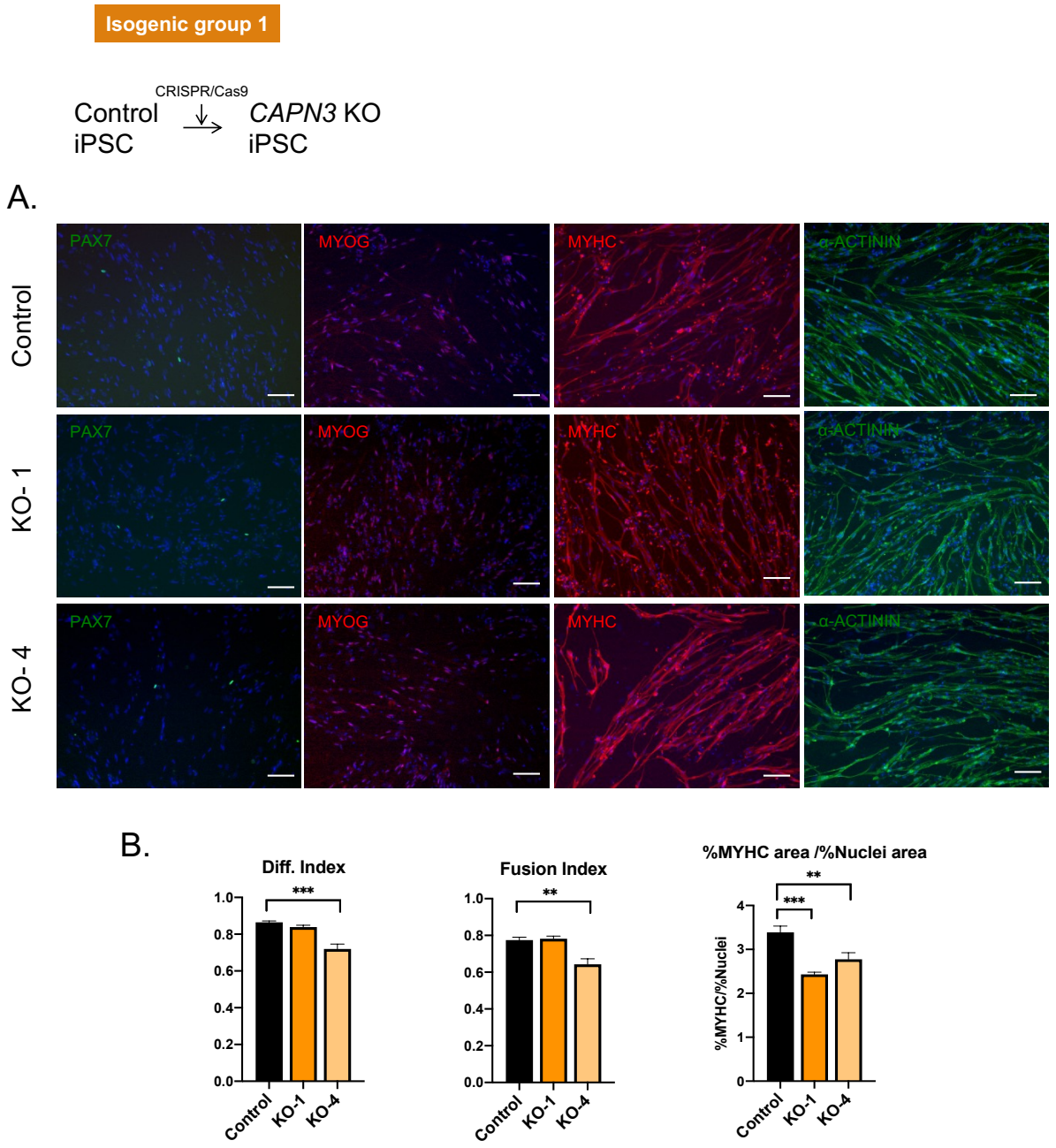

Figure 35. Terminal differentiation of myogenic progenitors from isogenic group 1. A) Representative images of immunofluorescence detection of PAX7, MYOGENIN (MYOG), MYHC and α-ACTININ at day 8 of differentiation. Nuclei were counterstained with Hoechst (blue). Scale bars: 100 µm. B) Differentiation index (Diff. index), Fusion index, and MYHC area per Nuclei area levels observed at day 8 of differentiation. Data expressed as mean ± SEM of 4 biological replicates. One-way Anova was used to calculate p-value. *p<0.05, **p<0.01, ***p<0.001.

Gene expression analysis was performed in these cells to evaluate expression of myogenic regulatory factors and differentiation indicators during differentiation at days 0, 3 and 8. *PAX7* expression was decreased in all lines as differentiation progressed and *MYOD1* and *MYOGENIN* were induced. In the case of the latter, KO-4 had higher levels of its expression in day 3. Despite having similar levels to the control in these myogenic factors,

KO lines showed decreased levels of *MYH3* and *MYH2* at day 8 of differentiation, consistent with the observations in the immunofluorescence analysis. Dystrophin levels also appeared significantly lower at day 8 in the KO-4 line (Figure 36).

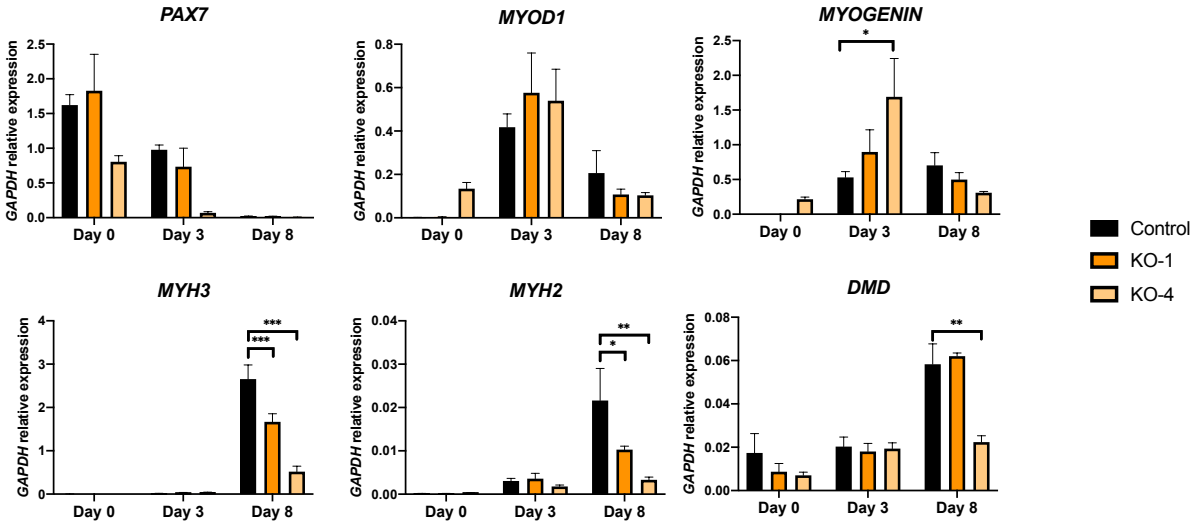

Figure 36. Gene expression analysis of myogenic progenitors from isogenic group 1 in terminal differentiation day 0, 3 and 8. Early myogenic marker genes *PAX7*, *MYOD1*, *MYOGENIN* and advanced myogenic markers *MYH3*, *MYH2* and *DMD* were analysed. Data expressed as mean ± SEM of 3 biological replicates. One-way Anova was used to calculate p-value. *p<0.05, **p<0.01, ***p<0.001.

Protein levels at day 3 and day 8 were also analysed in these differentiations. At day 3, MYOD1 and MYOGENIN levels were very variable among the three lines, which could be due to a different pace of differentiation, and myogenic repressor MYBBP1A levels were similar in all the lines. At this point of the differentiation, p-mTOR and PGC1A, key regulators of muscle growth and mitochondrial biogenesis respectively, were significantly upregulated in the KO lines, although mitochondrial TOM20 levels were not changed (Figure 37A-B).

At day 8 of differentiation, the differences in some of these proteins changed. MYOGENIN was significantly reduced in the KO lines, and MYH3 seemed to be lower in the KO lines too. Myogenic regulatory proteins MYBBP1A and CSRP3 were variable between the lines, the latter being significantly lower in KO-4 than in KO-1. SERCA-2 was significantly lower in the KO lines, consistent with what has been described in calpain 3 downregulated muscle (Toral-Ojeda et al., 2016). At this point of the differentiation, p-AMPK levels seemed to be increased in the KO lines, particularly in the KO-1 line, while PGC1A was reduced, significantly for the KO-4, and TOM20 showed a similar profile (Figure 37C-D).

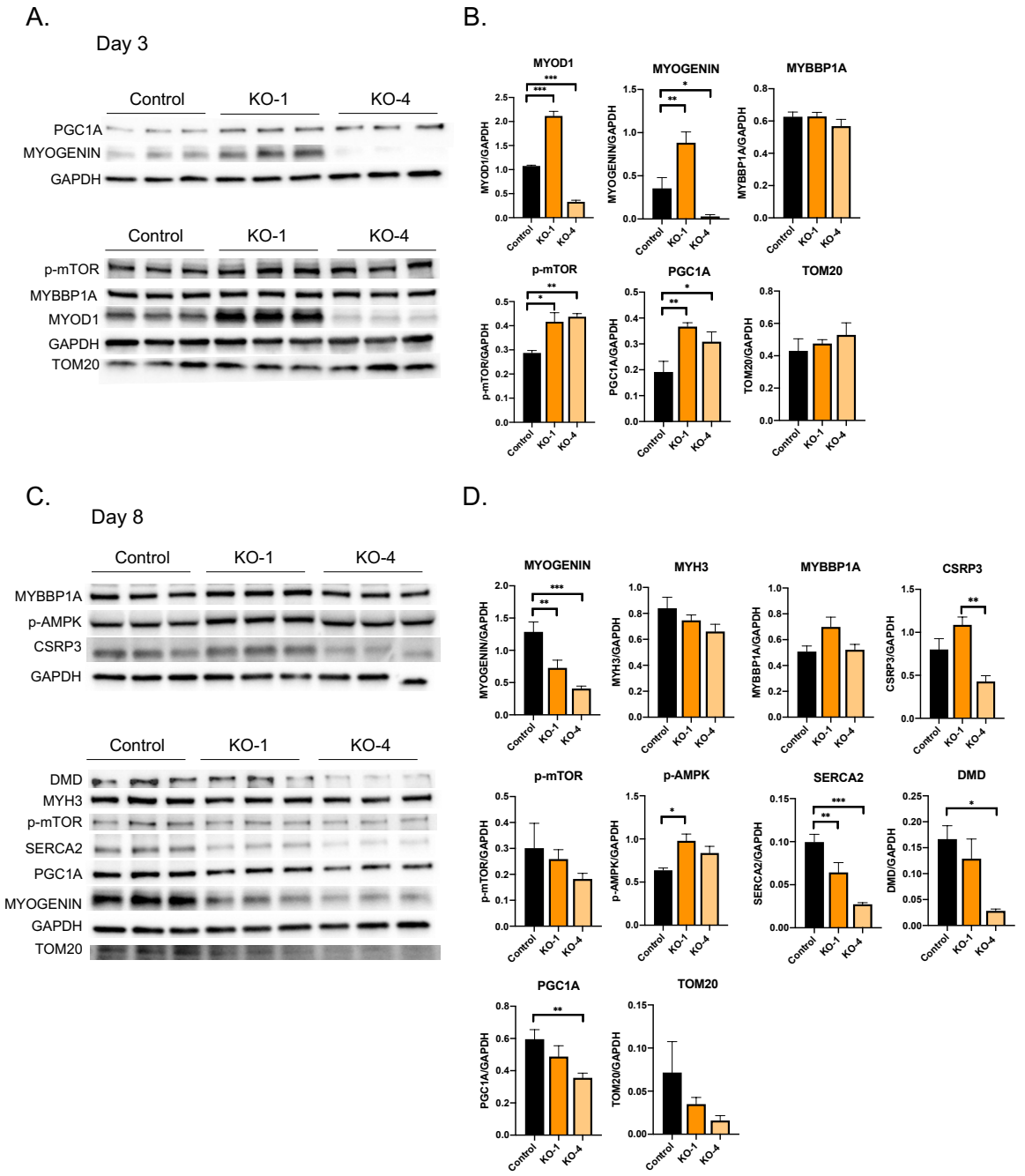

Figure 37. Western blot analysis of myogenic progenitors from isogenic group 1 in differentiation day 3 and 8. A) Protein levels at day 3 of differentiation analysing myogenic regulatory proteins MYOD1, MYOGENIN and MYBBP1A, and p-mTOR, PGC1A and mitochondrial TOM20. B) Quantification of protein levels detected in (A) through densitometry and normalized to GAPDH protein levels. C) Protein levels at day 8 of differentiation, analysing myogenic regulatory proteins, MYOGENIN, MYBBP1A, and CSRP3, differentiation markers MYH3, DMD, and calcium transporter SERCA2, and p-mTOR, p-AMPK, PGC1A and mitochondrial TOM20. D) Quantification of protein levels detected in (C) through densitometry and normalized to GAPDH protein levels. Data expressed as mean ± SEM of 3 biological replicates. One-way Anova was used to calculate p-value. *p<0.05, **p<0.01, ***p<0.001.

In the same way, these experiments were carried out with the isogenic group 2. These isogenic lines were also terminally differentiated into myotubes. In this case also, both the patient-derived line (08-26) and the calpain 3 gene corrected lines (C5 and C10) were able to differentiate, formed myotubes and showed differentiation markers MYOGENIN, MYHC and α-ACTININ in immunofluorescence analysis, as well as a few PAX7 positive nuclei. The differentiation index measured was significantly higher in the gene corrected lines, as well as the fusion index and the ratio of MYHC area per nuclei area, consistent with what was observed in the isogenic group 1 (Figure 38).

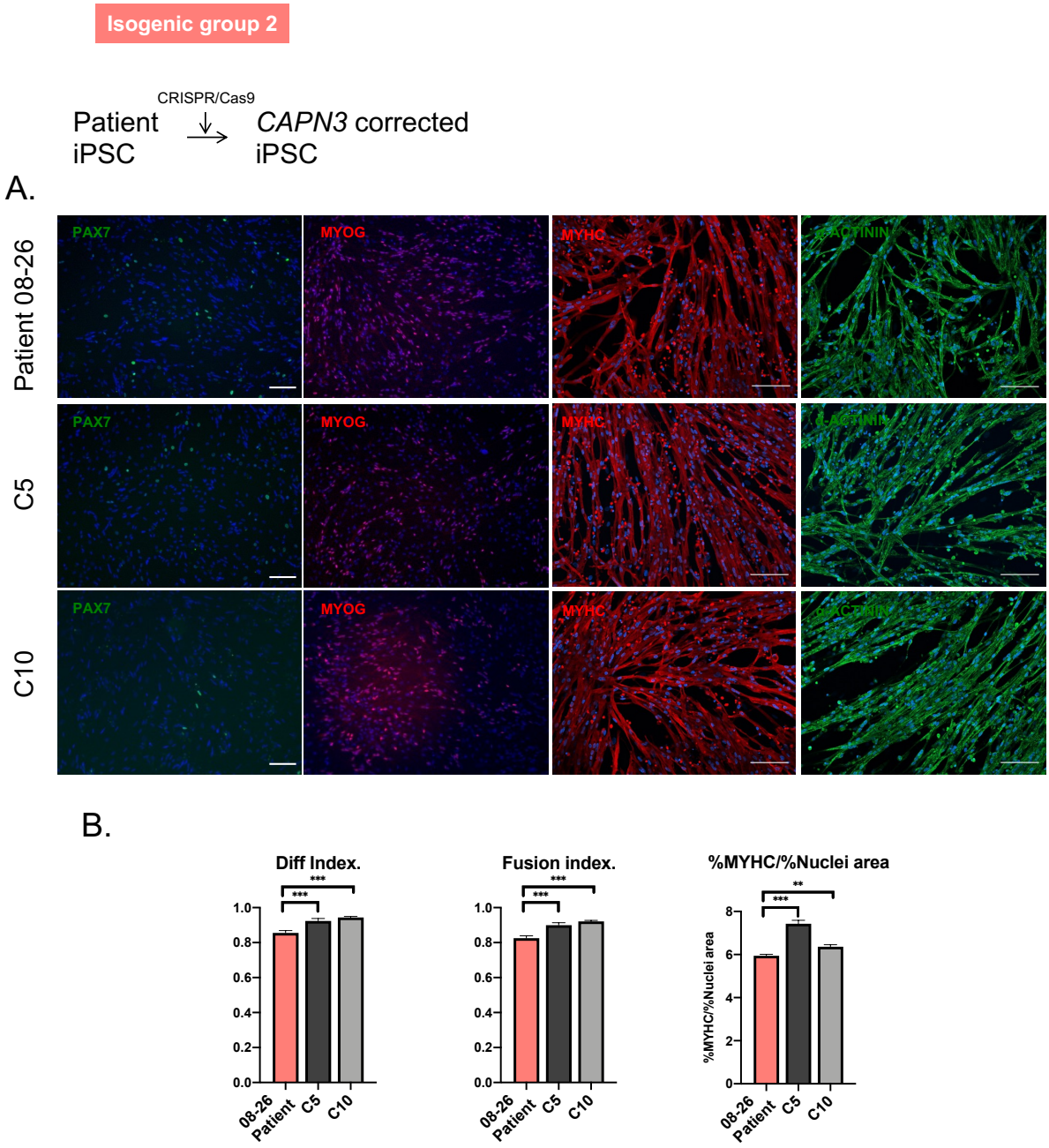

Figure 38. Terminal differentiation of myogenic progenitors from isogenic group 2. A) Representative images of immunofluorescence detection of PAX7, MYOGENIN (MYOG), MYHC, and α-ACTININ at day 8 of differentiation. Nuclei were counterstained with Hoechst (blue). Scale bars: 100 µm. B) Differentiation index (Diff. index), Fusion index, and MYHC area per nuclei area levels observed at day 8 of differentiation. Data expressed as mean ± SEM of 4 biological replicates. One-way Anova was used to calculate p-value. *p<0.05, **p<0.01, ***p<0.001.

When performing gene expression analysis of these lines, the gene expression pattern was similar to isogenic group 1. *PAX7* expression decreased as differentiation progressed and *MYOD1* and *MYOGENIN* were induced after the 3rd day. Differentiation indicators of *MYH3, MYH2* and *DMD* were highest at day 8 of differentiation, and although the *MYH3* and *MYH2* averages were slightly higher on the gene-corrected lines, the differences were not statistically significant (Figure 39).

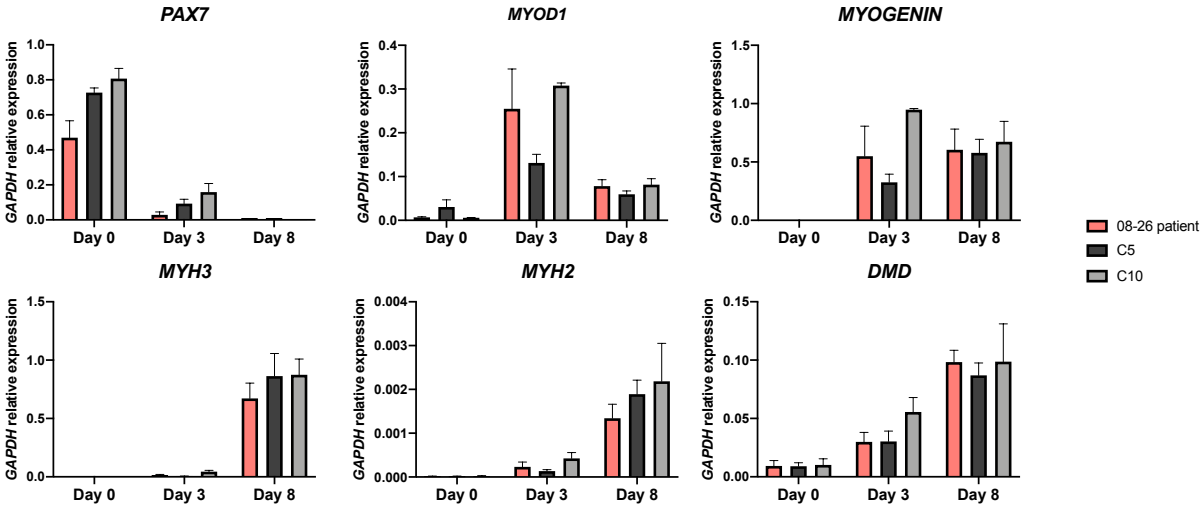

Figure 39. Gene expression analysis of myogenic progenitors from isogenic group 2 in terminal differentiation day 0, 3 and 8. Early myogenic marker genes PAX7, MYOD1, MYOGENIN and advanced myogenic markers MYH3, MYH2 and DMD were analysed. Data expressed as mean ± SEM of 3 biological replicates. One-way Anova was used to calculate p-value. *p<0.05, **p<0.01, ***p<0.001.

At the protein level, the differences in this isogenic group were also less noticeable than the differences found in the isogenic group 1. In this case, at day 3 myogenic repressor MYBBP1A was variable but appeared higher in the corrected clones, while p-mTOR was up significantly in line C10. At day 8 of differentiation, corrected lines did seem to have higher levels of MYH3 and p-mTOR, which were significant for line C10, as well as for the higher levels of MYBBP1A (Figure 40).

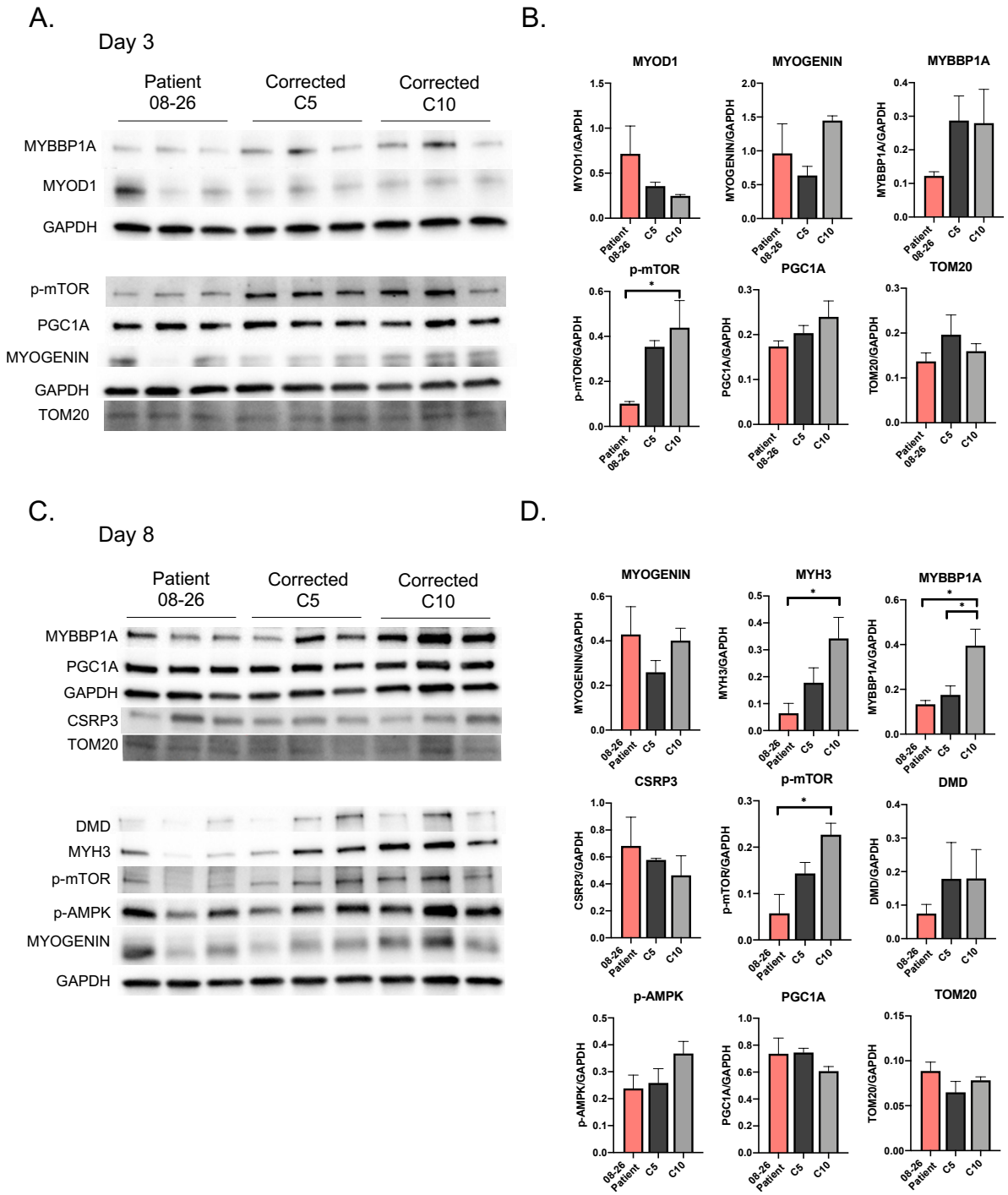

Figure 40. Western blot analysis of proteins in myogenic progenitors from isogenic group 2 in differentiation day 3 and 8. A) Protein levels at day 3 of differentiation analysing myogenic regulatory proteins, MYOD1, MYOGENIN, and MYBBP1A, and p-mTOR, PGC1A and mitochondrial TOM20. B) Quantification of protein levels detected in (A) through densitometry and normalized to GAPDH protein levels. C) Protein levels at day 8 of differentiation. Myogenic regulatory proteins, MYOGENIN, MYBBP1A, and CSRP3, differentiation markers MYH3 and DMD, and p-mTOR, p-AMPK, PGC1A and mitochondrial TOM20. D) Quantification of protein levels detected in (C) through densitometry and normalized to GAPDH protein levels. Data expressed as mean ± SEM of 3 biological replicates. One-way Anova was used to calculate p-value. *p<0.05

ER stress and mTOR/Akt pathways in young and old C3KO mice

Considering the pathways and proteins that were affected in the damage response proteomic study and the fact that old but not young C3KO mice showed alterations in proliferative and myogenic capacity in their SCs, a set of related proteins were analysed in TA and soleus of young and old C3KO (Figure 41). Among these proteins, ER stress/UPR and mTOR/Akt pathway proteins were analysed, since these pathways are key in maintaining protein homeostasis and the proteomic data indicated that the protein folding process was dysregulated, as well as previous studies also indicated proteostatic issues such as insoluble aggregates (Kramerova et al., 2005), and an altered ubiquitin proteasomal pathway (Rajakumar et al., 2013).

In TA, old C3KO had significantly higher levels of AKT protein, and also seemed to have higher mTOR and β-CATENIN. On the other hand, GSK3β, substrate of AKT and key protein inducing protein degradation and muscle wasting, appeared significantly higher only in young C3KO (Figure 41A-B). In the soleus, mTOR levels were significantly higher in young C3KO, but AKT, β-CATENIN and GSK3β levels had a high variability and the differences were not significant, however a tendency for higher levels of GSK3β and β-CATENIN was observed in C3KO soleus muscles (Figure 41C-D).

ER stress/UPR associated proteins GRP94 and CHOP did not show significant differences, however, in the case of CHOP despite the high variability in the C3KO, a general tendency could be observed for higher levels in old mice both in WT and C3KO, and in both muscles. In the case of cytosolic chaperone HSP70, despite also having great variability, C3KO mice showed a tendency for higher levels both in young and old age and in both TA and soleus (Figure 41) which also appeared dysregulated in the proteomic study.

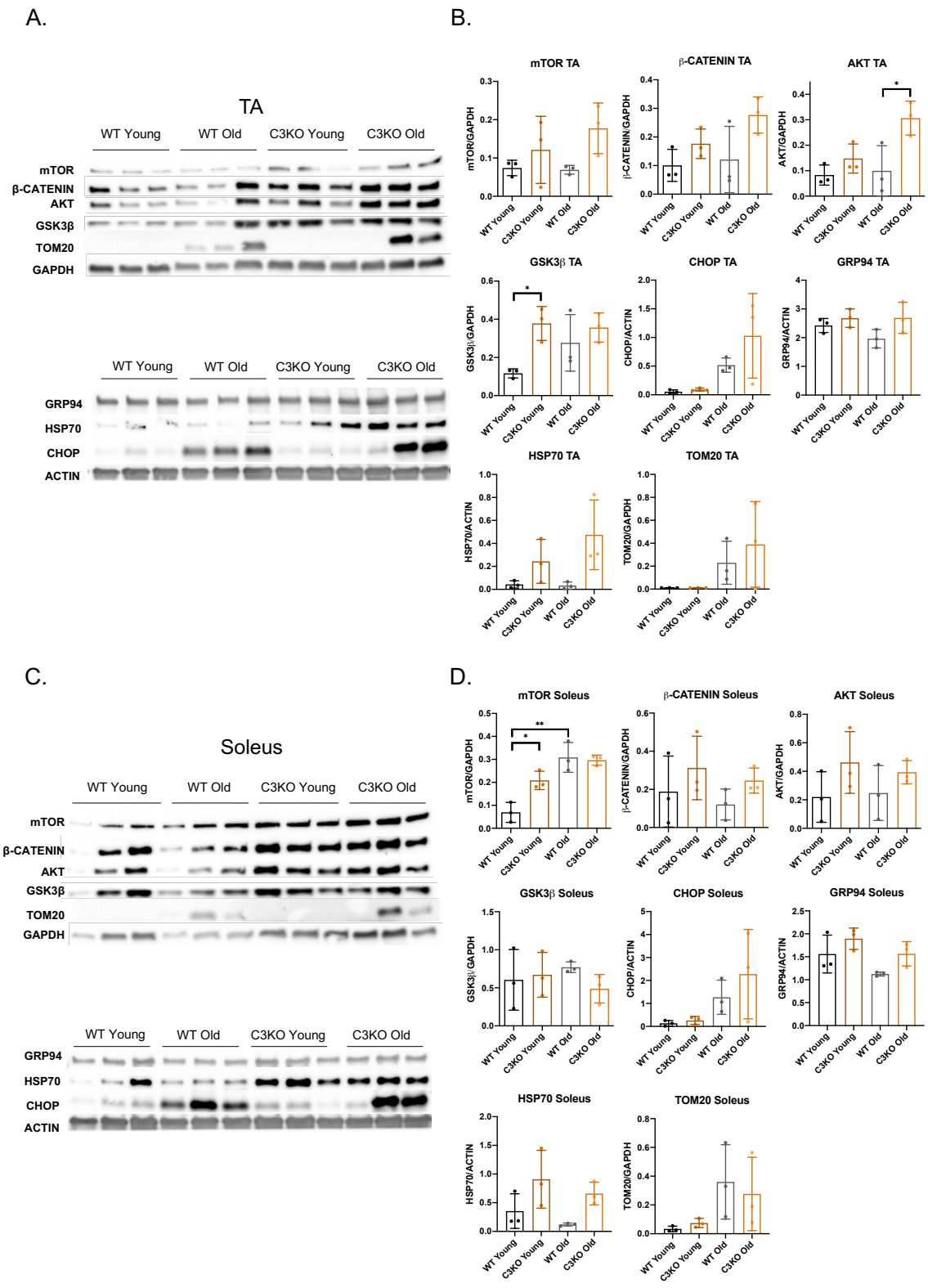

Figure 41. Western blot analysis of proteins from C3KO mouse TA and soleus muscles in young and old age. A) Protein levels analysed in TA muscles for signalling pathways mTOR, β-CATENIN, AKT, and GSK3β; and ER stress indicators CHOP and GRP94, chaperone HSP70, and mitochondrial protein TOM20. B) Quantification of protein levels detected in (A) through densitometry and normalized to GAPDH or ACTIN protein levels. C) Protein levels analysed in soleus muscles for the same set of proteins. D) Quantification of protein levels detected in (C) through densitometry and normalized to GAPDH or ACTIN protein levels. Data expressed as mean ± SD of 3 biological replicates. One-way Anova was used to calculate p-value. *p<0.05, **p<0.01.

Further focusing on the soleus muscle for being considered a more affected muscle than the TA, ER stress protein CALNEXIN appeared significantly upregulated in young mice, and similarly, myogenic repressor MYBBP1A was also significantly upregulated, however these differences were not significant in old age. Other analysed proteins like MYOD1, HSP27 and NF-κB showed high variability and no statistically significant differences could be observed (Figure 42).

Overall and despite the high degree of variability, some of the mTOR/Akt pathway proteins were observed altered in the C3KO muscles and in the case of ER/UPR indicators, only CALNEXIN was detected significantly increased in the young C3KO soleus.

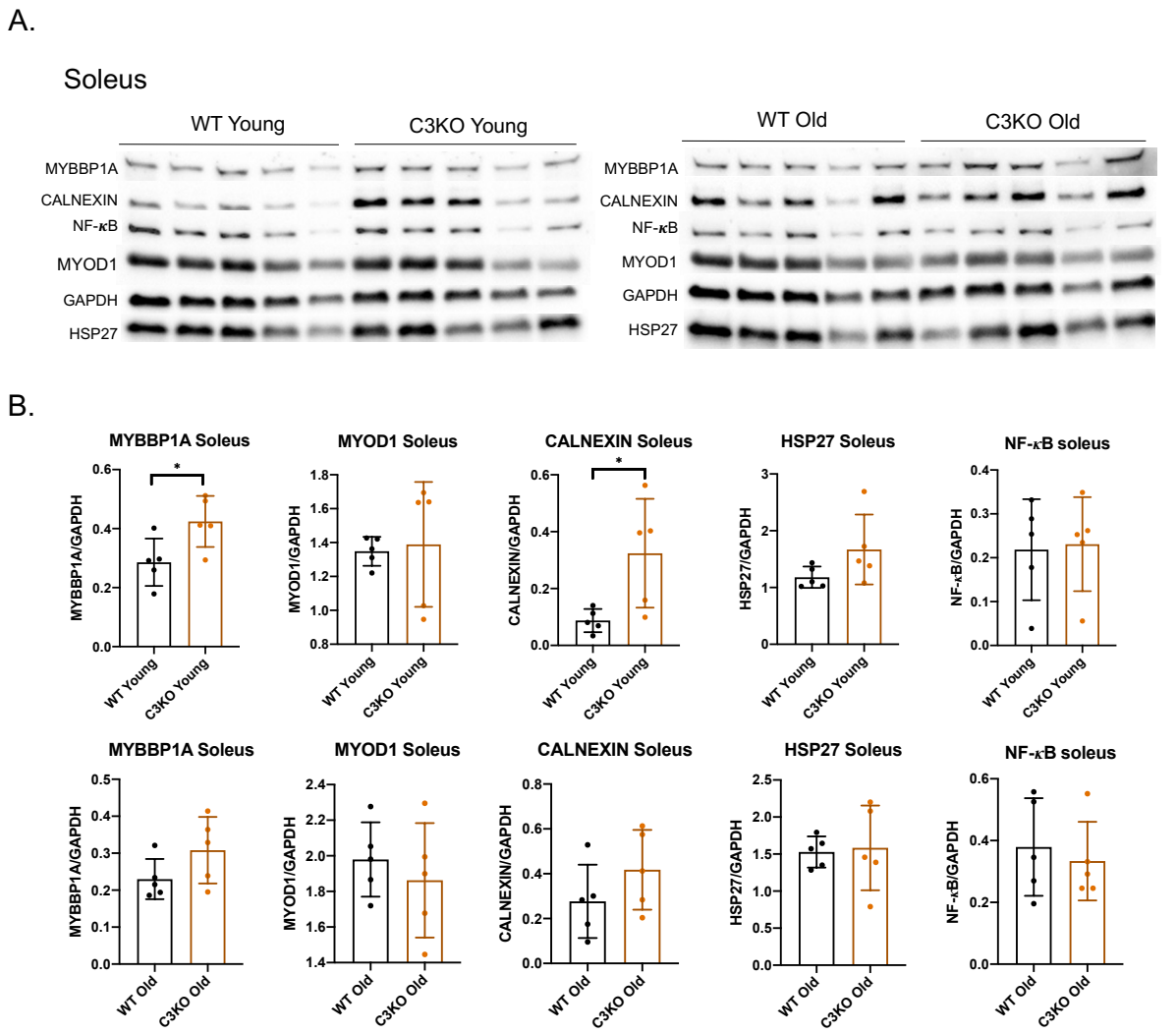

Figure 42. Western blot analysis of proteins in C3KO mouse soleus muscles in young and old age. A) Protein levels analysed in soleus muscles for myogenic regulators MYBBP1A and MYOD1; ER stress indicator CALNEXIN, pro-atrophic NF-κB and chaperone HSP27. B) Quantification of protein levels detected in (A) through densitometry and normalized to GAPDH protein levels. Data expressed as mean ± SD of 5 biological replicates. One-way Anova was used to calculate p-value. *p<0.05.

Exercise endurance and voluntary exercise in old C3KO mice and the effect of 4-PBA treatment

In order to evaluate the C3KO muscle response and motor function in a more physiological challenge than the CTX induced damage, running endurance tests and voluntary running experiments were performed. Exercise can be an inducer of ER stress/UPR and increase protein turnover and SCs activation (Darr & Schultz, 1987; Estébanez et al., 2018), and therefore any issues in maintaining proteostasis could be more apparent in a context where intense exercise is being performed. LGMDR1 is a progressive and degenerative human disease that leads to loss of muscle mass and ambulation, mostly affecting to proximal limb muscles, and which worsens with age. Aiming to have more affection in the C3KO model, old mice (18±1 months) were used for the study.

In addition to evaluating the differences between the WT and C3KO, the effect of sodium phenylbutyrate (4-PBA) treatment was tested. 4-PBA is a compound currently used to treat urea cycle disorders that also functions as a chemical chaperone, aiding in protein folding, reducing protein aggregation and oxidative stress (Perlmutter, 2002). Currently it is also being studied in RYR1-associated myopathies that are associated with ER stress (C. S. Lee et al., 2017) and in clinical trials for inclusion body myositis (ClinicalTrials.gov: NCT04421677). Since previous studies with the C3KO mouse reported insoluble protein aggregate formation in muscles (Kramerova et al., 2005), and the proteomic data presented here indicated chaperone-mediated protein folding could be an altered process, we thought that a 4-PBA treatment could potentially be used to reduce the effects of protein folding issues and an affected proteostasis.

Exhaustion test and voluntary running in old C3KO mice

Exhaustion and voluntary running tests were performed during 30 days, performing 3 exhaustion test per week and analysing voluntary running for 48h every 3 exhaustion tests. 9 WT, 5 C3KO and 5 C3KO with 4-PBA treatment were used, all around 18 months old (Figure 43A). For the exhaustion test, mice were put on an enclosed treadmill with progressively increasing speed until mice were unable to keep the pace while the time and distance run were being measured. In all the exhaustion tests, both the untreated and the 4-PBA treated C3KO mice were able to run significantly more distance and time in average than the WT mice (Figure 43B-D).

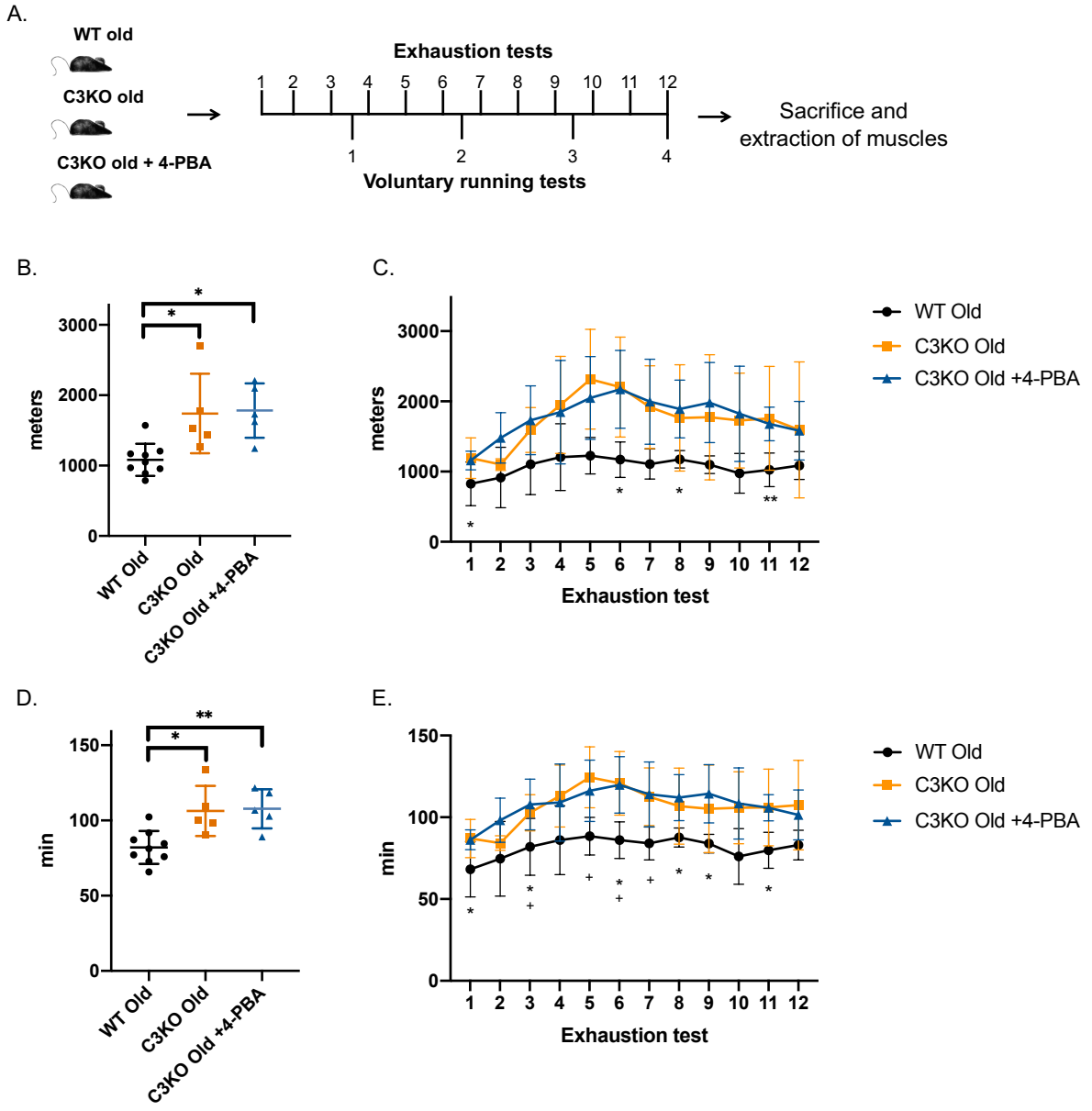

Figure 43. *In vivo* study of endurance by exhaustion tests and voluntary running in old C3KO mouse and old 4-PBA treated C3KO mouse. A) Schematic representation of the *in vivo* experiment. 12 exhaustion tests were performed over a period of 30 days and 4 voluntary running tests. B) Average distance run by each group in all exhaustion tests. C) Distance run by each group in each exhaustion test. D) Average time run by each group in all exhaustion tests. E) Average time run by each group in each exhaustion test. Data expressed as mean ± SD, n = 5 in C3KO, n = 5 in C3KO +4-PBA, and n = 9 in WT. One-way Anova was used to calculate p-value in (B) and (D) *p<0.05, **p<0.01. In (C) and (E) p-value was calculated with mixed-effects analysis: *p<0.05 (WT Old vs. C3KO Old + 4-PBA). $^{+}$p<0.05 (WT Old vs. C3KO Old).

To ensure the genotypes of the mice colonies were correct all the mice were genotyped and calpain 3 presence/absence was confirmed by Western blot (Figure 44A). Due to old age, some mice were visibly overweight, but no statistically significant differences were found between the groups (Figure 44B-C).

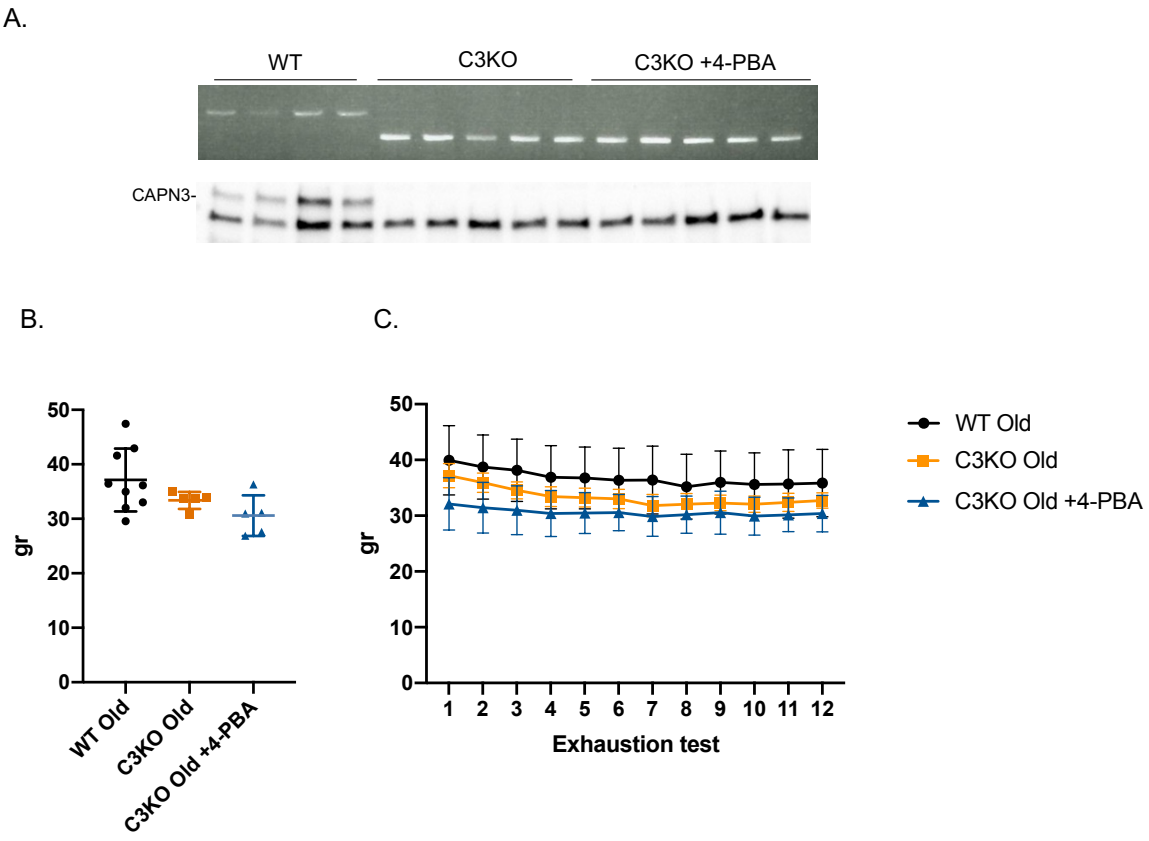

Figure 44. Genotype confirmation and weight measurements for the *in vivo* study of endurance by exhaustion tests and voluntary running. A) WT and C3KO genotyping by PCR and agarose gel electrophoresis (white bands in the upper gel) and CAPN3 protein detection by Western blot in muscles (top black bands in lower membrane image). B) Average weight of each group throughout the study. C) Weight of each group in each exhaustion test. Data expressed as mean ± SD, n = 5 in C3KO, n = 5 in C3KO +4-PBA, and n = 9 in WT.

In the voluntary running tests no statistically significant differences were found in the voluntary distance run by the 3 groups, with high variability between each mouse (Figure 45A-C). Regarding the maximum speed recorded for each group, there were no major differences between the groups, the C3KO being the group with the highest variability. However, 4-PBA treated C3KO had the highest average maximum speed and in the last voluntary running test, it did record significantly faster maximum speeds than the WT (Figure 45D).

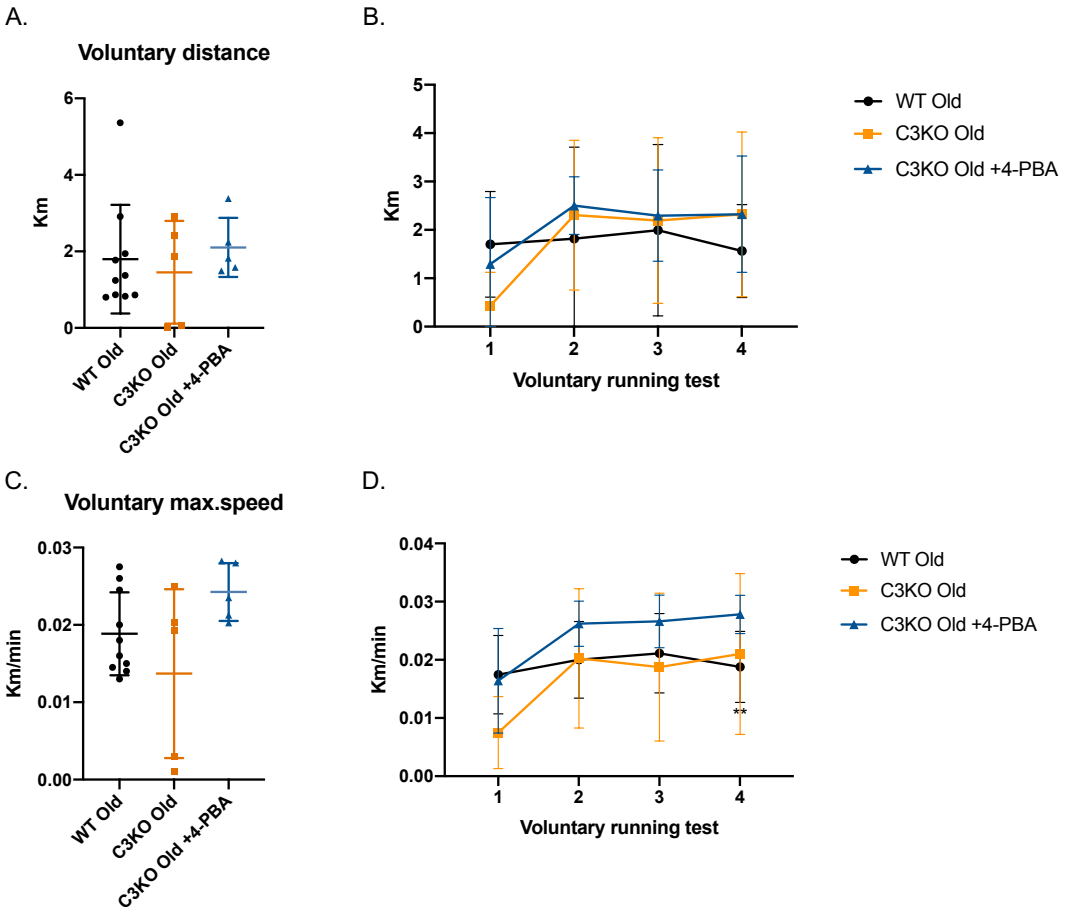

Figure 45. *In vivo* voluntary running in old C3KO mouse and old 4-PBA treated C3KO mouse. A) Average voluntary distance run by each group. B) Voluntary distance run by each group in each voluntary running test. C) Average voluntary maximum speed run by each group. D) Voluntary maximum speed run by each group in each voluntary running test. Data expressed as mean ± SD, n = 5 in C3KO, n = 5 in C3KO +4-PBA, and n = 9 in WT. p-value was calculated with mixed-effects analysis: *p<0.05 (WT Old - C3KO Old + 4-PBA).

TA and soleus muscles from these mice were analysed at the histological level by hematoxylin and eosin staining (Figure 46). Overall, there were no major differences in the appearance of the muscles between the WT, C3KO and the 4-PBA treated C3KO. One thing that could be noted was that soleus muscles did seem to have slightly higher levels of fibrotic tissue than the TA, but this was present in all groups and could probably be associated to the age of the mice. Similarly, regenerative centrally nucleated fibers could be detected in all groups, while no clear signs of increased atrophy or fatty acid infiltrations could be detected in any of the groups.

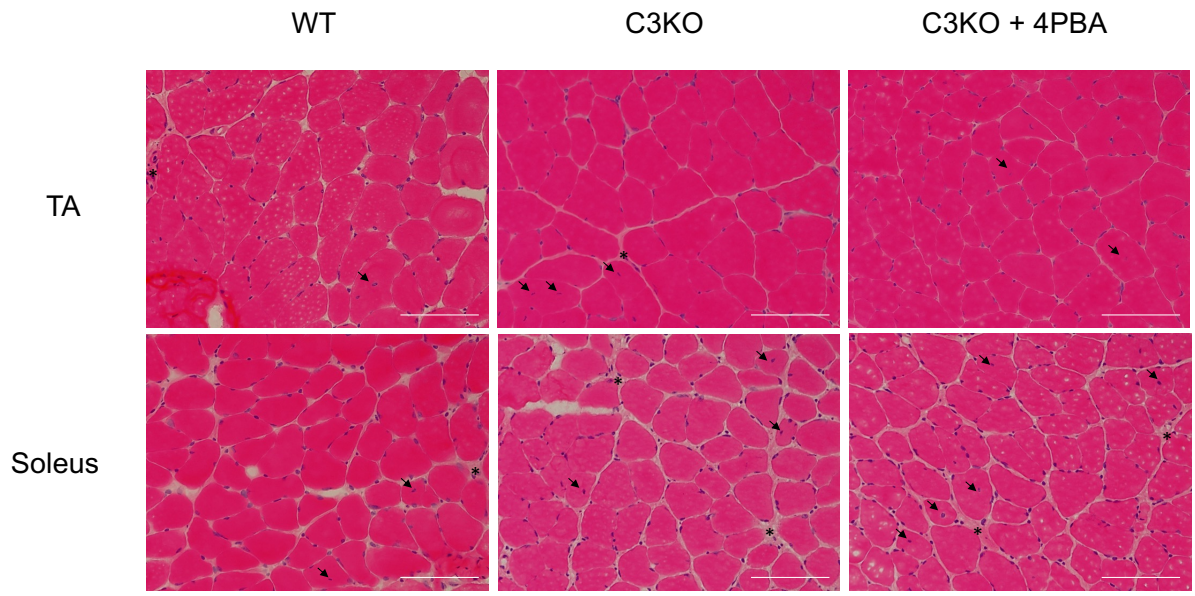

Figure 46. TA and soleus hematoxylin and eosin staining from the old WT, C3KO and 4-PBA treated C3KO mouse after the exhaustion tests. Black asterisks show fibrotic tissue and arrows central nuclei. Scale bar: 100µm.

Analysis of ER stress, protein homeostasis and metabolism indicators

Soleus muscles extracted after the exhaustion and voluntary running tests were taken to analyse protein levels from some of the pathways and functions that previous results indicated that could to be altered, particularly the functions and proteins that the proteomic study indicated that were dysregulated, and to evaluate whether the 4-PBA treatment had any effect in them. In this case, only the soleus muscle was analysed due to this muscle having more differences in the proteomic damage response analysis and also being described as one of the most affected ones in this model (Figure 47) (Kramerova et al., 2004). Levels of active phosphorylated p-mTOR, key regulator in maintaining muscle mass, were significantly upregulated in the C3KO mice, however in the 4-PBA treated group, these levels were significantly reduced to WT levels. Also, despite increased p-mTOR levels, p-S6, which is used as a marker of mTOR pathway activity, was not increased in the C3KO. Other key pathways that appeared affected in the proteomic data were associated with glucose metabolism and mitochondria. In this regard, insulin-regulated glucose transporter GLUT4 levels were significantly reduced in C3KO mice, and similarly, mitochondrial membrane protein TOM20 was significantly reduced. In these cases, the 4-PBA treated group did not have any significant effect. PGC1A, which regulates mitochondrial biogenesis, did not have significant differences, although there

was a tendency for higher levels in the WT (Figure 47B). Other key proteins that mediate in muscle metabolism changes with exercise such as p-CAMKII or p-GSK3β did not have significant differences either, although there was high variability between the samples (Figure 47B-D).

Myogenic repressor MYBBP1A, which appeared upregulated in the damage response of the C3KO soleus, also appeared upregulated after the exhaustion tests. In this case, C3KO soleus had significantly higher levels of this protein, but 4-PBA treatment significantly reduced MYBBP1A levels down to WT levels. Embryonic MYH3 levels, indicative of newly formed myotubes, seemed to be slightly higher in the WT group, but the results were not significant (Figure 47C). On the other hand, pro-atrophic NF-**κ**B levels were higher in both C3KO mice groups. When analysing levels of ubiquitination, the amount of high-molecular weight (MW) proteins that were ubiquitinated (above 150 KDa) was significantly higher in the C3KO group, and here too, 4-PBA treatment seemed to restore this increase (Figure 47D).

Regarding chaperones expression and ER stress/UPR related proteins (Figure 47E), these were only partially induced, where ER stress indicators CALNEXIN and BIP were significantly higher in the C3KO mice. 4-PBA treatment reduced the levels of both proteins back to WT levels, significantly reducing BIP levels when compared to the untreated C3KO. On the other hand, ER stress associated GRP94 chaperone and CHOP did not significantly differ between the groups. Among the cytosolic chaperones analysed, HSP27, which also appeared dysregulated in the proteomic analysis of damage response, was significantly higher in the C3KO mice, and here too 4-PBA treatment reduced its levels significantly back to WT levels. In the case of the other small cytosolic chaperone A-CRYSTALIN B, there were no significant differences observed between the groups. HSP70, which also seems to be affected in the C3KO mice, showed a tendency for higher levels in the C3KO but the differences were not statistically significant (Figure 47E).

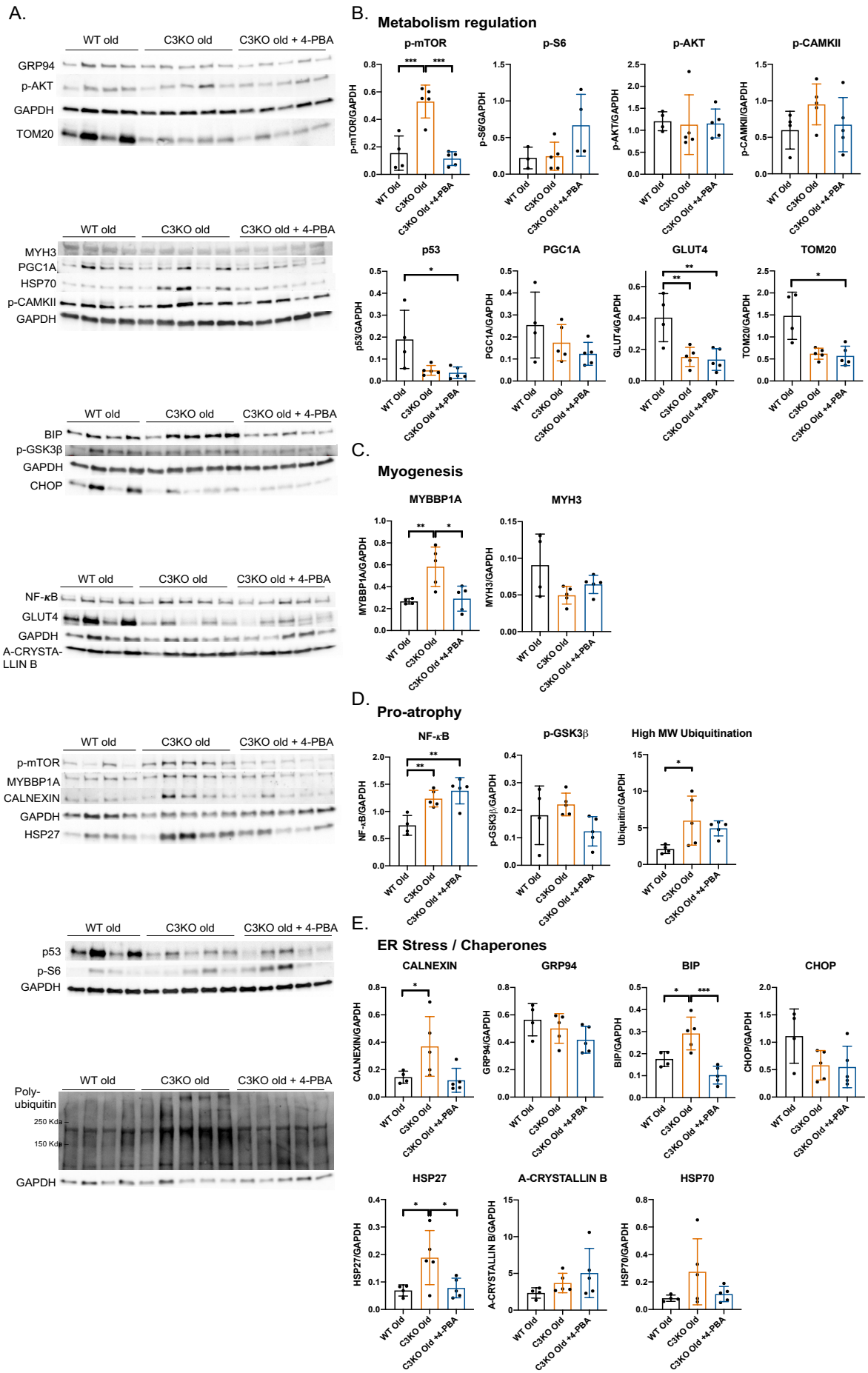
A.
WT old
C3KO old
C3KO old + 4-PBA
GRP94
p-AKT
GAPDH
TOM20
MYH3
PGC1A
HSP70
p-CAMKII
GAPDH
BIP
p-GSK3β
GAPDH
CHOP
NF-κB
GLUT4
GAPDH
A-CRYSTA-LLIN B
p-mTOR
MYBBP1A
CALNEXIN
GAPDH
HSP27
p53
p-S6
GAPDH
Poly-ubiquitin
250 Kda
150 Kda
GAPDH
B.
Metabolism regulation
p-mTOR
p-S6
p-AKT
p-CAMKII
p53
PGC1A
GLUT4
TOM20
C.
Myogenesis
MYBBP1A
MYH3
D.
Pro-atrophy
NF-κB
p-GSK3β
High MW Ubiquitination
E.
ER Stress / Chaperones
CALNEXIN
GRP94
BIP
CHOP
HSP27
A-CRYSTALLIN B
HSP70
WT Old
C3KO Old
C3KO Old +4-PBA

Figure 47. Western blot analysis of proteins in soleus of old WT, C3KO and 4-PBA treated C3KO mice after the exhaustion tests. A) Western blot membrane images of the protein analysed. Quantification of protein levels detected in (A) through densitometry normalized to GAPDH protein levels and grouped by their function/process in the muscle: B) Metabolism regulation, C) myogenesis, D) atrophy regulation, E) ER stress indicators and chaperone proteins. Data expressed as mean ± SD. n = 4 in WT n= 5 in C3KO, and n = 5 in 4-PBA treated. One-way Anova was used to calculate p-value. *p<0.05, **p<0.01, ***p<0.001.

Since TOM20 mitochondrial content indicator protein appeared lower in the C3KO, respiratory chain complex protein levels were also analysed. Overall, there were no statistically significant differences found between the groups in these proteins when normalized to TOM20, which indicates that mitochondrial content seems to be reduced in the C3KO mice but there are no alterations in the respiratory chain complex levels (Figure 48).

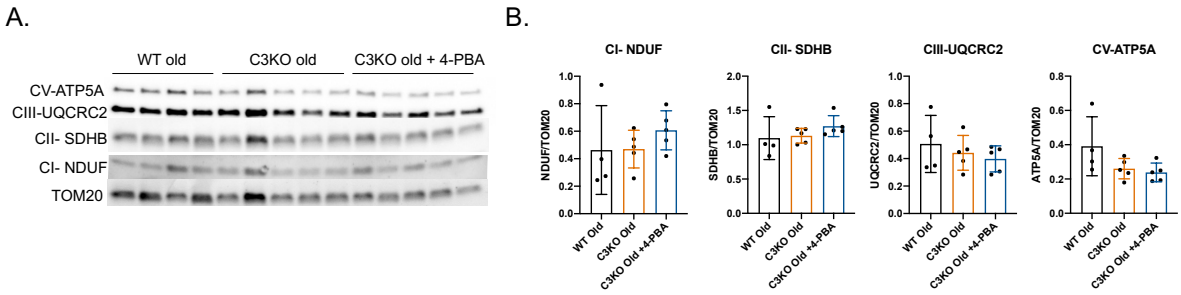

Figure 48. Western blot analysis of mitochondrial respiratory chain complex proteins in soleus of old WT, C3KO and 4-PBA treated C3KO mice after the exhaustion tests. A) Western blot membrane images of complex I (NDUF) complex II (SDHB), complex III (UBCRC2), complex V (ATP5A) and mitochondrial membrane protein TOM20. B) Quantification of protein levels detected in (A) through densitometry normalized to TOM20. Data expressed as mean ± SD. n = 4 in WT n= 5 in C3KO and 4-PBA treated. One-way Anova was used to calculate p-value.

Overall, the old C3KO soleus showed a molecular phenotype after the running tests with increased levels of some of the chaperones analysed, increased ubiquitination, and increased levels of MYBBP1A and p-mTOR, which were reversed by the use of 4-PBA. On the other hand, in the other proteins found with altered levels in the C3KO, p53, GLUT4, TOM20, and NF-κB, associated with glucose metabolism, mitochondria, and atrophy, the treatment did not show any effect.

Electrostimulation of human isogenic iPSCs derived myotubes

To evaluate whether some of the alterations found in the mice soleus after the exhaustion tests could be reproduced in human myotubes *in vitro*, the isogenic calpain 3 KO iPSC derived myotubes were used (isogenic group 1 and group 2) with an electric pulse stimulation (EPS). EPS of myotubes has been proposed as a potential *in vitro* exercise model, and can induce metabolic and biomechanical adaptations to stretch in processes such as glucose uptake, protein turnover, myotube hypertrophy and atrophy, or cytoskeleton adaption (Evers-Van Gogh et al., 2015; Ren et al., 2021), some of which seem to be altered in the absence of calpain 3. With this in mind, isogenic group 1-derived myotubes were differentiated for 6 days, and were cultured for 6 additional days under EPS (Figure 49A) before being collected at 14 days for RNA and protein analysis (Figure 49B and Figure 50 respectively).

At the gene expression level, from the ER stress/UPR associated genes analysed, it did seem like the KO lines had higher levels than the control upon EPS stimulation, particularly in the expression of *HSP90B1* and *HSPA5* (coding for proteins GRP94 and BIP), and spliced *XBP1* levels seemed to be higher in the KO-4 line too. However, the differences were not statistically significant (Figure 49B). In the case of cytosolic chaperones, the results also had high variability, however, *HSPA1A* (HSP70 protein) showed significantly higher levels in the control line after EPS (Figure 49C). Other genes analysed associated with the response to exercise had either high variability or showed little differences between lines and after EPS (Figure 49D).

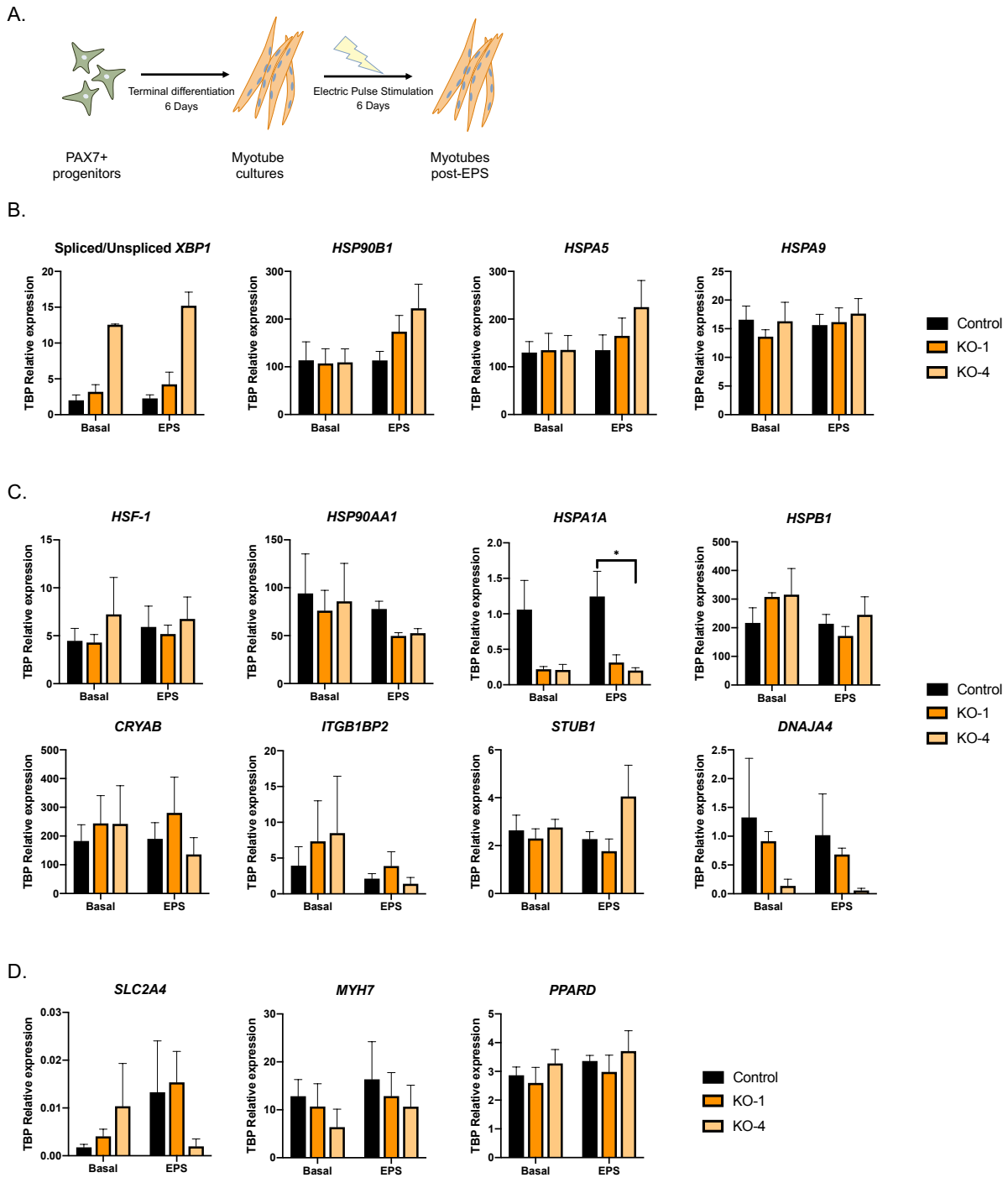

Figure 49. Gene expression analysis of myotubes derived from the iPSC isogenic group 1 without stimulation (basal) and after electric pulse stimulation (EPS). A) Schematic representation of the differentiation and stimulation of the myogenic progenitors and myotubes. B) Expression of ER stress associated genes *XBP1*, *HSP90B1*, *HSPA5* and *HSPA9*. C) Expression of chaperone expression inducer *HSF-1* and chaperones *HSP90A1, HSPA1A, HSPB1, CRYAB, ITGB1BP2, STUB1* and *DNAJ4*. D) Expression of genes associated with the response to exercise *SLC2A4, MYH7* and *PPARD*. Data expressed as relative to *TBP* expression mean ± SEM of 3 biological replicates. One-way Anova was used to calculate p-value. *p<0.05.

At the protein level, results had the same variability issues, where from one differentiation experiment to another, protein levels varied greatly, however, mitochondrial content indicator TOM20 appeared significantly reduced in line KO-4 at basal state (Figure 50A) and in both KO lines after EPS (Figure 50B).

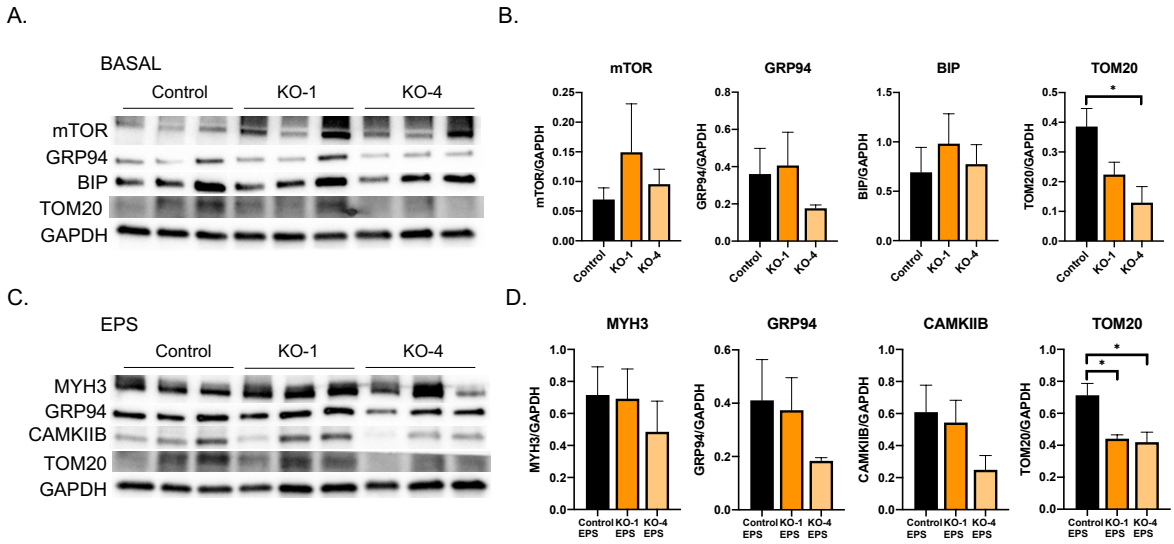

Figure 50. Western blot analysis of myotubes derived from the iPSC isogenic group 1 without stimulation (basal) and after electric pulse stimulation (EPS). A) Western blot of myotubes without stimulation at basal levels. Total mTOR, ER stress associated GRP94 and BIP, and mitochondrial TOM20 protein levels. B) Quantification of protein levels detected in (A) through densitometry and normalized to GAPDH protein levels. C) Western blot of myotubes with EPS for 4 days. Embryonic myosin MYH3, ER stress associated GRP94, calcium signal transducing CAMKIIB and mitochondrial TOM20 protein levels D) Quantification of protein levels detected in (C) through densitometry and normalized to GAPDH protein levels. Data expressed as mean ± SEM of 3 biological replicates. One-way Anova was used to calculate p-value. *p<0.05.

4-PBA treatment was tested in these cell lines to see if the effect could be detectable in EPS stimulated myotubes. Changes in expression of ER stress/UPR associated genes were not significant with this experimental setup, and the same happened when quantifying cytosolic chaperones (Figure 51).

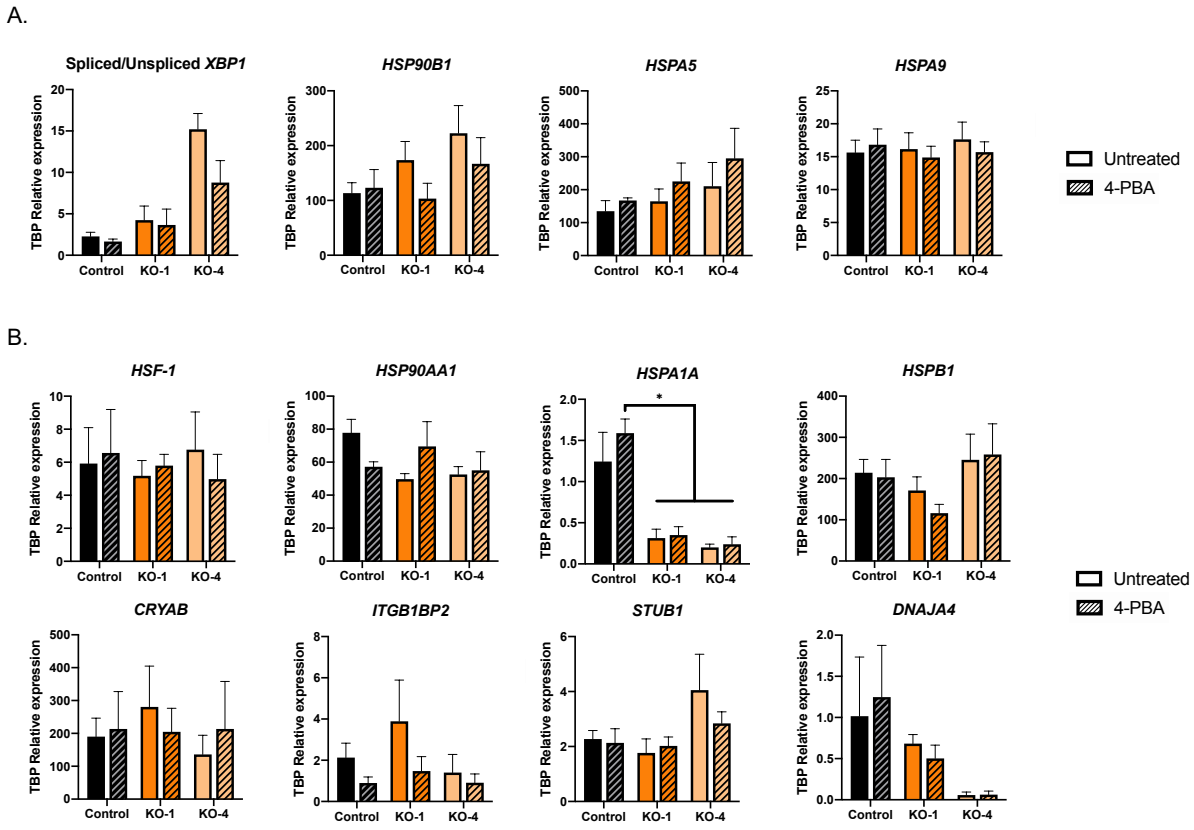

Figure 51. Gene expression analysis of myotubes derived from the iPSC isogenic group 1 with EPS and treated with 100 µM 4-PBA. A) ER stress associated genes *XBP1*, *HSP90B1*, *HSPA5* and *HSPA9*. B) Expression of chaperone inducer *HSF-1* and chaperones *HSP90A1, HSPA1A, HSPB1, CRYAB, ITGB1BP2, STUB1* and *DNAJ4*. Data expressed as relative to *TBP* expression mean ± SEM of 3 biological replicates. Solid bars represent untreated samples and dashed bars 4-PBA treated samples. One-way Anova was used to calculate p-value. *p<0.05.

In the case of the patient and mutation-corrected isogenic group 2, EPS stimulation had similar results at the gene expression level, and no statistically significant differences were found in the ER stress associated genes nor in the cytosolic chaperones analysed. It did seem the case that in the cytosolic chaperones, there was a tendency for the patient derived line to have higher averages in most cases, but no clear effect of the EPS could be detected (Figure 52). Since no differences were observed in the isogenic group 1 with the 4-PBA treatment, this was not tested in the isogenic group 2.

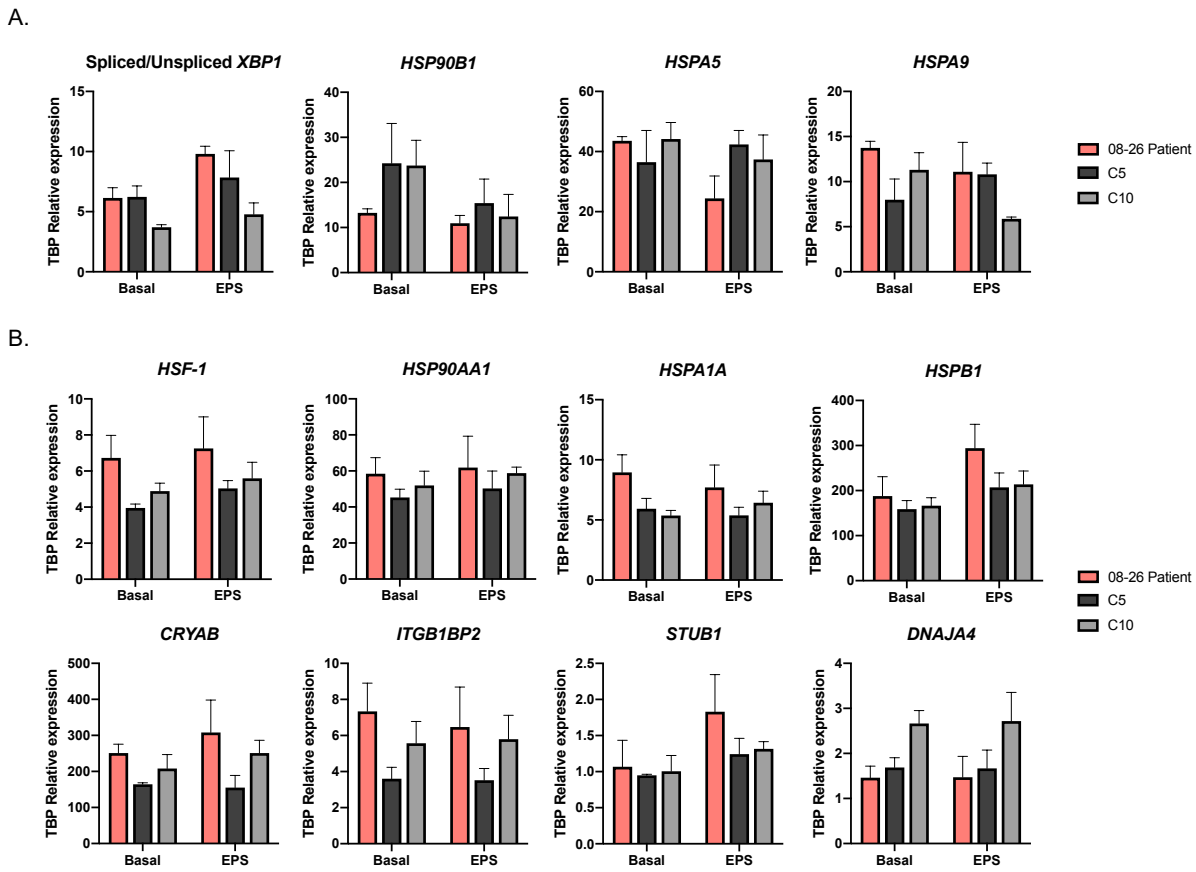

Figure 52. Gene expression analysis of myotubes derived from the iPSC isogenic group 2 without stimulation (basal) and after electric pulse stimulation (EPS). A) Expression of ER stress associated genes *XBP1*, *HSP90B1*, *HSPA5* and *HSPA9*. B) Expression of chaperone inducer *HSF-1* and chaperones *HSP90A1, HSPA1A, HSPB1, CRYAB, ITGB1BP2, STUB1* and *DNAJ4*. Data expressed as relative to *TBP* expression mean ± SEM of 3 biological replicates. One-way Anova was used to calculate p-value.

However, when stimulating the cultures with EPS some differences could be detected at the protein level. Most notably, GLUT4 levels were significantly higher in the patient line compared to the mutation-corrected lines, and in the case of HSP70 this chaperone was significantly decreased in the patient line (Figure 53). However, there was some variability between the lines and p-mTOR and p-CAMKII only were significantly increased in one of the mutation-corrected line and the ER stress/UPR associated proteins did not seem to be differentially expressed.

Overall, application of EPS to these myotube cultures did not seem to have a significant effect in the genes and proteins analysed. Despite EPS-induced contractions were visible in the culture (not shown), its effect could not be clearly detected and ER stress/UPR associated genes were not significantly induced, where only some tendencies could be observed. Also, there was high variability between the samples and there did not seem to

be great differences between the lines in most chaperone expression levels. However, *HSPA1A* (HSP70 protein) did appear significantly lower in the lines lacking calpain 3, and proteins TOM20, GLUT4, and p-mTOR, which had altered expression in the C3KO mouse, also showed differences in the EPS stimulated isogenic lines.

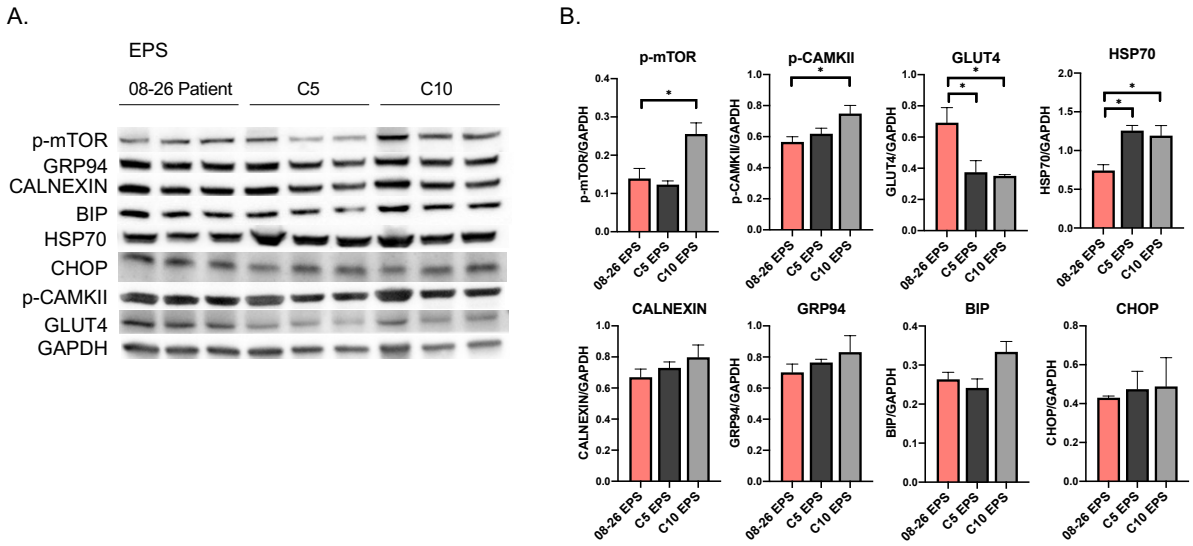

Figure 53. Western blot analysis of proteins from myotubes derived from the iPSC isogenic group 2 after electric pulse stimulation (EPS). A) Western blot membrane images of p-mTOR, p-CAMKII, GLUT4, and HSP70 and ER stress associated CALNEXIN, GRP94, BIP, and CHOP. B) Quantification of protein levels detected in (A) through densitometry and normalized to GAPDH protein levels. Data expressed as mean ± SEM of 3 biological replicates. One-way Anova was used to calculate p-value. *p<0.05.

Discussion

Muscle damage response in the C3KO mouse

Previous studies with the C3KO mouse have indicated that in the absence of calpain 3, these mice have an impaired capacity to regenerate muscle after acute damage by CTX and a reduced growth after atrophy by disuse (Kramerova et al., 2005, 2018; Yalvac et al., 2017). The muscle damage response proteomic analysis was performed to evaluate the differences that could be present in the early response to acute damage in these mice and how the response may differ from one muscle to another.

The CTX induced damage paradigm has been widely used to study the *in vivo* regenerative process in mice. Here, the initial necrosis and degeneration, followed by inflammation, initiates the activation of SCs and by the third day after the damage is induced, the degeneration and necrosis has concluded and new myofibers start to appear (Musarò, 2014). Since our analysis was done in the third day after damage, this means that tissue was in the initial phase of regeneration, with activated SCs forming new myofibers.

Before comparing the damage response, the differences in basal undamaged muscle already showed that the absence of calpain 3 has a different effect in the TA and the soleus, as the proteins differentially expressed compared to the WT and their associated functions, were very different in each muscle and only two proteins, isovaleryl-CoA dehydrogenase and flavin reductase, coincided to be downregulated and upregulated respectively, in both C3KO muscles. Interestingly, these two proteins appeared among the most down/up-regulated ones in the WT after the damage, but not in the C3KO after the damage. This seems to indicate that the C3KO in the basal state, could be already having a response to some kind of damage, as the changes in these two proteins seems to occur after the damage in the WT. Metabolically, isovaleryl-CoA dehydrogenase participates in the degradation of branched chain amino acids (BCAA), which have been described to improve muscle recovery (Doma et al., 2021; Khemtong et al., 2021), and leucine in particular is known to alter mTOR signalling in the muscle (Gulati & Thomas, 2007), therefore such an acute downregulation of isovaleryl-CoA dehydrogenase could be a response aimed at improving BCAAs availability in the muscle. A similar reduction in

isovaleryl-CoA dehydrogenase levels has been previously reported in a mouse model of collagen VI myopathy (de Palma et al., 2013).

One of the reasons why each muscle is affected differently could be because of its fiber type composition. Around 40% of the fibers in the mice soleus muscle are type I slow oxidative fibers, while in the TA, slow oxidative fibers are mostly absent and all the fibers are fast glycolytic type IIa and IIb (Augusto et al., 2004). In fact, it has been described that the soleus is one of the most affected muscles in calpain 3 KO mouse models (Kramerova et al., 2004; Richard et al., 2000), and that these mice have issues in activating the slow phenotype associated genes in response to exercise (Kramerova et al., 2012). Our proteomic data shows that both at basal state and after the damage the profile of altered proteins in the C3KO are quite different for each muscle, and while at basal state the C3KO TA has more dysregulated proteins, after the damage, the C3KO soleus seems to have more dysregulated proteins.

The damage response analysis revealed several proteins and associated functions that are altered in the C3KO. On one side there are the normal changes that occur in response to damage in the WT, that are not present in the C3KO, and on the other side, the specific changes that only occur in the C3KO muscles. From these C3KO specific changes, some of them will likely be involved in the pathogenesis of the disease, while others can be compensatory mechanisms activated by the muscle to compensate the absence of calpain 3, and while distinguishing between the two requires further experiments, the obtained results can help to point out some of these proteins and functions.

In the C3KO soleus damage response, three myogenic regulators appeared strongly deregulated indicating myogenic repression. Two of these were positive regulators of myogenesis, cysteine and glycine-rich protein 3 (CSRP3), a mechanosensor associated with autophagy (Cui et al., 2020; Rashid et al., 2015) and ankyrin repeat domain-containing protein 2 (ANKRD2), also involved in mechanotransduction and in the response to oxidative stress (Cenni et al., 2011, 2019), and both were among the most downregulated proteins. On the other hand, among the most upregulated proteins was myb-binding protein 1A (MYBBP1A) which has been described as an epigenetic repressor of myogenesis, acting on the MYOD1 genomic region (Yang et al., 2012), and also a suppressor of mitochondrial respiration by repressing PGC1A expression (Fan et al., 2004). Some previous studies indicated that myogenic capacity was reduced in C3KO

myoblasts (Kramerova et al., 2006; Yalvac et al., 2017), however, the mechanism by which this occurs is not clear. Our results indicate that such reduced myogenic capacity could be mediated by these proteins in the C3KO soleus. Moreover, dystrophin levels were also reduced, which we previously also found reduced in patient iPSC-derived myogenic progenitors and myotubes, which is also known to play a role in the correct divisions of SCs and generation of myogenic progenitors (Dumont et al., 2015; Mateos-Aierdi et al., 2021). Of note, these proteins were not found deregulated in the TA muscle, supporting the idea that the TA is less affected.

Another major set of deregulated proteins found in the proteomic study pointed towards mitochondrial proteins and process, as well as processes related to glucose metabolism as being altered in the C3KO mouse. Already in the basal state, the altered proteins in the C3KO soleus, which given its slow fiber type composition is a lot richer in mitochondria, were linked to the mitochondrial matrix and the respiratory chain, and in the case of the TA, glycolysis and gluconeogenesis pathways appeared altered. In response to damage, the C3KO soleus showed alterations in pyruvate metabolism and the mitochondrial acetyl-CoA biosynthesis from pyruvate. Here, the most upregulated protein was Ras-related protein Rab11A (RAB11A), which regulates the exocytosis of glucose receptor GLUT4 to the cell membrane, and its overexpression has been shown to decrease GLUT4 levels (Uhlig et al., 2005). In the response to damage in the C3KO TA, again glucose metabolism appeared altered. These results indicate that alterations in glucose metabolism and in mitochondrial functions are affected in the C3KO muscles, and while these could be associated to perhaps a reduced myogenesis or other differences in the response to the damage, the alterations are also present at basal state, which indicates that this is a dysregulation that is constant in the C3KO muscle.

Previous studies with the C3KO mouse and patient samples have also pointed out mitochondrial abnormalities like abnormal distribution, a reduced ATP production, as well as a reduction in PGC1A, and mitochondrial biogenesis in the C3KO mouse (Kramerova et al., 2009; Yalvac et al., 2017), and abnormal spatial distribution of the intermyofibrillar mitochondria, increased cytosolic cytochrome C levels, and dysregulated genes also related with glucose metabolism have been reported in patient samples (Baghdiguian et al., 1999; Sáenz et al., 2008). Our results align with the previous, showing dysregulated expression of mitochondrial proteins and indicate that in the issues with glucose metabolism, RAB11A and glucose transporter GLUT4 could be playing an

important role. Although the mechanisms by which the lack of calpain 3 could be affecting mitochondria is not clear, it has been suggested this could be occurring due to the altered Ca^{2+} levels as a consequence of the absence of calpain 3 in the triad, and consequent altered CAMKII signaling (Kramerova et al., 2008, 2012).

Finally, another group of proteins that appeared deregulated in both muscles were chaperones. Basal C3KO soleus had an increase in a mitochondrial 10 KDa heat shock protein, and in damage response, chaperones HSP70, HSP27, alpha-crystallin B, and DNAJA4 were among the most downregulated proteins in the C3KO soleus. In the C3KO TA, HSP70 was upregulated in the basal state, while after the damage HSP27 and DNAJA1 appeared both upregulated. Intriguingly, HSP27 appeared downregulated in the damage response of the soleus and upregulated in the TA.

Different chaperones have been found to be dysregulated throughout the studies in LGMDR1, however their role in the disease has not been clarified. In the C3KO mouse, accumulation of HSP70 was found in insoluble fractions of the muscle, however, despite this accumulation, it was reported that C3KO mice fail to induce appropriate levels of HSP70, which is necessary to induce muscle growth after atrophy by disuse (Kramerova et al., 2005, 2018). In human patients of LGMDR1, gene expression analysis of different muscles showed significant upregulation of *DNAJA4* and melusin (*ITGB1BP2*) chaperones in one study (Sáenz et al., 2008), and another also reported the increase of small chaperones HSP27 and alpha-crystallin B (Unger et al., 2017). These last two small chaperones have been shown to translocate to the sarcomeric Z-disc/I-band regions of skeletal myofibers under stress or disease conditions (Paulsen et al., 2009), and in LGMDR1 they translocate to the titin spring, and while they are able to prevent the aggregation of titin, they have been shown to increase the passive tension of LGMDR1 myofibers (Kötter et al., 2014; Unger et al., 2017).

Our results align with these previous studies and also point out to most of these chaperones as being dysregulated, however, not all of the chaperones appear dysregulated on both muscles, and it seems that in the context of damage response, they are downregulated in the soleus. However, the altered expression of chaperones seems to align with the hypothesis that the C3KO muscles have issues in maintaining protein homeostasis in the sarcomeres. It is important to note that the proteomic analysis performed here focused on proteins with a differential expression greater that 1.5

upregulation or down regulation, therefore there could be other proteins also dysregulated under this threshold that we did not consider but could be relevant to the changes observed.

Myogenesis in the absence of calpain 3

So far, the studies involving myogenesis in the C3KO mouse focused on the myogenic capacity of primary myoblasts, but no studies have been done directly isolating or studying C3KO SCs. Moreover, the results of these studies were inconsistent as one study indicated an increased fusion of the myoblasts with an abnormal distribution of the nuclei (Kramerova et al., 2006), while other reported a reduced fusion capacity (Yalvac et al., 2017). In LGMDR1 patients, there is an increase of central nucleation, indicating that new regenerative fibers do appear, but these are less abundant than in similarly affected patients of other MDs, and more frequently they appear irregularly shaped, which indicates problems in myofibrilogenesis (Hauerslev et al., 2012). It has also been reported that patients have an increased number of PAX7+ SCs, which was suggested that it could be due to an increased activation and proliferation, despite they probably present an impairment in differentiation (Rosales et al., 2013).

Considering that the C3KO mouse model has been described to have a very mild phenotype, we included 18 months old mice when studying SCs and their ability to form spheres and differentiate, to evaluate the differences between the C3KO and WT and whether the differences would be accentuated in older age. In those experiments, we observed that the number of spheres that old C3KO SCs formed was significantly reduced compared to the old WT and young C3KO, while there were no statistically significant differences in their size. Similarly, when the spheres were induced to terminally differentiate into myotubes, the differentiation index was significantly lower only in the old C3KO. This seems to indicate that *in vitro*, after isolation and the sphere formation, the myogenic capacity of the C3KO SCs is reduced in older age.

When performing the myogenesis studies with the human isogenic calpain 3 KO iPSC lines, the results also pointed towards a reduced myogenic capacity in the absence of calpain 3. In general, all the lines with or without calpain 3 were able to differentiate and form myotubes, however the myogenic capacity appeared reduced in some aspects. In the isogenic group 1, while only the KO-4 line had significantly lower differentiation and

fusion index, both KO lines had a reduced ratio of MYHC area per nuclei, and in the case of the isogenic group 2, the lines that had the calpain 3 mutation-corrected had better differentiation parameters overall. At the gene expression level in the isogenic group 1, the results indicated that despite properly inducing myogenic factors *MYOD1* and *MYOGENIN* at day 3 of differentiation, with a tendency that even seemed higher than in the control, at day 8 of differentiation markers *MYH3* and *MYH2* were significantly lower in the KO lines. This also supports the idea that while the myogenic program seems to be properly induced, appropriate levels of differentiation are not achieved in the absence of calpain 3.

At the protein level, there were some significant differences between each of the KO lines at day 3 that could be due to a different pace of differentiation in each line. At this point in the differentiation, p-mTOR and PGC1A appeared significantly upregulated in the KOs, which in theory would lead to more growth and increased mitochondrial biogenesis, however, at day 8 these proteins as well as the mitochondrial marker TOM20 had a tendency to be less expressed. MYOGENIN and SERCA2 were also significantly reduced in the KO lines which in case of SERCA2 confirms what previously has been described in calpain 3 silenced immortalized myoblasts (Toral-Ojeda et al., 2016), and DMD was also significantly lower in KO-4, in line with data previously described (Mateos-Aierdi et al., 2021). Also at day 8, p-AMPK seemed to be higher in KO lines which could indicate an energetic shortage. In the isogenic group 2, despite the mutation-corrected lines showed better differentiation, the differences were less noticeable at the gene expression level and at the protein level, however, at day 8 of differentiation the corrected lines did seem to have a tendency for increased MYH3, DMD, and p-mTOR.

Considering the results in the C3KO mouse proteomic analysis, myogenic repressor MYBBP1A was also analysed in the isogenic lines to evaluate whether it could be playing a role in the decreased myogenic capacity in the human cell line context. However, this protein was not significantly changed in day 3 nor in day 8 in the isogenic group 1, and in the isogenic group 2 there was a tendency for its higher expression in the corrected lines at day 3 and was significantly higher in C10 at day 8. This suggests that either MYBBP1A does not play such a critical role in this model and its only relevant in the mouse model, or that in this context of iPSC-derived myogenic progenitors that usually are more representative of the embryonic myogenesis rather than the adult myogenesis, this regulatory protein is not key in the observed reduced myogenic capacity. It would have

been interesting to also evaluate the other myogenic regulatory proteins CSRP3 and ANKRD2 that in the mouse proteomic analysis appeared downregulated, however, we were unable to detect these proteins by Western blot. Despite at first it does not seem that MYBBP1A is key in the iPSC-derived myogenic progenitors, it would be interesting to study the pattern of MYBBP1A, CSRP3, and ANKRD2 expression in more detail in the differentiation of the progenitors, other human samples, or cultures of LGMDR1 to see if they could be playing a role in the disease and the reduced myogenic capacity.

Old C3KO mice lack motor function impairment despite showing a molecular phenotype

LGMDR1 is a slowly progressive degenerative disease that worsens with age and considering that calpain 3 KO mouse models have been described to have a very mild phenotype (Fougerousse et al., 2003; Kramerova et al., 2004), we decided to use old mice of 18 months with the expectation that any phenotype in this model would be more easily noticeable. In the literature, the initial study published with the C3KO model measuring performance reported no significant differences in the amount of voluntary running and treadmill running in 3-4 month old mice (Kramerova et al., 2012) and the same was reported in another recent study (Lasa-Elgarresta et al., 2022). Nevertheless, in other studies that used the same run to exhaustion test that we have performed here but with 5-6 month old C3KO mice, they did show a significant decrease in the time, distance and maximum speed reached by the C3KO (Kramerova et al., 2016; J. Liu et al., 2020). The experiment with the oldest C3KO mice used was by another group using a similar treadmill protocol with 15 month old mice where they saw a decrease in the distance run by the C3KO and where an AAV therapy was tested (Sahenk et al., 2021).

Despite of what has been described in some previous studies, when the exhaustion tests were performed, we observed that the old C3KO, both the treated with 4-PBA and the untreated, not only did not perform worse than the WT, but were able to run significantly more than the age matched WT mice. Also, the repetition of the test over time did not deteriorate or significantly alter the performance of any of the groups, indicating that within this experimental setup the C3KO do not seem to have problems facing repeated physiological stress induced by exercise.

To make sure that our results were not the consequence of an error or problem with the mouse colonies, we genotyped all the mice and confirmed the lack of calpain 3 in the C3KO by Western blot. In addition, we made sure with the responsible of the animal facilities that all the animals and particularly the WT colonies were healthy and free of pathogens. Also, the WT mice included in the experiment came from different cages with no prior contact with each other and all WT were from the same background as the one used in the literature to compare to the C3KO (C57BL/6). The WT mice did have a slightly higher weight than the C3KO, although the difference was not significant, and when we compared the individual performance of the WT mice, the ones that were most notably overweight were not the ones running less, therefore the overweight mice were not particularly lowering the WT performance numbers. Also, the same ratio of males and females were used in all the groups.

This led us to conclude that in fact at 18 months of age, the C3KO mice does not have an impairment in the ability to run nor present a reduced resistance, and actually performed better than age matched WT in a statistically significant manner.

Moreover, at the histological level the C3KO muscles also looked similar to WT and did not show more noticeable atrophy or fatty infiltration at the qualitative level. Another aspect that pointed towards old C3KO having less differences was that when we compared old and young WT and C3KO muscle protein levels in normal conditions without any exercise regime, we did observe that some differences that could be indicators of the C3KO phenotype, were more apparent when comparing young WT vs. young C3KO than when comparing them in old age. For instance, when comparing to the age matched WT, GSK3β levels were significantly higher in the young C3KO TA, but not in the old C3KO TA. Similarly, mTOR, MYBBP1A and CALNEXIN had significant differences in the young soleus muscles, while in old age the differences were not significant.

Finally, another hint pointing towards old C3KO having less issues than the young, comes from one of the published studies where they subjected the C3KO mice to an AAV calpain 3 gene therapy in young (2 months) and old (10 months) groups and performed a similar exhaustion test 20 weeks after the treatment (Sahenk et al., 2021). Here they observed that the old group had an improvement of up to 142% over the untreated C3KO, while the young group had an improvement of up to 88%. This is contrary to what is known for muscular dystrophy gene therapies, where early treatment in young age generally seems

to improve the efficacy of the gene therapy (Hjartarson et al., 2022; Mirea et al., 2021). In fact, despite they did have a reduced performance in the untreated old C3KO, after the treatment the C3KO showed notably higher average distance run over the WT, although they did not mention or provide a p-value for that comparison (Sahenk et al., 2021).

Despite that at the functional level the C3KO performed better than the WT and there were no significant differences between the C3KO and the 4-PBA treated C3KO, at the molecular level some significant differences could be observed in the levels of some proteins, where the effect of 4-PBA could be noted in the soleus muscles.

The use of 4-PBA was aimed at aiding in potential proteostatic issues with protein folding or aggregates that could be causing an increase in ER stress/UPR and chaperone expression (Kolb et al., 2015). In this aspect, we observed a significant increase in ER chaperones CALNEXIN and BIP in the C3KO soleus after the exhaustion tests, while in the 4-PBA treated group, this did not occur and the levels were comparable to those of the WT group. Similarly, HSP27 levels were significantly increased in the C3KO, and the 4-PBA treatment significantly reduced its levels. In addition to this, high MW protein ubiquitination levels were also significantly increased in the C3KO group, but not in the treated group, and a similar tendency could be observed with HSP70.

This is interesting because in human LGMDR1 patients, atrophy programme appears to depend mainly upon the activation of the ubiquitin-proteasome system (Fanin et al., 2013) and HSP27 levels have also been found increased in patient fibers where this chaperone translocates to the sarcomere and binds to titin (Unger et al., 2017), therefore 4-PBA could potentially be used to treat these aspects of the disease. In relation to this, in the case of IBM, a myopathy where 4-PBA is being tested in clinical trials, a study has shown that there is a functional calpainopathy occurring with ER stress and calcium dysregulation in IBM (Amici et al., 2017), which together with the fact that 4-PBA is already an FDA and EMA approved drug, makes it also an interesting candidate for clinical trials in LGMDR1.

In addition to these changes, myogenic repressor MYBBP1A also appeared significantly upregulated in the C3KO after the exhaustion tests, and here too, 4-PBA significantly reduced its levels. This suggests that this myogenic repressor could be induced in response to proteostatic issues, to prevent further protein expression and myogenic differentiation,

and although further characterization is required, it would be interesting to see if 4-PBA could in fact restore the reduced myogenic capacity we observed when differentiating the spheres obtained from the C3KO SCs. In parallel to this effect, p-mTOR levels were also significantly increased in the C3KO and 4-PBA treatment significantly reduced this back to WT levels. However, whether mTOR pathway is more active in the C3KO is not clear since downstream p-S6 levels were not increased.

On the other hand, there were also some differences observed in the C3KO where 4-PBA did not have an effect. For instance, NF-***κ***B levels were significantly increased in treated and untreated C3KO, which also has been found activating pro-apoptotic signaling in LGMDR1 patient samples (Benayoun et al., 2008; Rajakumar et al., 2013), and TOM20, P53, and GLUT4 were also reduced in C3KO. Regarding TOM20 reduced levels, this is often used as a marker for mitochondrial content, and although this should be confirmed also with other methods, it most likely indicates a reduction in mitochondria. However, when we analysed levels of respiratory chain complex proteins, these did not change relative to TOM20 levels, which indicates that despite reduced mitochondria the respiratory chain complex protein levels are not affected.

From our results, it seems evident that C3KO mice have compensatory mechanisms to deal with calpain 3 deficiency, and despite showing some molecular and myogenic capacity differences, they do not develop the dystrophic loss of muscle function, and on the contrary, seem to actually perform better than the WT in old age. This issue requires further research and study both to better understand the model and because those compensatory mechanisms could actually indicate therapeutic targets for humans where such compensatory mechanisms are not present. In this regard, we hypothesize that a possible reason why the old C3KO run more than the WT could be related with the fiber type changes and the fast-to-slow fiber type transition that occurs during age-related sarcopenia (Larsson et al., 2019; Short et al., 2005). In C3KO, it has been reported that these mice have reduced amounts of type I slow fibers and issues in transitioning from type II fast to type I slow fibers, and inducing the expression of genes associated with the slow phenotype (Kramerova et al., 2012, 2018). Thus, if the C3KO mouse avoids atrophy by compensatory mechanisms and could have more type II fibers in old age due to inability to transitioning to type I fibers, it could mean that they could retain more strength to perform the exhaustion test where by the end of the test, mice are running intensely at high speeds and where type II fibers might be important. The fact that the WT soleus had

significantly higher levels of TOM20, indicative of more mitochondrial content, as well as increased amounts of GLUT4, which both are significantly higher in type I myofibers, could be due to reduced type I fiber levels in the soleus, as it has been previously suggested (Kramerova et al., 2012). This clearly requires further experiments to evaluate fiber types and sarcopenia indicators in old C3KO and WT mice, but it could be playing an important role in the observed results. In any case, the C3KO model is clearly a poor model to test therapies looking to show functional improvements.

Electrostimulation of human isogenic iPSCs derived myotubes

EPS has been used to *in vitro* stimulate myotube cultures and induce changes associated with exercise and muscle contraction (Carter et al., 2018). Similar to *in vivo* exercise, the response depends on the type of EPS stimulus, where short-term, high frequency stimulation has been proposed as a model of high-intensity exercise, inducing upregulation of glucose uptake, reduced phosphocreatine and lactate production, and the activation of contraction-related signaling pathways (Manabe et al., 2012; Nikolić et al., 2012, 2017). In contrast, chronically stimulating myotube cultures with low-frequency pulses has been used to resemble changes seen after exercise training with effects similar to exercise-mediated signal transduction such as *PGC1A* expression, AMPK signalling, Ca^{2+} transients, enhanced glucose uptake (Carter et al., 2018), myotube hypertrophy (Tarum et al., 2017), increased mitochondrial content (Nikolić et al., 2012) and sarcomeric structure formation, this latter one being mediated by calpains (Fujita et al., 2007).

In order to evaluate if the altered pathways or proteins that were found dysregulated in the mouse after the exhaustion tests would also be affected in human cells, the iPSC derived isogenic lines were used cultured with EPS, with a particular focus on evaluating the expression of different chaperones and also to evaluate whether 4-PBA treatment could have similar effects as it had in the mice. A low-frequency chronic EPS was used to induce contractility of the culture. The protocol that was chosen aimed at inducing visible contractions in the culture and to maintaining contractibility of the culture over the four days of the culture with EPS, with the expectation that any negative effect that the repeated contractions could have in the cells lacking calpain 3, could accumulate and become more apparent.

Despite the EPS protocol kept contractions visible throughout the culture time, we encountered limited effects in the EPS stimulated cultures in the expression of chaperones, ER stress associated genes, and genes associated with the response to exercise, all of which are described to be increased after exercise (Carter et al., 2018; Noble et al., 2008; Wu et al., 2011). Similarly, when we tested the 4-PBA treatment on the cells from the isogenic group 1, we could not observe significant differences in the expression of chaperones. This could partially due to the high variability we had with these cultures, where from one experiment to the other the expression levels of certain genes varied greatly despite it being the same line and protocol each time. Also, the EPS protocol should be optimized to assess which parameters induce more the adaptative changes to exercise. In this aspect, the protocol that we were using was on the lower end in terms of frequency (0.1 Hz) compared to what has been used in the literature, however, when we tested some higher frequency protocols, we found that the culture would stop contracting after 1 or 2 days, and due to time constrains to further optimize the EPS protocol, we decided to use the one with 0.1 Hz, based on the observation that the cultures were still contracting after 4 days. However, an EPS protocol optimization and a larger number of experimental replicates would be necessary to be able to evaluate EPS induced changes.

Despite that based on the measured parameters we did not achieve to significantly emulate exercise *in vitro,* some significant differences between the control and calpain 3 KO lines could be observed in the EPS stimulated cultures. In the case of *HSPA1A* (coding for HSP70), it was significantly higher in the control line than in the KO-4, and the same tendency was observed for KO-1, and at the protein level, mitochondrial protein TOM20 levels were significantly lower in the KO lines. On the other hand, when performing the experiments with the isogenic group 2, while at gene expression level there were no statistically significant differences, at the protein level HSP70 was significantly higher in the mutation-corrected lines, aligning with the observation in the isogenic group 1 of lower levels of HSP70 induction in the absence of calpain 3.

It is interesting to see that despite the doubts that the C3KO mouse generates and the fact that the *in vivo* context of damage response or the effect of treadmill running in old C3KO mouse might not be comparable to the *in vitro* setup with the EPS stimulated myotubes, some of the proteins that were dysregulated in the C3KO were also dysregulated in the human iPSC derived myotubes, which indicates that it is very likely that these proteins are in fact dysregulated in the absence of calpain 3 and could be

implicated in the disease. In both species, TOM20 levels were reduced significantly, pointing towards a reduced mitochondrial content in the absence of calpain 3. HSP70 also appeared dysregulated in both cases, in the proteomic study of the C3KO mice and in the EPS stimulated myotubes. And finally, levels of GLUT4 and p-mTOR were also both significantly altered. Unfortunately, with our *in vitro* setup we were not able to clearly appreciate the effects of EPS *in vitro* and 4-PBA treatment did not seem to exert a significant effect, although improvements in the *in vitro* EPS protocol would probably be necessary to allow for a better assessment.

CHAPTER 3

CHAPTER 3: GENERATION OF A LGMDR1 PIG MODEL WITH CRISPR/CAS9

Hypothesis and objectives

Available animal models of LGMDR1 such as the C3KO mouse, while being useful to study some molecular aspects of the disease, fail to recapitulate key aspects of the disease such as a severe muscle atrophy and loss of motor functions and ambulation with disease progression. Thus, alternative models are required to overcome current limitations in the study of LGMDR1 and the development of new therapies.

We hypothesize that an animal model of LGMDR1 KO for calpain 3 based in pig will represent a better disease model and will have a clinical phenotype more similar to humans than the murine models.

Therefore, in order to obtain a calpain 3 KO pig, the following specific objectives were set:

1- To design and test CRISPR/Cas9 guides to generate calpain 3 KOs in pig fibroblasts.
2- To test and optimize the obtention of calpain 3 KO embryos in pigs and transfer the embryos to recipient sows to obtain a calpain 3 KO pig.
3- To characterize the obtained calpain 3 KO pig model.

Results

Obtention of a calpain 3 KO pig with CRISPR/Cas9

Aiming to obtain a calpain 3 KO pig model of LGMDR1, different CRISPR/Cas9 guides and strategies were designed. Unlike it occurs in other species like mice, rats, cattle or humans, the efficiencies of certain techniques when handling pig oocytes and embryos becomes a limiting factor due to their impact on the viability of pig embryos (Chen et al., 2021, 2022). For instance, cryopreservation of oocytes, *in vitro* maturation of oocytes, somatic cell nuclear transfer (SCNT) for cloning, or embryo vitrification for preimplantation genetic diagnosis, greatly reduce the viability of the embryos when transferred to recipient sows, where large numbers of embryos are generally transferred and low implantation and birth rates are obtained (Chen et al., 2021; Li et al., 2021). For this reason, it was decided to optimize CRISPR/Cas9 guide design, with more than one strategy to generate the KOs and also to test the most efficient and viable way to deliver CRISPR/Cas9 into pig embryos and subsequent transfers into recipient sows with the highest possible number of KO embryos. Compared to SCNT, this method has the disadvantage of not knowing the outcome of the CRISPR/Cas9 modification in the transferred embryos, but allows to reduce embryo manipulation and increase viability, which is one of the main concerns in the *in vitro* generation of pig embryos.

CRISPR/Cas9 guide design and testing in pig fibroblasts

A set of guides were designed targeting the start codon in exon 1 of the porcine calpain 3 gene. In a similar way to the guides used for the iPSCs, these guides were designed to be used in pairs as a dual-guide strategy in order to generate a deletion of the sequence between both guides, where the start codon of calpain 3 is located. For this reason, the guides targeting sites upstream of the start codon (guides #1 - #3) had to be paired with guides targeting sites downstream the start codon (guides #4 - #7) (Figure 54A-B). In addition to these guides, another pair of guides were also designed targeting exon 22 of calpain 3 and in particular, one of the guides directly targeted codon ARG788. In humans, a frameshift and early stop codon causing mutation (Arg788Serfs*14) is known to cause a severe phenotype (Urtasun et al., 1998) and therefore, these guides were designed as an alternative strategy to be used either as a pair or using only the guide that directly targeted ARG788 to mutate this codon (Figure 54C-D-E).

A.

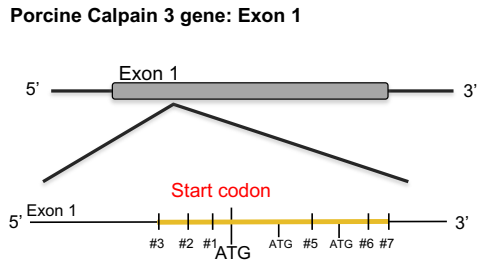

B.

#	Strand	Sequence	Ontarget	Score
1	-	GTCGGCATGACAGGCAAATTTGG	1	86.5
2	-	CAGGCAAATTTGGAAGGGAAAGG	1	51.3
3	-	ACAAGATACGGCTACCTTTAAGG	1	91.7
4	-	ATAGACGCGCTAATGACAGTCGG	1	96.6
5	+	TTAGCGCGTCTATGGCCCCACGG	1	95.3
6	+	GTCCCCAGGACCGATGCCCCAGG	1	72.6
7	-	ATGGCTGAGTATTTACCACCTGG	1	88.6

C.

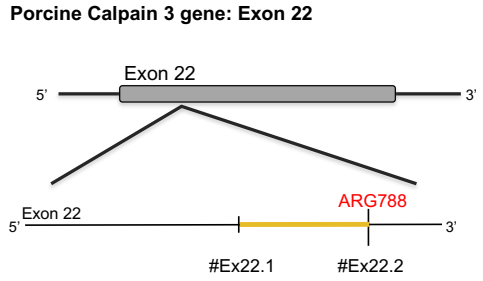

D.

#	Strand	Sequence	Ontarget	Score
Ex22.1	+	TCTATGACATCATCACCATGCGG	1	76.4
Ex22.2	+	TATCTGCTGCTTCGTCAGGCTGG	1	87.2

E.

```
CAPN3_PIG    780 DSFICCFVRLEGMFRAFNAFDKDGDGIIKLNVLEWLQLTMYA
CAPN3_HUMAN  780 DSFICCFVRLEGMFRAFHAFDKDGDGIIKLNVLEWLQLTMYA
```

Figure 54. CRISPR/Cas9 guide design strategy for porcine calpain 3 KO generation. A) Schematic representation of start codon in exon 1 of porcine calpain 3 gene and CRISPR/Cas9 guides flanking the main and the alternative start codons. B) Designed guide sequences for exon 1. PAM sequences are highlighted in orange, "ontarget" stands for the number of *loci* found containing a matching sequence, and the score given by the software. C) Schematic representation of exon 22 and CRISPR/Cas9 guides targeting codon ARG788. D) Designed guide sequences for exon 22. E) Porcine calpain 3 amino acid sequence aligned with the human sequence around residue ARG788.

To test the designed guides, fibroblasts were obtained and cultured from a pig skin sample and the different guide combinations were tested by electroporating them in the form of ribonucleoprotein (RNP) with Cas9 protein. The electroporated fibroblasts were analysed in pools without clonal selection, therefore different outcomes were present in the sample. The deletions generated by the different guide combinations could be observed in the form of smaller than control (WT) DNA bands in agarose electrophoresis gels from the PCR products of exon 1 (Figure 55A), besides also having the WT sized band from the unmodified fibroblasts in the pool. The size difference of the DNA bands from the electroporated fibroblasts corresponded with the estimated PCR product size if the sequence between both guides would be deleted, and thus the efficiencies were calculated based on the intensity of the bands with the deletion compared to the WT size band in the same sample. It was observed that the guide combination #2+#5 obtained significantly higher efficiencies than the combinations #2+#5, #3+#6 and #3+#7 (Figure 55B), however, guide #5 was leaving an alternative in-frame start codon outside the deletion, which could

result in potentially functional calpain 3 expression. Guide #4 had the same problem, and the deletions using guide #1 upstream the start codon were considered too small as it was the guide closest to the start codon in the upstream side (data not shown). Given these design considerations and the fact that guide #2 had the lowest score in the guide design software (indicating more potential off-target effects), guide pairs #3+#6 and #3+#7 were selected for further tests in exon 1. Next, the use of RNA guides in the form of duplexed guides (crRNA:tracrRNA) against using them as single-guide RNA molecules (sgRNA) in the formation of the RNP complex was compared. The efficiencies obtained with the sgRNA molecules were significantly higher with both guide combinations tested, and when using sgRNAs, the guide pair #3+#6 showed significantly higher efficiencies than the pair #3+#7 (Figure 55C).

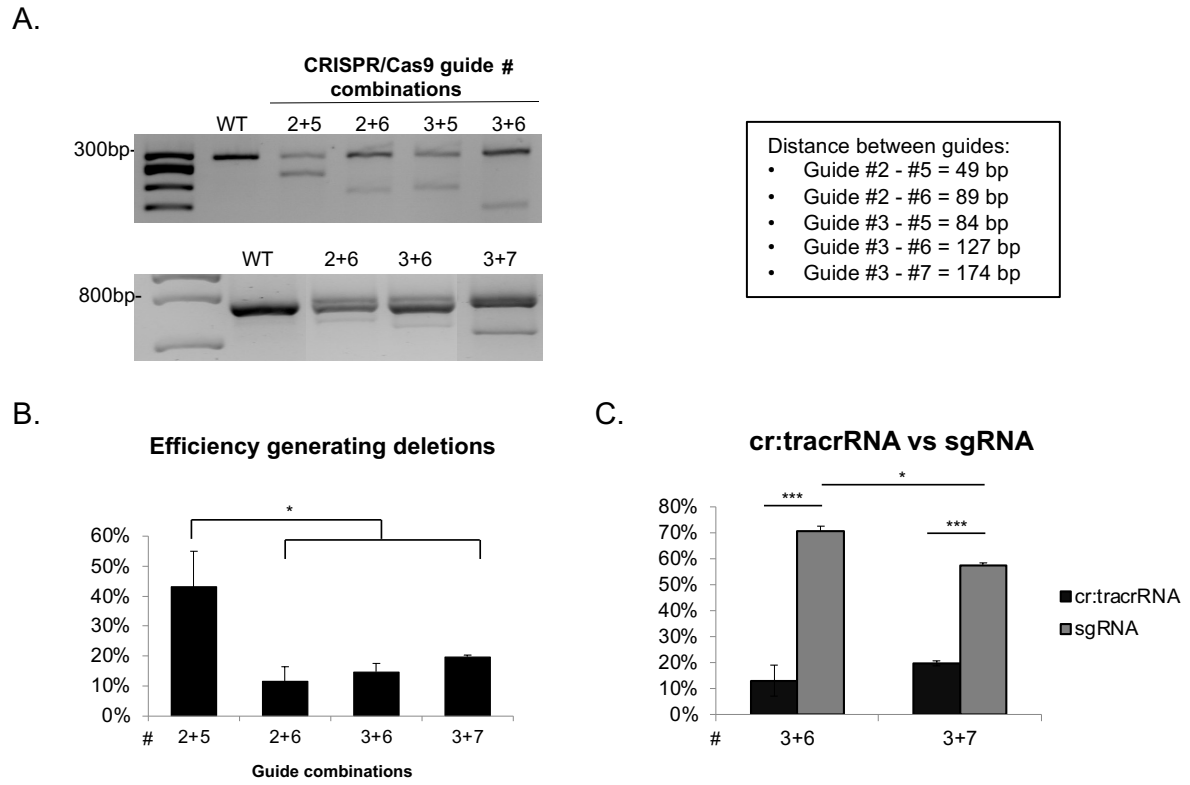

Figure 55. CRISPR/Cas9 calpain 3 exon 1 guide testing in pig fibroblasts. A) DNA electrophoresis images of PCR products of exon 1 start codon region, from fibroblast pools nucleofected with different CRISPR/Cas9 guide combinations, with smaller PCR bands resulting from the generated deletions. Gel image was cut to show different combinations in one image. On the right, distance between the different guides in base pairs. B) Bar graph of the efficiencies obtained with each guide combination, measured by band image densitometry analysis. C) Comparison of the efficiencies generating deletions obtained when using duplexed guides (cr:tracrRNA) or single-guides (sgRNA) tested with guide combinations #3+#6 and #3+#7. Bar graphs show average ±SEM of 3 biological replicates. One-way Anova was used to calculate p-value *p<0.05, ***p<0.001.

When testing the guides designed for exon 22, the use of both guides as a pair were able to generate a deletion of a size approximately corresponding to the distance between both guides (61bp), detectable in the PCR product of the pool of electroporated fibroblasts (Figure 56A). When using only guide #Ex22.2 to only target codon ARG788, it also worked and caused mutations detectable by sequencing the PCR product of exon 22 (Figure 56B). Further analysis of the mutations generated with this guide by inference of sanger trace data using ICE software (Conant et al., 2022) revealed that the efficiency was around 58% where the most frequent mutation (29%) was a 1 base insertion causing a reading frameshift and an early stop codon 8 codons later (ARG788fs*8), followed by 2 different 1 base deletions (18% and 11% frequency respectively) both also causing a reading frameshift and early stop codon (ARG788Glyfs*23 and ARG788Serfs*24 respectively) (Figure 56C). This indicated that the use of guide #Ex22.2 was very likely to generate a mutation causing a frameshift and an early stop codon similar to that encountered in the human mutation ARG788Serfs*14.

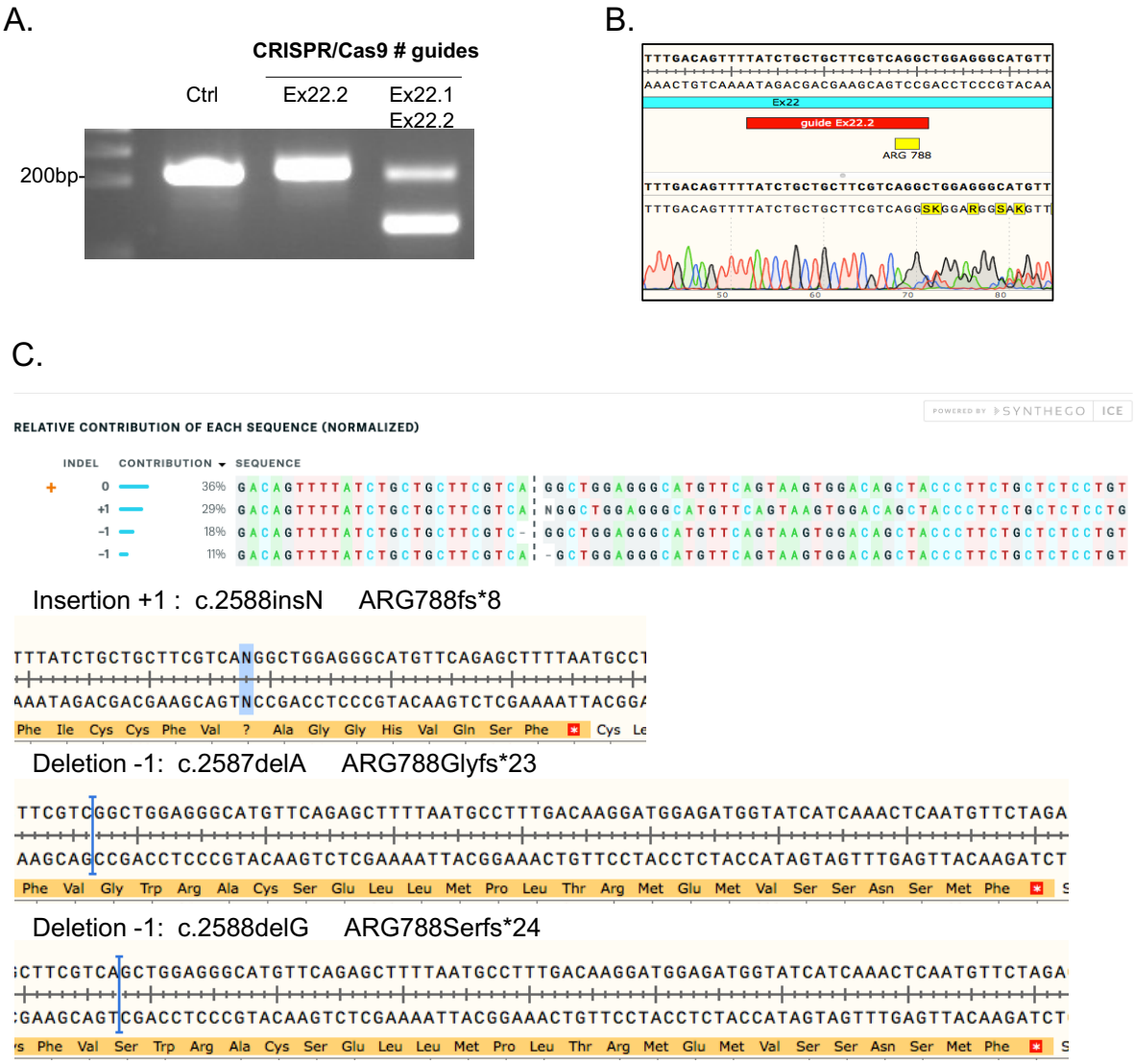

Figure 56. CRISPR/Cas9 calpain 3 exon 22 guide testing in pig fibroblasts. A) DNA electrophoresis images of PCR products of exon 22 codon ARG788 region, from fibroblast pools nucleofected with one guide (#Ex22.2) or two guides (#Ex22.1+#Ex22.2) targeting codon ARG788. B) Sequencing chromatogram of PCR product from fibroblasts nucleofected with one guide (#Ex22.2) showing mutations in codon ARG788. C) ICE analysis of the probability to obtain specific mutations from using guide #Ex22.2, and their translation to protein sequence. Vertical blue bar in the sequence indicates where the mutation occurs and the asterisk in red indicates a stop codon.

Finally, it was evaluated whether the use of the guide #3 and guide #Ex22.2 as a pair could generate a large deletion spanning from exon 1 to exon 22. Both guides were electroporated and a PCR was performed with DNA from the fibroblast pools with the forward primer in exon 1 and the reverse primer in exon 22. The PCR only amplified a product in the electroporated fibroblasts and not in the control, with the PCR product size corresponding to what would be expected if the 52 Kbp long sequence between both guides would be deleted (around 438 bp) (Figure 57A). Sanger sequencing of the purified PCR product confirmed this had the exon 1 sequence in the 5' end and the exon 22 sequence in

the 3' end, indicating that the large deletion had likely occurred in some of the fibroblasts and it was possible to delete the calpain 3 gene sequence from exon 1 to 22 with this guide combination (Figure 57B).

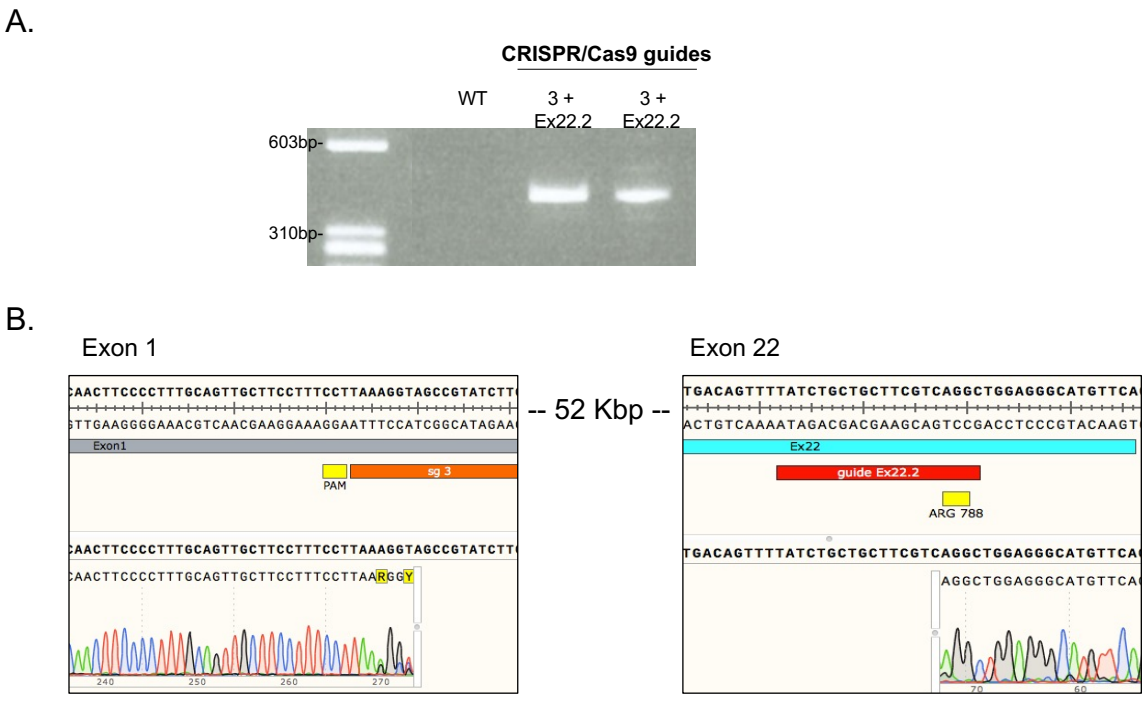

Figure 57. Calpain 3 gene deletions from exon 1 to exon 22 in pig fibroblasts. A) DNA electrophoresis images of PCR products using forward primers in exon 1 and reverse primers in exon 22, from fibroblast pools nucleofected with one guide targeting exon 1 (guide #3) and other targeting exon 22 (#Ex22.2). Each lane represents one experiment. B) PCR products from (A) forward and reverse sequenced with chromatograms aligned with exon 1 and exon 22 sequences respectively.

CRISPR/Cas9 guide testing in pig blastocysts

Following the experiments in pig fibroblasts, the designed CRISPR/Cas9 strategies to generate a calpain 3 KO were tested in pig embryos. The process aimed at high efficiencies obtaining biallelic KOs while also keeping viability high. For this, immature oocytes were extracted from ovaries obtained from a slaughterhouse and matured *in vitro* for 48 hours, at which point CRISPR/Cas9 RNP was either electroporated or microinjected into the oocyte right before *in vitro* fertilization for 24 hours. The zygote was then cultured for another day (day 2 embryo) or until the blastocyst stage in day 6, before being either used for analysis or transferred into recipient sows (Figure 58).

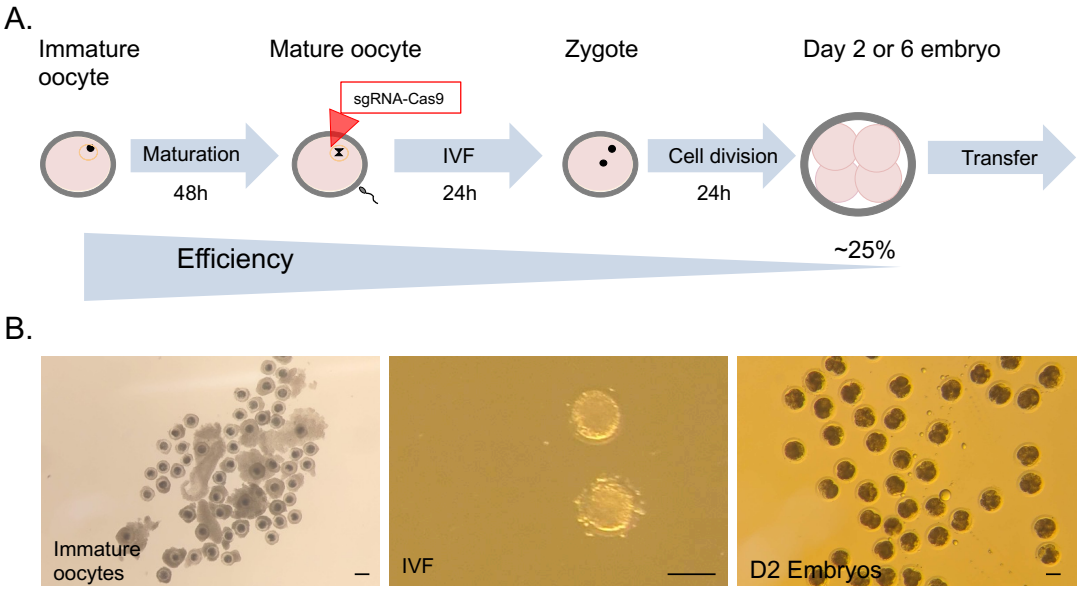

Figure 58. In vitro production of CRISPR/Cas9 edited pig embryos. A) Schematic representation of the embryo production process from oocyte maturation to day 2 embryos. B) Representative images of immature oocytes, mature oocytes with sperm cells around them in *in vitro* fertilization (IVF) and day 2 (D2) embryos. Scale bars: 100 µm.

To genotype the embryos, two methods were used depending on the exon being analysed. To analyse deletions generated by guide pairs in exon 1, these were analysed in the same way as the fibroblast pools, but since each embryo was independently analysed it could be determined whether the deletion had occurred in heterozygosis (HZ), in both alleles (KO) or none (WT) (Figure 59A). To generate mutations in exon 22 of the embryos, only guide #Ex22.2 was used to targeted codon ARG788. To evaluate the mutations in this site, PCR products were run through capillary electrophoresis where insertions or deletions could be precisely detected for each allele and determine whether the embryo was WT, HZ or had the biallelic mutation (Figure 59B).

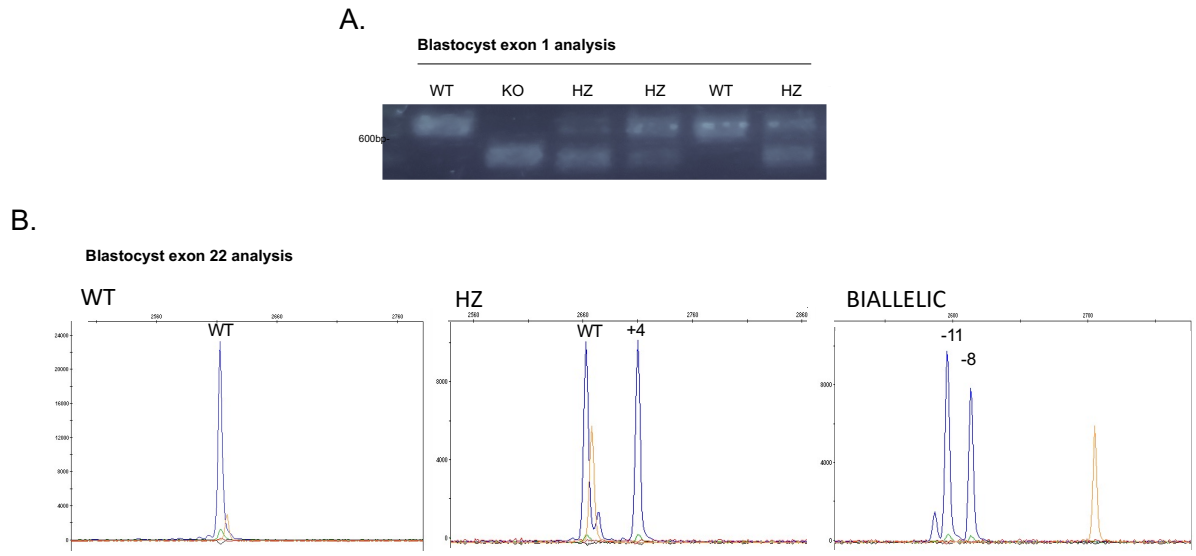

Figure 59. CRISPR/Cas9 calpain 3 guide testing in pig embryos: Mutation analysis. A) Agarose electrophoresis to evaluate deletions in exon 1, showing negative control band of 645bp (WT blastocysts), biallelic deletion with a single smaller band (KO blastocyst) and heterozygous for the deletion, showing both bands (HZ). B) Capillary electrophoresis to evaluate mutation in exon 22. WT: sample with wildtype allele. HZ sample with wildtype allele and KO allele (insertion of +4 bp). KO: sample with KO alleles (deletion of -11 bp and -8 bp).

It is important to mention that in exon 1, it was evaluated whether both guides had worked and generated the deletion of the sequence between the two guides, however if only one of the two guides had worked, generating a small insertion or deletion, this would not be detected, and therefore the real efficiency and rate of mutations could be higher. In a similar way in exon 22, despite of the fact that when using a single-guide CRISPR/Cas9 generally produces and insertion or deletion, if instead the guide only generated a base replacement, this mutation would not be detected since the amplicon size would not vary, therefore the real mutation rate could be higher.

To assess the effect in the embryo viability of the CRISPR/Cas9 introduction on the oocytes and optimize the obtention of biallelic deletions, different CRISPR/Cas9 RNP introduction methods were evaluated. Oocytes were either microinjected or electroporated with 4 or 6 pulses (30V 1ms, 100ms intervals) with the pair of guides #3 + #6 at 100 ng/µL Cas9 and 12.5 ng/µL guide #3 and guide #6 (1:1 Cas9:sgRNA ratio) and the effects in viability were compared to uninjected controls or mock-injected controls. For this, cleavage rate (two cell embryos per total number of inseminated oocytes) and blastocyst rate (blastocyst obtained per total number of inseminated oocytes) were analysed. Cleavage rate was not affected by microinjections, however electroporation did have an effect. In the case of 4 pulses, it increased the cleavage rate significantly, while 6 pulses

were detrimental and reduced the cleavage rate (Figure 60A). Regarding the percentage of embryos that reached the blastocyst stage, this was significantly reduced if the oocyte had been microinjected or electroporated. The rate was reduced from around 32% to 20% in the cases it was injected or electroporated, with no significant differences between injection control and injection or electroporation with CRISPR/Cas9, while it was reduced to around 10% if electroporated with 6 pulses (Figure 60B). When comparing the deletion rate in exon 1 with the different methods, microinjection obtained a significantly higher deletion rate compared to electroporation, and the number of biallelic deletions obtained were also higher (Figure 60C-D).

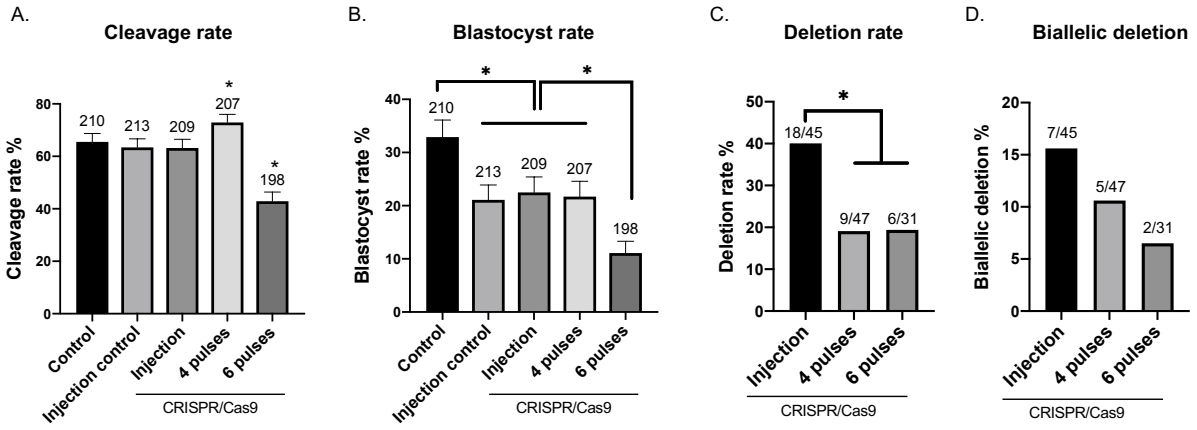

Figure 60. CRISPR/Cas9 calpain 3 guide testing in pig embryos: Effect of microinjection and electroporation in viability and efficiency. A) Cleavage rate: Two cell embryos per total number of inseminated oocytes B) Blastocyst rate: Blastocyst obtained per total number of inseminated oocytes C) Deletion rate: Percentage of embryos with at least one allele with the deletion relative to total embryos and D) Biallelic deletion rate: Percentage of embryos with both alleles with the deletion relative to total embryos. Data expressed as mean percentage ± SEM, with number on top of each bar indicating sample size. *In vitro* matured oocytes were electroporated or microinjected at 100 ng/µL Cas9 and 12.5 ng/µL guide #3 and guide #6 (1:1 Cas9:sgRNA).

Aiming to improve the efficiency of the guides and obtain the highest possible percentage of mutated embryos for embryo transfers, the Cas9:sgRNA molar ratio was doubled (1:2) for the electroporated oocytes and the simultaneous use of a guide pair targeting exon 1 and a guide targeting exon 22 was tested. The sgRNA ratio was not increased for microinjections because previous experience had shown reduced viability (data not shown). No significant differences were found in the blastocyst rate between the 3 guide combinations in microinjection or 4-pulse electroporation (Figure 61A) and the blastocyst rates were similar to the ones previously obtained.

The mutation rate and distribution of mutations was also analysed. The percentage of embryos with mutations was between 76% and 87% with no significant differences between using microinjection, electroporation or guide combinations #3+#6+#Ex22.2 or #3+#7+#Ex22.2. From these embryos, between 32% and 39% had both a deletion in exon 1 and a mutation in exon 22, between 28% and 40% had mutations only in exon 22, and between 5% and 13% only had mutations in exon 1 (Figure 61B). In the case of biallelic mutations, in exon 1 approximately 20% of the microinjected embryos had a biallelic deletion, whereas for the electroporated ones it was between 16-17%. For the exon 22 biallelic mutations, the efficiency was lower than 3% in all cases (Figure 61C). Overall, there were no statistically significant differences in the efficiency to obtain mutations and deletions between the 3 guide combinations tested and whether they were microinjected or electroporated, indicating that the increase of the Cas9:sgRNA molar ration to 1:2 in 4 pulse electroporation was able to match efficiencies obtained with microinjection and any of these methods and guide combinations could be used to obtain up 80% of the embryos with at least one of the designed modifications.

A.

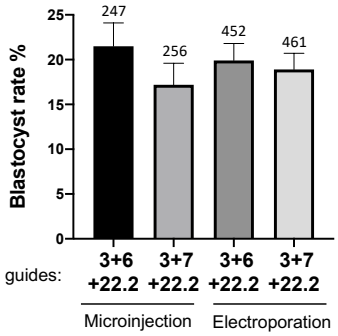

B.

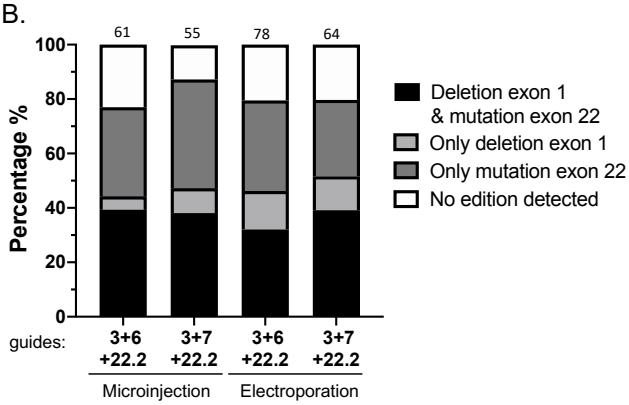

C.

	Microinjection		Electroporation		p value
sgRNA	3+6+22.2	3+7+22.2	3+6+22.2	3+7+22.2	
Exon 1 biallelic deletion (%)	20.5 (16/78)	20.3 (16/79)	16.7 (13/78)	17.2 (11/64)	0.9
Exon 22 biallelic mutation (%)	3.2 (2/63)	1.8 (1/56)	1.3 (1/80)	0 (0/80)	0.46

Figure 61. CRISPR/Cas9 calpain 3 guide testing in pig embryos: Effect of doubling sgRNA concentration and distribution of mutations obtained with different strategies. A) Effect of doubling sgRNA concentration in electroporation in viability measured in blastocyst rate with different guide combinations Data expressed as mean percentage ± SEM. Blastocyst rate: Blastocyst obtained per total number of inseminated oocytes. B) Distribution of mutations obtained with guide combinations #3+#6+#22.2 or #3+#7+#22.2 in microinjection and in electroporation. C) Table with biallelic deletion efficiencies. *In vitro* matured oocytes were microinjected at 100 ng/µL Cas9 and 12.5 ng/µL of each guide (1:1 Cas9:sgRNA) or electroporated at 100 ng/µL Cas9 and 25 ng/µL of each guide (1:2 Cas9:sgRNA). Numbers on top of each bar indicate sample size.

Embryo transfers to recipient pigs

Using the optimized CRISPR guides and the tested methods, a set of embryo transfers were performed to recipient pigs. Guide combinations #3+#6 and #3+#7 were used in microinjection and D2 embryos were transferred surgically into the uterotubal junction in the uterus. For guide combinations #3+#6+#22.2, #3+#7+#22.2 or only #22.2, these were used in electroporation and D2 embryos were surgically transferred either to the uterotubal junction or the oviduct, while embryos developed *in vitro* until D6 were non surgically transferred to the uterus. From the 45 embryo transfers performed 12 pregnancies were detected, however only two completed the gestation while the others resulted in natural abortions. From the two completed gestations, each of them only gave birth to a single piglet, which in both cases were WT and were dead at birth (Table 14).

Pig ID	**Guides #**	**Embryo Day**	**Embryos transferred**	**CRISPR method**	**Transfer method**	**Gestation**	**Result**
1	3+7	D2	117	Microinj.	Q1	Negative	-
2	3+7	D2	116	Microinj.	Q1	Negative	-
3	3+6	D2	140	Microinj.	Q1	Negative	-
4	3+6	D2	150	Microinj.	Q1	Negative	-
5	3+6	D2	110	Microinj.	Q1	Negative	-
6	3+6	D2	111	Microinj.	Q1	Negative	-
7	3+6	D2	60	Microinj.	Q1	Negative	
8	3+6	D2	60	Microinj.	Q1	Negative	-
9	3+7	D2	88	Microinj.	Q1	Negative	-
10	3+6+22.2	D6	38	Electrop.	NoQ	**Positive**	**Abortion**
11	3+6+22.2	D6	29	Electrop.	NoQ	Negative	-
12	3+6+22.2	D6	40	Electrop.	NoQ	Negative	-
13	3+6+22.2	D6	40	Electrop.	NoQ	Negative	-
14	3+6+22.2	D6	80	Electrop.	NoQ	**Positive**	**Abortion**
15	3+7+22.2	D6	80	Electrop.	NoQ	Negative	-
16	3+7+22.2	D6	67	Electrop.	NoQ	**Positive**	**Abortion**
17	3+6+22.2	D2	92	Electrop.	Q1	Negative	-
18	3+6+22.2	D6	52	Electrop.	NoQ	**Positive**	**Abortion**

19	3+6+22.2	D2	100	Electrop.	Q2	Negative	-
20	3+6+22.2	D2	100	Electrop.	Q1	**Positive**	**Abortion**
21	3+6+22.2	D6	38	Electrop.	NoQ	**Positive**	**1 WT (Dead)**
22	3+6+22.2	D2	100	Electrop.	Q2	Negative	-
23	3+6+22.2	D2	100	Electrop.	Q1	Negative	-
24	3+6+22.2	D6	48	Electrop.	NoQ	Negative	-
25	3+6+22.2	D6	47	Electrop.	NoQ	**Positive**	**Abortion**
26	3+6+22.2	D6	65	Electrop.	NoQ	**Positive**	**Abortion**
27	3+6+22.2	D2	100	Electrop.	Q1	Negative	-
28	3+6+22.2	D6	52	Electrop.	NoQ	Negative	-
29	22.2	D2	55	Electrop.	Q1	Negative	-
30	22.2	D2	65	Electrop.	Q1	Negative	-
31	22.2	D2	89	Electrop.	Q1	Negative	-
32	22.2	D2	86	Electrop.	Q1	**Positive**	**Abortion**
33	22.2	D2	86	Electrop.	Q1	Negative	-
34	22.2	D2	106	Electrop.	Q1	Negative	-
35	22.2	D2	106	Electrop.	Q1	Negative	-
36	22.2	D6	50	Electrop.	NoQ	Negative	-
37	22.2	D2	50	Electrop.	Q1	**Positive**	**Abortion**
38	22.2	D2	50	Electrop.	Q1	Negative	-
39	22.2	D2	92	Electrop.	Q1	Negative	-
40	22.2	D2	92	Electrop.	Q1	Negative	-
41	22.2	D2	94	Electrop.	Q1	Negative	-
42	22.2	D2	40	Electrop.	Q1	**Positive**	**Abortion**
43	22.2	D2	40	Electrop.	Q1	Negative	-
44	22.2	D2	40	Electrop.	Q1	Negative	-
45	22.2	D2	40	Electrop.	Q1	**Positive**	**1 WT (Dead)**

Table 14. Embryo transfers made with different guides and transfer methods. Embryo day: Days of development of the transferred embryo. CRISPR method: method of introduction of CRISPR/Cas9 in matured oocytes (4 pulse electroporation or Microinjection). Embryo transfer method: Q1: Surgical, Uterotubal junction transfer; Q2: Surgical, oviduct transfer; NoQ: Non-surgical transfer to uterus.

Discussion

Guide designs

Obtaining genetically modified pigs requires embryo technologies and procedures that compared to other species, remain challenging in pigs. Currently, the primary problem with the *in vitro* produced embryos is the low pregnancy rate after the embryo transfers and the small litter sizes that are obtained, which in part could be due to the micromanipulation procedures (Chen et al., 2022).

In order to face the embryo transfers with a high percentage of embryos that would carry the mutations in the calpain 3 gene, while maintaining viability as much as possible, we focused on optimizing the *in vitro* aspects of CRISPR/Cas9 design and delivery. Based in our successful experience generating calpain 3 KO iPSC lines, we followed a similar strategy when designing the RNA guides for the porcine calpain 3 gene, targeting the start codon in exon 1 with different guide combinations and additionally designing guides for codon ARG788 in exon 22.

Testing the designed guides in the pig fibroblasts first before moving into pig embryos proved to be an efficient way to analyse the efficiencies and the mutations that were being obtained with each guide. Ideally, it would have been better to test the guides in a cell type that expressed detectable levels of calpain 3 protein in order to evaluate its knockdown levels with each guide in the pool of cells, however, for that we would have needed to grow primary pig myoblasts, electroporate them with CRISPR/Cas9 and differentiate them, which was not considered appropriate given the time requirements that those protocols have. From the designed guides for exon 1, these were designed given the available PAM sequences that Cas9 requires around exon 1. From these guides, the pair #3+#6 and #3+#7 were selected mostly due design considerations rather than their efficiency, due to guide #2 showing a much higher off-targeting potential (lower score) despite its higher efficiency, and guide #5 and #4 leaving other potential start codons outside the deletions. The efficiency of the guides in fibroblasts were greatly improved when using the single-guide sgRNA guides instead of the two-part cr:tracerRNA guides, which has been previously suggested due to the higher stability of the sgRNA (Hendel et al., 2015; Ryan et al., 2018).

Regarding the guides for exon 22, the adjacent PAM sequence to codon ARG788 allowed to directly target this codon with one guide, and since using just the guide #Ex22.2 efficiently targeted codon ARG788 generating frameshift mutations and early stop codons, and having the human mutation with frameshift and early stop codon (ARG788Serfs*) found in humans as a reference, using a single-guide to target exon 22 was considered more optimal. In addition to this, it was interesting to find that when using guide #3 in exon 1 and guide #Ex22.2 in exon 22, the entire 52 Kbp sequence of the calpain 3 gene between both guides could be deleted. We did not evaluate with what frequency this event was occurring compared to only the small deletion by one or two guides, however it is known that the greater the distance between the two guides the lower is the probability of a large deletion, which varies depending on the guides and genomic region where this is occurring, (Song et al., 2016, 2017).

In vitro production of pig embryos and CRISPR/Cas9 guide testing

Despite *in vitro* production of embryos has been adopted for other species such as horses, cattle and small ruminants, the swine industry has been reluctant to adopt these technologies. Unlike in other species like mice, *in vitro* generated embryos exhibit reduced quality and ability to establish a pregnancy after the embryo transfer (Chen et al., 2021; van der Weijden et al., 2021). And a significant amount of effort is still being dedicated to improve each step of the process in pigs (Bauer et al., 2010; Casillas et al., 2018; Navarro-Serna et al., 2021; París-Oller et al., 2022).

Producing embryos *in vitro* is an essential part of the process and a key element in assisted reproductive technologies, necessary to generate porcine models, and the recent development of CRISPR/Cas gene editing has considerably expanded the interest in porcine models for biomedical and agricultural purposes (Hryhorowicz et al., 2020; H. Yang & Wu, 2018). Since pigs have similar physiology and a more relevant organ and body sizes to humans when compared to other laboratory species, pig models can be used to test relevant doses of therapeutics or medical devices, as well as to understand disease progression better. And in the particular case of MDs, they have been proven useful in Duchenne's muscular dystrophy where different therapies have been tested (Gutierrez et al., 2015; Klymiuk et al., 2016; Stirm et al., 2022).

Most of the porcine embryo production systems are comprised of 3 main steps: oocyte maturation, *in vitro* fertilization, and embryo culture. First, oocytes are aspirated from ovaries from sows or gilts, which are then matured *in vitro*. Then, matured oocytes are *in vitro* fertilized and the putative zygotes are cultured *in vitro* prior to the embryo transfer. To create genetically modified pigs, the manipulation of oocytes and embryos is required, where the most common method for introducing mutations is by microinjection of CRISPR/Cas9 either as mRNA or a RNP complex, into the porcine zygote or oocyte, or by transfection of fetal fibroblasts to generate donor cells for SCNT. Both methods have been used to generate genetically modified pigs, where the gene editing by microinjection or electroporation into the zygote or oocyte generates pigs with heterogeneous mutations, while SCNT results in pigs with the same mutation as the donor cell, allowing to select exact genetic modifications of interest *in vitro* in the fibroblast cultures before the transfer. However, SCNT is a technically demanding method that lowers the overall efficiency of obtaining blastocysts and successful pregnancies (P. R. Chen et al., 2021; G. Li et al., 2014; Zhao et al., 2010).

For the mentioned reasons as well as the for the fact that in order to generate a KO a precise modification is not required and different mutations can result in a disruption of the mRNA translation and a gene KO, it was opted to use microinjection and electroporation directly in the oocytes. Since electroporation is considered an easier and faster method than microinjection, electroporation was also optimized to obtain the highest percentage of modified embryos possible prior to the transfers.

Other aspects were also taken into account when deciding to use CRISPR/Cas9 as a RNP in mature oocytes. Delivery of macromolecules into oocytes and zygotes are limited due to the presence of the zona pellucida (ZP), the glycoprotein layer surrounding the plasma membrane of mammalian oocytes, which blocks molecules larger than 170 kDa in matured oocytes and 110 kDa in zygotes (Legge, 1995). This makes oocytes more amenable to introduce proteins like Cas9, which is nearly 160 kDa, and despite there have been several genetically modified pigs generated using zygote electroporation either with Cas9 in mRNA form (Tanihara et al., 2016) or as a RNP (Hirata et al., 2019; Nishio et al., 2018; Tanihara et al., 2018), introducing CRISPR/Cas9 in mature oocytes or early zygotes before DNA replication occurs has been shown to reduce the possibility of obtaining mosaic embryos, with the efficiencies being higher with Cas9 in RNP form (Lamas-Toranzo et al., 2019; Su et al., 2019).

Optimizing electroporation conditions is important to maximize the rates of mutations and minimize pig embryo damage. Previous studies have adjusted parameters like pulse duration, number of pulses, voltage and the use of unipolar or bipolar currents (Hirata et al., 2019; Le et al., 2021; Tanihara et al., 2016). In our results, electroporation had similar mutation rates with 4 or 6 pulses, however the blastocyst rate was lower with 6 pulses, and no differences could be detected between injection control, and the CRISPR/Cas9 RNP injection or 4 pulse electroporation. Despite not being a good indicator of viability, it could be observed that the cleavage rate was increased with 4 pulses, as it is known that electrical stimuli can induce oocyte activation (Zhu et al., 2002), however 6 pulses also seemed to be detrimental for cleavage as this rate was also reduced. Initially, a lower mutation rate was obtained with electroporation compared with microinjection when the same conditions of RNP delivery were used with a 1:1 equimolar Cas9:sgRNA concentration (100 ng/mL Cas9 and 12.5 ng/mL each guide). However, when the sgRNA concentration was doubled, the efficiencies obtained were similar to the ones obtained with microinjection without affecting the blastocyst rate obtained. In previous studies modified pigs have been obtained by electroporating CRISPR/Cas9 as a RNP, where similar concentrations of Cas9 (50-100 ng/mL) and even higher concentrations of sgRNA have been used (100-200 ng/mL) with ratios up to 1:16 of Cas9:sgRNA (Hirata et al., 2019; Le et al., 2021; Tanihara et al., 2019).

Once the Cas9:sgRNA ratio was increased, we found no differences in embryo development or mutation rates when using microinjection or electroporation. We designed this strategy to use 3 guides that simultaneously remove the start codon and generate an INDEL in exon 22, and despite we were using lower sgRNA concentrations than previous studies, we found that nearly 80% of embryos had at least one type of the expected mutations in the calpain 3 gene, and around 17-20% were biallelic for the deletion of the start codon. It should be noted that the efficiency of the system could be even higher because mutations caused by sgRNA 6 or 7 without causing the deletion of the start codon were not evaluated, and also the entire deletion of 52 Kbp from exon 1 to exon 22, which in fibroblasts we were able to detect, was not evaluated in these embryos, therefore, some of the embryos in the 20% that were considered WT, could in fact still have a mutation.

Embryo transfers

Aiming to obtain a calpain 3 biallelic KO pig, the different combinations of guides tested in blastocysts were used for the embryo transfers. From the 45 embryo transfers performed to recipient sows, in 9 of them only a guide pair targeting exon 1 was introduced by microinjection in the oocytes, in 19 of them the 3 guide combinations were used and introduced by electroporation, and in another 17 transfers oocytes were only electroporated with the guide #Ex22.2 for exon 22. Also, depending on the development days of the embryos that was being transferred, different surgical approaches were taken to place the embryos in the most appropriate place for its developmental state.

Despite the efforts and obtaining at least 12 pregnancies, no piglets were obtained and the only two that were born died at birth and were genotyped as WT. Pregnancy and birth rates with *in vitro* produced and manipulated embryos are known to be very low for the porcine species compared to others (Chen et al., 2022), however given the amount of embryo transfers that were performed we would have expected to obtain at least some animals. The embryo production and transfer protocols were carried out in the Physiology Dept. of the University of Murcia, as part of a collaborative project with Prof. J. Gadea's group, where previous work using the same embryo production and transfer protocols proved to work well to obtain a TPC2 KO pig (Navarro-Serna, et al., 2021). However, this made us question the methods and protocols that we were using and evaluated where the possible issue could be residing.

Clarifying the reason why the pregnancies were not successful would require a deeper characterization work that stands outside the scope of this work, but there are 3 main aspects that could be resulting in the low pregnancy and birth rates observed.

The first case could be a specific toxicity or lethality generated by the calpain 3 gene or sgRNA guides utilized. We believe it is quite unlikely that a calpain 3 KO pig would result in embryonic lethality, since in humans and mice lacking calpain 3, there have not been any developmental issues reported. Despite we cannot completely discard this option, the efficiency for a biallelic KO with our CRISPR/Cas9 system was 20% in the best cases, therefore even if there was an embryonic lethality in pigs in the absence of calpain 3, there should still be 80% of viable embryos in heterozygosis, or at least around 20% of WT embryos that would not have any mutation that should have been born, which was not

the case in our transfers. Another explanation could be that the sgRNA guides used, would have an off-target activity responsible for the toxicity or lethality. Even though we did not analyse off-target activity in the pig embryos mostly because we were waiting to do so only in the born piglets, it is also unlikely to think such a scenario because even if it is likely that there could be some off-target mutations in some cases, it would need to be constantly causing a lethal mutation off-target with high efficiency. Initially we did the transfers with embryos that had either a pair of guides for exon 1 or 3 simultaneous guides for exon 1 and exon 22 aiming to obtain biallelic KOs. However, once we were aware of the low pregnancy rates, we decided to only use one guide for exon 22 in the last embryo transfers. This means that there were transfers done with embryos that not always had the same guides, and again to think that more than one guide was having a lethal off-target effect, with such a high efficiency as to affect to all the embryos transferred does not seem likely.

The second case could be an unspecific toxicity associated with CRISPR/Cas9 RNP microinjection and electroporation that would be damaging the oocytes and embryos. In this aspect both our Cas9 and sgRNA concentrations were within what has been described in the literature, (100 ng/mL Cas9 and up to 25 ng/mL of each sgRNA guide) (Hirata et al., 2019; Le et al., 2021; Tanihara et al., 2019) therefore this should not be the main issue. There is however certain level of toxicity attributed to the *in vitro* embryo development that is increased when microinjection or electroporation of CRISPR/Cas9 occurs. Current studies report that the embryos that reach the blastocyst stage on day 6 are about 20-40% of initial oocytes, with significant embryo loss or arrest at earlier stages (Chen et al., 2020; Redel et al., 2016; Tanihara et al., 2019). In our case this number was similar around 20% for the CRISPR/Cas9 treated, while the controls were at around 30%. One known issue with *in vitro* developed embryos is associated with epigenetic changes. Regulation of DNA methylation is a major epigenetic event that occurs during preimplantation development in mammals and is critical for normal embryo development (Reik et al., 2001). Fertilized oocytes undergo a significant decrease in global DNA methylation during embryo development from gametes to blastocyst stage (Messerschmidt et al., 2014), and it has been reported that artificial intrusions during *in vitro* embryo development such as *in vitro* maturation, culture and varying oxygen concentrations are expected to influence the epigenome of *in vitro* developed embryos (Deshmukh et al., 2011; el Hajj & Haaf, 2013; Sirard, 2017). Still, the full-term pregnancy rate after transferring IVF embryos

microinjected with CRISPR/Cas9 is reported to be around 40% with an average of 5.7 live piglets per litter (Chen et al., 2022).

Finally, the issues could also be occurring in the embryo culture and transfer methods. Compared to other species, since *in vitro* produced embryos have a lower viability, large numbers of embryos are transferred to increase the probability of obtaining a pregnancy. For 1-2 cell stage embryos, it is common to transfer up to 150 embryos, while for day 6 blastocyst stage embryos, transfers are commonly done with around 30-40 embryos (Chen et al., 2022; E. A. Martinez et al., 2015; Sheets et al., 2018). However unlike on other species, non-surgical transfers in pigs have been limited due to the complex anatomy of their female reproductive tract which makes it harder to reach the uterus as well as the uterine horns, which are long and narrow. Alternatively, the *in vitro* developed embryos are transferred via midventral laparotomy into the ovary and oviduct, with the additional risks and stress that this procedure can carry. Usually, when a pregnancy is lost during gestation, the majority of loss occurs between days 25 to 45 by resorption, and in rare cases, the surrogate will abort the pregnancy after day 45 (Lai & Prather, 2004).

Overall, we have designed and tested effective CRISPR/Cas9 guides and strategies to knockout the porcine calpain 3 gene from pig embryos, with high efficiency and similar *in vitro* embryo viability as other studies have obtained up to day 6 of development, with electroporation optimized as a viable alternative to microinjection. However, for reasons that we still haven't identify, we have not been able so far to produce a calpain 3 KO pig.

GENERAL DISCUSSION

GENERAL DISCUSSION

So far, LGMDR1 has proven to be a hard disease to model and study. With a very limited amount of patient samples available for research, there is a need for good models that will recapitulate the disease characteristics, both molecularly and phenotypically. This would be ideal in order to study pathogenic mechanisms arising from the absence of calpain 3, as well as to test potential treatments. However, each of the current models presents its own limitation that in combination with the fact that calpain 3 seems to be involved in several different functions in the muscle, makes it hard to determine the chain of pathological events that ultimately lead to atrophy in humans.

In vitro models have proven to be useful to study the differences in signaling pathways, myogenesis or calcium regulation, however the physiological complexity and maturation levels achieved *in vitro* are still far from representing the complexity of the human muscle tissue. Also, most of the observations made *in vitro,* even when using human patient derived cell cultures, do not seem to clearly indicate an increased pro-atrophic signaling nor show a clearly deteriorated myotube cultures, therefore stablishing which of the *in vitro* observed differences in the absence of calpain 3 causes pathology and leads to atrophy remains challenging. On the other hand, the *in vivo* models developed in mouse have a very mild phenotype, if any, and they do not develop clear signs of atrophy at the histological level with functional motor measurements being highly variable.

Altogether this means that first of all, better models would be highly valuable to study the disease and test new therapies, at the same time, the observations and conclusions that are made in the mouse models, and in the *in vitro* models, should be taken with caution and ideally, they should be tested in more than one model to confirm that such observations are not a consequence of the model being used. Ultimately, if the type of analysis allows it, the observations should be confirmed in patient samples.

In this work we have aimed at tackling LGMDR1 research in two main aspects. On the one hand, we aimed to provide new research models, one *in vitro* and the other one *in vivo,* that we expect could improve some of the limitations found in current models, and on the other hand, we aimed to clarify and test some of the previous knowledge in existing

as well as new calpain 3 KO models and to obtain new insights of disease mechanisms and treatment possibilities.

The generated *in vitro* model consists of isogenic calpain 3 KO iPSC lines generated from a control line with CRISPR/Cas9. The KO lines maintained their iPSC characteristics after the biallelic mutation in calpain 3, and we did not observe any CRISPR/Cas9 off-target effects. This provided us with continuous cell lines with the same genetic background that only differed in the generated mutations, and from where we obtained myogenic progenitors and multinucleated myotubes through a PAX7 overexpression protocol. From there, we optimized the terminal differentiation protocol to obtain more mature myotubes with increased contraction levels to a point where we considered appropriate. Here, having the model based in iPSC lines offers the opportunity to not only further optimize the differentiation and maturation protocols in order to obtain a more advanced *in vitro* system in the future, but also to use different myogenic induction protocols or to generate advanced muscle organoids with multiple cell types, starting from the same isogenic lines, which could offer further advantages to model this disease in the future.

Once we generated the *in vitro* model, we aimed to evaluate different aspects that could be affecting the disease using our isogenic iPSC lines as well as the C3KO mouse model.

First, we performed a proteomic study to evaluate CTX damage response in the C3KO mouse. Here, we observed that the damage response was different in the C3KO with many proteins dysregulated when compared to the WT damage response, but also, that there were significant differences between the TA and the soleus muscles, the latter being described as a more affected one. Also, we observed that the differences in protein levels pointed towards altered mitochondrial processes, glucose metabolism, protein folding and myogenesis in the C3KO muscles, and identified some proteins that could be key in these processes such as the myogenic regulators MYBBP1A, CSRP3 and ANKRD2, as well as several chaperones. Following this, we observed that in the absence of calpain 3, the myogenic capacity appears to be reduced, which we observed both in the human isogenic iPSC lines as well as in the old C3KO mouse derived SCs cultures.

However, despite these differences, when we performed several exhaustion tests in old C3KO mice, we did not observe any motor impairments, on the contrary, the C3KO mice

showed increased endurance, and at the histological level there were no clear signs of atrophy either. This made us suspect that the compensatory mechanisms that the mice are believed to have to avoid the dystrophy that humans develop in the absence of calpain 3, could be more evident in the old C3KO and perhaps the lack of atrophy and the potential differences in fiber types could even be making the C3KO perform better in these tests. This issue clearly requires further experiments and characterization to understand the differences in the old C3KO and WT muscles, but the results clearly rise doubts on the C3KO model and on whether the molecular changes that can be observed in this mouse have any pathological effect and whether they are occurring at all in the LGMDR1 patients. At the molecular level, we did observe significant differences in proteins from mitochondria, glucose metabolism, and cytosolic as well as ER stress/UPR associated chaperones after run to exhaustion tests, and observed that the 4-PBA treatment that we tested, significantly reduced some of the increased protein levels such as chaperones in the C3KO without affecting the performance in the run to exhaustion tests. We also tried to evaluate whether some of these observed changes and pathways would also be affected on the human myotubes obtained from our isogenic iPSC lines, for which we induced contractions of the myotubes *in vitro* for prolonged periods, and observed that alterations in TOM20, HSP70, GLUT4 and p-mTOR protein levels are present in both C3KO mice after the exhaustion tests and human iPSC derived myotubes lacking calpain 3 after EPS.

Finally, and after the clear signs that a better *in vivo* LGMDR1 model is needed, we focused on generating a new model by generating a calpain 3 KO pig with CRISPR/Cas9, that we expect based on other muscular dystrophy models generated in pigs, would develop a more severe atrophy and a clinical phenotype more similar to humans. We optimized the process to obtain pig embryos with a high mutation rate and viability *in vitro,* but unfortunately after several embryo transfers and few gestations, we could not achieve to obtain a calpain 3 KO pig. The reason why we obtained such a low success rate in obtaining live piglets requires further experiments, however, we expect that the tools and optimized protocols we obtained here will be helpful in future attempts that will be made to obtain the calpain 3 KO pig, and which also could be useful to develop porcine models for other MDs.

CONCLUSIONS

CONCLUSIONS

CHAPTER 1: Generation of isogenic calpain 3 KO iPSC lines with CRISPR/Cas9

1- Targeting the start codon of calpain 3 with CRISPR/Cas9 effectively generated biallelic knockouts both using a single-guide or dual-guide strategy.
2- The generated isogenic calpain 3 KO lines maintained pluripotency, and no chromosomal aberrations or off-target mutations were detected.
3- The generated isogenic calpain 3 KO lines were able to undergo myogenic differentiation into PAX7-GFP+ myogenic progenitors and to terminally differentiate into multinucleated myotubes.
4- The use of a cultrex-HA substrate and differentiation mediums S-Dex and DM-2 were determined as the best to induce terminal differentiation and maturation of the PAX7-GFP+ myogenic progenitors among the tested protocols.

CHAPTER 2: Damage response, myogenesis and protein homeostasis in calpain 3 KO models of LGMDR1.

5- Myogenic capacity is reduced in the absence of calpain 3 both in mouse SCs and derived cultures and in human iPSC derived myogenic progenitors.
6- TA and soleus are differentially affected in the C3KO mouse and have different responses to acute damage by CTX.
7- Mitochondria, glucose metabolism and protein folding processes are among the most dysregulated in the C3KO acute damage response by CTX.
8- MYBBP1A, CSRP3 and ANKRD2 appear as novel negative effectors of myogenesis in C3KO mouse soleus.
9- Old C3KO soleus shows altered levels of proteins from mitochondria, glucose metabolism, and chaperones after run to exhaustion tests, as well as increased protein ubiquitination, p-mTOR and NF-κB levels.
10- Despite reduced myogenic capacity and a molecular phenotype, 18 month old C3KO mice lack motor impairment and are able to run more than WT in run to exhaustion tests.

11- 4-PBA is an effective treatment to restore increased ER and cytosolic chaperone levels in the old C3KO, as well as the increased p-mTOR, MYBBP1A and ubiquitination levels, without affecting running performance.
12- Alterations in TOM20, HSP70, GLUT4 and p-mTOR levels are present in both C3KO mice after the exhaustion tests and human iPSC derived myotubes lacking calpain 3 after EPS.

CHAPTER 3: Generation of a LGMDR1 pig model with CRISPR/Cas9

13- The functionality of CRISPR/Cas9 guides in pig fibroblasts is also maintained when using them in pig oocytes prior to IVF.
14- Using a dual-guide strategy worked efficiently to delete the start codon of calpain 3 in porcine fibroblasts and embryos.
15- Using the dual-guide strategy for exon 1 and a single-guide for exon 22 resulted in high mutation rates of around 80% in pig embryos while maintaining the blastocyst rate comparable to empty microinjection controls.
16- Using guides separated by 52 Kbp can generate large deletions of the entire fragment between the guides in the calpain 3 gene, opening the possibility to delete the entire gene.
17- Using CRISPR/Cas9 guides as sgRNA is more efficient than using the duplexed crRNA:tracrRNA guides when electroporating pig fibroblasts with Cas9 RNP.
18- Mutation and viability rates obtained with 4 pulses of 30V and 1ms with 100ms pulse intervals, can be comparable to the ones obtained by microinjection with the same Cas9 concentration, by only duplicating the sgRNA guide concentrations.

BIBLIOGRAPHY

BIBLIOGRAPHY

Aartsma-Rus, A., Ginjaar, I. B., & Bushby, K. (2016). The importance of genetic diagnosis for Duchenne muscular dystrophy. *Journal of Medical Genetics*, *53*(3), 145. https://doi.org/10.1136/JMEDGENET-2015-103387

Aasen, T., Raya, A., Barrero, M. J., Garreta, E., Consiglio, A., Gonzalez, F., Vassena, R., Bilić, J., Pekarik, V., Tiscornia, G., Edel, M., Boué, S., & Belmonte, J. C. I. (2008). Efficient and rapid generation of induced pluripotent stem cells from human keratinocytes. *Nature Biotechnology*, *26*(11), 1276–1284. https://doi.org/10.1038/NBT.1503

Abujarour, R., Bennett, M., Valamehr, B., Lee, T. T., Robinson, M., Robbins, D., Le, T., Lai, K., & Flynn, P. (2014). Myogenic Differentiation of Muscular Dystrophy-Specific Induced Pluripotent Stem Cells for Use in Drug Discovery. *Stem Cells Translational Medicine*, *3*(2), 149–160. https://doi.org/10.5966/SCTM.2013-0095/-/DC1

Adli, M. (2018). The CRISPR tool kit for genome editing and beyond. *Nature Communications 2018 9:1*, *9*(1), 1–13. https://doi.org/10.1038/s41467-018-04252-2

Afroze, D., & Kumar, A. (2019). ER stress in skeletal muscle remodeling and myopathies. In *FEBS Journal* (Vol. 286, Issue 2, pp. 379–398). Blackwell Publishing Ltd. https://doi.org/10.1111/febs.14358

Ajalik, R. E., Alenchery, R. G., Cognetti, J. S., Zhang, V. Z., Mcgrath, J. L., Miller, B. L., Awad, H. A., Sheyn, D., Pelled, G., & Rothbauer, M. (2022). *Human Organ-on-a-Chip Microphysiological Systems to Model Musculoskeletal Pathologies and Accelerate Therapeutic Discovery*. *10*. https://doi.org/10.3389/fbioe.2022.846230

Alderton, J. M., & Steinhardt, R. A. (2000). How calcium influx through calcium leak channels is responsible for the elevated levels of calcium-dependent proteolysis in dystrophic myotubes. *Trends in Cardiovascular Medicine*, *10*(6), 268–272. https://doi.org/10.1016/S1050-1738(00)00075-X

Amici, D. R., Pinal-Fernandez, I., Mázala, D. A. G., Lloyd, T. E., Corse, A. M., Christopher-Stine, L., Mammen, A. L., & Chin, E. R. (2017). Calcium dysregulation, functional calpainopathy, and endoplasmic reticulum stress in sporadic inclusion body myositis. *Acta Neuropathologica Communications*, *5*(1), 24. https://doi.org/10.1186/S40478-017-0427-7

Anders, C., Niewoehner, O., Duerst, A., & Jinek, M. (2014). Structural basis of PAM-dependent target DNA recognition by the Cas9 endonuclease. *Nature*, *513*(7519), 569–573. https://doi.org/10.1038/NATURE13579

Anderson, L. V. B., & Davison, K. (1999). Multiplex Western blotting system for the analysis of muscular dystrophy proteins. *The American Journal of Pathology*, *154*(4), 1017–1022. https://doi.org/10.1016/S0002-9440(10)65354-0

Artrong, R. B., Warren, G. L., & Warren, J. A. (1991). Mechanisms of exercise-induced muscle fibre injury. *Sports Medicine (Auckland, N.Z.)*, *12*(3), 184–207. https://doi.org/10.2165/00007256-199112030-00004

Assou, S., Girault, N., Plinet, M., Bouckenheimer, J., Sansac, C., Combe, M., Mianné, J., Bourguignon, C., Fieldes, M., Ahmed, E., Se Commes, T., Boureux, A., Lemaıˆtre, J.-M. L., & de Vos, J. (2020). Stem Cell Reports Report Recurrent Genetic Abnormalities in Human Pluripotent Stem Cells: Definition and Routine Detection in Culture Supernatant by Targeted Droplet Digital PCR. *Stem Cell Reports*, *14*, 1–8. https://doi.org/10.1016/j.stemcr.2019.12.004

Augusto, V., Padovani, C. R., & Rocha Campos, G. E. (2004). Skeletal muscle fiber types in C57Bl6J mice. *Braz. J. Morphol. Sci*, *21*(2), 89–94.

Awaya, T., Kato, T., Mizuno, Y., Chang, H., Niwa, A., Umeda, K., Nakahata, T., & Heike, T. (2012). Selective Development of Myogenic Mesenchymal Cells from Human Embryonic and Induced Pluripotent Stem Cells. *PLOS ONE*, *7*(12), e51638. https://doi.org/10.1371/JOURNAL.PONE.0051638

Baghdadi, M. B., & Tajbakhsh, S. (2018). Regulation and phylogeny of skeletal muscle regeneration. *Developmental Biology*, *433*(2), 200–209. https://doi.org/10.1016/J.YDBIO.2017.07.026

Baghdiguian, S., Martin, M., Richard, I., Pons, F., Astier, C., Bourg, N., Hay, R. T., Chemaly, R., Halaby, G., Loiselet, J., Anderson, L. V. B., de Munain, A. L., Fardeau, M., Mangeat, P., Beckmann, J. S., & Lefranc, G. (1999). Calpain 3 deficiency is associated with myonuclear apoptosis and profound perturbation of the IκBα/NF-κB pathway in limb-girdle muscular dystrophy type 2A. *Nature Medicine*, *5*(5), 503–511. https://doi.org/10.1038/8385

Bakooshli, M. A., Lippmann, E. S., Mulcahy, B., Iyer, N., Nguyen, C. T., Tung, K., Stewart, B. A., van den Dorpel, H., Fuehrmann, T., Shoichet, M., Bigot, A., Pegoraro, E., Ahn, H., Ginsberg, H., Zhen, M., Ashton, R. S., & Gilbert, P. M. (2019). A 3D culture model of innervated human skeletal muscle enables studies of the adult neuromuscular junction. *ELife*, *8*. https://doi.org/10.7554/ELIFE.44530

Bandi, E., Jevšek, M., Mars, T., Jurdana, M., Formaggio, E., Sciancalepore, M., Fumagalli, G., Grubič, Z., Ruzzier, F., & Lorenzon, P. (2008). Neural agrin controls maturation of the excitation-contraction coupling mechanism in human myotubes developing in vitro. *American Journal of Physiology - Cell Physiology*, *294*(1), 66–73. https://doi.org/10.1152/AJPCELL.00248.2007/ASSET/IMAGES/LARGE/ZH00010854960009.JPEG

Barp, A., Laforet, P., Bello, L., Tasca, G., Vissing, J., Monforte, M., Ricci, E., Choumert, A., Stojkovic, T., Malfatti, E., Pegoraro, E., Semplicini, C., Stramare, R., Scheidegger, O., Haberlova, J., Straub, V., Marini-Bettolo, C., Løkken, N., Diaz-Manera, J., … Carlier, R. Y. (2020). European muscle MRI study in limb girdle muscular dystrophy type R1/2A (LGMDR1/LGMD2A). *Journal of Neurology*, *267*(1), 45–56. https://doi.org/10.1007/S00415-019-09539-Y

Bartoli, M., Roudaut, C., Martin, S., Fougerousse, F., Suel, L., Poupiot, J., Gicquel, E., Noulet, F., Danos, O., & Richard, I. (2006). Safety and efficacy of AAV-mediated calpain 3 gene transfer in a mouse model of limb-girdle muscular dystrophy type 2A. *Molecular Therapy : The Journal of the American Society of Gene Therapy*, *13*(2), 250–259. https://doi.org/10.1016/J.YMTHE.2005.09.017

Barton, E. R., Pacak, C. A., Stoppel, W. L., & Kang, P. B. (2020). The ties that bind: functional clusters in limb-girdle muscular dystrophy. *Skeletal Muscle*, *10*(1). https://doi.org/10.1186/S13395-020-00240-7

Bauer, B. K., Isom, S. C., Spate, L. D., Whitworth, K. M., Spollen, W. G., Blake, S. M., Springer, G. K., Murphy, C. N., & Prather, R. S. (2010). Transcriptional profiling by deep sequencing identifies differences in mRNA transcript abundance in in vivo-derived versus in vitro-cultured porcine blastocyst stage embryos. *Biology of Reproduction*, *83*(5), 791–798. https://doi.org/10.1095/BIOLREPROD.110.085936

Baylies, M. K., Bate, M., & Gomez, M. R. (1998). Myogenesis: a view from Drosophila. *Cell*, *93*(6), 921–927. https://doi.org/10.1016/S0092-8674(00)81198-8

Beauchamp, J. R., Heslop, L., Yu, D. S. W., Tajbakhsh, S., Kelly, R. G., Wernig, A., Buckingham, M. E., Partridge, T. A., & Zammit, P. S. (2000). Expression of CD34 and Myf5 defines the majority of quiescent adult skeletal muscle satellite cells. *The Journal of Cell Biology*, *151*(6), 1221–1233. https://doi.org/10.1083/JCB.151.6.1221

Beckmann, J. S., & Spencer, M. (2008). Calpain 3, the "gatekeeper" of proper sarcomere assembly, turnover and maintenance. In *Neuromuscular Disorders* (Vol. 18, Issue 12, pp. 913–921). https://doi.org/10.1016/j.nmd.2008.08.005

Beekhuis-Hoekstra, S. D., Watanabe, K., Werme, J., de Leeuw, C. A., Paliukhovich, I., Li, K. W., Koopmans, F., Smit, A. B., Posthuma, D., & Heine, V. M. (2021). Systematic assessment of variability in the proteome of iPSC derivatives. *Stem Cell Research*, *56*, 102512. https://doi.org/10.1016/J.SCR.2021.102512

Belcastro, A. N., Shewchuk, L. D., & Raj, D. A. (1998). Exercise-induced muscle injury: a calpain hypothesis. *Molecular and Cellular Biochemistry*, *179*(1–2), 135–145. https://doi.org/10.1023/A:1006816123601

Benayoun, B., Baghdiguian, S., Lajmanovich, A., Bartoli, M., Daniele, N., Gicquel, E., Bourg, N., Raynaud, F., Pasquier, M., Suel, L., Lochmuller, H., Lefranc, G., & Richard, I. (2008). NF-kappaB-dependent expression of the antiapoptotic factor c-FLIP is regulated by calpain 3, the protein involved in limb-girdle muscular dystrophy type 2A. *FASEB Journal : Official Publication of the Federation of American Societies for Experimental Biology*, *22*(5), 1521–1529. https://doi.org/10.1096/FJ.07-8701COM

Bentzinger, C. F., Wang, Y. X., & Rudnicki, M. A. (2012). Building Muscle: Molecular Regulation of Myogenesis. *Cold Spring Harbor Perspectives in Biology*, *4*(2). https://doi.org/10.1101/CSHPERSPECT.A008342

Benziane, B., Burton, T. J., Scanlan, B., Galuska, D., Canny, B. J., Chibalin, A. v., Zierath, J. R., & Stepto, N. K. (2008). Divergent cell signaling after short-term intensified endurance training in human skeletal muscle. *American Journal of Physiology. Endocrinology and Metabolism*, *295*(6). https://doi.org/10.1152/AJPENDO.90428.2008

Berridge, M. J., Lipp, P., & Bootman, M. D. (2000). The versatility and universality of calcium signalling. *Nature Reviews. Molecular Cell Biology*, *1*(1), 11–21. https://doi.org/10.1038/35036035

Bian, W., & Bursac, N. (2012). Soluble miniagrin enhances contractile function of engineered skeletal muscle. *The FASEB Journal*, *26*(2), 955–965. https://doi.org/10.1096/FJ.11-187575

Blain, A. M., & Straub, V. W. (2011). δ-Sarcoglycan-deficient muscular dystrophy: from discovery to therapeutic approaches. *Skeletal Muscle*, *1*(1), 1–12. https://doi.org/10.1186/2044-5040-1-13/FIGURES/2

Blázquez, L., Azpitarte, M., Sáenz, A., Goicoechea, M., Otaegui, D., Ferrer, X., Illa, I., Gutierrez-Rivas, E., Vilchez, J. J., & Munain, A. L. de. (2008). Characterization of novel CAPN3 isoforms in white blood cells: An alternative approach for limb-girdle muscular dystrophy 2A diagnosis. *Neurogenetics*, *9*(3), 173–182. https://doi.org/10.1007/s10048-008-0129-1

Bodine, S. C., Stitt, T. N., Gonzalez, M., Kline, W. O., Stover, G. L., Bauerlein, R., Zlotchenko, E., Scrimgeour, A., Lawrence, J. C., Glass, D. J., & Yancopoulos, G. D. (2001). Akt/mTOR pathway is a crucial regulator of skeletal muscle hypertrophy and can prevent muscle atrophy in vivo. *Nature Cell Biology*, *3*(11), 1014–1019. https://doi.org/10.1038/NCB1101-1014

Bohnert, K. R., McMillan, J. D., & Kumar, A. (2018). Emerging roles of ER stress and unfolded protein response pathways in skeletal muscle health and disease. *Journal of Cellular Physiology*, *233*(1), 67–78. https://doi.org/10.1002/JCP.25852

Bolster, D. R., Crozier, S. J., Kimball, S. R., & Jefferson, L. S. (2002). AMP-activated protein kinase suppresses protein synthesis in rat skeletal muscle through down-regulated mammalian target of rapamycin (mTOR) signaling. *The Journal of Biological Chemistry*, *277*(27), 23977–23980. https://doi.org/10.1074/JBC.C200171200

Booth, F. W., & Thomason, D. B. (1991). Molecular and cellular adaptation of muscle in response to exercise: perspectives of various models. *Physiological Reviews*, *71*(2), 541–585. https://doi.org/10.1152/PHYSREV.1991.71.2.541

Bou Saada, Y., Dib, C., Dmitriev, P., Hamade, A., Carnac, G., Laoudj-Chenivesse, D., Lipinski, M., & Vassetzky, Y. S. (2016). Facioscapulohumeral dystrophy myoblasts efficiently repair moderate levels of oxidative DNA damage. *Histochemistry and Cell Biology*, *145*(4), 475–483. https://doi.org/10.1007/S00418-016-1410-2/FIGURES/4

Broomfield, J., Hill, M., Guglieri, M., Crowther, M., & Abrams, K. (2021). Life Expectancy in Duchenne Muscular Dystrophy. *Neurology*, *97*(23), e2304–e2314. https://doi.org/10.1212/WNL.0000000000012910

Buckingham, M., & Rigby, P. W. J. (2014). Gene regulatory networks and transcriptional mechanisms that control myogenesis. *Developmental Cell*, *28*(3), 225–238. https://doi.org/10.1016/J.DEVCEL.2013.12.020

Calve, S., Odelberg, S. J., & Simon, H. G. (2010). A transitional extracellular matrix instructs cell behavior during muscle regeneration. *Developmental Biology*, *344*(1), 259–271. https://doi.org/10.1016/J.YDBIO.2010.05.007

Campbell, R. L., & Davies, P. L. (2012). Structure-function relationships in calpains. *The Biochemical Journal*, *447*(3), 335–351. https://doi.org/10.1042/BJ20120921

Canovas, S., Ivanova, E., Romar, R., García-Martínez, S., Soriano-Úbeda, C., García-Vázquez, F. A., Saadeh, H., Andrews, S., Kelsey, G., & Coy, P. (2017). DNA methylation and gene expression changes derived from assisted reproductive technologies can be decreased by reproductive fluids. *ELife*, *6*. https://doi.org/10.7554/ELIFE.23670

Carlisle, C., Prill, K., & Pilgrim, D. (2017). Chaperones and the Proteasome System: Regulating the Construction and Demolition of Striated Muscle. *International Journal of Molecular Sciences*, *19*(1). https://doi.org/10.3390/IJMS19010032

Carter, G. T., Joyce, N. C., Abresch, A. L., Smith, A. E., & VandeKeift, G. K. (2012). Using palliative care in progressive neuromuscular disease to maximize quality of life. *Physical Medicine and*

Rehabilitation Clinics of North America, *23*(4), 903–909. https://doi.org/10.1016/J.PMR.2012.08.002

Carter, S., & Solomon, T. P. J. (2018). In vitro experimental models for examining the skeletal muscle cell biology of exercise: the possibilities, challenges and future developments. *Pflügers Archiv - European Journal of Physiology 2018 471:3*, *471*(3), 413–429. https://doi.org/10.1007/S00424-018-2210-4

Casillas, F., Betancourt, M., Cuello, C., Ducolomb, Y., López, A., Juárez-Rojas, L., & Retana-Márquez, S. (2018). An efficiency comparison of different in vitro fertilization methods: IVF, ICSI, and PICSI for embryo development to the blastocyst stage from vitrified porcine immature oocytes. *Porcine Health Management*, *4*(1). https://doi.org/10.1186/S40813-018-0093-6

Cenni, V., Bavelloni, A., Beretti, F., Tagliavini, F., Manzoli, L., Lattanzi, G., Maraldi, N. M., Cocco, L., & Marmiroli, S. (2011). Ankrd2/ARPP is a novel Akt2 specific substrate and regulates myogenic differentiation upon cellular exposure to H(2)O(2). *Molecular Biology of the Cell*, *22*(16), 2946–2956. https://doi.org/10.1091/MBC.E10-11-0928

Cenni, V., Kojic, S., Capanni, C., Faulkner, G., & Lattanzi, G. (2019). Ankrd2 in Mechanotransduction and Oxidative Stress Response in Skeletal Muscle: New Cues for the Pathogenesis of Muscular Laminopathies. *Oxidative Medicine and Cellular Longevity*, *2019*. https://doi.org/10.1155/2019/7318796

Chae, J., Minami, N., Jin, Y., Nakagawa, M., Murayama, K., Igarashi, F., & Nonaka, I. (2001). Calpain 3 gene mutations: genetic and clinico-pathologic findings in limb-girdle muscular dystrophy. *Neuromuscular Disorders : NMD*, *11*(6–7), 547–555. https://doi.org/10.1016/S0960-8966(01)00197-3

Chal, J., al Tanoury, Z., Hestin, M., Gobert, B., Aivio, S., Hick, A., Cherrier, T., Nesmith, A. P., Parker, K. K., & Pourquié, O. (2016). Generation of human muscle fibers and satellite-like cells from human pluripotent stem cells in vitro. *Nature Protocols 2016 11:10*, *11*(10), 1833–1850. https://doi.org/10.1038/nprot.2016.110

Chal, J., Oginuma, M., al Tanoury, Z., Gobert, B., Sumara, O., Hick, A., Bousson, F., Zidouni, Y., Mursch, C., Moncuquet, P., Tassy, O., Vincent, S., Miyanari, A., Bera, A., Garnier, J. M., Guevara, G., Hestin, M., Kennedy, L., Hayashi, S., … Pourquie, O. (2015). Differentiation of pluripotent stem cells to muscle fiber to model Duchenne muscular dystrophy. *Nature Biotechnology*, *33*(9), 962–969. https://doi.org/10.1038/NBT.3297

Chan, S. S. K., Arpke, R. W., Filareto, A., Xie, N., Pappas, M. P., Penaloza, J. S., Perlingeiro, R. C. R., & Kyba, M. (2018). Skeletal Muscle Stem Cells from PSC-Derived Teratomas Have Functional Regenerative Capacity. *Cell Stem Cell*, *23*(1), 74-85.e6. https://doi.org/10.1016/j.stem.2018.06.010

Chang, N. C., & Rudnicki, M. A. (2014). Satellite cells: the architects of skeletal muscle. *Current Topics in Developmental Biology*, *107*, 161–181. https://doi.org/10.1016/B978-0-12-416022-4.00006-8

Chapman, J. R., Taylor, M. R. G., & Boulton, S. J. (2012). Playing the end game: DNA double-strand break repair pathway choice. *Molecular Cell*, *47*(4), 497–510. https://doi.org/10.1016/J.MOLCEL.2012.07.029

Chazaud, B., Brigitte, M., Yacoub-Youssef, H., Arnold, L., Gherardi, R., Sonnet, C., Lafuste, P., & Chretien, F. (2009). Dual and beneficial roles of macrophages during skeletal muscle regeneration. *Exercise and Sport Sciences Reviews*, *37*(1), 18–22. https://doi.org/10.1097/JES.0B013E318190EBDB

Chemello, F., Bean, C., Cancellara, P., Laveder, P., Reggiani, C., & Lanfranchi, G. (2011). Microgenomic Analysis in Skeletal Muscle: Expression Signatures of Individual Fast and Slow Myofibers. *PLOS ONE*, *6*(2), e16807. https://doi.org/10.1371/JOURNAL.PONE.0016807

Chen, J. F., Tao, Y., Li, J., Deng, Z., Yan, Z., Xiao, X., & Wang, D. Z. (2010). microRNA-1 and microRNA-206 regulate skeletal muscle satellite cell proliferation and differentiation by repressing Pax7. *The Journal of Cell Biology*, *190*(5), 867–879. https://doi.org/10.1083/JCB.200911036

Chen, P. R., Lee, |, Spate, D., Leffeler, E. C., Benne, J. A., Raissa, |, Cecil, F., Hord, T. K., & Prather, R. S. (2020). Removal of hypotaurine from porcine embryo culture medium does not impair development of in vitro-fertilized or somatic cell nuclear transfer-derived embryos at low oxygen tension. *Mol Reprod Dev*. https://doi.org/10.1002/mrd.23393

Chen, P. R., Redel, B. K., Kerns, K. C., Spate, L. D., & Prather, R. S. (2021). Challenges and Considerations during In Vitro Production of Porcine Embryos. *Cells 2021, Vol. 10, Page 2770*, *10*(10), 2770. https://doi.org/10.3390/CELLS10102770

Chen, P., Uh, K., Redel, B. K., Reese, E. D., Prather, R. S., & Lee, K. (2022). Production of Pigs From Porcine Embryos Generated in vitro. *Frontiers in Animal Science*, *0*, 15. https://doi.org/10.3389/FANIM.2022.826324

Chen, Y., Zheng, Y., Kang, Y., Yang, W., Niu, Y., Guo, X., Tu, Z., Si, C., Wang, H., Xing, R., Pu, X., Yang, S. H., Li, S., Ji, W., & Li, X. J. (2015). Functional disruption of the dystrophin gene in rhesus monkey using CRISPR/Cas9. *Human Molecular Genetics*, *24*(13), 3764–3774. https://doi.org/10.1093/HMG/DDV120

Chin, E. R. (2010). Intracellular Ca2+ signaling in skeletal muscle: decoding a complex message. *Exercise and Sport Sciences Reviews*, *38*(2), 76–85. https://doi.org/10.1097/JES.0B013E3181D495D2

Choi, I. Y., Lim, H. T., Estrellas, K., Mula, J., Cohen, T. v., Zhang, Y., Donnelly, C. J., Richard, J. P., Kim, Y. J., Kim, H., Kazuki, Y., Oshimura, M., Li, H. L., Hotta, A., Rothstein, J., Maragakis, N., Wagner, K. R., & Lee, G. (2016). Concordant but Varied Phenotypes among Duchenne Muscular Dystrophy Patient-Specific Myoblasts Derived using a Human iPSC-Based Model. *Cell Reports*, *15*(10), 2301–2312. https://doi.org/10.1016/J.CELREP.2016.05.016

Choi, J., Costa, M. L., Mermelstein, C. S., Chagas, C., Holtzer, S., & Holtzer, H. (1990). MyoD converts primary dermal fibroblasts, chondroblasts, smooth muscle, and retinal pigmented epithelial cells into striated mononucleated myoblasts and multinucleated myotubes. *Proceedings of the National Academy of Sciences of the United States of America*, *87*(20), 7988–7992. https://doi.org/10.1073/PNAS.87.20.7988

Choulika, A., Perrin, A., Dujon, B., & Ois Nicolas, J. (1995). Induction of homologous recombination in mammalian chromosomes by using the I-SceI system of Saccharomyces cerevisiae. *Molecular and Cellular Biology*, *15*(4), 1968. https://doi.org/10.1128/MCB.15.4.1968

Clarke, B. A., Drujan, D., Willis, M. S., Murphy, L. O., Corpina, R. A., Burova, E., Rakhilin, S. v., Stitt, T. N., Patterson, C., Latres, E., & Glass, D. J. (2007). The E3 Ligase MuRF1 degrades myosin heavy chain protein in dexamethasone-treated skeletal muscle. *Cell Metabolism*, *6*(5), 376–385. https://doi.org/10.1016/J.CMET.2007.09.009

Coffey, V. G., & Hawley, J. A. (2007). The molecular bases of training adaptation. *Sports Medicine (Auckland, N.Z.)*, *37*(9), 737–763. https://doi.org/10.2165/00007256-200737090-00001

Cohen, E., Bonne, G., Rivier, F., & Hamroun, D. (2021). The 2022 version of the gene table of neuromuscular disorders (nuclear genome). *Neuromuscular Disorders*, *31*, 1313–1357. https://doi.org/10.1016/j.nmd.2021.11.004

Cohen, N., Kudryashova, E., Kramerova, I., Anderson, L. V. B., Beckmann, J. S., Bushby, K., & Spencer, M. J. (2006). Identification of putative in vivo substrates of calpain 3 by comparative proteomics of overexpressing transgenic and nontransgenic mice. *Proteomics*, *6*(22), 6075–6084. https://doi.org/10.1002/PMIC.200600199

Cohen, S., Brault, J. J., Gygi, S. P., Glass, D. J., Valenzuela, D. M., Gartner, C., Latres, E., & Goldberg, A. L. (2009). During muscle atrophy, thick, but not thin, filament components are degraded by MuRF1-dependent ubiquitylation. *The Journal of Cell Biology*, *185*(6), 1083–1095. https://doi.org/10.1083/JCB.200901052

Conant, D., Hsiau, T., Rossi, N., Oki, J., Maures, T., Waite, K., Yang, J., Joshi, S., Kelso, R., Holden, K., Enzmann, B. L., & Stoner, R. (2022). Inference of CRISPR Edits from Sanger Trace Data. *The CRISPR Journal*, *5*(1), 123–130. https://doi.org/10.1089/CRISPR.2021.0113

Cone, S. G., Warren, P. B., & Fisher, M. B. (2017). Rise of the Pigs: Utilization of the Porcine Model to Study Musculoskeletal Biomechanics and Tissue Engineering During Skeletal Growth. *Tissue Engineering. Part C, Methods*, *23*(11), 763. https://doi.org/10.1089/TEN.TEC.2017.0227

Cong, L., Ran, F. A., Cox, D., Lin, S., Barretto, R., Habib, N., Hsu, P. D., Wu, X., Jiang, W., Marraffini, L. A., & Zhang, F. (2013). Multiplex genome engineering using CRISPR/Cas systems. *Science (New York, N.Y.)*, *339*(6121), 819–823. https://doi.org/10.1126/SCIENCE.1231143

Cooper, S. T., Kizana, E., Yates, J. D., Lo, H. P., Yang, N., Wu, Z. H., Alexander, I. E., & North, K. N. (2007). Dystrophinopathy carrier determination and detection of protein deficiencies in muscular dystrophy using lentiviral MyoD-forced myogenesis. *Neuromuscular Disorders : NMD*, *17*(4), 276–284. https://doi.org/10.1016/J.NMD.2006.12.010

Coy, P., Martínez, E., Ruiz, S., Vázquez, J. M., Roca, J., & Gadea, J. (1993). Environment and medium volume influence in vitro fertilisation of pig oocytes. *Zygote (Cambridge, England)*, *1*(3), 209–213. https://doi.org/10.1017/S0967199400001489

Cradick, T. J., Qiu, P., Lee, C. M., Fine, E. J., & Bao, G. (2014). COSMID: A Web-based Tool for Identifying and Validating CRISPR/Cas Off-target Sites. *Molecular Therapy. Nucleic Acids*, *3*(12), e214. https://doi.org/10.1038/MTNA.2014.64

Croall, D. E., & Ersfeld, K. (2007). The calpains: Modular designs and functional diversity. *Genome Biology*, *8*(6), 1–11. https://doi.org/10.1186/GB-2007-8-6-218/TABLES/2

Crociara, P., Chieppa, M. N., Vallino Costassa, E., Berrone, E., Gallo, M., lo Faro, M., Pintore, M. D., Iulini, B., D'Angelo, A., Perona, G., Botter, A., Formicola, D., Rainoldi, A., Paulis, M., Vezzoni, P., Meli, F., Peverali, F. A., Bendotti, C., Trolese, M. C., … Corona, C. (2019). Motor neuron degeneration, severe myopathy and TDP-43 increase in a transgenic pig model of SOD1-linked familiar ALS. *Neurobiology of Disease*, *124*, 263–275. https://doi.org/10.1016/J.NBD.2018.11.021

Cui, C., Han, S., Tang, S., He, H., Shen, X., Zhao, J., Chen, Y., Wei, Y., Wang, Y., Zhu, Q., Li, D., & Yin, H. (2020). The Autophagy Regulatory Molecule CSRP3 Interacts with LC3 and Protects Against Muscular Dystrophy. *International Journal of Molecular Sciences*, *21*(3). https://doi.org/10.3390/IJMS21030749

Cullot, G., Boutin, J., Toutain, J., Prat, F., Pennamen, P., Rooryck, C., Teichmann, M., Rousseau, E., Lamrissi-Garcia, I., Guyonnet-Duperat, V., Bibeyran, A., Lalanne, M., Prouzet-Mauléon, V., Turcq, B., Ged, C., Blouin, J. M., Richard, E., Dabernat, S., Moreau-Gaudry, F., & Bedel, A. (2019). CRISPR-Cas9 genome editing induces megabase-scale chromosomal truncations. *Nature Communications 2019 10:1*, *10*(1), 1–14. https://doi.org/10.1038/s41467-019-09006-2

Darabi, R., Arpke, R. W., Irion, S., Dimos, J. T., Grskovic, M., Kyba, M., & Perlingeiro, R. C. R. (2012). Human ES- and iPS-derived myogenic progenitors restore DYSTROPHIN and improve contractility upon transplantation in dystrophic mice. *Cell Stem Cell*, *10*(5), 610–619. https://doi.org/10.1016/j.stem.2012.02.015

Darabi, R., & Perlingeiro, R. C. R. (2016). Derivation of skeletal myogenic precursors from human pluripotent stem cells using conditional expression of PAX7. *Methods in Molecular Biology*, *1357*, 423–439. https://doi.org/10.1007/7651_2014_134

Darr, K. C., & Schultz, E. (1987). Exercise-induced satellite cell activation in growing and mature skeletal muscle. *Journal of Applied Physiology (Bethesda, Md.: 1985)*, *63*(5), 1816–1821. https://doi.org/10.1152/JAPPL.1987.63.5.1816

Dayanithi, G., Richard, I., Viero, C., Mazuc, E., Mallie, S., Valmier, J., Bourg, N., Herasse, M., Marty, I., Lefranc, G., Mangeat, P., & Baghdiguian, S. (2009). Alteration of Sarcoplasmic Reticulum Ca2+ Release in Skeletal Muscle from Calpain 3-Deficient Mice. *International Journal of Cell Biology*, *2009*, 1–12. https://doi.org/10.1155/2009/340346

de Haro, M., Al-Ramahi, I., de Gouyon, B., Ukani, L., Rosa, A., Faustino, N. A., Ashizawa, T., Cooper, T. A., & Botas, J. (2006). MBNL1 and CUGBP1 modify expanded CUG-induced toxicity in a Drosophila model of myotonic dystrophy type 1. *Human Molecular Genetics*, *15*(13), 2138–2145. https://doi.org/10.1093/HMG/DDL137

de Palma, S., Leone, R., Grumati, P., Vasso, M., Polishchuk, R., Capitanio, D., Braghetta, P., Bernardi, P., Bonaldo, P., & Gelfi, C. (2013). Changes in Muscle Cell Metabolism and Mechanotransduction Are Associated with Myopathic Phenotype in a Mouse Model of Collagen VI Deficiency. *PLoS ONE*, *8*(2). https://doi.org/10.1371/JOURNAL.PONE.0056716

Deegan, S., Saveljeva, S., Gorman, A. M., & Samali, A. (2013). Stress-induced self-cannibalism: on the regulation of autophagy by endoplasmic reticulum stress. *Cellular and Molecular Life Sciences : CMLS*, *70*(14), 2425–2441. https://doi.org/10.1007/S00018-012-1173-4

Delaporte, C., Dautreaux, B., Rouche, A., & Fardeau, M. (1990). Changes in surface morphology and basal lamina of cultured muscle cells from Duchenne muscular dystrophy patients. *Journal of the Neurological Sciences*, *95*(1), 77–88. https://doi.org/10.1016/0022-510X(90)90118-7

der Vartanian, A., Quétin, M., Michineau, S., Auradé, F., Hayashi, S., Dubois, C., Rocancourt, D., Drayton-Libotte, B., Szegedi, A., Buckingham, M., Conway, S. J., Gervais, M., & Relaix, F. (2019). PAX3 Confers Functional Heterogeneity in Skeletal Muscle Stem Cell Responses to Environmental Stress. *Cell Stem Cell*, *24*(6), 958-973.e9. https://doi.org/10.1016/J.STEM.2019.03.019

Deshmukh, R. S., Østrup, O., Østrup, E., Vejlsted, M., Niemann, H., Lucas-Hahn, A., Petersen, B., Li, J., Callesen, H., & Hyttel, P. (2011). DNA methylation in porcine preimplantation embryos developed in vivo and produced by in vitro fertilization, parthenogenetic activation and somatic cell nuclear transfer. *Epigenetics*, *6*(2), 177–187. https://doi.org/10.4161/EPI.6.2.13519

Diaz, B. G., Moldoveanu, T., Kuiper, M. J., Campbell, R. L., & Davies, P. L. (2004). Insertion sequence 1 of muscle-specific calpain, p94, acts as an internal propeptide. *The Journal of Biological Chemistry*, *279*(26), 27656–27666. https://doi.org/10.1074/JBC.M313290200

Dienes, J., Browne, S., Farjun, B., Amaral Passipieri, J., Mintz, E. L., Killian, G., Healy, K. E., & Christ, G. J. (2021). Semisynthetic Hyaluronic Acid-Based Hydrogel Promotes Recovery of the Injured Tibialis Anterior Skeletal Muscle Form and Function. *ACS Biomaterials Science and Engineering*, *7*(4), 1587–1599. https://doi.org/10.1021/ACSBIOMATERIALS.0C01751/ASSET/IMAGES/MEDIUM/AB0C01751_0012.GIF

DiFranco, M., Kramerova, I., Vergara, J. L., & Spencer, M. J. (2016). Attenuated Ca2+ release in a mouse model of limb girdle muscular dystrophy 2A. *Skeletal Muscle*, *6*(1), 1. https://doi.org/10.1186/s13395-016-0081-y

Doma, K., Singh, U., Boullosa, D., & Connor, J. D. (2021). The effect of branched-chain amino acid on muscle damage markers and performance following strenuous exercise: a systematic review and meta-analysis. *Applied Physiology, Nutrition, and Metabolism = Physiologie Appliquee, Nutrition et Metabolisme*, *46*(11), 1303–1313. https://doi.org/10.1139/APNM-2021-0110

Donnelly, K., Khodabukus, A., Philp, A., Deldicque, L., Dennis, R. G., & Baar, K. (2010). A novel bioreactor for stimulating skeletal muscle in vitro. *Tissue Engineering. Part C, Methods*, *16*(4), 711–718. https://doi.org/10.1089/TEN.TEC.2009.0125

Duan, D., Goemans, N., Takeda, S., Mercuri, E., & Aartsma-Rus, A. (2021). Duchenne muscular dystrophy. *Nature Reviews. Disease Primers*, *7*(1). https://doi.org/10.1038/S41572-021-00248-3

Dufaux, B., & Order, U. (1989). Complement activation after prolonged exercise. *Clinica Chimica Acta; International Journal of Clinical Chemistry*, *179*(1), 45–49. https://doi.org/10.1016/0009-8981(89)90021-1

Dumont, N. A., Bentzinger, C. F., Sincennes, M. C., & Rudnicki, M. A. (2015). Satellite Cells and Skeletal Muscle Regeneration. *Comprehensive Physiology*, *5*(3), 1027–1059. https://doi.org/10.1002/CPHY.C140068

Dumont, N. A., Wang, Y. X., von Maltzahn, J., Pasut, A., Bentzinger, C. F., Brun, C. E., & Rudnicki, M. A. (2015). Dystrophin expression in muscle stem cells regulates their polarity and asymmetric division. *Nature Medicine*, *21*(12), 1455–1463. https://doi.org/10.1038/NM.3990

Echigoya, Y., Trieu, N., Duddy, W., Moulton, H. M., Yin, H., Partridge, T. A., Hoffman, E. P., Kornegay, J. N., Rohret, F. A., Rogers, C. S., & Yokota, T. (2021). A Dystrophin Exon-52 Deleted Miniature Pig Model of Duchenne Muscular Dystrophy and Evaluation of Exon Skipping. *International Journal of Molecular Sciences*, *22*(23). https://doi.org/10.3390/IJMS222313065

Ecob-Prince, M. S., & Leberer, E. (1989). Parvalbumin in mouse muscle in vivo and in vitro. *Differentiation*, *40*(1), 10–16. https://doi.org/10.1111/J.1432-0436.1989.TB00808.X

Egan, B., Dowling, P., O'Connor, P. L., Henry, M., Meleady, P., Zierath, J. R., & O'Gorman, D. J. (2011). 2-D DIGE analysis of the mitochondrial proteome from human skeletal muscle reveals time course-dependent remodelling in response to 14 consecutive days of endurance exercise training. *Proteomics*, *11*(8), 1413–1428. https://doi.org/10.1002/PMIC.201000597

Egan, B., & Zierath, J. R. (2013). Exercise metabolism and the molecular regulation of skeletal muscle adaptation. *Cell Metabolism*, *17*(2), 162–184. https://doi.org/10.1016/J.CMET.2012.12.012

Egorova, T. v., Galkin, I. I., Ivanova, Y. v., & Polikarpova, A. v. (2021). Duchenne Muscular Dystrophy Animal Models. *Preclinical Animal Modeling in Medicine*. https://doi.org/10.5772/INTECHOPEN.96738

el Hajj, N., & Haaf, T. (2013). Epigenetic disturbances in in vitro cultured gametes and embryos: implications for human assisted reproduction. *Fertility and Sterility*, *99*(3), 632–641. https://doi.org/10.1016/J.FERTNSTERT.2012.12.044

El-Khoury, R., Traboulsi, S., Hamad, T., Lamaa, M., Sawaya, R., & Ahdab-Barmada, M. (2019). Divergent Features of Mitochondrial Deficiencies in LGMD2A Associated With Novel Calpain-3 Mutations. *Journal of Neuropathology and Experimental Neurology*, *78*(1), 88–98. https://doi.org/10.1093/JNEN/NLY113

Ellwood, R. A., Piasecki, M., & Szewczyk, N. J. (2021). Caenorhabditis elegans as a Model System for Duchenne Muscular Dystrophy. *International Journal of Molecular Sciences*, *22*(9). https://doi.org/10.3390/IJMS22094891

Emery, A. E. H. (2002). The muscular dystrophies. *Lancet (London, England)*, *359*(9307), 687–695. https://doi.org/10.1016/S0140-6736(02)07815-7

Engler, A. J., Griffin, M. A., Sen, S., Bönnemann, C. G., Sweeney, H. L., & Discher, D. E. (2004). Myotubes differentiate optimally on substrates with tissue-like stiffness: pathological implications for soft or stiff microenvironments. *The Journal of Cell Biology*, *166*(6), 877–887. https://doi.org/10.1083/JCB.200405004

Engler, A. J., Sen, S., Sweeney, H. L., & Discher, D. E. (2006). Matrix elasticity directs stem cell lineage specification. *Cell*, *126*(4), 677–689. https://doi.org/10.1016/J.CELL.2006.06.044

Estébanez, B., de Paz, J. A., Cuevas, M. J., & González-Gallego, J. (2018). Endoplasmic Reticulum Unfolded Protein Response, Aging and Exercise: An Update. *Frontiers in Physiology*, *9*. https://doi.org/10.3389/FPHYS.2018.01744

Evans, J. S., & Turner, M. D. (2007). Emerging functions of the calpain superfamily of cysteine proteases in neuroendocrine secretory pathways. *Journal of Neurochemistry*, *103*(3), 849–859. https://doi.org/10.1111/J.1471-4159.2007.04815.X

Evers-Van Gogh, I. J. A., Alex, S., Stienstra, R., Brenkman, A. B., Kersten, S., & Kalkhoven, E. (2015). Electric Pulse Stimulation of Myotubes as an In Vitro Exercise Model: Cell-Mediated and Non-Cell-Mediated Effects. *Scientific Reports 2015 5:1*, *5*(1), 1–11. https://doi.org/10.1038/srep10944

Fan, M., Rhee, J., St-Pierre, J., Handschin, C., Puigserver, P., Lin, J., Jäeger, S., Erdjument-Bromage, H., Tempst, P., & Spiegelman, B. M. (2004). Suppression of mitochondrial respiration through recruitment of p160 myb binding protein to PGC-1α: modulation by p38 MAPK. *Genes & Development*, *18*(3), 278. https://doi.org/10.1101/GAD.1152204

Fanin, M., & Angelini, C. (2015). Protein and genetic diagnosis of limb girdle muscular dystrophy type 2A: The yield and the pitfalls. *Muscle & Nerve*, *52*(2), 163–173. https://doi.org/10.1002/MUS.24682

Fanin, M., Nardetto, L., Nascimbeni, A. C., Tasca, E., Spinazzi, M., Padoan, R., & Angelini, C. (2007). Correlations between clinical severity, genotype and muscle pathology in limb girdle muscular dystrophy type 2A. *Journal of Medical Genetics*, *44*(10), 609–614. https://doi.org/10.1136/JMG.2007.050328

Fanin, M., Nascimbeni, A. C., & Angelini, C. (2007). Screening of calpain-3 autolytic activity in LGMD muscle: a functional map of CAPN3 gene mutations. *Journal of Medical Genetics*, *44*(1), 38–43. https://doi.org/10.1136/JMG.2006.044859

Fanin, M., Nascimbeni, A. C., & Angelini, C. (2013). Muscle atrophy in Limb Girdle Muscular Dystrophy 2A: A morphometric and molecular study. *Neuropathology and Applied Neurobiology*, *39*(7), 762–771. https://doi.org/10.1111/nan.12034

Fanin, M., Nascimbeni, A. C., Fulizio, L., Trevisan, C. pietro, Meznaric-Petrusa, M., & Angelini, C. (2003). Loss of calpain-3 autocatalytic activity in LGMD2A patients with normal protein expression. *The American Journal of Pathology*, *163*(5), 1929–1936. https://doi.org/10.1016/S0002-9440(10)63551-1

Fardeau, M., Eymard, B., Mignard, C., Tomé, F. M. S., Richard, I., & Beckmann, J. S. (1996). Chromosome 15-linked limb-girdle muscular dystrophy: clinical phenotypes in Reunion Island and French metropolitan communities. *Neuromuscular Disorders : NMD*, *6*(6), 447–453. https://doi.org/10.1016/S0960-8966(96)00387-2

Fardeau, M., Hillaire, D., Mignard, C., Feingold, N., Feingold, J., Mignard, D., de Ubeda, B., Collin, H., Tomé, F. M. S., Richard, I., & Beckmann, J. (1996). Juvenile limb-girdle muscular dystrophy. Clinical, histopathological and genetic data from a small community living in the Reunion Island. *Brain : A Journal of Neurology*, *119 (Pt 1)*(1), 295–308. https://doi.org/10.1093/BRAIN/119.1.295

Fareed, M. U., Evenson, A. R., Wei, W., Menconi, M., Poylin, V., Petkova, V., Pignol, B., & Hasselgren, P. O. (2006). Treatment of rats with calpain inhibitors prevents sepsis-induced muscle proteolysis independent of atrogin-1/MAFbx and MuRF1 expression. *American*

Journal of Physiology. Regulatory, Integrative and Comparative Physiology, *290*(6). https://doi.org/10.1152/AJPREGU.00668.2005

Feng, X., Adiarte, E. G., & Devoto, S. H. (2006). Hedgehog acts directly on the zebrafish dermomyotome to promote myogenic differentiation. *Developmental Biology*, *300*(2), 736–746. https://doi.org/10.1016/J.YDBIO.2006.08.056

Fernando, P., Kelly, J. F., Balazsi, K., Slack, R. S., & Megeney, L. A. (2002). Caspase 3 activity is required for skeletal muscle differentiation. *Proceedings of the National Academy of Sciences of the United States of America*, *99*(17), 11025–11030. https://doi.org/10.1073/PNAS.162172899

Fougerousse, F., Durand, M., Suel, L., Pourquié, O., Delezoide, A. L., Romero, N. B., Abitbol, M., & Beckmann, J. S. (1998). Expression of Genes (CAPN3, SGCA, SGCB, and TTN) Involved in Progressive Muscular Dystrophies during Early Human Development. *Genomics*, *48*(2), 145–156. https://doi.org/10.1006/GENO.1997.5160

Fougerousse, F., Gonin, P., Durand, M., Richard, I., & Raymackers, J. M. (2003). Force impairment in calpain 3-deficient mice is not correlated with mechanical disruption. *Muscle & Nerve*, *27*(5), 616–623. https://doi.org/10.1002/MUS.10368

Franco, S. J., & Huttenlocher, A. (2005). Regulating cell migration: calpains make the cut. *Journal of Cell Science*, *118*(Pt 17), 3829–3838. https://doi.org/10.1242/JCS.02562

Frenette, J., Cai, B., & Tidball, J. G. (2000). Complement activation promotes muscle inflammation during modified muscle use. *The American Journal of Pathology*, *156*(6), 2103–2110. https://doi.org/10.1016/S0002-9440(10)65081-X

Frontera, W. R., & Ochala, J. (2015). Skeletal muscle: a brief review of structure and function. *Calcified Tissue International*, *96*(3), 183–195. https://doi.org/10.1007/S00223-014-9915-Y

Fu, Y., Sander, J. D., Reyon, D., Cascio, V. M., & Joung, J. K. (2014). Improving CRISPR-Cas nuclease specificity using truncated guide RNAs. *Nature Biotechnology*, *32*(3), 279–284. https://doi.org/10.1038/NBT.2808

Fujita, H., Nedachi, T., & Kanzaki, M. (2007). Accelerated de novo sarcomere assembly by electric pulse stimulation in C2C12 myotubes. *Experimental Cell Research*, *313*(9), 1853–1865. https://doi.org/10.1016/J.YEXCR.2007.03.002

Fukada, S., Uezumi, A., Ikemoto, M., Masuda, S., Segawa, M., Tanimura, N., Yamamoto, H., Miyagoe-Suzuki, Y., & Takeda, S. (2007). Molecular signature of quiescent satellite cells in adult skeletal muscle. *Stem Cells (Dayton, Ohio)*, *25*(10), 2448–2459. https://doi.org/10.1634/STEMCELLS.2007-0019

Gaina, G., & Popa, A. (2021). Muscular dystrophy: Experimental animal models and therapeutic approaches (Review). *Experimental and Therapeutic Medicine*, *21*(6). https://doi.org/10.3892/ETM.2021.10042

Galli, F., Bragg, L., Meggiolaro, L., Rossi, M., Caffarini, M., Naz, N., Santoleri, S., & Cossu, G. (2018). Gene and Cell Therapy for Muscular Dystrophies: Are We Getting There? *Human Gene Therapy*, *29*(10), 1098. https://doi.org/10.1089/HUM.2018.151

García-Parra, P., Cavaliere, F., Maroto, M., Bilbao, L., Obieta, I., de Munain, A. L., Álava, J. I., & Izeta, A. (2012). Modeling neural differentiation on micropatterned substrates coated with neural matrix components. *Frontiers in Cellular Neuroscience*, *6*(MARCH). https://doi.org/10.3389/FNCEL.2012.00010

García-Parra, P., Maroto, M., Cavaliere, F., Naldaiz-Gastesi, N., Álava, J. I., García, A. G., López de Munain, A., & Izeta, A. (2013). A neural extracellular matrix-based method for in vitro hippocampal neuron culture and dopaminergic differentiation of neural stem cells. *BMC Neuroscience*, *14*. https://doi.org/10.1186/1471-2202-14-48

García-Parra, P., Naldaiz-Gastesi, N., Maroto, M., Padín, J. F., Goicoechea, M., Aiastui, A., Fernández-Morales, J. C., García-Belda, P., Lacalle, J., Álava, J. I., García-Verdugo, J. M., García, A. G., Izeta, A., & de Munain, A. L. (2014). Murine muscle engineered from dermal precursors: an in vitro model for skeletal muscle generation, degeneration, and fatty infiltration. *Tissue Engineering. Part C, Methods*, *20*(1), 28–41. https://doi.org/10.1089/TEN.TEC.2013.0146

García-Prat, L., Perdiguero, E., Alonso-Martín, S., Dell'Orso, S., Ravichandran, S., Brooks, S. R., Juan, A. H., Campanario, S., Jiang, K., Hong, X., Ortet, L., Ruiz-Bonilla, V., Flández, M., Moiseeva, V., Rebollo, E., Jardí, M., Sun, H. W., Musarò, A., Sandri, M., … Muñoz-Cánoves, P. (2020). FoxO maintains a genuine muscle stem-cell quiescent state until geriatric age. *Nature Cell Biology*, *22*(11), 1307–1318. https://doi.org/10.1038/S41556-020-00593-7

Gaudelli, N. M., Komor, A. C., Rees, H. A., Packer, M. S., Badran, A. H., Bryson, D. I., & Liu, D. R. (2017). Programmable base editing of A•T to G•C in genomic DNA without DNA cleavage. *Nature 2017 551:7681*, *551*(7681), 464–471. https://doi.org/10.1038/nature24644

Gavin, T. P., Ruster, R. S., Carrithers, J. A., Zwetsloot, K. A., Kraus, R. M., Evans, C. A., Knapp, D. J., Drew, J. L., McCartney, J. S., Garry, J. P., & Hickner, R. C. (2007). No difference in the skeletal muscle angiogenic response to aerobic exercise training between young and aged men. *The Journal of Physiology*, *585*(Pt 1), 231. https://doi.org/10.1113/JPHYSIOL.2007.143198

Gilbert, P. M., Havenstrite, K. L., Magnusson, K. E. G., Sacco, A., Leonardi, N. A., Kraft, P., Nguyen, N. K., Thrun, S., Lutolf, M. P., & Blau, H. M. (2010). Substrate elasticity regulates skeletal muscle stem cell self-renewal in culture. *Science (New York, N.Y.)*, *329*(5995), 1078–1081. https://doi.org/10.1126/SCIENCE.1191035

Goll, D. E., Neti, G., Mares, S. W., & Thompson, V. F. (2008). Myofibrillar protein turnover: the proteasome and the calpains. *Journal of Animal Science*, *86*(14 Suppl). https://doi.org/10.2527/JAS.2007-0395

Goll, D. E., Thompson, V. F., Li, H., Wei, W., & Cong, J. (2003). The calpain system. *Physiological Reviews*, *83*(3), 731–801. https://doi.org/10.1152/PHYSREV.00029.2002

Gomes, M. D., Lecker, S. H., Jagoe, R. T., Navon, A., & Goldberg, A. L. (2001). Atrogin-1, a muscle-specific F-box protein highly expressed during muscle atrophy. *Proceedings of the National Academy of Sciences of the United States of America*, *98*(25), 14440–14445. https://doi.org/10.1073/PNAS.251541198

Goñi-Balentziaga, O., Ortega-Saez, I., Vila, S., & Azkona, G. (2022). A survey on the use of mice, pigs, dogs and monkeys as animal models in biomedical research in Spain. *Laboratory Animal Research 2022 38:1*, *38*(1), 1–9. https://doi.org/10.1186/S42826-022-00124-5

González-Mera, L., Ravenscroft, G., Cabrera-Serrano, M., Ermolova, N., Domínguez-González, C., Arteche-López, A., Soltanzadeh, P., Evesson, F., Navas, C., Mavillard, F., Clayton, J., Rodrigo, P., Servián-Morilla, E., Cooper, S. T., Waddell, L., Reardon, K., Corbett, A., Hernandez-Laín, A., Sanchez, A., … Olivé, M. (2021). Heterozygous CAPN3 missense variants causing autosomal-dominant calpainopathy in seven unrelated families. *Neuropathology and Applied Neurobiology*, *47*(2), 283–296. https://doi.org/10.1111/NAN.12663

Grassl, E. D., Oegema, T. R., & Tranquillo, R. T. (2002). Fibrin as an alternative biopolymer to type-I collagen for the fabrication of a media equivalent. *Journal of Biomedical Materials Research*, *60*(4), 607–612. https://doi.org/10.1002/JBM.10107

Grefte, S., Vullinghs, S., Kuijpers-Jagtman, A. M., Torensma, R., & von Den Hoff, J. W. (2012). Matrigel, but not collagen I, maintains the differentiation capacity of muscle derived cells in vitro. *Biomedical Materials (Bristol, England)*, *7*(5). https://doi.org/10.1088/1748-6041/7/5/055004

Grumati, P., Coletto, L., Schiavinato, A., Castagnaro, S., Bertaggia, E., Sandri, M., & Bonaldo, P. (2011). Physical exercise stimulates autophagy in normal skeletal muscles but is detrimental for collagen VI-deficient muscles. *Autophagy*, *7*(12), 1415–1423. https://doi.org/10.4161/AUTO.7.12.17877

Gulati, P., & Thomas, G. (2007). Nutrient sensing in the mTOR/S6K1 signalling pathway. *Biochemical Society Transactions*, *35*(2), 236–238. https://doi.org/10.1042/BST0350236

Guroff, G. (1964). A Neutral, Calcium-activated Proteinase from the Soluble Fraction of Rat Brain. *Journal of Biological Chemistry*, *239*(1), 149–155. https://doi.org/10.1016/S0021-9258(18)51762-2

Gutierrez, K., Dicks, N., Glanzner, W. G., Agellon, L. B., & Bordignon, V. (2015). Efficacy of the porcine species in biomedical research. *Frontiers in Genetics*, *6*(SEP). https://doi.org/10.3389/fgene.2015.00293

Guyon, J. R., Kudryashova, E., Potts, A., Dalkilic, I., Brosius, M. A., Thompson, T. G., Beckmann, J. S., Kunkel, L. M., & Spencer, M. J. (2003). Calpain 3 cleaves filamin C and regulates its ability to interact with gamma- and delta-sarcoglycans. *Muscle & Nerve*, *28*(4), 472–483. https://doi.org/10.1002/MUS.10465

H. Dehkordi, M., Tashakor, A., O'Connell, E., & Fearnhead, H. O. (2020). Apoptosome-dependent myotube formation involves activation of caspase-3 in differentiating myoblasts. *Cell Death & Disease 2020 11:5*, *11*(5), 1–12. https://doi.org/10.1038/s41419-020-2502-4

Halievski, K., Xu, Y., Haddad, Y. W., Tang, Y. P., Yamada, S., Katsuno, M., Adachi, H., Sobue, G., Breedlove, S. M., & Jordan, C. L. (2020). Muscle BDNF improves synaptic and contractile

muscle strength in Kennedy's disease mice in a muscle-type specific manner. *The Journal of Physiology*, *598*, 2719–2739. https://doi.org/10.1113/JP279987

Han, D. S., Yang, W. S., & Kao, T. W. (2017). Dexamethasone Treatment at the Myoblast Stage Enhanced C2C12 Myocyte Differentiation. *International Journal of Medical Sciences*, *14*(5), 434–443. https://doi.org/10.7150/IJMS.18427

Hargreaves, M., & Spriet, L. L. (2020). Skeletal muscle energy metabolism during exercise. *Nature Metabolism 2020 2:9*, *2*(9), 817–828. https://doi.org/10.1038/s42255-020-0251-4

Hata, S., Doi, N., Shinkai-Ouchi, F., & Ono, Y. (2020). A muscle-specific calpain, CAPN3, forms a homotrimer. *Biochimica et Biophysica Acta. Proteins and Proteomics*, *1868*(7). https://doi.org/10.1016/J.BBAPAP.2020.140411

Hauerslev, S., Sveen, M. L., Duno, M., Angelini, C., Vissing, J., & Krag, T. O. (2012). Calpain 3 is important for muscle regeneration: Evidence from patients with limb girdle muscular dystrophies. *BMC Musculoskeletal Disorders*, *13*. https://doi.org/10.1186/1471-2474-13-43

He, R., Li, H., Wang, L., Li, Y., Zhang, Y., Chen, M., Zhu, Y., & Zhang, C. (2020). Engraftment of human induced pluripotent stem cell-derived myogenic progenitors restores dystrophin in mice with duchenne muscular dystrophy. *Biological Research*, *53*(1), 1–16. https://doi.org/10.1186/S40659-020-00288-1/FIGURES/6

He, Z. H., Bottinelli, R., Pellegrino, M. A., Ferenczi, M. A., & Reggiani, C. (2000). ATP consumption and efficiency of human single muscle fibers with different myosin isoform composition. *Biophysical Journal*, *79*(2), 945. https://doi.org/10.1016/S0006-3495(00)76349-1

Hendel, A., Bak, R. O., Clark, J. T., Kennedy, A. B., Ryan, D. E., Roy, S., Steinfeld, I., Lunstad, B. D., Kaiser, R. J., Wilkens, A. B., Bacchetta, R., Tsalenko, A., Dellinger, D., Bruhn, L., & Porteus, M. H. (2015). Chemically modified guide RNAs enhance CRISPR-Cas genome editing in human primary cells. *Nature Biotechnology 2015 33:9*, *33*(9), 985–989. https://doi.org/10.1038/nbt.3290

Henriksson, J. (1995). Muscle fuel selection: effect of exercise and training. *The Proceedings of the Nutrition Society*, *54*(1), 125–138. https://doi.org/10.1079/PNS19950042

Herasse, M., Ono, Y., Fougerousse, F., Kimura, E., Stockholm, D., Beley, C., Montarras, D., Pinset, C., Sorimachi, H., Suzuki, K., Beckmann, J. S., & Richard, I. (1999). Expression and Functional Characteristics of Calpain 3 Isoforms Generated through Tissue-Specific Transcriptional and Posttranscriptional Events. *Molecular and Cellular Biology*, *19*(6), 4047. https://doi.org/10.1128/MCB.19.6.4047

Hermanová, M., Zapletalová, E., Sedláčková, J., Chrobáková, T., Letocha, O., Kroupová, I., Zámečník, J., Vondráček, P., Mazanec, R., Maříková, T., Voháňka, S., & Fajkusová, L. (2006). Analysis of histopathologic and molecular pathologic findings in Czech LGMD2A patients. *Muscle & Nerve*, *33*(3), 424–432. https://doi.org/10.1002/MUS.20480

Hetz, C. (2012). The unfolded protein response: controlling cell fate decisions under ER stress and beyond. *Nature Reviews Molecular Cell Biology 2012 13:2*, *13*(2), 89–102. https://doi.org/10.1038/nrm3270

Hetz, C., Chevet, E., & Oakes, S. A. (2015). Proteostasis control by the unfolded protein response. *Nature Cell Biology*, *17*(7), 829–838. https://doi.org/10.1038/NCB3184

Hinds, S., Bian, W., Dennis, R. G., & Bursac, N. (2011). The role of extracellular matrix composition in structure and function of bioengineered skeletal muscle. *Biomaterials*, *32*(14), 3575–3583. https://doi.org/10.1016/J.BIOMATERIALS.2011.01.062

Hirata, M., Tanihara, F., Wittayarat, M., Hirano, T., Nguyen, N. T., Le, Q. A., Namula, Z., Nii, M., & Otoi, T. (2019). Genome mutation after introduction of the gene editing by electroporation of Cas9 protein (GEEP) system in matured oocytes and putative zygotes. *In Vitro Cellular and Developmental Biology - Animal*, *55*(4), 237–242. https://doi.org/10.1007/S11626-019-00338-3/FIGURES/2

Hjartarson, H. T., Nathorst-Böös, K., & Sejersen, T. (2022). Disease Modifying Therapies for the Management of Children with Spinal Muscular Atrophy (5q SMA): An Update on the Emerging Evidence. *Drug Design, Development and Therapy*, *16*, 1865–1883. https://doi.org/10.2147/DDDT.S214174

Hollinger, K., Yang, C. X., Montz, R. E., Nonneman, D., Ross, J. W., & Selsby, J. T. (2014). Dystrophin insufficiency causes selective muscle histopathology and loss of dystrophin-glycoprotein complex assembly in pig skeletal muscle. *FASEB Journal*, *28*(4), 1600–1609. https://doi.org/10.1096/fj.13-241141

Home - ClinicalTrials.gov. (n.d.). Retrieved June 19, 2022, from https://www.clinicaltrials.gov/ct2/home

Hosoyama, T., McGivern, J. v., van Dyke, J. M., Ebert, A. D., & Suzuki, M. (2014). Derivation of myogenic progenitors directly from human pluripotent stem cells using a sphere-based culture. *Stem Cells Translational Medicine*, *3*(5), 564–574. https://doi.org/10.5966/SCTM.2013-0143

Hryhorowicz, M., Lipiński, D., Hryhorowicz, S., Nowak-Terpiłowska, A., Ryczek, N., & Zeyland, J. (2020). Application of Genetically Engineered Pigs in Biomedical Research. *Genes*, *11*(6), 1–22. https://doi.org/10.3390/GENES11060670

Hsu, P. D., Scott, D. A., Weinstein, J. A., Ran, F. A., Konermann, S., Agarwala, V., Li, Y., Fine, E. J., Wu, X., Shalem, O., Cradick, T. J., Marraffini, L. A., Bao, G., & Zhang, F. (2013). DNA targeting specificity of RNA-guided Cas9 nucleases. *Nature Biotechnology 2013 31:9*, *31*(9), 827–832. https://doi.org/10.1038/nbt.2647

Huang, J., & Forsberg, N. E. (1998). Role of calpain in skeletal-muscle protein degradation. *Proceedings of the National Academy of Sciences of the United States of America*, *95*(21), 12100–12105. https://doi.org/10.1073/PNAS.95.21.12100

Huang, Y. C., Dennis, R. G., & Baar, K. (2006). Cultured slow vs. fast skeletal muscle cells differ in physiology and responsiveness to stimulation. *American Journal of Physiology. Cell Physiology*, *291*(1). https://doi.org/10.1152/AJPCELL.00366.2005

Hunt, L. C., Gorman, C., Kintakas, C., McCulloch, D. R., Mackie, E. J., & White, J. D. (2013). Hyaluronan synthesis and myogenesis: a requirement for hyaluronan synthesis during myogenic differentiation independent of pericellular matrix formation. *The Journal of Biological Chemistry*, *288*(18), 13006–13021. https://doi.org/10.1074/JBC.M113.453209

Iberite, F., Gruppioni, E., & Ricotti, L. (2022). Skeletal muscle differentiation of human iPSCs meets bioengineering strategies: perspectives and challenges. In *npj Regenerative Medicine* (Vol. 7, Issue 1). Nature Research. https://doi.org/10.1038/s41536-022-00216-9

Incitti, T., Magli, A., Darabi, R., Yuan, C., Lin, K., Arpke, R. W., Azzag, K., Yamamoto, A., Stewart, R., Thomson, J. A., Kyba, M., & Perlingeiro, R. C. R. (2019). Pluripotent stem cell-derived myogenic progenitors remodel their molecular signature upon in vivo engraftment. *Proceedings of the National Academy of Sciences of the United States of America*, *116*(10), 4346–4351. https://doi.org/10.1073/pnas.1808303116

Isaacs, W. B., Kim, I. S., Struve, A., & Fulton, A. B. (1989). Biosynthesis of titin in cultured skeletal muscle cells. *The Journal of Cell Biology*, *109*(5), 2189–2195. https://doi.org/10.1083/JCB.109.5.2189

Iyer, V., Shen, B., Zhang, W., Hodgkins, A., Keane, T., Huang, X., & Skarnes, W. C. (2015). Off-target mutations are rare in Cas9-modified mice. *Nature Methods*, *12*(6), 479. https://doi.org/10.1038/NMETH.3408

Jäer, S., Handschin, C., St-Pierre, J., & Spiegelman, B. M. (2007). AMP-activated protein kinase (AMPK) action in skeletal muscle via direct phosphorylation of PGC-1alpha. *Proceedings of the National Academy of Sciences of the United States of America*, *104*(29), 12017–12022. https://doi.org/10.1073/PNAS.0705070104

Jagannathan, S., de Greef, J. C., Hayward, L. J., Yokomori, K., Gabellini, D., Mul, K., Sacconi, S., Arjomand, J., Kinoshita, J., & Harper, S. Q. (2022). Meeting report: the 2021 FSHD International Research Congress. *Skeletal Muscle*, *12*(1). https://doi.org/10.1186/S13395-022-00287-8

Jahnke, V. E., Peterson, J. M., Meulen, J. H. van der, Boehler, J., Uaesoontrachoon, K., Johnston, H. K., Defour, A., Phadke, A., Yu, Q., Jaiswal, J. K., & Nagaraju, K. (2020). Mitochondrial dysfunction and consequences in calpain-3-deficient muscle. *Skeletal Muscle*, *10*(1). https://doi.org/10.1186/s13395-020-00254-1

Jaka, O., Casas-Fraile, L., Azpitarte, M., Aiastui, A., López de Munain, A., & Sáenz, A. (2017). FRZB and melusin, overexpressed in LGMD2A, regulate integrin β1D isoform replacement altering myoblast fusion and the integrin-signalling pathway. *Expert Reviews in Molecular Medicine*, *19*. https://doi.org/10.1017/ERM.2017.3

Jaka, O., Casas-Fraile, L., López De Munain, A., & Sáenz, A. (2015). Costamere proteins and their involvement in myopathic processes. In *Expert Reviews in Molecular Medicine* (Vol. 17). Cambridge University Press. https://doi.org/10.1017/erm.2015.9

Jánossy, J., Ubezio, P., Apáti, Á., Magócsi, M., Tompa, P., & Friedrich, P. (2004). Calpain as a multi-site regulator of cell cycle. *Biochemical Pharmacology*, *67*(8), 1513–1521. https://doi.org/10.1016/J.BCP.2003.12.021

Jasin, M., & Haber, J. E. (2016). The democratization of gene editing: Insights from site-specific cleavage and double-strand break repair. *DNA Repair*, *44*, 6–16. https://doi.org/10.1016/J.DNAREP.2016.05.001

Jinek, M., Chylinski, K., Fonfara, I., Hauer, M., Doudna, J. A., & Charpentier, E. (2012). A programmable dual RNA-guided DNA endonuclease in adaptive bacterial immunity. *Science (New York, N.Y.)*, *337*(6096), 816. https://doi.org/10.1126/SCIENCE.1225829

Jones, T. I., Parilla, M., & Jones, P. L. (2016). Transgenic Drosophila for Investigating DUX4 and FRG1, Two Genes Associated with Facioscapulohumeral Muscular Dystrophy (FSHD). *PloS One*, *11*(3). https://doi.org/10.1371/JOURNAL.PONE.0150938

Joyce, N. C., Oskarsson, B., & Jin, L. W. (2012). Muscle Biopsy Evaluation in Neuromuscular Disorders. *Physical Medicine and Rehabilitation Clinics of North America*, *23*(3), 609. https://doi.org/10.1016/J.PMR.2012.06.006

Judson, R. N., & Rossi, F. M. V. (2020). Towards stem cell therapies for skeletal muscle repair. *Npj Regenerative Medicine 2020 5:1*, *5*(1), 1–6. https://doi.org/10.1038/s41536-020-0094-3

Kahn, B. B., Alquier, T., Carling, D., & Hardie, D. G. (2005). AMP-activated protein kinase: ancient energy gauge provides clues to modern understanding of metabolism. *Cell Metabolism*, *1*(1), 15–25. https://doi.org/10.1016/J.CMET.2004.12.003

Kang, Y., Chu, C., Wang, F., & Niu, Y. (2019). CRISPR/Cas9-mediated genome editing in nonhuman primates. *Disease Models & Mechanisms*, *12*(10). https://doi.org/10.1242/DMM.039982

Karatzaferi, C., de Haan, A., Ferguson, R. A., van Mechelen, W., & Sargeant, A. J. (2001). Phosphocreatine and ATP content in human single muscle fibres before and after maximum dynamic exercise. *Pflugers Archiv : European Journal of Physiology*, *442*(3), 467–474. https://doi.org/10.1007/S004240100552

Kawabata, Y., Hata, S., Ono, Y., Ito, Y., Suzuki, K., Abe, K., & Sorimachi, H. (2003). Newly identified exons encoding novel variants of p94/calpain 3 are expressed ubiquitously and overlap the alpha-glucosidase C gene. *FEBS Letters*, *555*(3), 623–630. https://doi.org/10.1016/S0014-5793(03)01324-3

Khemtong, C., Kuo, C. H., Chen, C. Y., Jaime, S. J., & Condello, G. (2021). Does Branched-Chain Amino Acids (BCAAs) Supplementation Attenuate Muscle Damage Markers and Soreness after Resistance Exercise in Trained Males? A Meta-Analysis of Randomized Controlled Trials. *Nutrients*, *13*(6). https://doi.org/10.3390/NU13061880

Khodabukus, A. (2021). Tissue-Engineered Skeletal Muscle Models to Study Muscle Function, Plasticity, and Disease. *Frontiers in Physiology*, *12*, 115. https://doi.org/10.3389/FPHYS.2021.619710/BIBTEX

Khodabukus, A., & Baar, K. (2012). Defined electrical stimulation emphasizing excitability for the development and testing of engineered skeletal muscle. *Tissue Engineering. Part C, Methods*, *18*(5), 349–357. https://doi.org/10.1089/TEN.TEC.2011.0364

Khodabukus, A., Baehr, L. M., Bodine, S. C., & Baar, K. (2015). Role of contraction duration in inducing fast-to-slow contractile and metabolic protein and functional changes in engineered muscle. *Journal of Cellular Physiology*, *230*(10), 2489–2497. https://doi.org/10.1002/JCP.24985

Khodabukus, A., Prabhu, N., Wang, J., & Bursac, N. (2018). In Vitro Tissue-Engineered Skeletal Muscle Models for Studying Muscle Physiology and Disease. *Advanced Healthcare Materials*, *7*(15). https://doi.org/10.1002/ADHM.201701498

Khonsary, S. A. (2017). Guyton and Hall: Textbook of Medical Physiology. *Surgical Neurology International*, *8*(1), 275. https://doi.org/10.4103/SNI.SNI_327_17

Kim, D., Bae, S., Park, J., Kim, E., Kim, S., Yu, H. R., Hwang, J., Kim, J. il, & Kim, J. S. (2015). Digenome-seq: genome-wide profiling of CRISPR-Cas9 off-target effects in human cells. *Nature Methods*, *12*(3), 237–243. https://doi.org/10.1038/NMETH.3284

Kinbara, K., Ishiura, H., Tomioka, S., Sorimachi, H., Jeong, S. Y., Amano, S., Kawasaki, H., Kolmerer, B., Kimura, S., Labeit, S., & Suzuki, K. (1998). Purification of native p94, a muscle-specific calpain, and characterization of its autolysis. *The Biochemical Journal*, *335 (Pt 3)*(Pt 3), 589–596. https://doi.org/10.1042/BJ3350589

Kitajima, Y., & Suzuki, N. (2017). Role of the ubiquitin-proteasome pathway in skeletal muscle. In *The Plasticity of Skeletal Muscle: From Molecular Mechanism to Clinical Applications* (pp. 37–54). Springer Singapore. https://doi.org/10.1007/978-981-10-3292-9_2

Klymiuk, N., Blutke, A., Graf, A., Krause, S., Burkhardt, K., Wuensch, A., Krebs, S., Kessler, B., Zakhartchenko, V., Kurome, M., Kemter, E., Nagashima, H., Schoser, B., Herbach, N., Blum, H., Wanke, R. diger, Aartsma-Rus, A., Thirion, C., Lochmü ller, H., … Wolf, E. (2013). Dystrophin-deficient pigs provide new insights into the hierarchy of physiological derangements of dystrophic muscle. *Human Molecular Genetics*, *22*(21), 4368–4382. https://doi.org/10.1093/hmg/ddt287

Klymiuk, N., Seeliger, F., Bohlooly-Y, M., Blutke, A., Rudmann, D. G., & Wolf, E. (2016). Tailored Pig Models for Preclinical Efficacy and Safety Testing of Targeted Therapies. In *Toxicologic Pathology* (Vol. 44, Issue 3, pp. 346–357). SAGE Publications Inc. https://doi.org/10.1177/0192623315609688

Kodaka, Y., Rabu, G., & Asakura, A. (2017). Skeletal Muscle Cell Induction from Pluripotent Stem Cells. *Stem Cells International*, *2017*. https://doi.org/10.1155/2017/1376151

Kolb, P. S., Ayaub, E. A., Zhou, W., Yum, V., Dickhout, J. G., & Ask, K. (2015). The therapeutic effects of 4-phenylbutyric acid in maintaining proteostasis. *The International Journal of Biochemistry & Cell Biology*, *61*, 45–52. https://doi.org/10.1016/J.BIOCEL.2015.01.015

Kornegay, J. N., Spurney, C. F., Nghiem, P. P., Brinkmeyer-Langford, C. L., Hoffman, E. P., & Nagaraju, K. (2014). Pharmacologic Management of Duchenne Muscular Dystrophy: Target Identification and Preclinical Trials. *ILAR Journal*, *55*(1), 119. https://doi.org/10.1093/ILAR/ILU011

Kosicki, M., Tomberg, K., & Bradley, A. (2018). Repair of double-strand breaks induced by CRISPR-Cas9 leads to large deletions and complex rearrangements. *Nature Biotechnology*, *36*(8), 765–771. https://doi.org/10.1038/NBT.4192

Kötter, S., Unger, A., Hamdani, N., Lang, P., Vorgerd, M., Nagel-Steger, L., & Linke, W. A. (2014). Human myocytes are protected from titin aggregation-induced stiffening by small heat shock proteins. *The Journal of Cell Biology*, *204*(2), 187. https://doi.org/10.1083/JCB.201306077

Krahn, M., Goicoechea, M., Hanisch, F., Groen, E., Bartoli, M., Pécheux, C., Garcia-Bragado, F., Leturcq, F., Jeannet, P. Y., Lobrinus, J. A., Jacquemont, S., Strober, J., Urtizberea, J. A., Saenz, A., Bushby, K., Lévy, N., & Lopez de Munain, A. (2011). Eosinophilic infiltration related to CAPN3 mutations: a pathophysiological component of primary calpainopathy? *Clinical Genetics*, *80*(4), 398–402. https://doi.org/10.1111/J.1399-0004.2010.01620.X

Krahn, M., Lopez De Munain, A., Streichenberger, N., Bernard, R., Pécheux, C., Testard, H., Pena-Segura, J. L., Yoldi, E., Cabello, A., Romero, N. B., Poza, J. J., Bouillot-Eimer, S., Ferrer, X., Goicoechea, M., Garcia-Bragado, F., Leturcq, F., Urtizberea, J. A., & Lévy, N. (2006). CAPN3 mutations in patients with idiopathic eosinophilic myositis. *Annals of Neurology*, *59*(6), 905–911. https://doi.org/10.1002/ANA.20833

Krajacic, P., Hermanowski, J., Lozynska, O., Khurana, T. S., & Lamitina, T. (2009). C. elegans dysferlin homolog fer-1 is expressed in muscle, and fer-1 mutations initiate altered gene expression of muscle enriched genes. *Physiological Genomics*, *40*(1), 8–14. https://doi.org/10.1152/PHYSIOLGENOMICS.00106.2009

Kramerova, I., Beckmann, J. S., & Spencer, M. J. (2007). Molecular and cellular basis of calpainopathy (limb girdle muscular dystrophy type 2A). *Biochimica et Biophysica Acta*, *1772*(2), 128–144. https://doi.org/10.1016/J.BBADIS.2006.07.002

Kramerova, I., Ermolova, N., Eskin, A., Hevener, A., Quehenberger, O., Armando, A. M., Haller, R., Romain, N., Nelson, S. F., & Spencer, M. J. (2016). Failure to up-regulate transcription of genes necessary for muscle adaptation underlies limb girdle muscular dystrophy 2A (calpainopathy). *Human Molecular Genetics*, *25*(11), 2194–2207. https://doi.org/10.1093/hmg/ddw086

Kramerova, I., Kudryashova, E., Ermolova, N., Saenz, A., Jaka, O., López de munain, A., & Spencer, M. J. (2012). Impaired calcium calmodulin kinase signaling and muscle adaptation response in the absence of calpain 3. *Human Molecular Genetics*, *21*(14), 3193–3204. https://doi.org/10.1093/HMG/DDS144

Kramerova, I., Kudryashova, E., Tidball, J. G., & Spencer, M. J. (2004). Null mutation of calpain 3 (p94) in mice causes abnormal sarcomere formation in vivo and in vitro. *Human Molecular Genetics*, *13*(13), 1373–1388. https://doi.org/10.1093/HMG/DDH153

Kramerova, I., Kudryashova, E., Venkatraman, G., & Spencer, M. J. (2005). Calpain 3 participates in sarcomere remodeling by acting upstream of the ubiquitin - Proteasome pathway. *Human Molecular Genetics*, *14*(15), 2125–2134. https://doi.org/10.1093/hmg/ddi217

Kramerova, I., Kudryashova, E., Wu, B., Germain, S., Vandenborne, K., Romain, N., Haller, R. G., Verity, M. A., & Spencer, M. J. (2009). Mitochondrial abnormalities, energy deficit and oxidative stress are features of calpain 3 deficiency in skeletal muscle. *Human Molecular Genetics*, *18*(17), 3194–3205. https://doi.org/10.1093/hmg/ddp257

Kramerova, I., Kudryashova, E., Wu, B., Ottenheijm, C., Granzier, H., & Spencer, M. J. (2008). Novel role of calpain-3 in the triad-associated protein complex regulating calcium release in skeletal muscle. *Human Molecular Genetics*, *17*(21), 3271. https://doi.org/10.1093/HMG/DDN223

Kramerova, I., Kudryashova, E., Wu, B., & Spencer, M. J. (2006). Regulation of the M-Cadherin-ß-Catenin Complex by Calpain 3 during Terminal Stages of Myogenic Differentiation. *Molecular and Cellular Biology*, *26*(22), 8437. https://doi.org/10.1128/MCB.01296-06

Kramerova, I., Marinov, M., Owens, J., Lee, S. J., Becerra, D., & Spencer, M. J. (2020). Myostatin inhibition promotes fast fibre hypertrophy but causes loss of AMP-activated protein kinase signalling and poor exercise tolerance in a model of limb-girdle muscular dystrophy R1/2A. *The Journal of Physiology*, *598*(18), 3927–3939. https://doi.org/10.1113/JP279943

Kramerova, I., Torres, J. A., Eskin, A., Nelson, S. F., & Spencer, M. J. (2018). Calpain 3 and CaMKIIß signaling are required to induce HSP70 necessary for adaptive muscle growth after atrophy. *Human Molecular Genetics*, *27*(9), 1642–1653. https://doi.org/10.1093/hmg/ddy071

Kuang, S., Kuroda, K., le Grand, F., & Rudnicki, M. A. (2007). Asymmetric self-renewal and commitment of satellite stem cells in muscle. *Cell*, *129*(5), 999–1010. https://doi.org/10.1016/J.CELL.2007.03.044

Kucherenko, M. M., Pantoja, M., Yatsenko, A. S., Shcherbata, H. R., Fischer, K. A., Maksymiv, D. v., Chernyk, Y. I., & Ruohola-Baker, H. (2008). Genetic Modifier Screens Reveal New Components that Interact with the Drosophila Dystroglycan-Dystrophin Complex. *PLOS ONE*, *3*(6), e2418. https://doi.org/10.1371/JOURNAL.PONE.0002418

Kumamoto, T., Kleese, W. C., Cong, J., Goll, D. E., Pierce, P. R., & Allen, R. E. (1992). Localization of the Ca2+-dependent proteinases and their inhibitor in normal, fasted, and denervated rat skeletal muscle. *Anatomical Record*, *232*(1), 60–77. https://doi.org/10.1002/AR.1092320108

Lagirand-Cantaloube, J., Offner, N., Csibi, A., Leibovitch, M. P., Batonnet-Pichon, S., Tintignac, L. A., Segura, C. T., & Leibovitch, S. A. (2008). The initiation factor eIF3-f is a major target for atrogin1/MAFbx function in skeletal muscle atrophy. *The EMBO Journal*, *27*(8), 1266–1276. https://doi.org/10.1038/EMBOJ.2008.52

Lai, L., & Prather, R. S. (2004). Production of Cloned Pigs by Using Somatic Cells as Donors. *Https://Home.Liebertpub.Com/Clo*, *5*(4), 233–241. https://doi.org/10.1089/153623003772032754

Lamas-Toranzo, I., Galiano-Cogolludo, B., Cornudella-Ardiaca, F., Cobos-Figueroa, J., Ousinde, O., & Bermejo-Álvarez, P. (2019). Strategies to reduce genetic mosaicism following CRISPR-mediated genome edition in bovine embryos. *Scientific Reports*, *9*(1). https://doi.org/10.1038/S41598-019-51366-8

Larcher, T., Lafoux, A., Tesson, L., Remy, S. V., Thepenier, V., François, V., Guiner, C. le, Goubin, H., Dutilleul, M. V., Guigand, L., Toumaniantz, G., de Cian, A., Boix, C., Renaud, J. B., Cherel, Y., Giovannangeli, C., Concordet, J. P., Anegon, I., & Huchet, C. (2014). Characterization of dystrophin deficient rats: a new model for Duchenne muscular dystrophy. *PloS One*, *9*(10). https://doi.org/10.1371/JOURNAL.PONE.0110371

Lars Larsson, X., Degens, H., Li, M., Salviati, L., il Lee, Y., Thompson, W., Kirkland, J. L., Sandri, M., & Kogod, A. (2019). SARCOPENIA: AGING-RELATED LOSS OF MUSCLE MASS AND FUNCTION. *Physiol Rev*, *99*, 427–511. https://doi.org/10.1152/physrev.00061

Lasa-Elgarresta, J., Mosqueira-Martín, L., González-Imaz, K., Marco-Moreno, P., Gerenu, G., Mamchaoui, K., Mouly, V., López de Munain, A., & Vallejo-Illarramendi, A. (2022). Targeting the Ubiquitin-Proteasome System in Limb-Girdle Muscular Dystrophy With CAPN3 Mutations. *Frontiers in Cell and Developmental Biology*, *10*. https://doi.org/10.3389/FCELL.2022.822563

Lasa-Elgarresta, J., Mosqueira-Martín, L., Naldaiz-Gastesi, N., Sáenz, A., de Munain, A. L., & Vallejo-Illarramendi, A. (2019). Calcium Mechanisms in Limb-Girdle Muscular Dystrophy

with CAPN3 Mutations. In *International Journal of Molecular Sciences* (Vol. 20, Issue 18). MDPI AG. https://doi.org/10.3390/ijms20184548

Laurent, R. (2010). DISORDERS OF SKELETAL MUSCLE. *The Musculoskeletal System: Systems of the Body Series*, 109–122. https://doi.org/10.1016/B978-0-7020-3377-3.00008-1

le Grand, F., Jones, A. E., Seale, V., Scimè, A., & Rudnicki, M. A. (2009). Wnt7a activates the planar cell polarity pathway to drive the symmetric expansion of satellite stem cells. *Cell Stem Cell*, *4*(6), 535–547. https://doi.org/10.1016/J.STEM.2009.03.013

le Grand, F., & Rudnicki, M. A. (2007). Skeletal muscle satellite cells and adult myogenesis. *Current Opinion in Cell Biology*, *19*(6), 628–633. https://doi.org/10.1016/J.CEB.2007.09.012

Le, Q. A., Tanihara, F., Wittayarat, M., Namula, Z., Sato, Y., Lin, Q., Takebayashi, K., Hirata, M., & Otoi, T. (2021). Comparison of the effects of introducing the CRISPR/Cas9 system by microinjection and electroporation into porcine embryos at different stages. *BMC Research Notes*, *14*(1), 1–7. https://doi.org/10.1186/S13104-020-05412-8/FIGURES/2

Lecker, S. H., Jagoe, R. T., Gilbert, A., Gomes, M., Baracos, V., Bailey, J., Price, S. R., Mitch, W. E., & Goldberg, A. L. (2004). Multiple types of skeletal muscle atrophy involve a common program of changes in gene expression. *FASEB Journal : Official Publication of the Federation of American Societies for Experimental Biology*, *18*(1), 39–51. https://doi.org/10.1096/FJ.03-0610COM

Lee, C. S., Hanna, A. D., Wang, H., Dagnino-Acosta, A., Joshi, A. D., Knoblauch, M., Xia, Y., Georgiou, D. K., Xu, J., Long, C., Amano, H., Reynolds, C., Dong, K., Martin, J. C., Lagor, W. R., Rodney, G. G., Sahin, E., Sewry, C., & Hamilton, S. L. (2017). A chemical chaperone improves muscle function in mice with a RyR1 mutation. *Nature Communications*, *8*. https://doi.org/10.1038/ncomms14659

Lee, J. H., Yu, S., Nam, T. W., Roh, J. il, Jin, Y., Han, J. P., Cha, J. Y., Kim, Y. K., Yeom, S. C., Nam, K. T., & Lee, H. W. (2020). The position of the target site for engineered nucleases improves the aberrant mRNA clearance in in vivo genome editing. *Scientific Reports 2020 10:1*, *10*(1), 1–9. https://doi.org/10.1038/s41598-020-61154-4

Lee, P. H. U., & Vandenburgh, H. H. (2013). Skeletal muscle atrophy in bioengineered skeletal muscle: a new model system. *Tissue Engineering. Part A*, *19*(19–20), 2147–2155. https://doi.org/10.1089/TEN.TEA.2012.0597

Legge, M. (1995). Oocyte and zygote zona pellucida permeability to macromolecules. *Journal of Experimental Zoology*, *271*(2), 145–150. https://doi.org/10.1002/JEZ.1402710210

Li, G., Jia, Q., Zhao, J., Li, X., Yu, M., Samuel, M. S., Zhao, S., Prather, R. S., & Li, C. (2014). Dysregulation of genome-wide gene expression and DNA methylation in abnormal cloned piglets. *BMC Genomics*, *15*(1). https://doi.org/10.1186/1471-2164-15-811

Li, M., Hromowyk, K. J., Amacher, S. L., & Currie, P. D. (2017). Muscular dystrophy modeling in zebrafish. *Methods in Cell Biology*, *138*, 347–380. https://doi.org/10.1016/BS.MCB.2016.11.004

Li, M., Tang, X., You, W., Wang, Y., Chen, Y., Liu, Y., Yuan, H., Gao, C., Chen, X., Xiao, Z., Ouyang, H., & Pang, D. (2021). HMEJ-mediated site-specific integration of a myostatin inhibitor increases skeletal muscle mass in porcine. *Molecular Therapy. Nucleic Acids*, *26*, 49–62. https://doi.org/10.1016/J.OMTN.2021.06.011

Lin, J. W., Huang, Y. M., Chen, Y. Q., Chuang, T. Y., Lan, T. Y., Liu, Y. W., Pan, H. W., You, L. R., Wang, Y. K., Lin, K. hui, Chiou, A., & Kuo, J. C. (2021). Dexamethasone accelerates muscle regeneration by modulating kinesin-1-mediated focal adhesion signals. *Cell Death Discovery 2021 7:1*, *7*(1), 1–16. https://doi.org/10.1038/s41420-021-00412-4

Liu, G., Lin, Q., Jin, S., & Gao, C. (2022). The CRISPR-Cas toolbox and gene editing technologies. *Molecular Cell*, *82*(2), 333–347. https://doi.org/10.1016/J.MOLCEL.2021.12.002

Liu, J., Campagna, J., John, V., Damoiseaux, R., Mokhonova, E., Becerra, D., Meng, H., McNally, E. M., Pyle, A. D., Kramerova, I., & Spencer, M. J. (2020). A Small-Molecule Approach to Restore a Slow-Oxidative Phenotype and Defective CaMKIIß Signaling in Limb Girdle Muscular Dystrophy. *Cell Reports Medicine*, *1*(7). https://doi.org/10.1016/j.xcrm.2020.100122

Liu, N., Bezprozvannaya, S., Shelton, J. M., Frisard, M. I., Hulver, M. W., McMillan, R. P., Wu, Y., Voelker, K. A., Grange, R. W., Richardson, J. A., Bassel-Duby, R., & Olson, E. N. (2011). Mice lacking microRNA 133a develop dynamin 2–dependent centronuclear myopathy. *The Journal of Clinical Investigation*, *121*(8), 3258–3268. https://doi.org/10.1172/JCI46267

Liu, Q., Jones, T. I., Tang, V. W., Brieher, W. M., & Jones, P. L. (2010). Facioscapulohumeral muscular dystrophy region gene-1 (FRG-1) is an actin-bundling protein associated with

muscle-attachment sites. *Journal of Cell Science*, *123*(Pt 7), 1116–1123. https://doi.org/10.1242/JCS.058958

López-Manzaneda, S., Ojeda-Pérez, I., Zabaleta, N., García-Torralba, A., Alberquilla, O., Torres, R., Sánchez-Domínguez, R., Torella, L., Olivier, E., Mountford, J., Ramírez, J. C., Bueren, J. A., González-Aseguinolaza, G., & Segovia, J. C. (2020). In Vitro and In Vivo Genetic Disease Modeling via NHEJ-Precise Deletions Using CRISPR-Cas9. *Molecular Therapy. Methods & Clinical Development*, *19*, 426–437. https://doi.org/10.1016/J.OMTM.2020.10.007

Lostal, W., Roudaut, C., Faivre, M., Charton, K., Suel, L., Bourg, N., Best, H., Smith, J. E., Gohlke, J., Corre, G., Li, X., Elbeck, Z., Knöll, R., Deschamps, J. Y., Granzier, H., & Richard, I. (2019). Titin splicing regulates cardiotoxicity associated with calpain 3 gene therapy for limb-girdle muscular dystrophy type 2A. *Science Translational Medicine*, *11*(520). https://doi.org/10.1126/SCITRANSLMED.AAT6072

Louis, E., Raue, U., Yang, Y., Jemiolo, B., & Trappe, S. (2007). Time course of proteolytic, cytokine, and myostatin gene expression after acute exercise in human skeletal muscle. *Journal of Applied Physiology (Bethesda, Md.: 1985)*, *103*(5), 1744–1751. https://doi.org/10.1152/JAPPLPHYSIOL.00679.2007

LOVD Database. (2022). LOVD Database. https://www.lovd.nl/

Lunney, J. K. (2007). Advances in swine biomedical model genomics. *International Journal of Biological Sciences*, *3*(3), 179–184. https://doi.org/10.7150/IJBS.3.179

Maffioletti, S. M., Sarcar, S., Henderson, A. B. H., Mannhardt, I., Pinton, L., Moyle, L. A., Steele-Stallard, H., Cappellari, O., Wells, K. E., Ferrari, G., Mitchell, J. S., Tyzack, G. E., Kotiadis, V. N., Khedr, M., Ragazzi, M., Wang, W., Duchen, M. R., Patani, R., Zammit, P. S., … Tedesco, F. S. (2018). Three-Dimensional Human iPSC-Derived Artificial Skeletal Muscles Model Muscular Dystrophies and Enable Multilineage Tissue Engineering. *Cell Reports*, *23*(3), 899. https://doi.org/10.1016/J.CELREP.2018.03.091

Magli, A., Incitti, T., Kiley, J., Swanson, S. A., Darabi, R., Rinaldi, F., Selvaraj, S., Yamamoto, A., Tolar, J., Yuan, C., Stewart, R., Thomson, J. A., & Perlingeiro, R. C. R. (2017). PAX7 Targets, CD54, Integrin α9β1, and SDC2, Allow Isolation of Human ESC/iPSC-Derived Myogenic Progenitors. *Cell Reports*, *19*(13), 2867–2877. https://doi.org/10.1016/j.celrep.2017.06.005

Mah, J. K., Korngut, L., Fiest, K. M., Dykeman, J., Day, L. J., Pringsheim, T., & Jette, N. (2015). A Systematic Review and Meta-analysis on the Epidemiology of the Muscular Dystrophies. *Canadian Journal of Neurological Sciences*, *43*(1), 163–177. https://doi.org/10.1017/cjn.2015.311

Mahoney, D. J., Parise, G., Melov, S., Safdar, A., & Tarnopolsky, M. A. (2005). Analysis of global mRNA expression in human skeletal muscle during recovery from endurance exercise. *FASEB Journal : Official Publication of the Federation of American Societies for Experimental Biology*, *19*(11), 1498–1500. https://doi.org/10.1096/FJ.04-3149FJE

Maleiner, B., Tomasch, J., Heher, P., Spadiut, O., Rünzler, D., & Fuchs, C. (2018). The Importance of Biophysical and Biochemical Stimuli in Dynamic Skeletal Muscle Models. *Frontiers in Physiology*, *9*(AUG), 1130. https://doi.org/10.3389/FPHYS.2018.01130

Mali, P., Yang, L., Esvelt, K. M., Aach, J., Guell, M., DiCarlo, J. E., Norville, J. E., & Church, G. M. (2013). RNA-Guided Human Genome Engineering via Cas9. *Science (New York, N.Y.)*, *339*(6121), 823. https://doi.org/10.1126/SCIENCE.1232033

Mamchaoui, K., Trollet, C., Bigot, A., Negroni, E., Chaouch, S., Wolff, A., Kandalla, P. K., Marie, S., di Santo, J., St Guily, J. L., Muntoni, F., Kim, J., Philippi, S., Spuler, S., Levy, N., Blumen, S. C., Voit, T., Wright, W. E., Aamiri, A., … Mouly, V. (2011). Immortalized pathological human myoblasts: Towards a universal tool for the study of neuromuscular disorders. *Skeletal Muscle*, *1*(1), 1–11. https://doi.org/10.1186/2044-5040-1-34/FIGURES/4

Manabe, Y., Miyatake, S., Takagi, M., Nakamura, M., Okeda, A., Nakano, T., Hirshman, M. F., Goodyear, L. J., & Fujii, N. L. (2012). Characterization of an Acute Muscle Contraction Model Using Cultured C2C12 Myotubes. *PLOS ONE*, *7*(12), e52592. https://doi.org/10.1371/JOURNAL.PONE.0052592

Martí, M., Mulero, L., Pardo, C., Morera, C., Carrió, M., Laricchia-Robbio, L., Esteban, C. R., & Belmonte, J. C. I. (2013). Characterization of pluripotent stem cells. *Nature Protocols 2013 8:2*, *8*(2), 223–253. https://doi.org/10.1038/nprot.2012.154

Martinez, E. A., Martinez, C. A., Nohalez, A., Sanchez-Osorio, J., Vazquez, J. M., Roca, J., Parrilla, I., Gil, M. A., & Cuello, C. (2015). Nonsurgical deep uterine transfer of vitrified, in vivo-

derived, porcine embryos is as effective as the default surgical approach. *Scientific Reports 2015 5:1*, *5*(1), 1–9. https://doi.org/10.1038/srep10587

Martinez, F. O., & Gordon, S. (2014). The M1 and M2 paradigm of macrophage activation: Time for reassessment. *F1000Prime Reports*, *6*. https://doi.org/10.12703/P6-13

Mason, E. A., Mar, J. C., Laslett, A. L., Pera, M. F., Quackenbush, J., Wolvetang, E., & Wells, C. A. (2014). Gene Expression Variability as a Unifying Element of the Pluripotency Network. *Stem Cell Reports*, *3*(2), 365. https://doi.org/10.1016/J.STEMCR.2014.06.008

Mateos-Aierdi, A. J., Dehesa-Etxebeste, M., Goicoechea, M., Aiastui, A., Goicoechea, M., Richaud-Patin, Y., Jiménez-Delgado, S., Raya, A., Naldaiz-Gastesi, N., & López de Munain, A. (2021). Patient-specific iPSC-derived cellular models of LGMDR1. *Stem Cell Research*, *53*, 102333. https://doi.org/10.1016/J.SCR.2021.102333

Mateos-Aierdi, A. J., Goicoechea, M., Aiastui, A., Torrón, R. F., Garcia-Puga, M., Matheu, A., & de Munain, A. L. (2015). Muscle wasting in myotonic dystrophies: a model of premature aging. *Frontiers in Aging Neuroscience*, *7*(JUN). https://doi.org/10.3389/FNAGI.2015.00125

Matsakas, A., & Patel, K. (2009). Intracellular signalling pathways regulating the adaptation of skeletal muscle to exercise and nutritional changes. *Histology and Histopathology*, *24*(2), 209–222. https://doi.org/10.14670/HH-24.209

Mauro, A. (1961). Satellite cell of skeletal muscle fibers. *The Journal of Biophysical and Biochemical Cytology*, *9*(2), 493–495. https://doi.org/10.1083/JCB.9.2.493

Maxwell, P. H., Wlesener, M. S., Chang, G. W., Clifford, S. C., Vaux, E. C., Cockman, M. E., Wykoff, C. C., Pugh, C. W., Maher, E. R., & Ratcliffe, P. J. (1999). The tumour suppressor protein VHL targets hypoxia-inducible factors for oxygen-dependent proteolysis. *Nature*, *399*(6733), 271–275. https://doi.org/10.1038/20459

McGreevy, J. W., Hakim, C. H., McIntosh, M. A., & Duan, D. (2015). Animal models of Duchenne muscular dystrophy: From basic mechanisms to gene therapy. *DMM Disease Models and Mechanisms*, *8*(3), 195–213. https://doi.org/10.1242/DMM.018424/-/DC1

McKeown, K. A., Downes, G. B., & Hutson, L. D. (2009). Modular laboratory exercises to analyze the development of zebrafish motor behavior. *Zebrafish*, *6*(2), 179–185. https://doi.org/10.1089/ZEB.2008.0564

Mensch, A., & Zierz, S. (2020). Cellular Stress in the Pathogenesis of Muscular Disorders—From Cause to Consequence. *International Journal of Molecular Sciences*, *21*(16), 1–27. https://doi.org/10.3390/IJMS21165830

Mercuri, E., Bönnemann, C. G., & Muntoni, F. (2019). Muscular dystrophies. *Lancet (London, England)*, *394*(10213), 2025–2038. https://doi.org/10.1016/S0140-6736(19)32910-1

Mercuri, E., Bushby, K., Ricci, E., Birchall, D., Pane, M., Kinali, M., Allsop, J., Nigro, V., Sáenz, A., Nascimbeni, A., Fulizio, L., Angelini, C., & Muntoni, F. (2005). Muscle MRI findings in patients with limb girdle muscular dystrophy with calpain 3 deficiency (LGMD2A) and early contractures. *Neuromuscular Disorders : NMD*, *15*(2), 164–171. https://doi.org/10.1016/J.NMD.2004.10.008

Mercuri, E., & Muntoni, F. (2013). Muscular dystrophies. *Lancet (London, England)*, *381*(9869), 845–860. https://doi.org/10.1016/S0140-6736(12)61897-2

Messerschmidt, D. M., Knowles, B. B., & Solter, D. (2014). DNA methylation dynamics during epigenetic reprogramming in the germline and preimplantation embryos. *Genes & Development*, *28*(8), 812. https://doi.org/10.1101/GAD.234294.113

Michalak, M., Parker, J. M. R., & Opas, M. (2002). Ca2+ signaling and calcium binding chaperones of the endoplasmic reticulum. *Cell Calcium*, *32*(5–6), 269–278. https://doi.org/10.1016/S0143416002001884

Milic, A., Daniele, N., Lochmüller, H., Mora, M., Comi, G. P., Moggio, M., Noulet, F., Walter, M. C., Morandi, L., Poupiot, J., Roudaut, C., Bittner, R. E., Bartoli, M., & Richard, I. (2007). A third of LGMD2A biopsies have normal calpain 3 proteolytic activity as determined by an in vitro assay. *Neuromuscular Disorders : NMD*, *17*(2), 148–156. https://doi.org/10.1016/J.NMD.2006.11.001

Mirauta, B. A., Seaton, D. D., Bensaddek, D., Brenes, A., Bonder, M. J., Kilpinen, H., Agu, C. A., Alderton, A., Danecek, P., Denton, R., Durbin, R., Gaffney, D. J., Goncalves, A., Halai, R., Harper, S., Kirton, C. M., Kolb-Kokocinski, A., Leha, A., McCarthy, S. A., … Lamond, A. I. (2020). Population-scale proteome variation in human induced pluripotent stem cells. *ELife*, *9*, 1–22. https://doi.org/10.7554/ELIFE.57390

Mirea, A., Shelby, E. S., Axente, M., Badina, M., Padure, L., Leanca, M., Dima, V., & Sporea, C. (2021). Combination Therapy with Nusinersen and Onasemnogene Abeparvovec-xioi in Spinal Muscular Atrophy Type I. *Journal of Clinical Medicine*, *10*(23). https://doi.org/10.3390/JCM10235540

Mitch, W. E., & Price, S. R. (2003). Mechanisms activating proteolysis to cause muscle atrophy in catabolic conditions. *Journal of Renal Nutrition : The Official Journal of the Council on Renal Nutrition of the National Kidney Foundation*, *13*(2), 149–152. https://doi.org/10.1053/JREN.2003.50019

Mojica, F. J. M., & Montoliu, L. (2016). On the Origin of CRISPR-Cas Technology: From Prokaryotes to Mammals. *Trends in Microbiology*, *24*(10), 811–820. https://doi.org/10.1016/J.TIM.2016.06.005

Moldoveanu, T., Hosfield, C. M., Lim, D., Elce, J. S., Jia, Z., & Davies, P. L. (2002). A Ca2+ Switch Aligns the Active Site of Calpain. *Cell*, *108*(5), 649–660. https://doi.org/10.1016/S0092-8674(02)00659-1

Molina, T., Fabre, P., & Dumont, N. A. (2021). Fibro-adipogenic progenitors in skeletal muscle homeostasis, regeneration and diseases. *Open Biology*, *11*(12), 210110. https://doi.org/10.1098/RSOB.210110

Montarras, D., Morgan, J., Colins, C., Relaix, F., Zaffran, S., Cumano, A., Partridge, T., & Buckingham, M. (2005). Direct isolation of satellite cells for skeletal muscle regeneration. *Science (New York, N.Y.)*, *309*(5743), 2064–2067. https://doi.org/10.1126/SCIENCE.1114758

Motohashi, N., Asakura, Y., & Asakura, A. (2014). Isolation, Culture, and Transplantation of Muscle Satellite Cells. *Journal of Visualized Experiments : JoVE*, *86*, 50846. https://doi.org/10.3791/50846

Musarò, A. (2014). The Basis of Muscle Regeneration. *Advances in Biology*, *2014*, 1–16. https://doi.org/10.1155/2014/612471

Nagaraju, K., & Willmann, R. (2009). Developing standard procedures for murine and canine efficacy studies of DMD therapeutics: report of two expert workshops on "Pre-clinical testing for Duchenne dystrophy": Washington DC, October 27th-28th 2007 and Zürich, June 30th-July 1st 2008. *Neuromuscular Disorders*, *19*(7), 502–506. https://doi.org/10.1016/j.nmd.2009.05.003

Naldaiz-Gastesi, N., Goicoechea, M., Aragón, I. M., Pérez-López, V., Fuertes-Alvarez, S., Herrera-Imbroda, B., López de Munain, A., de Luna-Diaz, R., Baptista, P. M., Fernández, M. A., Lara, M. F., & Izeta, A. (2019). Isolation and characterization of myogenic precursor cells from human cremaster muscle. *Scientific Reports*, *9*(1). https://doi.org/10.1038/S41598-019-40042-6

Navarro-Serna, S., Hachem, A., Canha-Gouveia, A., Hanbashi, A., Garrappa, G., Lopes, J. S., París-Oller, E., Sarriás-Gil, L., Flores-Flores, C., Bassett, A., Sánchez, R., Bermejo-Álvarez, P., Matás, C., Romar, R., Parrington, J., & Gadea, J. (2021). Generation of Nonmosaic, Two-Pore Channel 2 Biallelic Knockout Pigs in One Generation by CRISPR-Cas9 Microinjection Before Oocyte Insemination. *The CRISPR Journal*, *4*(1), 132–146. https://doi.org/10.1089/CRISPR.2020.0078

Navarro-Serna, S., París-Oller, E., Simonik, O., Romar, R., & Gadea, J. (2021). Replacement of Albumin by Preovulatory Oviductal Fluid in Swim-Up Sperm Preparation Method Modifies Boar Sperm Parameters and Improves In Vitro Penetration of Oocytes. *Animals : An Open Access Journal from MDPI*, *11*(5). https://doi.org/10.3390/ANI11051202

Nelson, W. B., Smuder, A. J., Hudson, M. B., Talbert, E. E., & Powers, S. K. (2012). Cross-talk between the calpain and caspase-3 proteolytic systems in the diaphragm during prolonged mechanical ventilation. *Critical Care Medicine*, *40*(6), 1857. https://doi.org/10.1097/CCM.0B013E318246BB5D

Nguyen-Tran, D. H., Hait, N. C., Sperber, H., Qi, J., Fischer, K., Ieronimakis, N., Pantoja, M., Hays, A., Allegood, J., Reyes, M., Spiegel, S., & Ruohola-Baker, H. (2014). Molecular mechanism of sphingosine-1-phosphate action in Duchenne muscular dystrophy. *DMM Disease Models and Mechanisms*, *7*(1), 41–54. https://doi.org/10.1242/DMM.013631/-/DC1

Nigro, V., Okazaki, Y., Belsito, A., Piluso, G., Matsuda, Y., Politano, L., Nigro, G., Ventura, C., Abbondanza, C., Molinari, A. M., Acampora, D., Nishimura, M., Hayashizaki, Y., & Puca, G. A. (1997). Identification of the Syrian hamster cardiomyopathy gene. *Human Molecular Genetics*, *6*(4), 601–607. https://doi.org/10.1093/HMG/6.4.601

Nikolić, N., Görgens, S. W., Thoresen, G. H., Aas, V., Eckel, J., & Eckardt, K. (2017). Electrical pulse stimulation of cultured skeletal muscle cells as a model for in vitro exercise - possibilities and limitations. *Acta Physiologica (Oxford, England)*, *220*(3), 310–331. https://doi.org/10.1111/APHA.12830

Nikolić, N., Skaret Bakke, S., Tranheim Kase, E., Rudberg, I., Flo Halle, I., Rustan, A. C., Thoresen, G. H., & Aas, V. (2012). Electrical pulse stimulation of cultured human skeletal muscle cells as an in vitro model of exercise. *PloS One*, *7*(3). https://doi.org/10.1371/JOURNAL.PONE.0033203

Nilsson, M. I., Macneil, L. G., Kitaoka, Y., Alqarni, F., Suri, R., Akhtar, M., Haikalis, M. E., Dhaliwal, P., Saeed, M., & Tarnopolsky, M. A. (2014). Redox state and mitochondrial respiratory chain function in skeletal muscle of LGMD2A patients. *PLoS ONE*, *9*(7). https://doi.org/10.1371/journal.pone.0102549

Nishikawa, K. (2020). Titin: A tunable spring in active muscle. *Physiology*, *35*(3), 209–217. https://doi.org/10.1152/PHYSIOL.00036.2019/ASSET/IMAGES/LARGE/PHY0032005090004.JPEG

Nishio, K., Tanihara, F., Nguyen, T. v., Kunihara, T., Nii, M., Hirata, M., Takemoto, T., & Otoi, T. (2018). Effects of voltage strength during electroporation on the development and quality of in vitro-produced porcine embryos. *Reproduction in Domestic Animals*, *53*(2), 313–318. https://doi.org/10.1111/RDA.13106

Noble, E. G., Milne, K. J., & Melling, C. W. J. (2008). Heat shock proteins and exercise: a primer. *Applied Physiology, Nutrition, and Metabolism = Physiologie Appliquee, Nutrition et Metabolisme*, *33*(5), 1050–1065. https://doi.org/10.1139/H08-069

Ohlendieck, K. (2011). Proteomic Profiling of Fast-To-Slow Muscle Transitions during Aging. *Frontiers in Physiology*, *2*. https://doi.org/10.3389/FPHYS.2011.00105

Ojima, K., Kawabata, Y., Nakao, H., Nakao, K., Doi, N., Kitamura, F., Ono, Y., Hata, S., Suzuki, H., Kawahara, H., Bogomolovas, J., Witt, C., Ottenheijm, C., Labeit, S., Granzier, H., Toyama-Sorimachi, N., Sorimachi, M., Suzuki, K., Maeda, T., … Sorimachi, H. (2010). Dynamic distribution of muscle-specific calpain in mice has a key role in physical-stress adaptation and is impaired in muscular dystrophy. *Journal of Clinical Investigation*, *120*(8), 2672–2683. https://doi.org/10.1172/JCI40658

Ojima, K., Ono, Y., Doi, N., Yoshioka, K., Kawabata, Y., Labeit, S., & Sorimachi, H. (2007). Myogenic Stage, Sarcomere Length, and Protease Activity Modulate Localization of Muscle-specific Calpain. *Journal of Biological Chemistry*, *282*(19), 14493–14504. https://doi.org/10.1074/JBC.M610806200

Ojima, K., Ono, Y., Ottenheijm, C., Hata, S., Suzuki, H., Granzier, H., & Sorimachi, H. (2011). Non-proteolytic functions of calpain-3 in sarcoplasmic reticulum in skeletal muscles. *Journal of Molecular Biology*, *407*(3), 439–449. https://doi.org/10.1016/j.jmb.2011.01.057

Oliveros, J. C., Franch, M., Tabas-Madrid, D., San-León, D., Montoliu, L., Cubas, P., & Pazos, F. (2016). Breaking-Cas-interactive design of guide RNAs for CRISPR-Cas experiments for ENSEMBL genomes. *Nucleic Acids Research*, *44*(W1), W267–W271. https://doi.org/10.1093/NAR/GKW407

Ono, Y., Ojima, K., Shinkai-Ouchi, F., Hata, S., & Sorimachi, H. (2016). An eccentric calpain, CAPN3/p94/calpain-3. *Biochimie*, *122*, 169–187. https://doi.org/10.1016/J.BIOCHI.2015.09.010

Ono, Y., Ojima, K., Torii, F., Takaya, E., Doi, N., Nakagawa, K., Hata, S., Abe, K., & Sorimachi, H. (2010). Skeletal muscle-specific calpain is an intracellular Na+-dependent protease. *The Journal of Biological Chemistry*, *285*(30), 22986–22998. https://doi.org/10.1074/JBC.M110.126946

Ono, Y., Shimada, H., Sorimach, H., Richard, I., Saido, T. C., Beckmann, J. S., Ishiura, S., & Suzuki, K. (1998). Functional defects of a muscle-specific calpain, p94, caused by mutations associated with limb-girdle muscular dystrophy type 2A. *The Journal of Biological Chemistry*, *273*(27), 17073–17078. https://doi.org/10.1074/JBC.273.27.17073

Ono, Y., Shindo, M., Doi, N., Kitamura, F., Gregorio, C. C., & Sorimachi, H. (2014). The N- and C-terminal autolytic fragments of CAPN3/p94/calpain-3 restore proteolytic activity by intermolecular complementation. *Proceedings of the National Academy of Sciences of the United States of America*, *111*(51), E5527–E5536. https://doi.org/10.1073/PNAS.1411959111

Ono, Y., Torii, F., Ojima, K., Doi, N., Yoshioka, K., Kawabata, Y., Labeit, D., Labeit, S., Suzuki, K., Abe, K., Maeda, T., & Sorimachi, H. (2006). Suppressed Disassembly of Autolyzing

p94/CAPN3 by N2A Connectin/Titin in a Genetic Reporter System *. *Journal of Biological Chemistry*, *281*(27), 18519–18531. https://doi.org/10.1074/JBC.M601029200

Pakos-Zebrucka, K., Koryga, I., Mnich, K., Ljujic, M., Samali, A., & Gorman, A. M. (2016). The integrated stress response. *EMBO Reports*, *17*(10), 1374–1395. https://doi.org/10.15252/EMBR.201642195

Pakula, A., Lek, A., Widrick, J., Mitsuhashi, H., Bugda Gwilt, K. M., Gupta, V. A., Rahimov, F., Criscione, J., Zhang, Y., Gibbs, D., Murphy, Q., Manglik, A., Mead, L., & Kunkel, L. (2019). Transgenic zebrafish model of DUX4 misexpression reveals a developmental role in FSHD pathogenesis. *Human Molecular Genetics*, *28*(2), 320–331. https://doi.org/10.1093/HMG/DDY348

París-Oller, E., Soriano-Úbeda, C., Belda-Pérez, R., Sarriás-Gil, L., Lopes, J. S., Canha-Gouveia, A., Gadea, J., Vieira, L. A., García-Vázquez, F. A., Romar, R., Cánovas, S., & Coy, P. (2022). Reproductive fluids, added to the culture media, contribute to minimizing phenotypical differences between in vitro-derived and artificial insemination-derived piglets. *Journal of Developmental Origins of Health and Disease*. https://doi.org/10.1017/S2040174421000702

Partha, S. K., Ravulapalli, R., Allingham, J. S., Campbell, R. L., & Davies, P. L. (2014). Crystal structure of calpain-3 penta-EF-hand (PEF) domain - a homodimerized PEF family member with calcium bound at the fifth EF-hand. *The FEBS Journal*, *281*(14), 3138–3149. https://doi.org/10.1111/FEBS.12849

Paulsen, G., Lauritzen, F., Bayer, M. L., Kalhovde, J. M., Ugelstad, I., Owe, S. G., Hallén, J., Bergersen, L. H., & Raastad, T. (2009). Subcellular movement and expression of HSP27, αB-crystallin, and HSP70 after two bouts of eccentric exercise in humans. *Journal of Applied Physiology*, *107*(2), 570–582. https://doi.org/10.1152/JAPPLPHYSIOL.00209.2009

Pavesi, A., Adriani, G., Rasponi, M., Zervantonakis, I. K., Fiore, G. B., & Kamm, R. D. (2015). Controlled electromechanical cell stimulation on-a-chip. *Scientific Reports 2015 5:1*, *5*(1), 1–12. https://doi.org/10.1038/srep11800

Perlmutter, D. H. (2002). Chemical Chaperones: A Pharmacological Strategy for Disorders of Protein Folding and Trafficking. *Pediatric Research 2002 52:6*, *52*(6), 832–836. https://doi.org/10.1203/00006450-200212000-00004

Pertille, A., de Carvalho, C. L. T., Matsumura, C. Y., Neto, H. S., & Marques, M. J. (2010). Calcium-binding proteins in skeletal muscles of the mdx mice: potential role in the pathogenesis of Duchenne muscular dystrophy. *International Journal of Experimental Pathology*, *91*(1), 63. https://doi.org/10.1111/J.1365-2613.2009.00688.X

Petters, R. M., & Wells, K. D. (1993). Culture of pig embryos. *Journal of Reproduction and Fertility. Supplement*, *48*, 61–73.

Plantié, E., Migocka-Patrzałek, M., Daczewska, M., & Jagla, K. (2015). Model Organisms in the Fight against Muscular Dystrophy: Lessons from Drosophila and Zebrafish. *Molecules*, *20*(4), 6237. https://doi.org/10.3390/MOLECULES20046237

Plomgaard, P., Penkowa, M., Leick, L., Pedersen, B. K., Saltin, B., & Pilegaard, H. (2006). The mRNA expression profile of metabolic genes relative to MHC isoform pattern in human skeletal muscles. *Journal of Applied Physiology (Bethesda, Md.: 1985)*, *101*(3), 817–825. https://doi.org/10.1152/JAPPLPHYSIOL.00183.2006

Powers, S. K., Duarte, J., Kavazis, A. N., & Talbert, E. E. (2010). Reactive oxygen species are signalling molecules for skeletal muscle adaptation. *Experimental Physiology*, *95*(1), 1–9. https://doi.org/10.1113/EXPPHYSIOL.2009.050526

Prescott, M. J. (2020). Ethical and Welfare Implications of Genetically Altered Non-Human Primates for Biomedical Research. *Journal of Applied Animal Ethics Research*, *2*(2), 151. https://doi.org/10.1163/25889567-BJA10002

Qin, W., Dion, S. L., Kutny, P. M., Zhang, Y., Cheng, A. W., Jillette, N. L., Malhotra, A., Geurts, A. M., Chen, Y. G., & Wang, H. (2015). Efficient CRISPR/Cas9-Mediated Genome Editing in Mice by Zygote Electroporation of Nuclease. *Genetics*, *200*(2), 423–430. https://doi.org/10.1534/GENETICS.115.176594

Rajakumar, D., Alexander, M., & Oommen, A. (2013). Oxidative Stress, NF-κB and the Ubiquitin Proteasomal Pathway in the Pathology of Calpainopathy. *Neurochemical Research 2013 38:10*, *38*(10), 2009–2018. https://doi.org/10.1007/S11064-013-1107-Z

Ramlee, M. K., Yan, T., Cheung, A. M. S., Chuah, C. T. H., & Li, S. (2015). High-throughput genotyping of CRISPR/Cas9-mediated mutants using fluorescent PCR-capillary gel electrophoresis. *Scientific Reports*, *5*. https://doi.org/10.1038/SREP15587

Ran, F. A., Hsu, P. D., Lin, C. Y., Gootenberg, J. S., Konermann, S., Trevino, A. E., Scott, D. A., Inoue, A., Matoba, S., Zhang, Y., & Zhang, F. (2013). Double nicking by RNA-guided CRISPR Cas9 for enhanced genome editing specificity. *Cell*, *154*(6). https://doi.org/10.1016/J.CELL.2013.08.021

Raney, M. A., & Turcotte, L. P. (2008). Evidence for the involvement of CaMKII and AMPK in Ca2+-dependent signaling pathways regulating FA uptake and oxidation in contracting rodent muscle. *Journal of Applied Physiology (Bethesda, Md.: 1985)*, *104*(5), 1366–1373. https://doi.org/10.1152/JAPPLPHYSIOL.01282.2007

Rangarajan, S., Madden, L., & Bursac, N. (2014). Use of flow, electrical, and mechanical stimulation to promote engineering of striated muscles. *Annals of Biomedical Engineering*, *42*(7), 1391–1405. https://doi.org/10.1007/S10439-013-0966-4

Rashid, M. M., Runci, A., Polletta, L., Carnevale, I., Morgante, E., Foglio, E., Arcangeli, T., Sansone, L., Russo, M. A., & Tafani, M. (2015). Muscle LIM protein/CSRP3: a mechanosensor with a role in autophagy. *Cell Death Discovery 2015 1:1*, *1*(1), 1–12. https://doi.org/10.1038/cddiscovery.2015.14

Rath, D., Long, C. R., Dobrinsky, J. R., Welch, G. R., Schreier, L. L., & Johnson, L. A. (1999). In vitro production of sexed embryos for gender preselection: high-speed sorting of X-chromosome-bearing sperm to produce pigs after embryo transfer. *Journal of Animal Science*, *77*(12), 3346–3352. https://doi.org/10.2527/1999.77123346X

Ravulapalli, R., Diaz, B. G., Campbell, R. L., & Davies, P. L. (2005). Homodimerization of calpain 3 penta-EF-hand domain. *The Biochemical Journal*, *388*(Pt 2), 585–591. https://doi.org/10.1042/BJ20041821

Raya, Á., Rodríguez-Piz, I., Guenechea, G., Vassena, R., Navarro, S., Barrero, M. J., Consiglio, A., Castell, M., Río, P., Sleep, E., González, F., Tiscornia, G., Garreta, E., Aasen, T., Veiga, A., Verma, I. M., Surrallés, J., Bueren, J., & Belmonte, J. C. I. (2009). Disease-corrected haematopoietic progenitors from Fanconi anaemia induced pluripotent stem cells. *Nature*, *460*(7251), 53–59. https://doi.org/10.1038/NATURE08129

Redel, B. K., Spate, L. D., Lee, K., Mao, J., Whitworth, K. M., & Prather, R. S. (2016). *Glycine Supplementation In Vitro Enhances Porcine Preimplantation Embryo Cell Number and Decreases Apoptosis but Does Not Lead to Live Births*. https://doi.org/10.1002/mrd.22618

Reik, W., Dean, W., & Walter, J. (2001). Epigenetic reprogramming in mammalian development. *Science (New York, N.Y.)*, *293*(5532), 1089–1093. https://doi.org/10.1126/SCIENCE.1063443

Relaix, F., Montarras, D., Zaffran, S., Gayraud-Morel, B., Rocancourt, D., Tajbakhsh, S., Mansouri, A., Cumano, A., & Buckingham, M. (2006). Pax3 and Pax7 have distinct and overlapping functions in adult muscle progenitor cells. *The Journal of Cell Biology*, *172*(1), 91–102. https://doi.org/10.1083/JCB.200508044

Ren, D., Song, J., Liu, R., Zeng, X., Yan, X., Zhang, Q., & Yuan, X. (2021). Molecular and Biomechanical Adaptations to Mechanical Stretch in Cultured Myotubes. *Frontiers in Physiology*, *12*, 1132. https://doi.org/10.3389/FPHYS.2021.689492/BIBTEX

Renzini, A., Benedetti, A., Bouchè, M., Silvestroni, L., Adamo, S., & Moresi, V. (2018). Culture conditions influence satellite cell activation and survival of single myofibers. *European Journal of Translational Myology*, *28*(2), 167–174. https://doi.org/10.4081/ejtm.2018.7567

Reynolds, B. A., & Weiss, S. (1992). Generation of neurons and astrocytes from isolated cells of the adult mammalian central nervous system. *Science (New York, N.Y.)*, *255*(5052), 1707–1710. https://doi.org/10.1126/SCIENCE.1553558

Richard, I., Broux, O., Allamand, V., Fougerousse, F., Chiannilkulchai, N., Bourg, N., Brenguier, L., Devaud, C., Pasturaud, P., Roudaut, C., Hillaire, D., Passos-Bueno, M. R., Zatz, M., Tischfield, J. A., Fardeau, M., Jackson, C. E., Cohen, D., & Beckmann, J. S. (1995). Mutations in the proteolytic enzyme calpain 3 cause limb-girdle muscular dystrophy type 2A. *Cell*, *81*(1), 27–40. https://doi.org/10.1016/0092-8674(95)90368-2

Richard, I., Hogrel, J. Y., Stockholm, D., Payan, C. A. M., Fougerousse, F., Eymard, B., Mignard, C., Lopez de Munain, A., Fardeau, M., & Urtizberea, J. A. (2016). Natural history of LGMD2A for delineating outcome measures in clinical trials. *Annals of Clinical and Translational Neurology*, *3*(4), 248–265. https://doi.org/10.1002/ACN3.287

Richard, I., Roudaut, C., Marchand, S., Baghdiguian, S., Herasse, M., Stockholm, D., Ono, Y., Suel, L., Bourg, N., Sorimachi, H., Lefranc, G., Fardeau, M., Sébille, A., & Beckmann, J. S. (2000). Loss of Calpain 3 Proteolytic Activity Leads to Muscular Dystrophy and to Apoptosis-

associated I B /Nuclear Factor B Pathway Perturbation in Mice. In *The Journal of Cell Biology* (Vol. 151, Issue 7). http://www.jcb.org/cgi/content/full/151/7/1583

Rico, A., Guembelzu, G., Palomo, V., Martínez, A., Aiastui, A., Casas-fraile, L., Valls, A., de Munain, A. L., & Sáenz, A. (2021). Allosteric modulation of GSK-3β as a new therapeutic approach in limb girdle muscular dystrophy R1 Calpain 3-related. *International Journal of Molecular Sciences*, *22*(14). https://doi.org/10.3390/ijms22147367

Rolfe, D. F. S., & Brown, G. C. (1997). Cellular energy utilization and molecular origin of standard metabolic rate in mammals. *Physiological Reviews*, *77*(3), 731–758. https://doi.org/10.1152/PHYSREV.1997.77.3.731

Rosales, X. Q., Malik, V., Sneh, A., Chen, L., Lewis, S., Kota, J., Gastier-Foster, J. M., Astbury, C., Pyatt, R., Reshmi, S., Rodino-Klapac, L. R., Clark, K. R., Mendell, J. R., & Sahenk, Z. (2013). Impaired regeneration in LGMD2A supported by increased PAX7-positive satellite cell content and muscle-specific microrna dysregulation. *Muscle and Nerve*, *47*(5), 731–739. https://doi.org/10.1002/mus.23669

Ross, J. J., & Tranquillo, R. T. (2003). ECM gene expression correlates with in vitro tissue growth and development in fibrin gel remodeled by neonatal smooth muscle cells. *Matrix Biology : Journal of the International Society for Matrix Biology*, *22*(6), 477–490. https://doi.org/10.1016/S0945-053X(03)00078-7

Ross, M. H., & Pawlina, W. (2016). *Histology : a text and atlas : with correlated cell and molecular biology* (7th ed.). Wolters Kluwer Health.

Roudaut, C., le Roy, F., Suel, L., Poupiot, J., Charton, K., Bartoli, M., & Richard, I. (2013). Restriction of calpain3 expression to the skeletal muscle prevents cardiac toxicity and corrects pathology in a murine model of limb-girdle muscular dystrophy. *Circulation*, *128*(10), 1094–1104. https://doi.org/10.1161/CIRCULATIONAHA.113.001340

Rudnicki, M. A., Schnegelsberg, P. N. J., Stead, R. H., Braun, T., Arnold, H. H., & Jaenisch, R. (1993). MyoD or Myf-5 is required for the formation of skeletal muscle. *Cell*, *75*(7), 1351–1359. https://doi.org/10.1016/0092-8674(93)90621-V

Ryan, D. E., Taussig, D., Steinfeld, I., Phadnis, S. M., Lunstad, B. D., Singh, M., Vuong, X., Okochi, K. D., McCaffrey, R., Olesiak, M., Roy, S., Yung, C. W., Curry, B., Sampson, J. R., Bruhn, L., & Dellinger, D. J. (2018). Improving CRISPR-Cas specificity with chemical modifications in single-guide RNAs. *Nucleic Acids Research*, *46*(2), 792–803. https://doi.org/10.1093/NAR/GKX1199

Sacco, A., Doyonnas, R., Kraft, P., Vitorovic, S., & Blau, H. M. (2008). Self-renewal and expansion of single transplanted muscle stem cells. *Nature*, *456*(7221), 502–506. https://doi.org/10.1038/NATURE07384

Sáenz, A., Azpitarte, M., Armañanzas, R., Leturcq, F., Alzualde, A., Inza, I., García-Bragado, F., la Herran, G. de, Corcuera, J., Cabello, A., Navarro, C., la Torre, C. de, Gallardo, E., Illa, I., & de Munain, A. L. (2008). Gene expression profiling in limb-girdle muscular dystrophy 2A. *PLoS ONE*, *3*(11). https://doi.org/10.1371/journal.pone.0003750

Sáenz, A., & de Munain, A. L. (2017). Dominant LGMD2A: Alternative diagnosis or hidden digenism? *Brain*, *140*(2), e7. https://doi.org/10.1093/brain/aww281

Sáenz, A., Leturcq, F., Cobo, A. M., Poza, J. J., Ferrer, X., Otaegui, D., Camaño, P., Urtasun, M., Vílchez, J., Gutiérrez-Rivas, E., Emparanza, J., Merlini, L., Paisán, C., Goicoechea, M., Blázquez, L., Eymard, B., Lochmuller, H., Walter, M., Bonnemann, C., … López De Munain, A. (2005). LGMD2A: Genotype-phenotype correlations based on a large mutational survey on the calpain 3 gene. *Brain*, *128*(4), 732–742. https://doi.org/10.1093/brain/awh408

Sáenz, A., Leturcq, F., Cobo, A. M., Poza, J. J., Ferrer, X., Otaegui, D., Camaño, P., Urtasun, M., Vílchez, J., Gutiérrez-Rivas, E., Emparanza, J., Merlini, L., Paisán, C., Goicoechea, M., Blázquez, L., Eymard, B., Lochmuller, H., Walter, M., Bonnemann, C., … Munain, A. L. de. (2005). LGMD2A: Genotype-phenotype correlations based on a large mutational survey on the calpain 3 gene. *Brain*, *128*(4), 732–742. https://doi.org/10.1093/brain/awh408

Sáenz, A., Ono, Y., Sorimachi, H., Goicoechea, M., Leturcq, F., Blázquez, L., García-Bragado, F., Marina, A., Poza, J. J., Azpitarte, M., Doi, N., Urtasun, M., Kaplan, J. C., & de Munain, A. L. (2011). Does the severity of the LGMD2A phenotype in compound heterozygotes depend on the combination of mutations? *Muscle and Nerve*, *44*(5), 710–714. https://doi.org/10.1002/mus.22194

Sahenk, Z., Ozes, B., Murrey, D., Myers, M., Moss, K., Yalvac, M. E., Ridgley, A., Chen, L., & Mendell, J. R. (2021). Systemic delivery of AAVrh74.tMCK.hCAPN3 rescues the phenotype

in a mouse model for LGMD2A/R1. *Molecular Therapy - Methods and Clinical Development*, *22*, 401–414. https://doi.org/10.1016/j.omtm.2021.06.010

Saibil, H. (2013). Chaperone machines for protein folding, unfolding and disaggregation. *Nature Reviews Molecular Cell Biology 2013 14:10*, *14*(10), 630–642. https://doi.org/10.1038/nrm3658

Sambasivan, R., Yao, R., Kissenpfennig, A., van Wittenberghe, L., Paldi, A., Gayraud-Morel, B., Guenou, H., Malissen, B., Tajbakhsh, S., & Galy, A. (2011). Pax7-expressing satellite cells are indispensable for adult skeletal muscle regeneration. *Development (Cambridge, England)*, *138*(17), 3647–3656. https://doi.org/10.1242/DEV.067587

Sánchez-Danés, A., Richaud-Patin, Y., Carballo-Carbajal, I., Jiménez-Delgado, S., Caig, C., Mora, S., di Guglielmo, C., Ezquerra, M., Patel, B., Giralt, A., Canals, J. M., Memo, M., Alberch, J., López-Barneo, J., Vila, M., Cuervo, A. M., Tolosa, E., Consiglio, A., & Raya, A. (2012). Disease-specific phenotypes in dopamine neurons from human iPS-based models of genetic and sporadic Parkinson's disease. *EMBO Molecular Medicine*, *4*(5), 380–395. https://doi.org/10.1002/EMMM.201200215

Sandri, M. (2008). Signaling in muscle atrophy and hypertrophy. *Physiology (Bethesda, Md.)*, *23*(3), 160–170. https://doi.org/10.1152/PHYSIOL.00041.2007

Sandri, M. (2010). Autophagy in skeletal muscle. *FEBS Letters*, *584*(7), 1411–1416. https://doi.org/10.1016/J.FEBSLET.2010.01.056

Sarcar, S., Tulalamba, W., Rincon, M. Y., Tipanee, J., Pham, H. Q., Evens, H., Boon, D., Samara-Kuko, E., Keyaerts, M., Loperfido, M., Berardi, E., Jarmin, S., In't Veld, P., Dickson, G., Lahoutte, T., Sampaolesi, M., de Bleser, P., VandenDriessche, T., & Chuah, M. K. (2019). Next-generation muscle-directed gene therapy by in silico vector design. *Nature Communications 2019 10:1*, *10*(1), 1–16. https://doi.org/10.1038/s41467-018-08283-7

Sargeant, A. J. (2007). Structural and functional determinants of human muscle power. *Experimental Physiology*, *92*(2), 323–331. https://doi.org/10.1113/EXPPHYSIOL.2006.034322

Sarig, R., Baruchi, Z., Fuchs, O., Nudel, U., & Yaffe, D. (2006). Regeneration and Transdifferentiation Potential of Muscle-Derived Stem Cells Propagated as Myospheres. *Stem Cells*, *24*(7), 1769–1778. https://doi.org/10.1634/STEMCELLS.2005-0547

Sartore, S., Gorza, L., & Schiaffino, S. (1982). Fetal myosin heavy chains in regenerating muscle. *Nature*, *298*(5871), 294–296. https://doi.org/10.1038/298294A0

Sato, T., Higashioka, K., Sakurai, H., Yamamoto, T., Goshima, N., Ueno, M., & Sotozono, C. (2019). Core Transcription Factors Promote Induction of PAX3-Positive Skeletal Muscle Stem Cells. *Stem Cell Reports*, *13*(2), 352–365. https://doi.org/10.1016/J.STEMCR.2019.06.006

Schiaffino, S., Dyar, K. A., Ciciliot, S., Blaauw, B., & Sandri, M. (2013). Mechanisms regulating skeletal muscle growth and atrophy. *The FEBS Journal*, *280*(17), 4294–4314. https://doi.org/10.1111/FEBS.12253

Schiaffino, S., & Mammucari, C. (2011). Regulation of skeletal muscle growth by the IGF1-Akt/PKB pathway: Insights from genetic models. *Skeletal Muscle*, *1*(1), 1–14. https://doi.org/10.1186/2044-5040-1-4/FIGURES/4

Scicchitano, B. M., Dobrowolny, G., Sica, G., & Musarò, A. (2018). Molecular Insights into Muscle Homeostasis, Atrophy and Wasting. *Current Genomics*, *19*(5), 356. https://doi.org/10.2174/1389202919666180101153911

Selsby, J. T., Ross, J. W., Nonneman, D., & Hollinger, K. (2015). Porcine models of muscular dystrophy. *ILAR Journal*, *56*(1), 116–126. https://doi.org/10.1093/ilar/ilv015

Selvaraj, S., Dhoke, N. R., Kiley, J., Mateos-Aierdi, A. J., Tungtur, S., Mondragon-Gonzalez, R., Killeen, G., Oliveira, V. K. P., López de Munain, A., & Perlingeiro, R. C. R. (2019). Gene Correction of LGMD2A Patient-Specific iPSCs for the Development of Targeted Autologous Cell Therapy. *Molecular Therapy*, *27*(12), 2147–2157. https://doi.org/10.1016/j.ymthe.2019.08.011

Selvaraj, S., Mondragon-Gonzalez, R., Xu, B., Magli, A., Kim, H., Lainé, J., Kiley, J., McKee, H., Rinaldi, F., Aho, J., Tabti, N., Shen, W., & Perlingeiro, R. C. (2019). Screening identifies small molecules that enhance the maturation of human pluripotent stem cell-derived myotubes. *ELife*, *8*. https://doi.org/10.7554/ELIFE.47970

Shansky, J., Chromiak, J., del Tatto, M., & Vandenburgh, H. (1997). A simplified method for tissue engineering skeletal muscle organoids in vitro. *In Vitro Cellular & Developmental Biology. Animal*, *33*(9), 659–661. https://doi.org/10.1007/S11626-997-0118-Y

Sheets, T. P., Park, K. E., Park, C. H., Swift, S. M., Powell, A., Donovan, D. M., & Telugu, B. P. (2018). Targeted Mutation of NGN3 Gene Disrupts Pancreatic Endocrine Cell Development in Pigs. *Scientific Reports 2018 8:1*, *8*(1), 1–10. https://doi.org/10.1038/s41598-018-22050-0

Sheridan, C. (2018). Keep calm and edit on. *Nature Biotechnology 2018 36:8*, *36*(8), 667–667. https://doi.org/10.1038/nbt.4221

Sherman, B. T., Hao, M., Qiu, J., Jiao, X., Baseler, M. W., Lane, H. C., Imamichi, T., & Chang, W. (2022). DAVID: a web server for functional enrichment analysis and functional annotation of gene lists (2021 update). *Nucleic Acids Research*. https://doi.org/10.1093/NAR/GKAC194

Shin, M. K., Bang, J. S., Lee, J. E., Tran, H. D., Park, G., Lee, D. R., & Jo, J. (2022). Generation of Skeletal Muscle Organoids from Human Pluripotent Stem Cells to Model Myogenesis and Muscle Regeneration. *International Journal of Molecular Sciences*, *23*(9). https://doi.org/10.3390/IJMS23095108

Shoji, E., Sakurai, H., Nishino, T., Nakahata, T., Heike, T., Awaya, T., Fujii, N., Manabe, Y., Matsuo, M., & Sehara-Fujisawa, A. (2015). Early pathogenesis of Duchenne muscular dystrophy modelled in patient-derived human induced pluripotent stem cells. *Scientific Reports 2015 5:1*, *5*(1), 1–13. https://doi.org/10.1038/srep12831

Short, K. R., Vittone, J. L., Bigelow, M. L., Proctor, D. N., Coenen-Schimke, J. M., Rys, P., & Nair, K. S. (2005). Changes in myosin heavy chain mRNA and protein expression in human skeletal muscle with age and endurance exercise training. *Journal of Applied Physiology*, *99*(1), 95–102. https://doi.org/10.1152/JAPPLPHYSIOL.00129.2005/ASSET/IMAGES/LARGE/ZDG0070539100006.JPEG

Siciliano, G., Simoncini, C., Giannotti, S., Zampa, V., Angelini, C., & Ricci, G. (2015). Muscle exercise in limb girdle muscular dystrophies: pitfall and advantages. In *Acta Myologica •: Vol. XXXIV*.

Silva, G., Poirot, L., Galetto, R., Smith, J., Montoya, G., Duchateau, P., & Pâques, F. (2011). Meganucleases and Other Tools for Targeted Genome Engineering: Perspectives and Challenges for Gene Therapy. *Current Gene Therapy*, *11*(1), 11. https://doi.org/10.2174/156652311794520111

Singh, P., Schimenti, J. C., & Bolcun-Filas, E. (2015). A mouse geneticist's practical guide to CRISPR applications. *Genetics*, *199*(1), 1–15. https://doi.org/10.1534/GENETICS.114.169771/-/DC1

Sirard, M. A. (2017). The influence of in vitro fertilization and embryo culture on the embryo epigenetic constituents and the possible consequences in the bovine model. *Journal of Developmental Origins of Health and Disease*, *8*(4), 411–417. https://doi.org/10.1017/S2040174417000125

Smith, D. A., Carland, C. R., Guo, Y., & Bernstein, S. I. (2014). Getting Folded: Chaperone proteins in muscle development, maintenance and disease. *Anatomical Record (Hoboken, N.J. : 2007)*, *297*(9), 1637. https://doi.org/10.1002/AR.22980

Smith, I. C., Bombardier, E., Vigna, C., & Tupling, A. R. (2013). ATP Consumption by Sarcoplasmic Reticulum Ca2+ Pumps Accounts for 40-50% of Resting Metabolic Rate in Mouse Fast and Slow Twitch Skeletal Muscle. *PLoS ONE*, *8*(7), 68924. https://doi.org/10.1371/JOURNAL.PONE.0068924

Song, Y., Lai, L., & Li, Z. (2017). Large-scale genomic deletions mediated by CRISPR/Cas9 system. *Oncotarget*, *8*(4), 5647. https://doi.org/10.18632/ONCOTARGET.14543

Song, Y., Yuan, L., Wang, Y., Chen, M., Deng, J., Lv, Q., Sui, T., Li, Z., & Lai, L. (2016). Efficient dual sgRNA-directed large gene deletion in rabbit with CRISPR/Cas9 system. *Cellular and Molecular Life Sciences : CMLS*, *73*(15), 2959–2968. https://doi.org/10.1007/S00018-016-2143-Z

Sonnet, C., Lafuste, P., Arnold, L., Brigitte, M., Poron, F., Authier, F. J., Chrétien, F., Gherardi, R. K., & Chazaud, B. (2006). Human macrophages rescue myoblasts and myotubes from apoptosis through a set of adhesion molecular systems. *Journal of Cell Science*, *119*(Pt 12), 2497–2507. https://doi.org/10.1242/JCS.02988

Sorimachi, H., Hata, S., & Ono, Y. (2011a). Calpain chronicle--an enzyme family under multidisciplinary characterization. *Proceedings of the Japan Academy. Series B, Physical and Biological Sciences*, *87*(6), 287–327. https://doi.org/10.2183/PJAB.87.287

Sorimachi, H., Hata, S., & Ono, Y. (2011b). Impact of genetic insights into calpain biology. *Journal of Biochemistry*, *150*(1), 23–37. https://doi.org/10.1093/JB/MVR070

Sorimachi, H., Imajoh-Ohmi$, S., Emori, Y., Kawasaki, H., Ohno, S., Minamio, Y., & Suzuki, K. (1989). Molecular cloning of a novel mammalian calcium-dependent protease distinct from both m-and μ-types: specific expression of the mRNA in skeletal muscle. *ASBMB*, *264*(33). https://doi.org/10.1016/S0021-9258(19)47225-6

Sorimachi, H., Kinbara, K., Kimura, S., Takahashi, M., Ishiura, S., Sasagawa, N., Sorimachi, N., Shimada, H., Tagawa, K., Maruyama, K., & Suzuki, K. (1995). Muscle-specific calpain, p94, responsible for limb girdle muscular dystrophy type 2A, associates with connectin through IS2, a p94-specific sequence. *The Journal of Biological Chemistry*, *270*(52), 31158–31162. https://doi.org/10.1074/JBC.270.52.31158

Stearns-Reider, K. M., D'Amore, A., Beezhold, K., Rothrauff, B., Cavalli, L., Wagner, W. R., Vorp, D. A., Tsamis, A., Shinde, S., Zhang, C., Barchowsky, A., Rando, T. A., Tuan, R. S., & Ambrosio, F. (2017). Aging of the skeletal muscle extracellular matrix drives a stem cell fibrogenic conversion. *Aging Cell*, *16*(3), 518–528. https://doi.org/10.1111/ACEL.12578

Stein, K. C., Bengoechea, R., Harms, M. B., Weihl, C. C., & True, H. L. (2014). Myopathy-causing mutations in an HSP40 chaperone disrupt processing of specific client conformers. *The Journal of Biological Chemistry*, *289*(30), 21120–21130. https://doi.org/10.1074/JBC.M114.572461

Stern, R. (2003). Devising a pathway for hyaluronan catabolism: are we there yet? *Glycobiology*, *13*(12). https://doi.org/10.1093/GLYCOB/CWG112

Stirm, M., Fonteyne, L. M., Shashikadze, B., Stöckl, J. B., Kurome, M., Keßler, B., Zakhartchenko, V., Kemter, E., Blum, H., Arnold, G. J., Matiasek, K., Wanke, R., Wurst, W., Nagashima, H., Knieling, F., Walter, M. C., Kupatt, C., Fröhlich, T., Klymiuk, N., … Wolf, E. (2022). Pig models for Duchenne muscular dystrophy – from disease mechanisms to validation of new diagnostic and therapeutic concepts. *Neuromuscular Disorders*. https://doi.org/10.1016/J.NMD.2022.04.005

Straub, V., & Bertoli, M. (2016). Where do we stand in trial readiness for autosomal recessive limb girdle muscular dystrophies? *Neuromuscular Disorders : NMD*, *26*(2), 111–125. https://doi.org/10.1016/J.NMD.2015.11.012

Straub, V., Murphy, A., & Udd, B. (2018). 229th ENMC international workshop: Limb girdle muscular dystrophies – Nomenclature and reformed classification Naarden, the Netherlands, 17–19 March 2017. *Neuromuscular Disorders*, *28*(8), 702–710. https://doi.org/10.1016/J.NMD.2018.05.007/ATTACHMENT/63091135-2517-4C16-8D6D-F5BBA0878469/MMC1.ZIP

Stuelsatz, P., Pouzoulet, F., Lamarre, Y., Dargelos, E., Poussard, S., Leibovitch, S., Cottin, P., & Veschambre, P. (2010). Down-regulation of MyoD by calpain 3 promotes generation of reserve cells in C2C12 myoblasts. *The Journal of Biological Chemistry*, *285*(17), 12670–12683. https://doi.org/10.1074/JBC.M109.063966

Stutzmann, G. E., & Mattson, M. P. (2011). Endoplasmic reticulum Ca(2+) handling in excitable cells in health and disease. *Pharmacological Reviews*, *63*(3), 700–727. https://doi.org/10.1124/PR.110.003814

Su, X., Chen, W., Cai, Q., Liang, P., Chen, Y., Cong, P., & Huang, J. (2019). Production of non-mosaic genome edited porcine embryos by injection of CRISPR/Cas9 into germinal vesicle oocytes. *Journal of Genetics and Genomics = Yi Chuan Xue Bao*, *46*(7), 335–342. https://doi.org/10.1016/J.JGG.2019.07.002

Sun, C., Choi, I. Y., Rovira Gonzalez, Y. I., Andersen, P., Conover Talbot, C., Iyer, S. R., Lovering, R. M., Wagner, K. R., & Lee, G. (2020). Duchenne muscular dystrophy hiPSC–derived myoblast drug screen identifies compounds that ameliorate disease in mdx mice. *JCI Insight*, *5*(11). https://doi.org/10.1172/JCI.INSIGHT.134287

Susan Standring. (2021). Gray's Anatomy: 42nd edition | | ISBN: 9780702077050 | ANZ Elsevier Health Bookshop : Books. *Gray's Anatomy*, 955–985. https://www.elsevierhealth.com.au/grays-anatomy-9780702077050.html

Sweeney, H. L., & Hammers, D. W. (2018). Muscle Contraction. *Cold Spring Harbor Perspectives in Biology*, *10*(2). https://doi.org/10.1101/CSHPERSPECT.A023200

Syverud, B. C., VanDusen, K. W., & Larkin, L. M. (2016). Growth Factors for Skeletal Muscle Tissue Engineering. *Cells, Tissues, Organs*, *202*(3–4), 169–179. https://doi.org/10.1159/000444671

Sztretye, M., Szabó, L., Dobrosi, N., Fodor, J., Szentesi, P., Almássy, J., Magyar, Z., Dienes, B., & Csernoch, L. (2020). From Mice to Humans: An Overview of the Potentials and Limitations

of Current Transgenic Mouse Models of Major Muscular Dystrophies and Congenital Myopathies. *International Journal of Molecular Sciences 2020, Vol. 21, Page 8935*, *21*(23), 8935. https://doi.org/10.3390/IJMS21238935

Tagawa, K., Taya, C., Hayashi, Y., Nakagawa, M., Ono, Y., Fukuda, R., Karasuyama, H., Toyama-Sorimachi, N., Katsui, Y., Hata, S., Ishiura, S., Nonaka, I., Seyama, Y., Arahata, K., Yonekawa, H., Sorimachi, H., & Suzuki, K. (2000). Myopathy phenotype of transgenic mice expressing active site-mutated inactive p94 skeletal muscle-specific calpain, the gene product responsible for limb girdle muscular dystrophy type 2A. In *Human Molecular Genetics* (Vol. 9, Issue 9).

Tajbakhsh, S. (2009). Skeletal muscle stem cells in developmental versus regenerative myogenesis. *Journal of Internal Medicine*, *266*(4), 372–389. https://doi.org/10.1111/J.1365-2796.2009.02158.X

Tajbakhsh, S., Rocancourt, D., Cossu, G., & Buckingham, M. (1997). Redefining the genetic hierarchies controlling skeletal myogenesis: Pax-3 and Myf-5 act upstream of MyoD. *Cell*, *89*(1), 127–138. https://doi.org/10.1016/S0092-8674(00)80189-0

Takahashi, K., & Yamanaka, S. (2006). Induction of pluripotent stem cells from mouse embryonic and adult fibroblast cultures by defined factors. *Cell*, *126*(4), 663–676. https://doi.org/10.1016/J.CELL.2006.07.024

Tanaka, A., Woltjen, K., Miyake, K., Hotta, A., Ikeya, M., Yamamoto, T., Nishino, T., Shoji, E., Sehara-Fujisawa, A., Manabe, Y., Fujii, N., Hanaoka, K., Era, T., Yamashita, S., Isobe, K. ichi, Kimura, E., & Sakurai, H. (2013). Efficient and Reproducible Myogenic Differentiation from Human iPS Cells: Prospects for Modeling Miyoshi Myopathy In Vitro. *PLOS ONE*, *8*(4), e61540. https://doi.org/10.1371/JOURNAL.PONE.0061540

Tanihara, F., Hirata, M., Nguyen, N. T., Le, Q. A., Hirano, T., Takemoto, T., Nakai, M., Fuchimoto, D. I., & Otoi, T. (2018). Generation of a TP53-modified porcine cancer model by CRISPR/Cas9-mediated gene modification in porcine zygotes via electroporation. *PLOS ONE*, *13*(10), e0206360. https://doi.org/10.1371/JOURNAL.PONE.0206360

Tanihara, F., Hirata, M., Nguyen, N. T., Le, Q. A., Hirano, T., Takemoto, T., Nakai, M., Fuchimoto, D. ichiro, & Otoi, T. (2019). Generation of PDX-1 mutant porcine blastocysts by introducing CRISPR/Cas9-system into porcine zygotes via electroporation. *Animal Science Journal*, *90*(1), 55–61. https://doi.org/10.1111/ASJ.13129

Tanihara, F., Hirata, M., & Otoi, T. (2021). Current status of the application of gene editing in pigs. *The Journal of Reproduction and Development*, *67*(3), 177. https://doi.org/10.1262/JRD.2021-025

Tanihara, F., Takemoto, T., Kitagawa, E., Rao, S., Do, L. T. K., Onishi, A., Yamashita, Y., Kosugi, C., Suzuki, H., Sembon, S., Suzuki, S., Nakai, M., Hashimoto, M., Yasue, A., Matsuhisa, M., Noji, S., Fujimura, T., Fuchimoto, D. ichiro, & Otoi, T. (2016). Somatic cell reprogramming-free generation of genetically modified pigs. *Science Advances*, *2*(9). https://doi.org/10.1126/SCIADV.1600803/SUPPL_FILE/1600803_SM.PDF

Tanoury, Z. al, Rao, J., Tassy, O., Gobert, B., Gapon, S., Garnier, J. M., Wagner, E., Hick, A., Hall, A., Gussoni, E., & Pourquié, O. (2020). Differentiation of the human PAX7-positive myogenic precursors/satellite cell lineage in vitro. *Development (Cambridge, England)*, *147*(12). https://doi.org/10.1242/DEV.187344

Tapscott, S. J. (2005). The circuitry of a master switch: Myod and the regulation of skeletal muscle gene transcription. *Development (Cambridge, England)*, *132*(12), 2685–2695. https://doi.org/10.1242/DEV.01874

Tarum, J., Folkesson, M., Atherton, P. J., & Kadi, F. (2017). Electrical pulse stimulation: an in vitro exercise model for the induction of human skeletal muscle cell hypertrophy. A proof-of-concept study. *Experimental Physiology*, *102*(11), 1405–1413. https://doi.org/10.1113/EP086581

Taveau, M., Bourg, N., Sillon, G., Roudaut, C., Bartoli, M., & Richard, I. (2003). Calpain 3 Is Activated through Autolysis within the Active Site and Lyses Sarcomeric and Sarcolemmal Components. *Molecular and Cellular Biology*, *23*(24), 9127–9135. https://doi.org/10.1128/mcb.23.24.9127-9135.2003

Taylor, M. v. (2013). *Comparison of Muscle Development in Drosophila and Vertebrates*. https://www.ncbi.nlm.nih.gov/books/NBK6226/

Tedesco, F. S., Gerli, M. F. M., Perani, L., Benedetti, S., Ungaro, F., Cassano, M., Antonini, S., Tagliafico, E., Artusi, V., Longa, E., Tonlorenzi, R., Ragazzi, M., Calderazzi, G., Hoshiya, H.,

Cappellari, O., Mora, M., Schoser, B., Schneiderat, P., Oshimura, M., … Cossu, G. (2012). Transplantation of genetically corrected human iPSC-derived progenitors in mice with limb-girdle muscular dystrophy. *Science Translational Medicine*, *4*(140). https://doi.org/10.1126/SCITRANSLMED.3003541

Tedesco, F. S., Moyle, L. A., & Perdiguero, E. (2017). Muscle Interstitial Cells: A Brief Field Guide to Non-satellite Cell Populations in Skeletal Muscle. *Methods in Molecular Biology (Clifton, N.J.)*, *1556*, 129–147. https://doi.org/10.1007/978-1-4939-6771-1_7

Terrill, J. R., Radley-Crabb, H. G., Iwasaki, T., Lemckert, F. A., Arthur, P. G., & Grounds, M. D. (2013). Oxidative stress and pathology in muscular dystrophies: focus on protein thiol oxidation and dysferlinopathies. *The FEBS Journal*, *280*(17), 4149–4164. https://doi.org/10.1111/FEBS.12142

Thomas, K., Engler, A. J., & Meyer, G. A. (2015). Extracellular matrix regulation in the muscle satellite cell niche. *Connective Tissue Research*, *56*(1), 1–8. https://doi.org/10.3109/03008207.2014.947369

Thorrez, L., DiSano, K., Shansky, J., & Vandenburgh, H. (2018). Engineering of human skeletal muscle with an autologous deposited extracellular matrix. *Frontiers in Physiology*, *9*(AUG), 1076. https://doi.org/10.3389/FPHYS.2018.01076/BIBTEX

Tidball, J. G. (2011). Mechanisms of muscle injury, repair, and regeneration. *Comprehensive Physiology*, *1*(4), 2029–2062. https://doi.org/10.1002/CPHY.C100092

Tintignac, L. A., Lagirand, J., Batonnet, S., Sirri, V., Leibovitch, M. P., & Leibovitch, S. A. (2005). Degradation of MyoD mediated by the SCF (MAFbx) ubiquitin ligase. *The Journal of Biological Chemistry*, *280*(4), 2847–2856. https://doi.org/10.1074/JBC.M411346200

Todd, P. K., Ackall, F. Y., Hur, J., Sharma, K., Paulson, H. L., & Dowling, J. J. (2014). Transcriptional changes and developmental abnormalities in a zebrafish model of myotonic dystrophy type 1. *DMM Disease Models and Mechanisms*, *7*(1), 143–155. https://doi.org/10.1242/DMM.012427/-/DC1

Toral-Ojeda, I., Aldanondo, G., Lasa-Elgarresta, J., Lasa-Fernández, H., Fernández-Torrón, R., de Munain, A. L., & Vallejo-Illarramendi, A. (2016). Calpain 3 deficiency affects SERCA expression and function in the skeletal muscle. *Expert Reviews in Molecular Medicine*, *18*. https://doi.org/10.1017/ERM.2016.9

Toral-Ojeda, I., Aldanondo, G., Lasa-Elgarresta, J., Lasa-Fernandez, H., Vesga-Castro, C., Mouly, V., Lasa-Elgarresta, J., Lasa-Fernandez, H., Vesga-Castro, C., Mouly, V., López de Munain, A., & Vallejo-Illarramendi, A. (2018). A Novel Functional In Vitro Model that Recapitulates Human Muscle Disorders. *Muscle Cell and Tissue - Current Status of Research Field*. https://doi.org/10.5772/INTECHOPEN.75903

Tsai, S. Q., Zheng, Z., Nguyen, N. T., Liebers, M., Topkar, V. v., Thapar, V., Wyvekens, N., Khayter, C., Iafrate, A. J., Le, L. P., Aryee, M. J., & Joung, J. K. (2014). GUIDE-seq enables genome-wide profiling of off-target cleavage by CRISPR-Cas nucleases. *Nature Biotechnology 2014 33:2*, *33*(2), 187–197. https://doi.org/10.1038/nbt.3117

Tuladhar, R., Yeu, Y., Tyler Piazza, J., Tan, Z., Rene Clemenceau, J., Wu, X., Barrett, Q., Herbert, J., Mathews, D. H., Kim, J., Hyun Hwang, T., & Lum, L. (2019). CRISPR-Cas9-based mutagenesis frequently provokes on-target mRNA misregulation. *Nature Communications 2019 10:1*, *10*(1), 1–10. https://doi.org/10.1038/s41467-019-12028-5

Uchimura, T., Otomo, J., Sato, M., & Sakurai, H. (2017). A human iPS cell myogenic differentiation system permitting high-throughput drug screening. *Stem Cell Research*, *25*, 98–106. https://doi.org/10.1016/J.SCR.2017.10.023

Uhlig, M., Passlack, W., & Eckel, J. (2005). Functional role of Rab11 in GLUT4 trafficking in cardiomyocytes. *Molecular and Cellular Endocrinology*, *235*(1–2), 1–9. https://doi.org/10.1016/J.MCE.2005.02.004

Unger, A., Beckendorf, L., Böhme, P., Kley, R., von Frieling-Salewsky, M., Lochmüller, H., Schröder, R., Fürst, D. O., Vorgerd, M., & Linke, W. A. (2017). Translocation of molecular chaperones to the titin springs is common in skeletal myopathy patients and affects sarcomere function. *Acta Neuropathologica Communications*, *5*(1), 72. https://doi.org/10.1186/S40478-017-0474-0

Urciuolo, A., Serena, E., Ghua, R., Zatti, S., Giomo, M., Mattei, N., Vetralla, M., Selmin, G., Luni, C., Vitulo, N., Valleid, G., Vitielloid, L., & Elvassore, N. (2020). *Engineering a 3D in vitro model of human skeletal muscle at the single fiber scale*. https://doi.org/10.1371/journal.pone.0232081

Urtasun, M., Sáenz, A., Roudaut, C., Poza, J. J., Urtizberea, J. A., Cobo, A. M., Richard, I., García Bragado, F., Leturcq, F., Kaplan, J. C., Martí Massó, J. F., Beckmann, J. S., & López de Munain, A. (1998). Limb-girdle muscular dystrophy in Guipúzcoa (Basque Country, Spain). *Brain : A Journal of Neurology*, *121 (Pt 9)*(9), 1735–1747. https://doi.org/10.1093/BRAIN/121.9.1735

Vakulskas, C. A., & Behlke, M. A. (2019). Evaluation and reduction of crispr off-target cleavage events. *Nucleic Acid Therapeutics*, *29*(4), 167–174. https://doi.org/10.1089/nat.2019.0790

Vallejo-Illarramendi, A., Toral-Ojeda, I., Aldanondo, G., & López de Munain, A. (2014). Dysregulation of calcium homeostasis in muscular dystrophies. *Expert Reviews in Molecular Medicine*, *16*, e16. https://doi.org/10.1017/ERM.2014.17

van der Velden, J. L. J., Langen, R. C. J., Kelders, M. C. J. M., Willems, J., Wouters, E. F. M., Janssen-Heininger, Y. M. W., & Schols, A. M. W. J. (2007). Myogenic differentiation during regrowth of atrophied skeletal muscle is associated with inactivation of GSK-3beta. *American Journal of Physiology. Cell Physiology*, *292*(5). https://doi.org/10.1152/AJPCELL.00504.2006

van der Weijden, V. A., Schmidhauser, M., Kurome, M., Knubben, J., Flöter, V. L., Wolf, E., & Ulbrich, S. E. (2021). Transcriptome dynamics in early in vivo developing and in vitro produced porcine embryos. *BMC Genomics*, *22*(1), 1–13. https://doi.org/10.1186/S12864-021-07430-7/FIGURES/6

van Putten, M., Lloyd, E. M., de Greef, J. C., Raz, V., Willmann, R., & Grounds, M. D. (2020). *Mouse models for muscular dystrophies: an overview*. https://doi.org/10.1242/dmm.043562

van Putten, M., Putker, K., Overzier, M., Adamzek, W. A., Pasteuning-Vuhman, S., Plomp, J. J., & Aartsma-Rus, A. (2019). Natural disease history of the D2-mdx mouse model for Duchenne muscular dystrophy. *The FASEB Journal*, *33*(7), 8110. https://doi.org/10.1096/FJ.201802488R

Vinciguerra, M., Musaro, A., & Rosenthal, N. (2010). Regulation of muscle atrophy in aging and disease. *Advances in Experimental Medicine and Biology*, *694*, 211–233. https://doi.org/10.1007/978-1-4419-7002-2_15

Vissing, J. (2016). Limb girdle muscular dystrophies: classification, clinical spectrum and emerging therapies. *Current Opinion in Neurology*, *29*(5), 635–641. https://doi.org/10.1097/WCO.0000000000000375

Vissing, J., Barresi, R., Witting, N., van Ghelue, M., Gammelgaard, L., Bindoff, L. A., Straub, V., Lochmüller, H., Hudson, J., Wahl, C. M., Arnardottir, S., Dahlbom, K., Jonsrud, C., & Duno, M. (2016). A heterozygous 21-bp deletion in CAPN3 causes dominantly inherited limb girdle muscular dystrophy. *Brain : A Journal of Neurology*, *139*(Pt 8), 2154–2163. https://doi.org/10.1093/BRAIN/AWW133

Vissing, J., Dahlqvist, J. R., Roudaut, C., Poupiot, J., Richard, I., Duno, M., & Krag, T. (2020). A single c.1715G>C calpain 3 gene variant causes dominant calpainopathy with loss of calpain 3 expression and activity. *Human Mutation*, *41*(9), 1507–1513. https://doi.org/10.1002/HUMU.24066

Volonte, D., Peoples, A. J., & Galbiati, F. (2003). Modulation of Myoblast Fusion by Caveolin-3 in Dystrophic Skeletal Muscle Cells: Implications for Duchenne Muscular Dystrophy and Limb-Girdle Muscular Dystrophy-1C. *Molecular Biology of the Cell*, *14*(10), 4075. https://doi.org/10.1091/MBC.E03-03-0161

Volpato, V., & Webber, C. (2020). Addressing variability in iPSC-derived models of human disease: guidelines to promote reproducibility. *Disease Models & Mechanisms*, *13*(1). https://doi.org/10.1242/DMM.042317

von Maltzahn, J., Chang, N. C., Bentzinger, C. F., & Rudnicki, M. A. (2012). Wnt signaling in myogenesis. *Trends in Cell Biology*, *22*(11), 602–609. https://doi.org/10.1016/J.TCB.2012.07.008

Wang, G., Yang, H., Yan, S., Wang, C. E., Liu, X., Zhao, B., Ouyang, Z., Yin, P., Liu, Z., Zhao, Y., Liu, T., Fan, N., Guo, L., Li, S., Li, X. J., & Lai, L. (2015). Cytoplasmic mislocalization of RNA splicing factors and aberrant neuronal gene splicing in TDP-43 transgenic pig brain. *Molecular Neurodegeneration*, *10*(1). https://doi.org/10.1186/S13024-015-0036-5

Wang, J., Khodabukus, A., Rao, L., Vandusen, K., Abutaleb, N., & Bursac, N. (2019). Engineered skeletal muscles for disease modeling and drug discovery. *Biomaterials*, *221*. https://doi.org/10.1016/J.BIOMATERIALS.2019.119416

Wang, Y. X., Feige, P., Brun, C. E., Hekmatnejad, B., Dumont, N. A., Renaud, J. M., Faulkes, S., Guindon, D. E., & Rudnicki, M. A. (2019). EGFR-Aurka Signaling Rescues Polarity and

Regeneration Defects in Dystrophin-Deficient Muscle Stem Cells by Increasing Asymmetric Divisions. *Cell Stem Cell*, *24*(3), 419-432.e6. https://doi.org/10.1016/J.STEM.2019.01.002

Warren, L., Manos, P. D., Ahfeldt, T., Loh, Y. H., Li, H., Lau, F., Ebina, W., Mandal, P. K., Smith, Z. D., Meissner, A., Daley, G. Q., Brack, A. S., Collins, J. J., Cowan, C., Schlaeger, T. M., & Rossi, D. J. (2010). Highly efficient reprogramming to pluripotency and directed differentiation of human cells with synthetic modified mRNA. *Cell Stem Cell*, *7*(5), 618–630. https://doi.org/10.1016/J.STEM.2010.08.012

Watt, K. I., Jaspers, R. T., Atherton, P., Smith, K., Rennie, M. J., Ratkevicius, A., & Wackerhage, H. (2010). SB431542 treatment promotes the hypertrophy of skeletal muscle fibers but decreases specific force. *Muscle & Nerve*, *41*(5), 624–629. https://doi.org/10.1002/MUS.21573

Waugh, T. A., Horstick, E., Hur, J., Jackson, S. W., Davidson, A. E., Li, X., & Dowling, J. J. (2014). Fluoxetine prevents dystrophic changes in a zebrafish model of Duchenne muscular dystrophy. *Human Molecular Genetics*, *23*(17), 4651–4662. https://doi.org/10.1093/HMG/DDU185

Wehrle, U., Düsterhöft, S., & Pette, D. (1994). Effects of chronic electrical stimulation on myosin heavy chain expression in satellite cell cultures derived from rat muscles of different fiber-type composition. *Differentiation; Research in Biological Diversity*, *58*(1), 37–46. https://doi.org/10.1046/J.1432-0436.1994.5810037.X

Wei, Y., Li, Y., Chen, C., Stoelzel, K., Kaufmann, A. M., & Albers, A. E. (2011). Human skeletal muscle-derived stem cells retain stem cell properties after expansion in myosphere culture. *Experimental Cell Research*, *317*(7), 1016–1027. https://doi.org/10.1016/J.YEXCR.2011.01.019

Weihl, C. C., Udd, B., Hanna, M., Ben-Zvi, A., Blaettler, T., Bryson-Richardson, R., Carra, S., Dimachkie, M., Findlay, A., Greensmith, L., Greenspan, S., Hanna, M., Höhfled, J., Jonson, P. H., Kampinga, H., Larsson, L., Linke, W., Lynch, G., Machado, P., … Zah, L. (2018). 234th ENMC International Workshop: Chaperone dysfunction in muscle disease December 8-10th 2017, Naarden, Netherlands. *Neuromuscular Disorders : NMD*, *28*(12), 1022. https://doi.org/10.1016/J.NMD.2018.09.004

Weisheit, I., Kroeger, J. A., Malik, R., Wefers, B., Lichtner, P., Wurst, W., Dichgans, M., & Paquet, D. (2021). Simple and reliable detection of CRISPR-induced on-target effects by qgPCR and SNP genotyping. *Nature Protocols*, *16*(3), 1714–1739. https://doi.org/10.1038/S41596-020-00481-2

Wells, D. J. (2018). Tracking progress: an update on animal models for Duchenne muscular dystrophy. *Disease Models & Mechanisms*, *11*(6). https://doi.org/10.1242/DMM.035774

Wernersson, R., Schierup, M. H., Jørgensen, F. G., Gorodkin, J., Panitz, F., Stærfeldt, H. H., Christensen, O. F., Mailund, T., Hornshøj, H., Klein, A., Wang, J., Liu, B., Hu, S., Dong, W., Li, W., Wong, G. K. S., Yu, J., Wang, J., Bendixen, C., … Bolund, L. (2005). Pigs in sequence space: a 0.66X coverage pig genome survey based on shotgun sequencing. *BMC Genomics*, *6*. https://doi.org/10.1186/1471-2164-6-70

Westerblad, H., Bruton, J. D., & Katz, A. (2010). Skeletal muscle: energy metabolism, fiber types, fatigue and adaptability. *Experimental Cell Research*, *316*(18), 3093–3099. https://doi.org/10.1016/J.YEXCR.2010.05.019

Westerman, K. A. (2015). Myospheres Are Composed of Two Cell Types: One That Is Myogenic and a Second That Is Mesenchymal. *PLOS ONE*, *10*(2), e0116956. https://doi.org/10.1371/JOURNAL.PONE.0116956

Westerman, K. A., Penvose, A., Yang, Z., Allen, P. D., & Vacanti, C. A. (2010). Adult muscle "stem" cells can be sustained in culture as free-floating myospheres. *Experimental Cell Research*, *316*(12), 1966–1976. https://doi.org/10.1016/J.YEXCR.2010.03.022

Whalen, R. G., Harris, J. B., Butler-Browne, G. S., & Sesodia, S. (1990). Expression of myosin isoforms during notexin-induced regeneration of rat soleus muscles. *Developmental Biology*, *141*(1), 24–40. https://doi.org/10.1016/0012-1606(90)90099-5

Winbanks, C. E., Wang, B., Beyer, C., Koh, P., White, L., Kantharidis, P., & Gregorevic, P. (2011). TGF-beta regulates miR-206 and miR-29 to control myogenic differentiation through regulation of HDAC4. *The Journal of Biological Chemistry*, *286*(16), 13805–13814. https://doi.org/10.1074/JBC.M110.192625

Wiśniewski, J. R., Zougman, A., Nagaraj, N., & Mann, M. (2009). Universal sample preparation method for proteome analysis. *Nature Methods*, *6*(5), 359–362. https://doi.org/10.1038/NMETH.1322

Wu, J., Ruas, J. L., Estall, J. L., Rasbach, K. A., Choi, J. H., Ye, L., Boström, P., Tyra, H. M., Crawford, R. W., Campbell, K. P., Rutkowski, D. T., Kaufman, R. J., & Spiegelman, B. M. (2011). The unfolded protein response mediates adaptation to exercise in skeletal muscle through a PGC-1α/ATF6α complex. *Cell Metabolism*, *13*(2), 160–169. https://doi.org/10.1016/J.CMET.2011.01.003

Xia, Q., Huang, X., Huang, J., Zheng, Y., March, M. E., Li, J., & Wei, Y. (2021). The Role of Autophagy in Skeletal Muscle Diseases. *Frontiers in Physiology*, *12*, 291. https://doi.org/10.3389/FPHYS.2021.638983/BIBTEX

Xie, N., Chu, S. N., Azzag, K., Schultz, C. B., Peifer, L. N., Kyba, M., Perlingeiro, R. C. R., & Chan, S. S. K. (2021). In vitro expanded skeletal myogenic progenitors from pluripotent stem cell-derived teratomas have high engraftment capacity. *Stem Cell Reports*, *16*(12), 2900–2912. https://doi.org/10.1016/J.STEMCR.2021.10.014

Xu, C., Tabebordbar, M., Iovino, S., Ciarlo, C., Liu, J., Castiglioni, A., Price, E., Liu, M., Barton, E. R., Kahn, C. R., Wagers, A. J., & Zon, L. I. (2013). A zebrafish embryo culture system defines factors that promote vertebrate myogenesis across species. *Cell*, *155*(4), 909. https://doi.org/10.1016/J.CELL.2013.10.023

Xu, M., Chen, X., Chen, D., Yu, B., & Huang, Z. (2017). FoxO1: a novel insight into its molecular mechanisms in the regulation of skeletal muscle differentiation and fiber type specification. *Oncotarget*, *8*(6), 10662. https://doi.org/10.18632/ONCOTARGET.12891

Yalvac, M. E., Amornvit, J., Braganza, C., Chen, L., Hussain, S. R. A., Shontz, K. M., Montgomery, C. L., Flanigan, K. M., Lewis, S., & Sahenk, Z. (2017). Impaired regeneration in calpain-3 null muscle is associated with perturbations in mTORC1 signaling and defective mitochondrial biogenesis. *Skeletal Muscle*, *7*(1). https://doi.org/10.1186/s13395-017-0146-6

Yang, C. C., Liu, H., Chen, S. L., Wang, T. H., Hsieh, C. L., Huang, Y., Chen, S. J., Chen, H. C., Yung, B. Y. M., & Tan, B. C. M. (2012). Epigenetic silencing of myogenic gene program by Myb-binding protein 1a suppresses myogenesis. *The EMBO Journal*, *31*(7), 1739–1751. https://doi.org/10.1038/EMBOJ.2012.24

Yang, H., & Wu, Z. (2018). Genome editing of pigs for agriculture and biomedicine. In *Frontiers in Genetics* (Vol. 9, Issue SEP). Frontiers Media S.A. https://doi.org/10.3389/fgene.2018.00360

Yang, W., & Hu, P. (2018). Skeletal muscle regeneration is modulated by inflammation. *Journal of Orthopaedic Translation*, *13*, 25–32. https://doi.org/10.1016/J.JOT.2018.01.002

Yang, X., Xue, P., Chen, H., Yuan, M., Kang, Y., Duscher, D., Machens, H. G., & Chen, Z. (2020). Denervation drives skeletal muscle atrophy and induces mitochondrial dysfunction, mitophagy and apoptosis via miR-142a-5p/MFN1 axis. *Theranostics*, *10*(3), 1415. https://doi.org/10.7150/THNO.40857

Yoon, S., Stadler, G., Beermann, M. L., Schmidt, E. v., Windelborn, J. A., Schneiderat, P., Wright, W. E., & Miller, J. B. (2013). Immortalized myogenic cells from congenital muscular dystrophy type1A patients recapitulate aberrant caspase activation in pathogenesis: A new tool for MDC1A research. *Skeletal Muscle*, *3*(1), 1–7. https://doi.org/10.1186/2044-5040-3-28/FIGURES/3

Yoshida, H., Matsui, T., Hosokawa, N., Kaufman, R. J., Nagata, K., & Mori, K. (2003). A Time-Dependent Phase Shift in the Mammalian Unfolded Protein Response. *Developmental Cell*, *4*(2), 265–271. https://doi.org/10.1016/S1534-5807(03)00022-4

Yoshioka, K., Kitajima, Y., Okazaki, N., Chiba, K., Yonekura, A., & Ono, Y. (2020). A Modified Pre-plating Method for High-Yield and High-Purity Muscle Stem Cell Isolation From Human/Mouse Skeletal Muscle Tissues. *Frontiers in Cell and Developmental Biology*, *8*, 793. https://doi.org/10.3389/FCELL.2020.00793/BIBTEX

Young, J., Margaron, Y., Fernandes, M., Duchemin-Pelletier, E., Michaud, J., Flaender, M., Lorintiu, O., Degot, S., & Poydenot, P. (2018). MyoScreen, a High-Throughput Phenotypic Screening Platform Enabling Muscle Drug Discovery. *SLAS Discovery*, *23*(8), 790–806. https://doi.org/10.1177/2472555218761102

Yu, H. H., Zhao, H., Qing, Y. B., Pan, W. R., Jia, B. Y., Zhao, H. Y., Huang, X. X., & Wei, H. J. (2016). Porcine zygote injection with Cas9/sgRNAResults in DMD-modified pig with muscle dystrophy. *International Journal of Molecular Sciences*, *17*(10). https://doi.org/10.3390/ijms17101668

Zak, R., Martin, A. F., Prior, G., & Rabinowitz, M. (1977). Comparison of Turnover of Several Myofibrillar Proteins and Critical Evaluation of Double Isotope Method*. *Journal of Biological Chemistry*, *252*(10), 3430–3435. https://doi.org/10.1016/S0021-9258(17)40409-1

Zambon, A. A., & Muntoni, F. (2021). Congenital muscular dystrophies: What is new? *Neuromuscular Disorders : NMD*, *31*(10), 931–942. https://doi.org/10.1016/J.NMD.2021.07.009

Zammit, P. S. (2017). Function of the myogenic regulatory factors Myf5, MyoD, Myogenin and MRF4 in skeletal muscle, satellite cells and regenerative myogenesis. *Seminars in Cell & Developmental Biology*, *72*, 19–32. https://doi.org/10.1016/J.SEMCDB.2017.11.011

Zammit, P. S., Relaix, F., Nagata, Y., Ruiz, A. P., Collins, C. A., Partridge, T. A., & Beauchamp, J. R. (2006). Pax7 and myogenic progression in skeletal muscle satellite cells. *Journal of Cell Science*, *119*(Pt 9), 1824–1832. https://doi.org/10.1242/JCS.02908

Zatz, M., de Paula, F., Starling, A., & Vainzof, M. (2003). The 10 autosomal recessive limb-girdle muscular dystrophies. In *Neuromuscular Disorders* (Vol. 13, Issues 7–8, pp. 532–544). Elsevier Ltd. https://doi.org/10.1016/S0960-8966(03)00100-7

Zhang, B. G. X., Quigley, A. F., Bourke, J. L., Nowell, C. J., Myers, D. E., Choong, P. F. M., & Kapsa, R. M. I. (2016). Combination of agrin and laminin increase acetylcholine receptor clustering and enhance functional neuromuscular junction formation In vitro. *Developmental Neurobiology*, *76*(5), 551–565. https://doi.org/10.1002/DNEU.22331

Zhang, H., Shang, R., & Bi, P. (2021). Feedback regulation of Notch signaling and myogenesis connected by MyoD–Dll1 axis. *PLOS Genetics*, *17*(8), e1009729. https://doi.org/10.1371/JOURNAL.PGEN.1009729

Zhang, J. P., Li, X. L., Li, G. H., Chen, W., Arakaki, C., Botimer, G. D., Baylink, D., Zhang, L., Wen, W., Fu, Y. W., Xu, J., Chun, N., Yuan, W., Cheng, T., & Zhang, X. B. (2017). Efficient precise knockin with a double cut HDR donor after CRISPR/Cas9-mediated double-stranded DNA cleavage. *Genome Biology*, *18*(1), 1–18. https://doi.org/10.1186/S13059-017-1164-8/FIGURES/6

Zhang, P., Liang, X., Shan, T., Jiang, Q., Deng, C., Zheng, R., & Kuang, S. (2015). mTOR is necessary for proper satellite cell activity and skeletal muscle regeneration. *Biochemical and Biophysical Research Communications*, *463*(1–2), 102–108. https://doi.org/10.1016/J.BBRC.2015.05.032

Zhang, X. H., Tee, L. Y., Wang, X. G., Huang, Q. S., & Yang, S. H. (2015). Off-target Effects in CRISPR/Cas9-mediated Genome Engineering. *Molecular Therapy. Nucleic Acids*, *4*(11), e264. https://doi.org/10.1038/MTNA.2015.37

Zhao, J., Whyte, J., & Prather, R. S. (2010). Effect of epigenetic regulation during swine embryogenesis and on cloning by nuclear transfer. *Cell and Tissue Research*, *341*(1), 13–21. https://doi.org/10.1007/S00441-010-1000-X/FIGURES/1

Zheng, Q., Cai, X., Tan, M. H., Schaffert, S., Arnold, C. P., Gong, X., Chen, C. Z., & Huang, S. (2014). Precise gene deletion and replacement using the CRISPR/Cas9 system in human cells. *BioTechniques*, *57*(3), 115–124. https://doi.org/10.2144/000114196/ASSET/IMAGES/LARGE/FIGURE4.JPEG

Zhu, J., Telfer, E. E., Fletcher, J., Springbett, A., Dobrinsky, J. R., de Sousa, P. A., & Wilmut, I. (2002). Improvement of an Electrical Activation Protocol for Porcine Oocytes. *Biology of Reproduction*, *66*(3), 635–641. https://doi.org/10.1095/BIOLREPROD66.3.635

Zschüntzsch, J., Meyer, S., Shahriyari, M., Kummer, K., Schmidt, M., Kummer, S., & Tiburcy, M. (2022). The Evolution of Complex Muscle Cell In Vitro Models to Study Pathomechanisms and Drug Development of Neuromuscular Disease. *Cells 2022, Vol. 11, Page 1233*, *11*(7), 1233. https://doi.org/10.3390/CELLS11071233

APPENDIX I: PUBLICATIONS

Published works during the PhD studies:

Navarro-Serna S, **Dehesa-Etxebeste M,** Piñeiro-Silva C, Romar R, Lopes J S, López de Munaín A, Gadea J, Generation of Calpain-3 knock-out porcine embryos by CRISPR-Cas9 electroporation and intracytoplasmic microinjection of oocytes before insemination. Theriogenology, 2022 186, 175-184. DOI:10.1016/j.theriogenology. 2022.04.012

Mateos-Aierdi AJ*, **Dehesa-Etxebeste M***, Goicoechea M, Aiastui A, Richaud-Patin Y, Jiménez-Delgado S, Raya A, Naldaiz-Gastesi N, López de Munain A. Patient-specific iPSC-derived cellular models of LGMDR1. Stem Cell Res. 2021 May;53:102333. doi: 10.1016/j.scr.2021.102333. *Co-first authors.

Juul-Madsen K, Qvist P, Bendtsen KL, Langkilde AE, Vestergaard B, Howard KA, **Dehesa-Etxebeste M**, Paludan SR, Andersen GR, Jensen PH, Otzen DE, Romero-Ramos M, Vorup-Jensen T. Size-Selective Phagocytic Clearance of Fibrillar α-Synuclein through Conformational Activation of Complement Receptor 4. J Immunol. 2020 Mar 1;204(5):1345-1361. doi: 10.4049.

APPENDIX II: FUNDING SOURCES

1. Ayudas destinadas a la financiación de la realización de una tesis doctoral mediante un contrato predoctoral. Departamento de Educación del Gobierno Vasco (PRE_2017_1_0235, PRE_2018_2_0232, PRE_2019_2_0135 y PRE_2020_2_0065).

2. **Project:** Function of calpain 3 in satellite cells during muscle regeneration and its pharmacological modulation as a possible treatment of LGMD2A (PI17/001841)
   Center: Biodonostia HRI **Principal Investigator:** Dr. Adolfo López de Munain
   Funding agency: Instituto de Salud Carlos III. **Period:** 2017-2021

3. **Project:** Development of porcine models of muscular disease with CRISPR/Cas9: Optimization of the in vitro fertilization and editing to obtain a LGMD2A pig model (DTS19/00061).
   Center: Biodonostia HRI **Principal Investigator:** Dr. Adolfo López de Munain
   Funding agency: Instituto de Salud Carlos III. **Period:** 2020-2022

4. **Funding agency:** Fundación Isabel Gemio.

5. **Funding agency:** CIBERNED, Instituto de Salud Carlos III.